# Investigating the delivery and secretion of effectors in the rice blast fungus *Magnaporthe oryzae*

Submitted by Clara Rodriguez Herrero

to the University of Exeter as a thesis for the degree of
Doctor of Philosophy in Biological Sciences
In November 2019



I certify that all material in this thesis which is not my own work has been identified and that no material has previously been submitted and approved for the award of a degree by this or any other University.

Clara Rodriguez Herrero

**Abstract**

*Magnaporthe oryzae* is a hemi-biotrophic fungus and the causal agent of rice blast disease, which is a serious threat to global rice production. During its biotrophic phase, the fungus feeds and develops within living plant cells. To facilitate this state, the fungus secretes effectors that suppress plant immunity and modify host cell structure, metabolism and function. Effectors in *M. oryzae* can be classified as either cytoplasmic effectors or apoplastic effectors, depending on where they are localised during host colonisation. Cytoplasmic effectors accumulate in a membrane-rich plant structure called the biotrophic interfacial complex (BIC), while apoplastic effectors are found between the fungal cell wall and the extra-invasive hyphal membrane which surrounds invasive hyphae. A previous report has provided evidence that different secretion pathways operate to drive effector secretion from fungal hyphae, including a non-conventional Golgi-independent pathway for secretion of cytoplasmic effectors. Little is known, however regarding how these secreted effectors are delivered to the correct domains and, in particular, how cytoplasmic effectors are translocated to plant cells. In this thesis, I report that the promoter and signal peptide sequences of effector-encoding genes are involved in delivering an effector into the correct domain. I generated a library of chimeric effectors that were systematically tested for localisation and translocation during *M. oryzae* growth inside the rice cell. This showed that when the promoter and signal peptide of a cytoplasmic effector gene was used to control expression of an apoplastic effector, then it was re-directed to the BIC and translocated into plant cells. Conversely, cytoplasmic effectors could be re-directed to the apoplast when expressed under control of the promoter and signal peptide region of an apoplastic effector gene. I also observed *M. oryzae* invasive hyphae in live cell imaging experiments with stable transgenic rice plants in which early endosomal compartments and the plant plasma membrane were fluorescent tagged. These transgenic rice lines allow the use of plasmolysis assays to observe effector translocation inside host cells and to visualise endosomal trafficking at the BIC structure. When considered together, the thesis provides evidence that effector secretion is controlled by sequences at the 5' end of effector genes that are sufficient to direct effector delivery into the appropriate pathway during plant infection. These signals are independent of the nature of the protein being secreted.

**Contents**

## List of figures

## List of tables

**Acknowledgements**

I would like to thank the Lawrence/Palmer Scholarship for providing me with funding to carry out this research. I am grateful for Michael Lawrence for his support and interest in these past four years, that has allowed me to present my research in various international scientific conferences and outreach events. I would like to thank my supervisor Nick Talbot for his supervision, mentorship and motivation during my PhD. Many thanks to everyone in lab 301 (Exeter) and The Sainsbury Laboratory in Norwich, especially my laboratory colleagues past and present for the many laughs and shared experiences. I am incredibly thankful to Dr Magdalena Martin Urdioz and Dr Miriam Oses Ruiz for their guidance, advice and support in and out the lab, I will always look up to both of you. Thank you to Dr Vincent Were and Alice Eseola for your encouraging words and making me laugh every day.

I would also like to thank Genna Davies and Felicity George for always being there for me and creating one of the most special friendships. To my friends who have shown me their support even if I was far away Regina, Laura, Maria, Albert, Claudi, Pol i Nat. Thank you to my parents Gabriel Rodriguez and Angela Herrero for their love and support, and to my family for their unconditional love. Finally, I would like to thank my fiancé Tim Peek for everything, your encouragement, patience and always showing me your love.

## Abbreviations

| | |
|---|---|
| bp | base pair |
| BIC | biotrophic interfacial complex |
| cAMP | cyclic 3', 5' adenosine monophosphate |
| CDS | coding sequence |
| CM | complete medium |
| °C | degrees Celcius |
| ddH20 | double distilled water |
| DNA | deoxyribonucleic acid |
| EIHM | extra-invsaive hyphal membrane |
| EIHMx | extra-invsaive hyphal membrane matrix |
| g | grams |
| $gL^{-1}$ | grams per litre |
| GFP | green flouresencent protein |
| hpi | hours post infection |
| IH | invasive hypahe |
| kb | kilobase |
| l | litre |
| µg | microgram |
| µl | microlitre |
| µm | micrometre |
| MAPK | mitogen-activated protein kinase |
| mCh | mCherry |
| mg | milligram |
| mL | millilitre |
| mm | millimetre |
| mM | millimolar |
| mRNA | messenger RNA |
| NLR | nucleotide-binding and leucine repeat domain |
| ng | nanogram |
| ORF | open reading frame |
| PCR | polymerase chain reaction |
| % | percentage |
| % w/v | percentage weight by volume |
| % v/v | percentage volume by volume |
| RNA | ribonucleic acid |
| Rnase | ribonuclease |
| ROS | reactive oxygen species |
| rpm | revolutions per minute |

# Chapter 1. General Introduction

## *1.1 Food security: The importance of plant diseases*

The expanding global population means that food production needs to double in the next 40 years (Godfray et al., 2010). The necessity for more food production, however, faces important challenges such as water shortages, the cost of energy, land degradation, political conditions, the climate emergency and the emergence and spread of pest and pathogens (Godfray et al., 2010). Pest and pathogens are responsible for the loss of at least 30% of the world's crop production (Strange and Scott, 2005). Of these losses, fungi generate the most significant diseases and are therefore a major threat to global food security and ecosystem health (Fisher et al., 2012). In spite of this, fungi are still the most neglected pathogens in terms of research funding, mostly in the medical field (Fisher et al., 2016). The most devastating crop pathogens globally are wheat stem rust, potato late blight, corn smut, Asian soybean rust and rice blast disease (Fisher et al., 2012).

This threat to global food production is intensified with climate change, because pathogens are moving polewards in a warming world. Research suggests that fungal diseases are moving 7.6 km per year since 1960, faster than wild species and nearly identically to that expected by temperature change (Bebber et al., 2013). This, and another human factors and mistakes, can lead to unexpected movement of crop diseases (Carvajal-Yepes et al., 2019). As a consequence, a Global Surveillance System (GSS) has been proposed to ensure fast networking between labs to respond to the spread of crop diseases. A recent example for this was the emergence of wheat blast disease, which appeared in Asia for the first time in 2016 (Islam et al., 2016; Carvajal-Yepes et al., 2019). The wheat blast outbreak in Bangladesh, caused loss of 16% of national wheat production in 2016 (Islam et al., 2016). Scientists obtained diseased samples from the field and carried out RNA-seq analysis to identify the pathogen very rapidly, which was then shared in an open science initiative (Open Wheat Blast). This example reinforces the need for collaboration and open science to tackle crop diseases (Islam et al., 2016; Carvajal-Yepes et al., 2019). As a result of this international collaboration, it was demonstrated that the wheat-infecting strain of *M. oryzae* from Bangladeshi fields was a wheat blast strain from South America (Islam et al., 2016). Wheat blast is caused by *Magnaporthe oryzae* and was first identified in South America (Islam et al., 2016). It originated from a host jump from a strain

of the fungus infecting perennial rye grass, *Lolium perenne* and has caused disease in Brazil since 1985. It is thought that contaminated grain from South America was shipped to Bangladesh and eventually found its way into seed stocks sown in 2015-16. *M. oryzae* is therefore not only tremendously important as the cause of rice blast disease, but also wheat blast disease. Sadly, wheat blast appears to be spreading within Bangladesh and potentially into India, the second major wheat producer in Asia (Islam et al., 2019).

### *1.2 The plant immune system*

Plants rely on innate immune responses that operate in each cell. Unlike humans, which have specialised immune defence cells, each plant cell is equipped to respond to danger signals (Zipfel, 2009). The operation of the plant immune system has been described as a "zigzag" model (Jones and Dangl, 2006) (Figure 1.1). First, the plant cell detects pathogen-associated molecular patterns (PAMPs) or microorganism-associated molecular patterns (MAMPs) by means of pattern recognition receptors (PRRs), which triggers PAMP-triggered immunity (PTI). This is the first layer of the plant immune response. PRRs are responsible for detecting pathogen molecules or stress signals in the apoplastic space. A large number of PAMPs have been characterised in fungi and bacteria but relatively few PRRs have been studied *in planta* (Boutrot and Zipfel, 2017). PRRs are surface-localised immune receptors and are either receptor kinases (RKs) or receptor-like proteins (RLPs). Because RKs carry a ligand-binding ectodomain, a single-pass transmembrane domain, an intracellular kinase domain but no signalling domains, it is thought that RKs and RLPs must form complexes to trigger PTI. The most well studied pair of PRRs is the FLS2 and EFR pair. FLS2 is a leucine-rich repeat receptor kinase that is involved in flagellin sensing and EFR responds to the EF-TU translation elongation factor PAMP (Chinchilla et al., 2006; Zipfel et al., 2006). PTI is a very important first layer of defence because it can stop a pathogen from spreading to neighbouring cells.

Pathogens are, however, able to overcome PTI by delivery of effectors, in a process known as effector-triggered susceptibility (ETS). In this way, effectors suppress PTI components, and inhibit defence-associated signalling mechanisms. In response to ETS, the plant has evolved a second layer of defence. Effectors can be recognized by proteins encoded by corresponding plant resistant genes (R genes), resulting in effector-triggered immunity (ETI).

This can lead to the hypersensitive cell death response (HR). The expression of two *M. oryzae* Avrs, AvrPita and AvrPii, in plants carrying the corresponding R genes has been shown, for example, to activate the HR in an incompatible rice-*M. oryzae* interaction (Ribot et al., 2013).

To overcome ETI and achieve successful colonisation, pathogens can lose effector genes that are recognised by R gene-encoding immune receptors. Effectors that are recognized by a resistance gene in the plant are called avirulence gene products (Avrs) (Jones and Dangl, 2006). In rice, some R genes are present as clusters at the same locus. For example, Pi2/Pi9/Piz-t, Pi3/Pii, Pish/Pi37/Pi35 and Pik/Pikp/Pil/Pkm. Many R genes encode intracellular immune receptors, known as NLRs, or nucleotide-binding, leucine-rice repeat receptor proteins. Plant NLRs contain Toll-interleukin1 receptor (TIR) or a coiled coil (CC) domain at the N-terminus, a nucleotide binding site (NBS) and a C-terminal leucine repeat domain (LRR), These sequences are mostly conserved except for the LRR domain which is variable and usually encodes the region where effector recognition occurs (Takken and Goverse, 2012).

Recent reports demonstrate that NLRs may work within NLR networks composed of “sensor” NLR proteins that are paired with “helper” NLRs to mediate immune signalling (Wu et al., 2017; Adachi et al., 2019a). Some NLRs, are known to trigger cell death and an insight into the mechanism underlying immune receptor activation was recently reported. The *Arabidopsis* CC-NLR ZAR1 (HOPZ-ACTIVATED RESISTANCE 1) is activated and adopts a wheel-like pentamer shaped complex that undergoes a conformational switch to expose a funnel-shaped structure formed by the N-terminal $\alpha$1 helices of the CC domain (Wang et al., 2019a). The exposed $\alpha$1 helix may disrupt the plasma membrane to trigger cell death. Following this finding, a conserved motif for the death switch was identified and has been named the MADA motif. The MADA motif was always found at the N-termini of NRC family proteins and is similar to the N-terminal $\alpha$1 helix of ZAR1 (Wu et al., 2017; Adachi et al., 2019b).

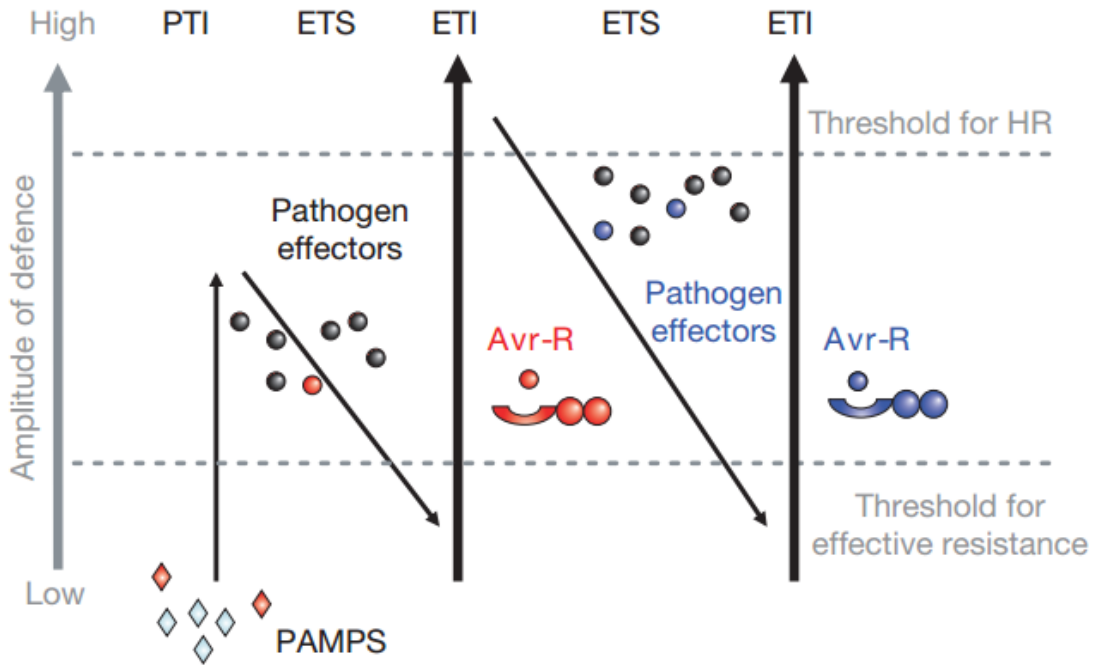


Figure 1.1 **The zigzag model of plant immunity.** The plant immune system as a zig zag model. Plant associated molecular patterns (PAMPs) are recognised by the plant which lead to plant triggered immune response (PTI), to attenuate it, pathogens secrete effectors (Avr-R) which switch on effector triggered immune response (ETI). ETI can be avoided if those effectors mutate and stop being recognised by the resistant gene in the plant and that is called effector triggered susceptibility (ETS). (Taken from Jones and Dang, 2006)

### *1.3 Integrated domains or decoys in NLR immune receptors*

There are various models that explain how an Avr protein is perceived by a corresponding NLR receptor (Wu et al., 2017). First, it was observed that NLRs act as singletons in a gene-for-gene relationship, consistent with Flor's original genetic model (Flor, 1942). The same NLR is therefore responsible for recognising an effector and the consequent immune signalling necessary for disease resistance. Some NLRs have, however, evolved into pairs of NLRs that require the action of one another. In these interactions, one NLR is responsible for recognition of the effector and the other is responsible for triggering immunity. There are four models that demonstrated how the recognition of effector works: direct binding of R-Avr, the guard model, the decoy model and the integrated decoy model (Van der Hoorn and Kamoun, 2008; Maqbool et al., 2015; Wu et al., 2017; Adachi et al., 2019a).

The direct binding of R-Avr, as described before, is when there is a direct recognition between the resistance gene and the effector. The guard model is when the interaction between an effector and NLR is not direct, but the NLR guards the effector target and is able to detect a modified target by the effector, triggering ETI. The decoy model is similar to the guard model but in this model a decoy protein acts as a mimic of the effector target protein, thereby binding to it with strong affinity. This triggers NLR activation, by a closely associated guard-like NLR, and a resistance response. A further elaboration of this model occurs when the decoy is integrated as a discrete protein domain within the NLR protein itself. This is called the integrated decoy model. The integrated decoy model normally requires corresponding NLRs to work in pairs. These NLRs have a similar structure except for the LRR domain. One NLR, contains the decoy protein domain in its LRR that binds to the effector. This allows the NLR to recognise the effector. Then, the other classical NLR, the sensor, triggers the cell death response (Dangl and Jones, 2001; Cesari et al., 2014a).

An example of such a NLR pair is the *RGA4/RGA5*-encoded NLR pair in rice which binds to the *M. oryzae* effectors AvrPia and Avr1CO39 by a Heavy-Metal Associated domain (HMA). Interestingly, an HMA domain in Pik-1/Pik-2 NLS pair also binds to another *M. oryzae* effector AvrPik (Maqbool et al., 2015). The HMA domain was found in RGA5 and Pik-1, therefore the Avrs do not bind to Pik-2 or RGA4. Research shows co-evolution between the plant and the pathogen of HMA

receptor specificities (De la Concepcion et al., 2018). The different allels of AvrPik show different affinities for the HMA domain in two different Pik NLR allels. Pikm is able to confer resistance to AvrPikD, AvrPikE and AvrPikA. However, Pikp is only able to interact with AvrPikD(De la Concepcion et al., 2018). The integrated decoy model has also been proposed for *Arabidopsis* with the NLR pair RRS1-R/RPS4, which are the target of different effectors in different pathogens. In this instance, the effector binds a conserved “WRKY”DNA-binding domain which is in the C-terminus of RRS1 (Le Roux et al., 2015).

### *1.4 Rice Blast disease*

*Magnaporthe oryzae* Couch (synonym of *Pyricularia oryzae*) is the causal agent of rice blast, the most serious disease of cultivated rice (*Oryza sativa*) (Kohn, 2002). The domestication of rice cultivars can be documented as far back as 7000 BC in the Yangtze Valley in China, and it is likely that other pathogenic forms *of M. oryzae* spread on to rice soon afterwards(Couch et al., 2005). Rice blast is a tremendous threat to global food security because rice consumption accounts for 23% of all human calorific intake (Wilson and Talbot, 2009). Because of the rapid increase in human population, there is a 3% rise in rice consumption per year (Wilson and Talbot, 2009). Losses due to rice blast are also increasing. In China 5.7 million hectares were destroyed between 2001 and 2005 (Veneault-Fourrey et al., 2006). There are 85 countries reported that are heavily affected by rice blast disease with losses from 10% to 30%. In 2009 in Mwea, Kenya, the total loss in production due to rice blast disease was 47.9% compared to 2008. (Howard and Valent, 1996; Kihoro et al., 2013; Nalley et al., 2016).

*M. oryzae* can also infect on more than 50 species of grass, such as wheat (*Triticum aestivum*), finger millet (*Eleusine coracana*) and barley (*Hordeum vulgare*) (Talbot, 2003). As described above, wheat blast is an emerging threat to food security (Islam et al., 2016). Finger millet is, however, also an important food security crop in India and southern and east African countries, which provides nutrition and essential minerals such as calcium, phosphorus and iron to low income rural communities. Finger millet blast is a severe disease that occurs before the grain is formed and can cause complete harvest loss (Talbot, 2003).

Rice plants are targeted by *M. oryzae* at all phases of growth and leaves, stems, nodes and panicles are all liable to infection (Wilson and Talbot, 2009). However, complete loss of grain can occur as a result of infection of the neck or panicle, especially if infection happens before formation of the grain (Talbot, 2003; Dean et al., 2012). Neck and panicle blast are therefore the most severe pathologies observed in the field.

In common with many crop diseases, selective breeding for disease resistance has been the predominant control method for rice blast disease. However, the rice blast fungus is able to mutate and overcome single gene resistance in rice within a time frame of 24 to 36 months, thus negating the breeding efforts to control it (Dean et al., 2012). Fundamental research into rice blast disease is therefore vital to provide diverse disease control strategies (Wilson and Talbot, 2009). In particular, it is clear that there needs to be a better understanding of the biology of the rice blast fungus.

### *1.5 The rice blast fungus Magnaporthe oryzae*

*M. oryzae* is a filamentous ascomycete fungus (Dean et al., 2012). *M. oryzae* was first isolated from rice by Cavara in 1892 and named *Pyricularia oryzae* (Perez-Nadales et al., 2014). The biology of the pathogen has since been extensively studied. This was accelerated by the ability to carry out classical and molecular genetics (Valent and Chumley, 1991). The discovery, 31 years of the fertile *MAT1-2* strain rice blast isolate Guy11 in French Guiana, for example, meant that mating could be carried out in rice blast fungus thereby facilitating classical genetic analysis and construction of the first genetic maps and gene isolation, thereby increasing its study as a model organism for understanding plant-microbe interactions (Wilson and Talbot, 2009; Dean et al., 2012).

The genome sequence of *M. oryzae* strain 70-15 was published in 2005 (Dean et al., 2005). The fungus has 7 chromosomes and is 41.7 Mb in size. The approximate number of genes is between 12,827 and 16,000, which means there is roughly one gene every 4 Kb. It is also important to mention that *M. oryzae* has 4,734 genes in common with *Saccharomyces cerevisiae* which is a model organism useful for studying functional relationships of genes across the eukaryotes (Perez-Nadales et al., 2014). The genome sequence, together with the ability to carry out DNA-mediated transformation of *M. oryzae* and advances

in new molecular genetics techniques make *M. oryzae* a valuable model to study plant-pathogen interactions (Dean et al., 2012).

### *1.6 The life cycle of Magnaporthe oryzae*

The life cycle of *M. oryzae* (Figure 1.2) begins when a three-celled spore, known as a conidium, lands on the hydrophobic leaf of a rice plant. The conidium is carried by a dew drop, as *M. oryzae* sporulates only under high humidity conditions (Talbot, 1995; Wilson and Talbot, 2009). The conidium becomes attached to the leaf surface by means of an adhesive called spore tip mucilage (STM), which is released from the apical tip of the conidium upon hydration and independently of the type of surface upon which the spore lands (Hamer et al., 1988). Hamer and co-workers showed that 20 minutes post inoculation, 90% of the conidia attach to the leaf surface and are therefore resistant to the flow of water and wind (Hamer et al., 1988).

Two hours after the spore attaches to the leaf, a polarized germ tube appears (Talbot, 2003). The germ tube normally develops from one of the apical cells and then compresses flat against the leaf surface. This is a process known as “hooking”, which is thought to be a recognition step prior to appressorium development (Bourett and Howard, 1990; Talbot, 2003). The germ tube is about 10-15 μm in length, composed mostly by cytoskeletal components with a bi-layered cell wall (Bourett and Howard, 1990). Once the germ tube appears, the nucleus of the apical cell from which the germ tube emerges migrates to the end of the germ tube. There, mitosis takes place 4 or 6 hours after germination (Saunders et al., 2010). Formation of the appressorium is regulated by a DNA replication dependent checkpoint and entry into S-phase is essential (Saunders et al., 2010). A temperature-sensitive mutation in the *NIMA* gene, which encodes a protein kinase necessary for mitosis, provided evidence that cell cycle control is necessary for the development of the appressorium, as the appressorium did not form when this protein was inactivated at non-permissive temperatures (Veneault-Fourrey et al., 2006). Equally, if mitosis is blocked by hydroxyurea, which blocks cell-cycle progression at the $G_1$/S, then appressorium formation is also inhibited (Veneault-Fourrey et al., 2006). In the laboratory, appressorium formation can be induced by *cis*-9,10-epoxy-18-hydroxyoctadecanoic acid or 1,16-hexadecanediol (Gilbert et al., 1996; Talbot, 2003; Ebbole, 2007). The absence of exogenous nutrients and a hard-hydrophobic surface are also

required for appressorium formation (Choi and Dean, 1997). After the appressorium has developed, appressorium maturation requires another S-phase check point that is dependent on turgor pressure generation (Oses-Ruiz et al., 2017). Once the appressorium is completely formed conidial cells collapse in a process requiring autophagy (Veneault-Fourrey et al., 2006; Kershaw and Talbot, 2009). In the autophagy mutant Δ*atg8*, the conidia do not collapse and although appressorium is formed it is unable to penetrate and cause infection (Veneault-Fourrey et al., 2006; Kershaw and Talbot, 2009) (Liu et al., 2007).

The appressorium is a dome-shaped cell with a highly differentiated cell wall, rich in chitin, and has a thick melanin layer (Bourett and Howard, 1990). The melanin layer prevents the efflux of glycerol and other solutes escaping from the appressorium. Therefore, enormous turgor pressure is generated in the appressorium (Bourett and Howard, 1990; Chumley, 1990; Howard et al., 1991; de Jong et al., 1997). Melanin-deficient mutants are not able to develop a successful appressorium due to lack of sufficient solute concentration (Chumley, 1990). The osmotic pressure inside the appressorium is as high as 8.0 MPa, and is translated into physical force at the appressorium base, which ruptures the rice leaf cuticle (Howard et al., 1991; de Jong et al., 1997). Then a rigid penetration peg emerges and enters the plant cell. Once it penetrates the host cell, the penetration peg undergoes a morphogenetic change from a primary invasive hypha (IH) into a bulbous secondary invasive hyphae, that will ramify throughout plant cells (Talbot, 2003; Kankanala et al., 2007). It has been reported that after 72 hours post-infection around 10% of biomass of a rice leaf is fungal biomass (Talbot et al., 1993a; Talbot et al., 1993b).

Ellipsoid necrotic lesions are visible on the surface of the leaf 3 to 4 days after infection (Talbot, 1995, 2003; Wilson and Talbot, 2009). Sporulation from these lesions is responsible for producing spores to infect other plants, completing *M. oryzae* life cycle (Perez-Nadales et al., 2014).

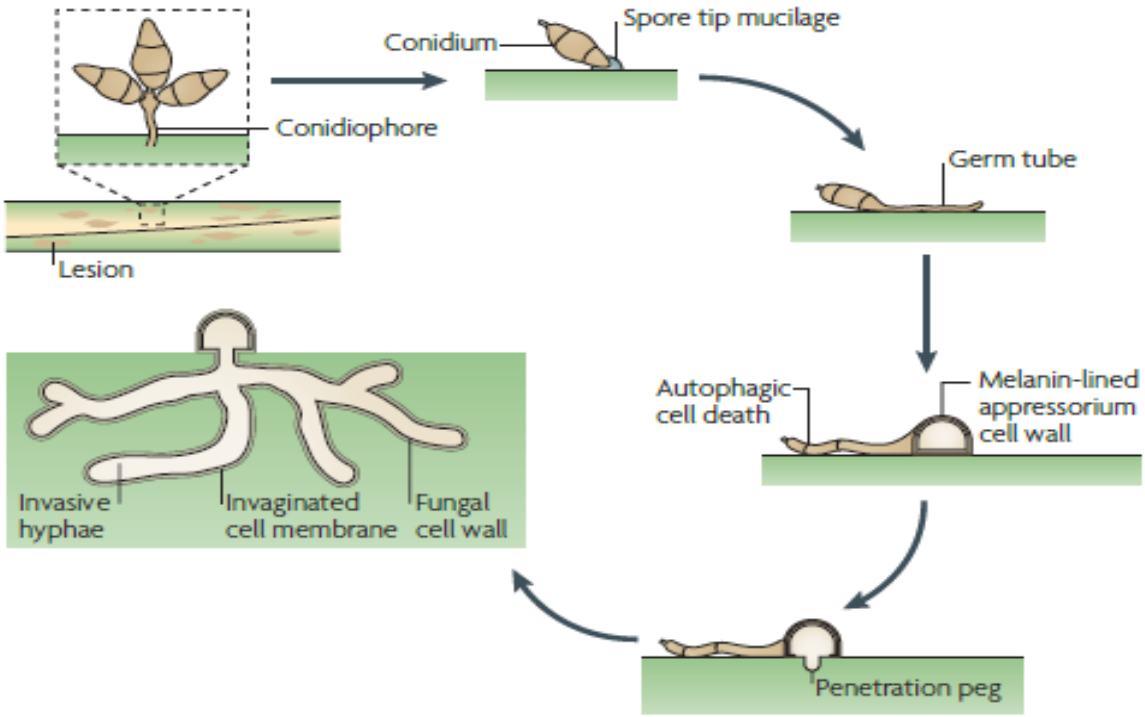


Figure 1.1 **The life cycle of *M. oryzae*.** The infection process is initiated when a spore lands on the hydrophobic surface of a rice leaf and attaches tightly to the cuticle. The spore forms a polarized germ tube, which extends before swelling at its tip, changing direction and becoming flattened against the surface. This process constitutes a recognition phase, which precedes development of a specialized infection cell, the appressorium. This dome-shaped cell generates enormous turgor pressure, which is translated into physical force at its base to rupture the rice leaf cuticle using a narrow, penetration peg that invades plant tissue. This penetration peg grows into a bulbous invasive hyphae that will move from cell to cell to colonise the host tissue. After 3 to 4 days the fungus sporulates on the surface of the leaf starting the cycle again. (Diagram taken from Wilson and Talbot, 2009)

## *1.7 Appressorium development in M. oryzae*

### 1.7.1 Cyclic AMP signalling

Appressorium formation requires a set of signalling pathways that detect and respond to the host cell surface and prevailing environment of the leaf surface. During the early stages of infection-related development, it has been demonstrated that transduction of these signals is regulated by the cyclic AMP (cAMP) response pathway (Choi and Dean, 1997). A putative adenylate cyclase known as *MAC1*, which is involved in the initiation of the cAMP pathway, is required for appressorium formation. Therefore, mutants lacking this gene are non-pathogenic (Choi and Dean, 1997).

Two other proteins, Mpg1 and Pth11, are also thought to be involved in the early events of appressorium formation, both serving a role in recognition of the host surface (Talbot et al., 1993a; DeZwaan et al., 1999). Mpg1 is a class I hydrophobin, which are a fungal-specific class of proteins (Talbot et al., 1993a; Bayry et al., 2012). Hydrophobins are secreted fungal proteins that assemble at hydrophobic-hydrophilic interfaces, such as the interface between the appressorium and the rice leaf cuticle (Bayry et al., 2012). Pth11 is an ascomycete-specific G-protein which encodes a membrane-localised receptor protein thought to be involved in detecting surface hardness and hydrophobicity (DeZwaan et al., 1999; Kulkarni et al., 2005). Appressorium formation in Δ*mpg1* and Δ*pth11* mutants was impaired. Pathogenicity of these mutants was restored with the addition of exogenous cAMP (Talbot et al., 1993a; DeZwaan et al., 1999). Exogenous cAMP was also able to rescue Δ*mac1* appressorium phenotype and pathogenicity (Talbot et al., 1993a).

### 1.7.2 MAPK signalling

Along with host surface signalling, pathogens use intracellular signals to initiate the differentiation of infection structures that are responsible for host entry (Hamel et al., 2012). There are three mitogen-activated protein kinases (MAPKs) in *M. oryzae* and all of them play a role in regulating infection-related development (Rispail et al., 2009). MAPKs work as components of signalling cascades that typically transmit a signal from the cell periphery to the nucleus of the cell to modulate gene expression (Talbot, 2003). Deletion of the *M. oryzae* MAP kinase

*PMK1* leads to non-pathogenic mutants unable to form an appressorium. Δ*pmk1* mutants are also unable to infect rice when wounded tissue is inoculated. (Xu and Hamer, 1996). Consistent with this observation, *PMK1* has been found to be responsible for cell-to-cell movement by *M. oryzae* inside the rice plant (Sakulkoo et al., 2018). Δ*pmk1* mutants are unable to generate an appressorium and therefore, it was difficult to study the function of this kinase during host colonisation. Sakulkoo and co-workers generated an analog-sensitive Pmk1 *M. oryzae* strain, *pmk1*$^{AS}$. The Pmk1 MAPK was modified by targeted mutation of the gatekeeper residue of adenosine triphosphate (ATP)-binding site into a glycine residue. The *pmk1*$^{AS}$ mutation allowed specific inhibition of Pmk1 to be carried out after initial infection and showed that the signalling pathway is necessary to cross to adjacent plant cells during intercellular growth. Interestingly, *PMK1* not only regulates cell-to-cell movement but also expression of effector genes such as *BAS1* and *BAS3* (Sakulkoo et al., 2018). Bas1 and Bas3 are effectors that translocate inside plant cells. These were found to be localised at cell wall crossing points. suggesting, Bas1 and Bas3 may be involved in modifying *M. oryzae* invasive hyphae crossing sites (Mosquera et al., 2009). Therefore, it has been proposed that the Pmk1 MAPK pathway may be necessary for hyphal constriction of *M. oryzae* invasive hyphae to move through plasmodesmata-rich pit fields and the expression of effectors that may suppress plasmodesmatal immunity (Sakulkoo et al., 2018).

### *1.8 Mechanism of M. oryzae fungal infection*

At the base of of the appressorium in direct contact with the surface of the leaf, is the appressorium pore from which the penetration peg emerges (Talbot, 2003). Initially, the appressorium pore is wall-less and lacks the thick melanin layer, and consequently the plasma membrane may be in direct contact with the surface of the leaf (Bourett and Howard, 1990). There, due to the high osmotic pressure, extreme membrane curvature develops as the rigid penetration peg is formed. Hence, penetration requires a developmental switch from isotropic growth of the appressorium to polarised, anisotropic growth of the penetration peg. This is accompanied by formation of a large F-actin network at the pore. Microscope observations showed this F-actin network as a ring at the base of the appressorium (Dagdas et al., 2012). The reorientation of F-actin is mediated by septin GTPases that provide rigidity to cell cortex to form the penetration peg.

The process is regulated by NADPH oxidases (Nox), because when antioxidants are applied, the F-actin network and ring formation around the pore is impaired (Ryder et al., 2013). Consequently, a hetero-oligomeric septin complex accumulates at the appressorium pore as a ring and act as a diffusion barrier for proteins such as the BAR domain proteins that are thought to be implicated in the process of membrane curvature to form the penetration peg (Dagdas et al., 2012).

Brown and Harvey in 1927 performed the famous 'gold leaf experiment', demonstrating that pathogenic fungi can break the plant cuticle only using force generated by appressorium turgor pressure. The 'gold leaf experiment' consisted of covering a rice leaf with a gold layer, which cannot be degraded by enzymes, and then inoculating with fungal spores. A few days later, when the gold layer was removed there were lesions on leaf indicating that appressoria can penetrate the host plant without using degrading enzymes (Talbot, 2019). Consistent with this, *M. oryzae* can penetrate plastic surfaces

### *1.9 Host plant colonisation by M. oryzae*

*M. oryzae* is a hemibiotrophic fungus that colonises living cell plant tissue before switching into a necrotrophic growth at the end of its life cycle (Koga et al., 2004; Kankanala et al., 2007).

During the biotrophic stage of infection, the primary hypha develops into a bulbous hypha that will branch and move from cell to cell (Kankanala et al., 2007). Interestingly, when the rice blast fungus enters the host and transitions into a bulbous invasive hypha, the fungus is bound to the rice cell plasma membrane (Mentlak et al., 2012). The rice plasma membrane wraps around the rice blast fungus and this membrane integrity is maintained as the fungus moves from cell to cell (Mentlak et al., 2012). The interface between the rice plasma membrane and the fungal cell wall is called the extra-invasive hyphal matrix (EIHMx) and to differentiate the plasma membrane of rice that forms a separate compartment around *M. oryzae* invasive hyphae, this has been named the extra-invasive hyphal membrane (EIHM) (Figure 1.3) (Khang et al., 2010). *M. oryzae* invasive hyphae and the EIHM form a sealed compartment, as it has been shown that the lipophilic styryl dye FM4-64 can stain the EIHM but not the *M. oryzae* invasive hyphae (Kankanala et al., 2007). It has also been proposed that the EIHM might

have a specific composition that is distinct from the rest of the rice plasma membrane (Kankanala et al., 2007).

*M. oryzae* is able to grow rapidly within living plant tissue because of the secretion of effectors. Effectors are pathogen molecules that are able to modify host cell structure, signalling, and metabolism, but which are best known as suppressors of host immunity (Giraldo and Valent, 2013). Effectors enable the rice blast fungus host colonisation by suppressing host immune responses, thereby facilitating fungal proliferation. These fungal proteins often interfere with immune signal pathways, either those required for host invasion or those that trigger host resistance (Khang et al., 2010; Giraldo et al., 2013). A broad classification of *M. oryzae* effectors has been made according to where they localise during host colonisation (Figure 1.3). Apoplastic effectors localise in the gap between the fungal cell wall and the extra-invasive hyphal membrane (EIHM) (Khang et al., 2010). These have suggested to have a role in suppressing apoplastic immune responses from the plant (Zhang and Xu, 2014). Cytoplasmic effectors, by contrast, accumulate at the biotrophic interfacial complex (BIC) (Khang et al., 2010; Giraldo et al., 2013). The BIC structure is thought to be involved in the translocation of effectors into the rice cytoplasm, where effectors have their targets (Zhang and Xu, 2014). The BIC is a plant membrane structure outside the fungal cell wall, and laser confocal microscopy demonstrates an accumulation of a rice plasma membrane marker, LTi6B, at the BIC (Mentlak et al., 2012). Fluorescence recovery after photobleaching (FRAP) experiments demonstrate that effectors are secreted into the BIC as the invasive hyphae grows and differentiates into bulbous hyphae, suggesting that the BIC is an active site of secretion, which is contradictory to our normal understanding that fungal secretion mechanisms normally occur at the hyphal tips of the growing fungus (Khang et al., 2010; Giraldo et al., 2013). As the fungus grows and differentiates inside the plant, the BIC localises adjacent to the first bulbous invasive hyphae for every plant cell invaded (Giraldo et al., 2013) (Figure 1.3).

Additionally, the rice blast fungus uses secondary metabolites to help colonize the plant and the ABC (ATP-binding cassette) superfamily of membrane transporters to remove toxic compounds from the host (Urban et al., 1999). The Abc3 transporter (Ebbole, 2007). The *ABC3* gene was identified as being induced during appressorium formation (Dean et al., 2005). The ∆*abc3* mutant was non

pathogenic in spite of being able to form an appressorium *in vitro* (Sun et al., 2006). The Abc3 transporter protein was localised to the plasma membrane of the early appressorium and once maturation happens it becomes vacuolar in its localisation (Sun et al., 2006). Furthermore, deletion mutants of another Abc transporter in *M. oryzae*, Abc1, die soon after penetration. It is thought that Abc1 acts as an efflux pump to make the rice blast fungus more resistant to toxic defence compounds generated by the plant (Urban et al., 1999).

Other proteins involved in colonisation of the host include members of the amino phospholipid translocase family, Pde1 and Apt2, which affect Golgi and secretory vesicle function (Balhadere and Talbot, 2001; Gilbert et al., 2006). Pde1 mutants have a penetration and pathogenicity defect, which suggests that amino phospholipid translocases play a role during the growth of penetration hyphae. *PDE1* is expressed in germinating conidia and the developing appressorium (Balhadere and Talbot, 2001). *APT2* is not important during hyphae development and germination. Nonetheless, Δ*apt2* mutants were affected in the secretion of extracellular enzymes that suggests that *APT2* plays a role in exocytic pathways during infection. *APT2* is required for both foliar and root infections (Gilbert et al., 2006). The *M. oryzae* zinc finger transcription factor *MoCRZ1* has been shown to regulate various virulence factors, such as *Pde1* and *Apt2* as shown by microarray expression studies and chromatin immunoprecipitation. *Mocrz1* mutants are defective in post appressorium penetration and establishment of biotrophic growth. Interestingly, *MoCRZ1* also regulates genes involved in vesicle-mediated secretion including the rhomboid family membrane protein, Sso1/2 type SNARE protein, homocysteine S-methyltransferase, Golgi apyrase, and a protein required for assembly of ER-to-Golgi SNARE complex. As a result, it has been suggested that *MoCRZ1* could be involved in regulation of effector secretion, although this has not been directly tested (Kim et al., 2010).

Movement of the rice blast fungus from cell to cell does not appear to be a random movement but more likely the hyphae going to specific sites (Khang et al., 2010; Giraldo et al., 2013). As mentioned above, the rice blast fungus moves by pit field sites that contain plasmodesmata. *M. oryzae* invasive hyphae narrows to 0–1 - 0.2 microns to go through those pit fields and get to the next cell (Kankanala et al., 2007; Sakulkoo et al., 2018). This extreme hyphal constriction that *M. oryzae* undergoes is mediated by the MAP kinase, Pmk1 (Sakulkoo et al., 2018).

On the other side of the infection, the plant immune responses fight pathogen colonisation. These are regulated by specific transcription factors such as NAC, ZN-finger, MYB, Bzip and WRKY, which regulate defence gene expression (Azizi et al., 2015). Plants also use membrane receptors such as CEBiP (chitin elicitor-binding protein) and immunity-associated plant hormones to trigger plant immune defences (Mentlak et al., 2012; Li et al., 2019). The salicylic acid (SA) and ethylene/jasmonate acid (ET/JA) mediated signalling pathways have been the most studied in model plant *A. thaliana*. SA- mediated defence response is thought to act against biotrophic pathogens, whereas ET/JA- immune response acts against necrotrophic pathogens (Li et al., 2019). However, recent findings demonstrate that Abm converts JA from the plant into hydroxylated JA (12OH-JA). 12OH-JA prevents the induction of plant immune responses enabling pathogen colonisation (Patkar et al., 2015). *M. oryzae* ∆abm mutants are able to penetrate and grow inside the first rice cell but are unable to colonise the plant. Interestingly, GFP localisation of Abm reveals it is at the cortical ER inside the fungus and secreted into the BIC. During host colonisation Amb colocalises with cytoplasmic effector Pwl2 inside the BIC suggesting that Abm might be an enzyme acting as a chemical effector (Patkar et al., 2015).

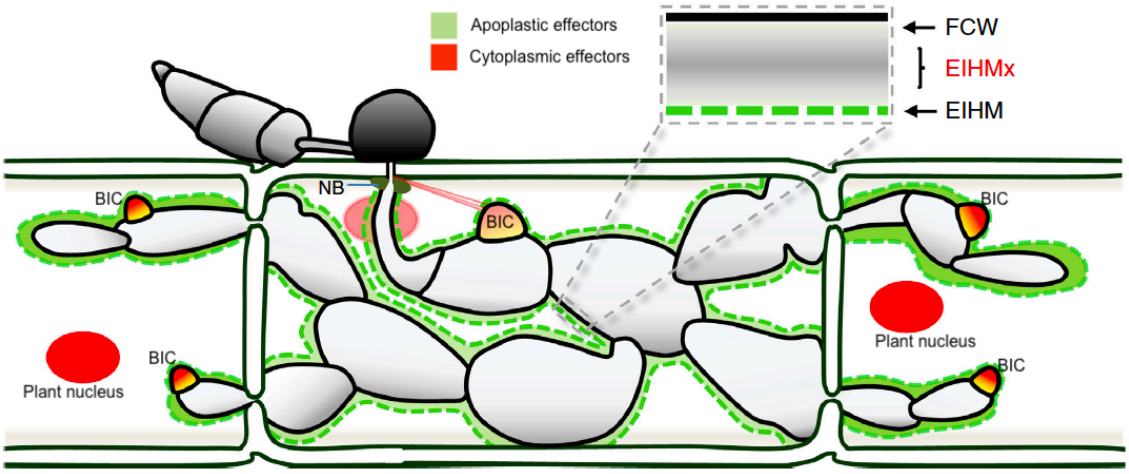


Figure 1.2 **Effector localisation during *M. oryzae* infection in the rice cell**. Schematic diagram showing effector localisation during *M. oryzae* during host cell colonisation. Cytoplasmic effectors are indicated in red, these preferably accumulate at the BIC and when fused to a nuclear signal in the plant nucleus. Apoplastic effectors are indicated in green, these preferably accumulate in the apoplastic space between the fungal cell wall (FCW) and the extra-invasive membrane (EIHM). The BIC is always represented in the first invasive hyphae. Adapted from Oliveira-Garcia and Valent, 2015.

## *1.10 Definition of effectors*

### 1.10.1 Classification of different classes of effector protein in the rice blast fungus

Effector proteins have been broadly classified as being either cytoplasmic or apoplastic according to where they localise during *M. oryzae* host colonisation.

Apoplastic effectors accumulate in the EIHMx that surrounds the fungus, and examples in *M. oryzae* include Slp1 and Bas4 (Mosquera et al., 2009; Khang et al., 2010; Mentlak et al., 2012). The apoplastic effector Slp1 is the only *M. oryzae* effector which has so far been functionally characterised. Slp1 is a LysM domain protein and binds chitin oligosaccharides competing with the chitin elicitor binding protein CEBiP to suppress the chitin-induced immunity in rice, including responses such as generation of ROS and expression of defence-related genes. Furthermore, ∆slp1 has reduced pathogenicity, indicating its suppression of PTI is sufficient to allow successful colonisation from the rice blast fungus (Mentlak et al., 2012). The function of Bas4 is unknown but it has been used to label the EIHM when it is fused to a fluorescent protein (Mosquera et al., 2009; Giraldo and Valent, 2013).

Effectors that localise at the BIC are cytoplasmic effectors, examples of which in *M. oryzae* include Pwl2 and AvrPita. Pwl2 is a host specificity determinant for *Eragrostis curvula* (weeping lovegrass). The gene was originally identified by genetic analysis which showed that the ability to infect weeping lovegrass was conditioned by a single gene, named *PWL2*. Strains of *M. oryzae* that possess Pwl2, such as many rice pathogenic strains, are unable to infect weeping lovegrass, whereas weeping lovegrass-infecting strains of the fungus do not possess Pwl2, or have a mutant allele. The function of Pwl2 is unknown, but it appears to interact with proteins associated with host immunity during infection (Kang et al., 1995; Sweigard et al., 1995) (Vincent Were and N. J Talbot, unpublished). AvrPita encodes a putative neutral zinc metalloprotease (Orbach et al., 2000). Interestingly, the promoter and signal peptide gene sequences of *AVRPITA* have been reported to be sufficient for BIC secretion (Khang et al., 2010).

The cytoplasmic delivery of effectors in *M. oryzae* has been investigated using live cell imaging to try to visualise effector localisation and movement in to plant

cells. By adding a nuclear localization signal (NLS) to the Pwl2 sequence and expressing this in *M. oryzae*, it has been shown that Pwl2, for example, is secreted into plant cells and that the Pwl2-NLS protein accumulates in the rice nucleus (Khang et al., 2010). Moreover, it was also observed that Pwl2 was able to move to adjacent cells before they were infected by the fungus, accumulating in their nuclei (Khang et al., 2010). It has been proposed that Pwl2 somehow prepares the cell for fungal invasion, together with Bas1 another cytoplasmic effector, which behaves in the same manner, perhaps by suppressing immunity responses ahead of cell invasion. The movement between cells may be dependent on the type of rice cell and effector protein size (Giraldo and Valent, 2013; Zhang and Xu, 2014). Cytoplasmic effectors universally appear to localise to the BIC during cell colonisation (Giraldo and Valent, 2013).

### 1.10.2 Identification of effectors in *M. oryzae*

There are known to be more than 200 effector-encoding genes in *M. oryzae* (Chen et al., 2013). There are therefore highly redundant sets of effector-encoding genes. A relatively small number of cytoplasmic effectors has, however been characterised to date, with around 40 Avr genes identified in *M. oryzae* so far (Zhang and Xu, 2014). The most well identified and characterised effectors in the rice blast fungus are Slp1, Bas1, Bas2, Bas3, Bas4, AvrPita, AvrCO39, Pwl1, Pwl2, Ace1, AvrPizt, AvrPia, AvrPii and AvrPik/km/kp (Valent and Chumley, 1991; Kang et al., 1995; Sweigard et al., 1995; Peyyala and Farman, 2006; Fudal et al., 2007; Mosquera et al., 2009; Yoshida et al., 2009; Mentlak et al., 2012). All of them are expressed during host colonisation, with the exception of *ACE1* which has also been found to be expressed in the appressorium (Fudal et al., 2007) (Zhang and Xu, 2014).

Most effectors have been identified as infection-specific genes by transcriptome analysis or earlier differential cDNA screening approaches, coupled with the bioinformatic prediction of a signal peptide sequence suggesting that they encode secreted proteins. The signal peptide sequence predicts that they encode proteins secreted outside the rice blast fungus and therefore into plant tissue (Mosquera et al., 2009; Mentlak et al., 2012).

Re-sequencing the genome of the rice blast strain INA168 and subsequent association genetics, helped unveil three novel Avr effectors. These were AvrPia, AvrPik/Km/Kp and AvrPii (Yoshida et al., 2009).

Using map-based cloning the effector AvrPib was isolated. It is a small 75-residue protein with a signal peptide (SP), and the corresponding gene located on chromosome 3 (Zhang et al., 2015). A host-driven selection may have occurred for the AvrPib effector, because the diversity of AvrPib population is greater from the north to the south regions of China, with many *M. oryzae* isolates having lost AvrPib function, thereby gaining virulence on Pib-containing rice cultivars. It has been shown that the gain of virulence was due to mutations in the signal peptide region, to abolish transcription, of the gene and transposable element (TE) insertions (Zhang et al., 2015).

Wu et al., 2015 identified the AvrPi9 gene by comparing the genome of two similar strains, R88-002 and R01-1, and they claim their method was faster than using conventional map-based cloning. Secreted proteins with identical SP sequences from Ina168 or 70-15 strains in R88-002 and R01-1 were analysed. Only one gene, R1434, was identified as a putative AvrPi9-encoding gene candidate because it showed a clear correlation across 26 avirulent strains. Its sequence in R88-002 and R01-1 was the same, but with a Mg-SINE insertion in R01-1 strain. By means of an allele swap/genetic complementation and targeted gene replacement of R1434 it was determined that R1434 is the *AVRPi9* gene (Wu et al., 2015).

Most Avrs identified to date, do not contain any known protein domains or show similarity in DNA sequence, making identification of novel Avrs difficult. AvrPikD and AvrPiz-t show no similarity in their amino acid sequences, but with the help of a protein folding bioinformatic tool (PDBeFold) it was possible to show that their protein structures were in fact very similar (Maqbool et al., 2015). This was also the case for AvrPia, AvrCO39 and an effector from *Pyrenophora tritici-repentis*, ToxB. Consequently, this information has been used to define a new effector family, the MAX-effectors (*Magnaporthe* Avrs and ToxB like), which are thought to act during biotrophic host colonization as they are secreted during early stages of infection (de Guillen et al., 2015).

### 1.10.3 *M. oryzae* effector function

Apoplastic effectors are thought to suppress extracellular plant immune responses in the apoplastic space between the fungus and the plant plasma membrane, whereas cytoplasmic effectors might target immune responses in the cytoplasm or different organelles inside host cells (Zhang and Xu, 2014). Effectors also appear to be highly redundant because only one gene (MC69) of 78 targeted gene deletion mutants of effector-encoding genes in *M. oryzae* showed a clear pathogenicity defect (Saitoh et al., 2012; Giraldo and Valent, 2013). It is important to mention that effector functions are not only carried out by proteins but also by secondary metabolites as well, such as the *M. oryzae* Avr gene *ACE1* (Fudal et al., 2007). *ACE1* encodes an enzyme involved in the synthesis of a secondary metabolite, that may be involved with cytoskeletal reorganisation of the host (Russell Cox and Marc-Henri Lebrun, personal communication). *ACE1* encodes a putative polyketide synthase/peptide synthetase without a detectable N-terminal secretion peptide (PKS-NRPS) the product of which is likely recognized by the Pi33 protein in rice (Bohnert et al., 2004).

The apoplastic effector Slp1 is the only effector in *M. oryzae* which has been functionally characterised. Slp1 is a LysM domain protein and binds chitin oligomers, thereby competing with the chitin elicitor binding protein CEBiP to suppress chitin-induced immunity in rice, including responses such as generation of ROS and expression of defence-related genes (Mentlak et al., 2012). Slp1 is dispensable for appressorium penetration but required for invasive growth *in planta* (Mentlak et al., 2012). Its chitin binding activity depends on Slp1 N-glycosylation at the protein sites Asn-48, Asn-104 and Asn-131 via Asparagine-Linked Glycosylation3 (Alg3). Alg3 not only intervenes in the N-glycosylation of Slp1, it also serves this role for other effectors such as Bas4 (Chen et al., 2014). The function of Bas4 is still unknown but due to its localisation in outlining the invasive hyphae and at the base of the BIC, it is thought that is could serve to protect the cell wall of *M. oryzae* invasive hyphae from plant immune responses. Bas4 is one of a family of effectors, which encode low molecular weight proteins, and have been termed biotrophy-associated secreted proteins (BAS). Bas1 and Bas107, for example, are translocated to the rice cytoplasm and move from cell

to cell, Bas2 and Bas3 accumulate at cell wall crossing points, and Bas113 has homology to glycosyl hydrolases and is a BFA-sensitive apoplastic effector (Mosquera et al., 2009; Giraldo and Valent, 2013).

The biochemical functions of AvrPita and AvrPiz-t are known. AvrPita encodes a putative neutral zinc metalloprotease and the gene is very close to the telomere, indeed its stop codon is only 48bp from the start of telomeric repeat sequences (Orbach et al., 2000). The secretion and activation of AvrPita can be impaired by disruption of an ER encoding chaperone gene, LSH1 (Yi et al., 2009). AvrPiz-t is a BIC localised effector which encodes a 108-amino-acid predicted secreted protein with 4 cysteine residues and unknown function (Li et al., 2009; Park et al., 2012; Zhang et al., 2013). AvrPiz-t has been shown to interact with twelve proteins known as APIP, AvrPiz-t interacting proteins (Park et al., 2012; Park et al., 2016; Wang et al., 2016; Tang et al., 2017; Wang et al., 2017a). These are different plant proteins involved at different stages of the plant immune response. Some examples are APIP6 and APIP10, ring E3 rice ubiquitin ligases (Park et al., 2012; Park et al., 2016), APIP12 a nucleoporin domain containing protein (Tang et al., 2017) and APIP5 a bZIP-type transcription factor (Wang et al., 2016). APIP5 and AvrPiz-t interaction happens at the necrotrophic stage (Wang et al., 2016). This is the only example in *M. oryzae* of an effector with various targets inside the host.

Avr-Pii has been reported to interact with an Exo70 sub-unit of the rice exocyst, perhaps indicating a role in suppression of targeted exocytosis from the host against the invading pathogen. Gene silencing of OsExo70-F3, which encodes an Exo70 protein, had an effect on the function of the rice resistance conferred by *Pii* in its recognition of Avr-Pii. This led to the conclusion that the exocyst protein might be involved in recognition of the effector by its cognate resistance gene, as Exo70 knockdown had no effect on the function of *Pia* and *Pik*. (Fujisaki et al., 2015).

AvrPi9 is 342 bp in size and encodes a secreted protein which is localised in the BIC. The protein is 91 amino acids long including an 18 amino acid signal peptide. The AvrPi9 locus is on chromosome 7 very near to AvrPiz-t. AvrPi9 function could be recognizing plant signals in the early stages of infection as it is when the Avr was mostly expressed (Wu et al., 2015).

One of the most used effectors in *M. oryzae* to study host colonisation, Pwl2 belongs to the PWL family. The PWL family of effectors are small and glycine rich proteins. The genome sequence of *M. oryzae* 70-15 strain encodes one sequence identical to Pwl2 and two others that are similar to Pwl3. When *M. oryzae* lacks Pwl2 or Pwl1, the rice blast fungus is able to infect weeping lovegrass. Despite the fact that this one of the most cited cytoplasmic effectors in *M. oryzae,* the function of Pwl2 is still unknown (Kang et al., 1995; Sweigard et al., 1995). Pwl2 does, however, serve a role in virulence as a CRISPR mutant lacking all three copies of Pwl2 in M. oryzae strain Guy11 does show reduced virulence (Vincent Were and N.J. Talbot, unpublished)

## *1.11 The unconventional secretion pathway and translocation of effectors into rice cells*

### 1.11.1 Different secretion pathways during M. oryzae host colonisation

Recent evidence suggests that *M. oryzae* effectors that are destined for delivery either to the cytoplasm or apoplast. Brefeldin A (BFA) (Pelham, 1991; Klausner et al., 1992), is a fungal metabolite that has been demonstrated to reversibly interfere with anterograde transport from the endoplasmic reticulum to the Golgi apparatus. It can therefore be used as an inhibitor of conventional Golgi-dependent exocytosis. When BFA is applied to *M. oryzae* the secretion of apoplastic effectors, such as Slp1 and Bas4 is inhibited, whereas cytoplasmic effectors such as Pwl2 and Bas1 are unaffected by BFA treatment. Apoplastic effectors are retained inside invasive hypha after such treatment, while cytoplasmic effectors are localised at the BIC and can be observed within plant cells after BFA treatment. The secretion of *M. oryzae* cytoplasmic effectors therefore appears to involve a Golgi-independent unconventional secretion pathway (Giraldo et al., 2013). It is still a mystery how this unconventional secretion pathway works and this was one of the motivations for the current study.

Interestingly, BFA has been used to investigate secretion pathways for effectors in the oomycete late blight pathogen of potato, *P. infestans*. Cytoplasmic effectors in *P. infestans* are also secreted in a BFA-insensitive way, similar to that observed in *M. oryzae* (Giraldo et al., 2013; Wang et al., 2017b; Wang et al., 2018). This remarkable comparative observation in very un-related pathogens will be explored further in the results and discussion chapters.

### 1.11.2 Secretion components during *M. oryzae* hyphal growth

Most of our understanding of the secretion pathway in filamentous fungi has been based on studies carried out on fungi growing in axenic culture, rather than on pathogenic species growing invasively. Secretion of proteins has been extensively observed at the hyphal tip. Filamentous fungal hyphae grow at their tips and this process involves polarised exocytosis to provide new cell wall constituents and localised membrane biogenesis, by means of vesicle docking at the tips of cells (Riquelme et al., 2007; Gupta et al., 2015; Steinberg et al., 2017; Riquelme et al., 2018). Secretory vesicles are transported to hyphal tips by microtubule-based transport over long distances and short-range actin microfilaments are then necessary for them to reach the hyphal tip. The Spitzenkörper is a visible region at the hyphal tip where secretory vesicles accumulate (Steinberg et al., 2017). The spitzenkörper acts as a vesicle supply centre, from which actin-based transport occurs for secretory vesicles to reach their final destination. The spitzenkörper works together with the polarisome and the exocyst complex at fungal hyphal tip to regulate growth and protein secretion at the hyphal apex (Riquelme, 2013).

The polarisome drives F-actin to the hyphal tip where polarized growth occurs (Sheu et al., 1998). Null mutants of *SPA2* in *M. oryzae* and *U. maydis,* which encodes a component of the polarisome, show defects in hyphal growth but not in pathogenicity. This unexpected result suggests that Spa2 is involved in polarity establishment and polarised fungal growth, but does not serve an important role in fungal invasive growth within plant tissue (Carbó and Pérez-Martín, 2008); (Li et al., 2014).

The exocyst complex is composed by 8 proteins: Sec3, Sec5, Sec6, Sec8, Sc10, Sec15, Exo70 and Exo84 and is involved in secretory vesicle docking at the plasma membrane. Secreted proteins are packed into vesicles which are transported via motor proteins along microtubules to the Spitzenkörper, and then via F-actin filaments to the tip. In order to be secreted, it is necessary for these vesicles to dock with the fungal plasma membrane. For this, t-SNARE proteins together with v-SNARE proteins, are necessary for vesicle fusion to occur at the plasma membrane (Gupta et al., 2015).

In vegetative hyphae of *M. oryzae*, secretory components, such as Snc1 and Mlc1 (located at the Spitzenkörper), Spa2 (a polarisome component), Exo70 and Sec5 (exocyst components), and Sso1 (a t-SNARE) all localise to regions within the hyphal tip. However, with the exception of Spa2, all of these components localise to sub-apically situated BIC-associated cells, when invasive hyphae colonise rice epidermal cells (Giraldo et al., 2013) (Figure 1.4). The BIC-associated cell may be a modified hyphal tip as the BIC is initially at the tip of the penetration hypha, where it is first observed. However, this cell then undergoes a budding type of growth to form bulbous invasive hyphae so that the BIC becomes sub-apically situated away from the growing apex of the fungus. Controversially, this observation in *M. oryzae* provides evidence that protein secretion might not occur predominantly at the hyphal tip, as it has been mostly studied before, but also from the BIC associated cell.

To test whether exocyst components and t-SNARE proteins are involved in the Golgi-independent pathway by which cytoplasmic effectors are secreted, Giraldo and co-workers generated a series of targeted gene deletion mutants. The exocyst mutants Δ*sec5* and Δ*exo70* showed impaired secretion of the cytoplasmic effector protein Pwl2, which accumulated inside invasive hyphae as well as in the BIC. By contrast, the t-SNARE mutant Δ*sso1* produced 2 different BICs within the same hypha. Vesicle fusion to the plasma membrane is therefore necessary for BIC development, which can be organisationally disrupted when this process is impeded by lack of t-SNARE activity (Giraldo et al., 2013). Additionally, it was also shown that F-actin and microtubules are essential for vesicle trafficking of apoplastic effector proteins to the hyphal tip, but play a less obvious role in delivery of cytoplasmic effectors into the BIC. Treatment with latranculin A (Lat A), an actin polymerisation inhibitor, and a microtubule polymerisation inhibitor methyl 1-(butylcarbamoyl)-2-benzimidazolecarbamate (MBC) resulted in Bas4, an apoplastic effector, showing impaired secretion, but did not seem to adversely affect the delivery of Pwl2 into the BIC (Giraldo et al., 2013).

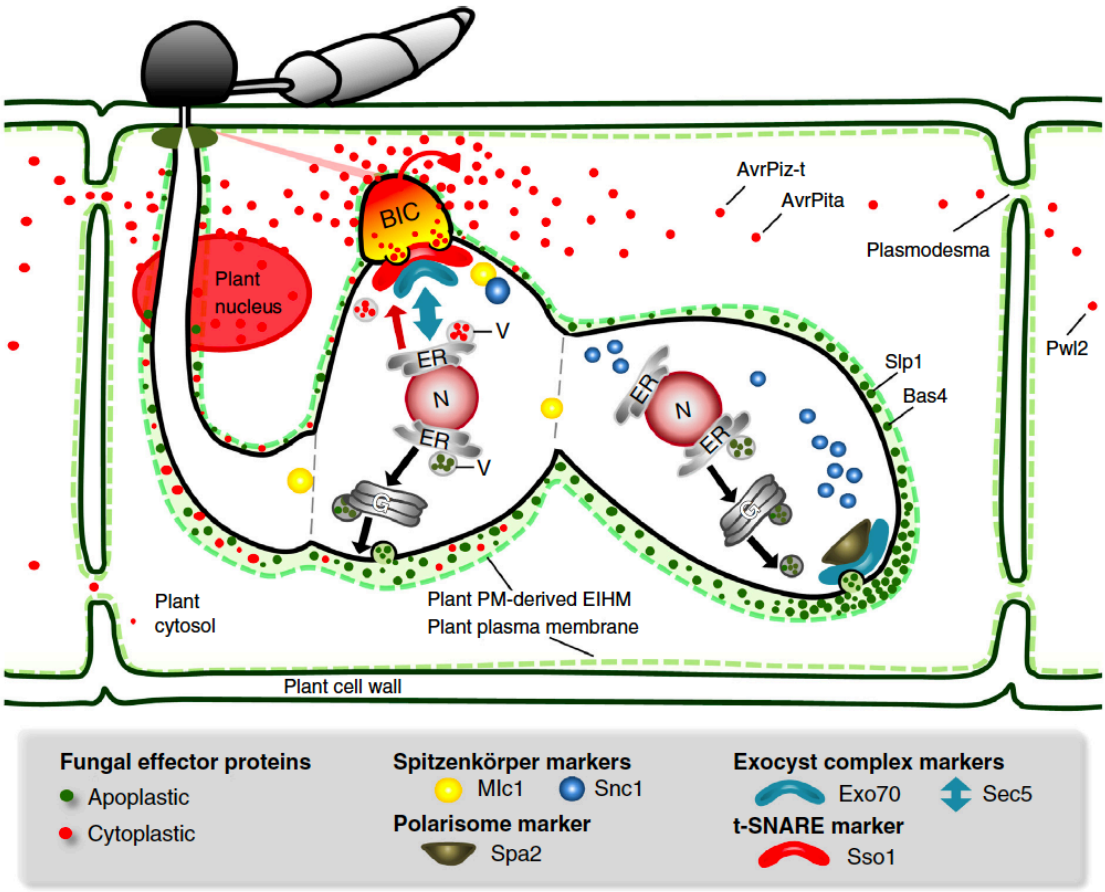


Figure 1.3 **Effector secretion during *M. oryzae* infection in the rice cell**. Schematic diagram showing effector localisation and proposed secretion pathways in *M. oryzae* during host cell colonisation. Taken from Oliveira-Garcia and Valent, 2015.

### 1.11.3 The translocation of effector proteins into plant cells

One of the most well characterised effector secretion systems is the type III secretion system (TTSS) that many gram-negative bacterial pathogens use to deliver effector into host cells. This is one of more than 9 specialised secretion sytems deployed by bacteria for protein secretion (Christie, 2019). The TTSS forms a needle-like structure that punctures the host delivering effector molecules from the bacteria and allowing protein to be delivered directly into the host cytoplasm (Alfano and Collmer, 2004). In fungi, a translocation motif has been found in only four effectors. However, none of these motifs are similar in the sequence or in structural properties (Petre and Kamoun, 2014) (see Chapter 5 for further details). A RALG translocation motif has been found necessary for symbiosis in *Laccaria bicolor* effector (Plett et al., 2011). In oomycetes, cytoplasmic effectors have been found to possess a conserved RXLR and LXFLAK translocation motifs (Schornack et al., 2010). The RXLR motif that was found to be necessary for entry into plant cells, but not for targeting the effector to the haustorium or for secretion (Whisson et al., 2007; Stam et al., 2013).

Although it appears that the RXLR motif is essential for translocation of effector proteins in oomycetes, the translocation mechanism has not been fully characterised (Ellis and Dodds, 2011). Kale and co-workers proposed that Avr1b from *P. sojae* interacted with phosphatidylinositol-3-phosphates (PIPs) in the plasma membrane mediated by the RXLR motif. They argued that this would allow the effector to bind to and traverse the plasma membrane (Kale et al., 2010). However, this observation has been challenging to reproduce and has therefore remained controversial. Yaeno and co-workers reported that whereas Avr3a from *P. infestans* could also bind to PIPs, it was able to do so without the RXLR sequence (Yaeno et al., 2011). This is also supported by the finding of an RXLR motif in an effector of an animal pathogenic oomycete *Saprolegnia parasitica*, SpHtp3 (Trusch et al., 2018). SpHtp3 enters the host in a pathogen-independent manner (Trusch et al., 2018). Various research groups have also carried out two main experiments to observe and demonstrate whether effector translocation could take place independent from the pathogen, based on the PIP interaction model (Tyler et al., 2013). Transient expression, which consists of bombardment or agroinfiltration of effectors with their complete sequence and signal peptide has been carried out to observe if cell re-entry was possible. A cell

root uptake assay, in which roots are submerged in a solution with the effector and uptake of the effector measured, has, however, been very difficult to reproduce (Petre and Kamoun, 2014). It has also been proposed that RXLR motif is proteolytically cleaved before secretion (Goldberg and Cowman, 2010; Marti and Spielmann, 2013; Wawra et al., 2013; Boddey et al., 2016; Wawra et al., 2017; Wang et al., 2018). This is similar to the mechanism proposed for the malaria parasite translocation motif, PEXEL motif, that strongly resembles RXLR (Goldberg and Cowman, 2010). The mechanism by which RXLR effectors cross the plant cell membrane is therefore still unknown.

In *M. oryzae* the mechanism that effectors use to enter the plant cell are unknown (Ribot et al., 2013). The fact that translocation motifs are not obvious in effector sequences also makes it difficult to classify *M. oryzae* effectors based on their amino acid sequence (Zhang and Xu, 2014). Unlike other pathogens, however, in *M. oryzae* it has been possible to use the fungus and host to visualise effector secretion. Microscopy techniques to visualise effector translocation inside the host in *M. oryzae* are discussed in detail in Chapter 5. Khang and co-workers have shown that without a signal peptide the promoter region of cytoplasmic effector genes is sufficient to drive expression of the effector, but with the signal peptide present, effectors localise predominantly at the BIC (Khang et al., 2010). This provides evidence that both the promoter and signal peptide sequences of cytoplasmic effectors are involved in secretion to the BIC. The main objective of the study described in this thesis is to understand the process of effector secretion by *M. oryzae*.

### *1.12 Introduction to the current study*

In this study, I set out to investigate the interaction between *M. oryzae* and the rice plant and, in particular, the biology of effector secretion during plant infection. The rapid colonisation of the rice plant by *M. oryzae* occurs because effector proteins are so efficient in suppressing plant immune responses. Little is known, however, regarding how the fungus secretes effectors into the plant. Previous work before this study had defined two different secretion mechanisms that may operate for delivery of cytoplasmic and apoplastic effectors, respectively (Giraldo et al., 2013). However, the nature of the unconventional secretion mechanism for cytoplasmic effectors in *M. oryzae* is not yet known. Previous research also suggested that the promoter and signal peptide region of a *M. oryzae* effector

gene was sufficient to secrete a fluorescent protein into the correct secretion domain– either the BIC or apoplast (Khang et al., 2010).

Here, I report an analysis of the roles of the promoter and signal peptide regions of both apoplastic and cytoplasmic effector-encoding genes. In this thesis, I present results of a study in which I constructed a series of chimeric gene fusion constructs and expressed them in *M. oryzae*. I then used live cell imaging to investigate the localisation of fluorescent proteins when the rice blast fungus is growing inside the plant. In this way I was able to define the relative importance and contribution of the promoter and signal peptide sequences of each effector class to the secretion and delivery of them into host tissue, during plant infection.

In Chapter 3, I present an analysis of the promoter and signal peptide regions of cytoplasmic effectors expressed as a translational fusion to a GFP reporter. In this series of studies, I observed that when the promoter and signal peptide regions were both present in a chimera, the GFP reporter was delivered to the BIC. When only the promoter was used to drive expression of the GFP marker, fluorescence stayed inside invasive hyphae of *M. oryzae*, confirming the requirement of a signal peptide for secretion. I then used the promoter and signal peptide regions from a group of cytoplasmic effectors to drive expression of apoplastic effectors in order to observe whether they were sufficient to drive the effector into the alternative secretory pathway, thereby sending them to the BIC and into plant cells. I was able to observe apoplastic effectors being delivered to the BIC in these experiments, suggesting that the promoter and signal peptide regions are pivotal to the correct secretory route of M. oryzae effectors. The conclusions from these results and the limitations of the experimental observations are described in Chapter 3.

In Chapter 4, I describe the reciprocal set of experiments in which I used the promoter and signal peptide regions from apoplastic effectors to drive expression and secretion of cytoplasmic effector proteins fused to GFP. These experiments showed that the promoter and signal peptide regions of apoplastic effectors are important for the apoplastic localisation of effectors. When the promoter and signal peptide regions of apoplastic effectors were fused to cytoplasmic effector genes, these were observed to adopt an apoplastic localisation. Furthermore, I present evidence that it is the promoter-signal peptide combination that is

important, and not simply the signal peptide sequence for this secretory mechanism.

In Chapter 5, I report an investigation into the nature of the secretion mechanism and the delivery of effectors into plant cells. In these experiments, I used the secretion pathway inhibitor drug BFA to confirm whether the two different secretory localisation patterns I observed– apoplastic or BIC-localised –were the result of alternative BFA-sensitive and BFA-insensitive secretion pathways. These experiments showed that when the promoter and signal peptide regions of a cytoplasmic effector were used to drive an apoplastic effector, the secretion becomes BFA insensitive, whereas apoplastic delivery was always BFA-sensitive. Therefore, these regions of each class of effector gene do appear to be necessary to re-direct an apoplastic effector into the unconventional secretion pathway. I then used plasmolysis assay was used to visualise the internalisation of effector proteins inside host cells. I also used transgenic rice plants with a GFP-tagged plant plasma membrane marker, so that membrane dynamics could be visualised during rice infection and effector delivery. These experiments provide evidence that the promoter and signal peptide region of a cytoplasmic effector are able to re-direct an apoplastic effector protein, or even a non-effector protein, into host cells. This suggests that the mechanism of effector uptake is probably independent of the effector protein itself and perhaps controlled instead from the 5'end of the effector transcript, either at the DNA or, more probably, the mRNA level.

In Chapter 6, these ideas are discussed in detail, both summarising and discussing all of the experimental results achieved from each part of the study, relating these to what is known in other pathogen-host interactions, and then identifying experimental strategies by which the secretory mechanism and plant cell uptake mechanism can be explored in future.

# Chapter 2. Materials and Methods

## *2.1 Growth and maintenance of fungal stocks*

All *Magnaporthe oryzae* strains used in this study are stored in the laboratory of N. J. Talbot (The Sainsbury Laboratory). For long-term storage, *M. oryzae* strains were grown through filter paper discs (3 mm, Whatman International), which were desiccated for at least 48 h and stored at -20ºC. The fungal strains were grown in solid complete medium (CM) and incubated in a controlled temperature room at 24ºC with a 12 h light and dark cycle. Complete medium consist of 10 g $l^{-1}$ glucose, 2 g $l^{-1}$ peptone, 1 g $l^{-1}$ yeast extract (BD Biosciences), 1 g $l^{-1}$ casamino acids, 0.1% (v/v) trace elements (zinc sulphate heptahydrate 22 mg $l^{-1}$, boric acid 11 mg $l^{-1}$, manganese(II) chloride tetrahydrate 5 mg $l^{-1}$, iron sulphate heptahydrate 5 mg $l^{-1}$, cobalt chloride hexahydrate 1.7 mg $l^{-1}$, copper sulphate pentahydrate 1.6 mg $l^{-1}$, sodium molybdate dehydrate 1.5 mg $l^{-1}$, ethylenediaminetetraacetic acid 50 mg $l^{-1}$), 0.1% (v/v) vitamin supplement (0.1 g $l^{-1}$ biotin, 0.1 g $l^{-1}$ pyridoxine, 0.1 g $l^{-1}$ thiamine, 0.1 g $l^{-1}$ riboflavin, 0.1 g $l^{-1}$ p-aminobenzoic acid, 0.1 g $l^{-1}$ nicotinic acid), nitrate salts (sodium nitrate 6 g $l^{-1}$, potassium chloride 0.5 g $l^{-1}$, magnesium sulphate heptahydrate 0.5 g $l^{-1}$, and potassium dihydrogen phosphate 1.5 g $l^{-1}$) to adjust the pH to 6.5. For solid medium, 15 g $l^{-1}$ agar was added to the medium. All chemicals were obtained from Sigma (Poole, Dorset), unless otherwise stated.

## *2.2 Nucleic acid analysis*

### 2.2.1 CTAB genomic DNA Extraction

Wild type and mutant strains of *M. oryzae* were grown in CM plate culture on a cellophane membrane. When it had covered the membrane, the cellophane was removed, wrapped in foil, snap frozen and stored at -80ºC.

The sample was placed in a mortar containing liquid nitrogen and ground until the sample was a very fine powder. The powder was then transferred to a 1.5 ml Eppendorf until about two thirds full. To this, 500 µl CTAB buffer was added (pre-warmed) (CTAB: 10g CTAB (hexadecyltrimethylammonium bromide) (2%); 6,06g TRIS BASE (100mM); 1,46g EDTA (10mM); 20,5g NaCl (0.7M); up to 500ml $dH_2O$), mixed well and incubated at 65ºC for 30 min. During this time, the tubes

were shaken every 10 min. In the fume cupboard, 500 µl CIA mix (24 Chloroform:1 Isoamylalcohol) was added to each tube. The tubes were shaken for 30 min, followed by centrifugation at 17,000 x *g* for 20 min using an Eppendorf 5415D Centrifuge. The top aqueous phase was transferred to a new 1.5 ml Eppendorf tube and 500 µl CIA added. The tubes were shaken for 5 min and a centrifugation process at 17,000 x *g* for 10 min. The CTAB and CIA solutions precipitate other cellular components to purify the DNA from the cell tissue. The top aqueous phase was removed to a new 1.5 ml Eppendorf tube and 1 ml of chilled Isopropanol was added, then mixed and incubated on ice for 5 min (or overnight) in order to allow the DNA to precipitate.

The tubes were processed by centrifugation at 17,000 x *g* for 10 min, then inverted on a paper towel and allowed to dry for 5 min. The pellet was resuspended in 500 µl sterile water and mixed by gently tapping the tube. When the pellet was no longer visible, one tenth of the volume was added (50 µl) of 3M NaOAc (pH 5.2) and two volumes (1 ml) of ice-cold 100% ethanol. The tubes were incubated at -20ºC for 10 min and then were subjected to centrifugation at 17,000 x *g* for 20 min. The supernatant was decanted and 400 µl of ice-cold 70% ethanol was added. The tubes were subjected to centrifugation at 17,000 x *g* for 5 min. The pellet was resuspended in 48 µl mili-Q (mQ) water and 2 µl RNase (10mg/ml), to remove RNA. The tubes were incubated at room temperature for 20 min. Genomic DNA was stored at -20ºC for further analyses.

### 2.2.2 Restriction Enzyme Digestion

Plasmid DNA and genomic DNA (gDNA), extracted with Midi prep kit or CTAB, were further analysed by digestion with restriction endonucleases. Plasmid DNA extraction was done to confirm it was the right construct, the sequence of the generated plasmid was known and so, the pattern of the resulted fragments can be predicted. The gDNA digestion with enzymes were used for southern blot protocol. The resulting fragments generated by digestion of the plasmid DNA or gDNA from different samples extracted, was checked by agarose gel electrophoresis. The mixture for the plasmid digestion was as follows: 1µl pDNA, 2µl buffer, 1µl restriction enzyme and 16µl mQ water. A negative control with the vector used as backbone was set for every enzyme used in the analysis. The

mixture for the genomic DNA digestion was routinely: 30ng of gDNA, 5 µl buffer, 1 µl restriction enzyme and up to 50 µl of mQ water. Digestion for plasmid DNA occurred at 37ºC for 2 h and overnight for gDNA.

### 2.2.3 Agarose Gel electrophoresis

For a middle size gel tray, 1.5 g of agarose was weighted in a 250 ml flask and 150 ml 1 x Tris- borate EDTA (TBE) buffer (0.09 M Tris- borate, 2 mM EDTA) poured and the solution melted. A 3 µl aliquot of a stock solution of Ethidium Bromide (0.5 µg $ml^{-1}$) were added to the tray and the agarose gel was poured in the tray with a gel comb. The gel was left to set and placed in an electrophoresis tank. Samples were loaded along with a 1 kb plus size ladder (Invitrogen) using 6x loading buffer (30% (v/v) glycerol, 0.25% (w/v) bromophenol blue and 0.25% (w/v) xylene cyanol FF). The DNA was visualized under a UV light transilluminator (image Master VDS) with a Fuji Thermal Imaging System, FTI-500 (Pharmacia Biotech).

### 2.2.4 Polymerase chain reaction (PCR)

DNA fragments were amplified using the Polymerase Chain Reaction with an Applied Biosystems GeneAmp® PCR System 2400 cycler using either GoTaq® Flexi DNA Polymerase (Promega), GoTaq® Green Master Mix (Promega), Phusion® high fidelity DNA Polymerase (New England Biolabs, Thermo Scientific®), Q5® High-Fidelity DNA Polymerase (New England Biolabs) or SapphireAmp® Fast PCR Master Mix for quick PCR (Takara), according to manufacturer's instructions.

For GoTaq® Flexi Polymerase reactions, 50-100 ng of template DNA was used for amplification, along with the GoTaq Flexi DNA Polymerase buffer (5 x), 10 nM $MgCl_2$, 100 nM each dNTP, 0.25 pM of each primer, 2 units of GoTaq® Flexi DNA Polymerase, made up to a final volume of 50 µl using sterile water (Sigma). The PCR was routinely carried out according to the following conditions: an initial denaturation step at 94°C for 5 min followed by 35 cycles of PCR cycling parameters of: denaturation at 94°C for 30 sec, annealing at 56-64°C for 30 sec

and extension 72°C for 1 min/kb target length, followed by a final extension at 72°C for 10 min and hold at 4°C.

For Phusion® high fidelity DNA Polymerase (New England Biolabs, Thermo Scientific®) reaction used for gene cloning experiments. In 50 µl reaction final reaction, 10 µl 5 x Phusion HF buffer, 200 µM dNTPs, 0.5 µM of each primer, 100-200 ng template DNA and 1 units of Phusion DNA polymerase was added in a microcentrifuge tube. PCR condition for Phusion® high fidelity DNA Polymerase (New England Biolabs, Thermo Scientific®) were: initial denaturation step at 98°C for 30 sec followed by 35 cycles of PCR cycling parameters of: denaturation at 98°C for 10 sec, annealing 58°C for 30 sec and extension 72°C for 30 sec/kb target length, followed by a final extension at 72°C for 10 min and hold at 4°C.

For Q5® High-Fidelity DNA Polymerase (New England Biolabs) when was also used in gene cloning experiments. A 50µl reaction final reaction, 10 µl 5 x Phusion HF buffer, 200 µM dNTPs, 0.5 µM of each primer, 100-200 ng template DNA and 1 unit of Q5® High-Fidelity DNA Polymerase was prepared in a microcentrifuge tube. PCR condition for Q5® High-Fidelity DNA Polymerase (New England Biolabs, Thermo Scientific®) was: initial denaturation step at 98°C for 30 sec followed by 35 cycles of PCR cycling parameters of: denaturation at 98°C for 10 sec, annealing 58°C for 30 sec and extension 72°C for 30 sec/kb target length, followed by a final extension at 72°C for 10 min and hold at 4°C.

SapphireAmp® Fast PCR Master Mix for quick PCR (Takara) was used to check for positive bacterial transformation, also referred to as colony PCR. In 25µl reaction final reaction, 12.5 µl 5 x SapphireAmp Fast PCR Master Mix (2X Premix), 0.5 µM of each primer, a single bacterial colony was added in a microcentrifuge tube. PCR condition for SapphireAmp® Fast PCR Master Mix for quick PCR (Takara) was: initial denaturation step at 94°C for 60 sec followed by 30 cycles of PCR cycling parameters of: denaturation at 98°C for 5 sec, annealing 55°C for 5 sec and extension 72°C for 1 min, followed by a final extension at 72°C for 7 min and hold at 4°C. Colony PCR was performed with the list of plasmids shown in Table 2.1.

Table 2.1 Primers used for the In-Fusion cloning and colony PCR

| Name of primer | Sequence of primer (5'-3') |
|---|---|
| BASTA_3 | GCAGGCATGCAAGCTGTCGACAGAAGATGATATTGAAG |
| BASTA_4 | GTCGACCTAAATCTCGGTGAC |
| GFP_1 | ATGGTGAGCAAGGGCGAG |
| TrC_1 | TGATTACGCCAAGCTAGTGGAGATGTGGAGTGG |
| Bar_p3_r | GTTATCGTGCACCAAGCAGCAGAT |
| natR-f | ATGTCACGCTTACATTCACGCCCT |

### 2.2.5 Gel purification of DNA fragments

DNA fragments were purified using a commercial kit, Wizard® SV Gel and PCR Clean-Up System kit (Promega). The DNA fragment was removed and placed in an Eppendorf tube. Membrane Binding Solution (4.5 M guanidine isothiocyanate, 0.5M potassium acetate, pH 5.0) was added to the tube (10 µl per 10 mg of gel slice), which was then incubated at 50-60ºC until the gel slice was completely dissolved. An SV Minicolumn was then inserted into the Collection Tube and the mixture incubated at room temperature for 1 min before it was subjected to centrifugation at 17,000 x *g* for 1 min.

The flow-through was discarded and 700 µl of membrane Wash Solution (potassium acetate, 10 mM (pH 5.0), ethanol, 80%, ethylenediaminetetraacetic acid, 16.7 µM (pH 8.0)) and subjected to centrifugation for 1 min at 17,000 x *g*, the flow-through was discarded. On the second wash, 500 µl of Membrane Wash Solution with ethanol were added and processed by centrifugation at 17,000 x *g* for 5 min. In order to make sure the ethanol evaporated the Collection Tube was emptied and the column was subjected to centrifugation at 17,000 x *g* for 1 min.

The last step consisted of eluting DNA with water. The Minicolumn was transferred to a clean 1.5 ml Eppendorf and 30 µl of mQ water were added and then DNA was recovered by centrifugation at 17,000 x *g* for 1 min. The Minicolumn was discarded and DNA stored at -20ºC. The DNA was quantified with a NanoDrop Spectrophotometer ND-1000.

## *2.3 DNA cloning*

### 2.3.1 In-Fusion Cloning Procedure for Spin-Column Purified PCR Fragments (Clontech)

This method was used to ligate previously amplified DNA fragments to a backbone vector to generate a new plasmid to be transformed into bacteria or yeast. The In-fusion reaction consisted of 2 µl 5x Infusion HD Enzyme Premix, 50-200 ng linearized vector, 10-200 ng purified PCR fragment and up to 10 µl with mQ water. After set up, the mix was incubated for 15 min at 50ºC, then

placed on ice or stored at -20ºC until bacterial transformation was carried out using Stellar™ competent cells.

### 2.3.2 Stellar™ Competent Cells Transformation (Clontech)

The Stellar™ Competent Cells were placed on ice to thaw before use. An aliquot of 50 µl of competent cells was placed into a 14 ml round bottom tube and 5 ng of DNA added for each transformation. The tubes were placed on ice for 30 min. The cells suffer a heat shock at 42ºC for exactly 45 seconds. Then, the tubes were incubated on ice for 2 min. B medium was added to bring the final volume to 500 µl. LB medium was first warmed to 37ºC. The tubes were incubated with shaking for 1 h at 37ºC. Finally, the 500 µl was divided and cultured on LB and ampicillin plates. Plates were incubated overnight at 37ºC. Positive colonies were then screened by colony PCR using SapphireAmp PCR master mix.

### 2.3.3 Plasmid purification for fungal transformation

After digestion with restriction endonucleases, a colony containing the desired plasmid was selected for further analysis. In order to obtain higher amounts of plasmid, the PureYield™ Plasmid Midi-Prep System (Promega) was used.

A positive colony was used to start a liquid culture. Then was grown in 100 ml LB liquid medium for 24 h at 37ºC with vigorous aeration (225 rpm) in an Innova 4000 rotary incubator (New Brunswick Scientific). For storage, 700 µl of the bacterial culture was incubated with 300µl glycerol at -80ºC. The rest was fractionated by centrifugation at 10,000 x *g* for 10 min. The pellet was resuspended in 3 ml of Cell Resuspension Solution (50 mM Tris (pH 7.5), 10mM EDTA and 100 µg $ml^{-1}$ of RNAse) and 3 ml of Cell Lysis Solution (0.2 M NaOH, 1% SDS). The samples were then inverted 5 times and left to incubate for 3 min at room temperature. After that, 5 ml of Neutralization solution (4.09 M guanidine hydrochloride, 0.759 M potassium acetate, 2.12 M glacial acetic acid (pH 4.2)) was added and samples inverted to mix. The next step was a centrifugation at 14,000 x *g* for 15 min. Next, the white PureYield Column (binding column) and the blue PureYield Clearing Column (clearing column) were placed in a vacuum manifold. The supernatant was poured into a clearing column as the vacuum was applied until all the liquid

passed through both columns. The blue column was then removed and 5 ml of Endotoxin Removal Wash were added. Vacuum was applied until the solution passed through. Then, 20 ml of the Column Wash Solution (60mM potassium acetate, 8.3 mM Tris-HCl (pH 7.5), 0.04 mM EDTA, 60% ethanol) was added to the binding column. Vacuum was applied until the solution passed through and the membrane was dried. Binding column was placed into a new 50 ml falcon tube and 600 µl of Nuclease-Free Water were added. After 1 min, the column was subjected to centrifugation at 1,500 x *g* for 5 min. Plasmid DNA was stored at 20ºC.

### *2.4 DNA-Mediated Transformation of M. oryzae*

A 2.5 $cm^2$ section of mycelium from a *M. oryzae* plate culture was transferred to 150 ml complete medium liquid and blended until small fragments of mycelium were formed. The liquid culture was incubated at 25ºC, shaking (125 rpm) in an orbital incubator for 48h.

Fresh ST (sucrose, 0.6M, Tris-HCl 0.1 M (pH 7), STC (sucrose, 1.2 M, Tris-HCl, 10 mM (pH 7.5)) and PTC (PRG 4000, 60%, Tris-HCl, 10 mM (pH 7.5), calcium chloride) buffers were made and they were stored at 4ºC.

The culture was harvested by filtration through sterile Miracloth and the mycelium was washed with sterile deionized water (SDW). The mycelium was transferred to a 50 ml falcon tube with 40 ml OM buffer (1.2 M magnesium sulfate, 10 mM sodium phosphate (pH5.8), Glucanex 5% (Novo Industries, Copenhagen)). The mycelium in the falcon with OM buffer was shaken gently to disperse hyphal clumps. Then, it was incubated at 30ºC with gentle (75 rpm) shaking, for 3 h.

The digested mycelium was transferred to two sterile polycarbonate Oakridge tubes (Nalgene) and overlaid with an equal volume of cold ST buffer. Resulting protoplast were recovered at the OM/ST interface by centrifugation at 5000 x *g*, for 15 min at 4ºC in a swinging bucket rotor (Beckman JS-13.1) in a Beckman J2.MC centrifuge. Protoplasts were recovered and transferred to a sterile Oakridge tube, which was then filled with cold STC buffer. The protoplasts were pelleted at 3,000 x *g* for 10 min (Beckman JS-13.1 rotor). This wash was carried out twice more with STC, with complete re-suspension of the pellet each time.

After the last wash, protoplasts were resuspended in 1 ml of STC and checked by microscopy.

In an Eppendorf tube, an aliquot of protoplasts was combined with 6 µg DNA. The mixture was incubated at room temperature for 30 min. After incubation, 1 ml of PTC was added in 2 aliquots, mixed gently by inversion and incubated at room temperature for 20 min.

The transformation mixture was added to 150 ml of molten agar medium and poured into 5 sterile Petri dishes. For selection of transformants on hygromycin B (Calbiochem), plate cultures were incubated in the dark for at least 16 h at 24ºC and then overlaid with approximately 15 ml of OCM/1% agar (CM osmotically stabilised with sucrose, 0.8M) containing 600µg $ml^{-1}$ hygromycin B. For selection of bialophos (Basta) resistant transformants, OCM was replaced with BDCM (yeast nitrogen base without amino acids and ammonium sulfate, 1.7 g $l^{-1}$ (Difco), ammonium nitrate, 2 g $l^{-1}$ asparagine, 1 g $l^{-1}$ glucose, 10 g $l^{-1}$ sucrose, 0.8 (pH 6)). In the overlay, CM was replaced by BDCM without sucrose and hygromycin B was replaced by glufosinate (30 µg $ml^{-1}$) stock was 100 $mgml^{-1}$ in DSW. For selection of sulfonylurea resistant transformants, OCM was replaced with BDCM and in the overlay, hygromycin B was replaced with chlorimuron ethyl, 50 30 µg $ml^{-1}$ freshly diluted from a stock solution, 100 mg $ml^{-1}$.

### *2.5 Southern Blot Analysis*

In this study Southern blot analysis was used to determine GFP copy number of *M. oryzae* transformants. Endonuclease digestion of *M. oryzae* transformants DNA was performed overnight and after fractionation by electrophoresis in an agarose gel at 100V. Fragments of DNA separated in agarose gels were transferred to Hybond-NX (Amersham Biosciences). Prior to blotting, partial depurination of DNA molecules was performed to enhance DNA transfer by submerging the agarose gel in 0.25 M with gentle rocking. Gels were then neutralised by replacing HCl with 0.4 M NaOH. For transfer of DNA from the agarose gel to the positively charge membrane, blots were carried out using a 0.4M NaOH transfer buffer that was drawn up through a wet paper wick (Whatman /international) supported by a Perspex panel onto which the agarose gel was placed. A sheet of Hybond-NX membrane was then laid upon the gel and positions of the wells were pencil marked. Three layers of Whatman 3MM paper

and a stack of paper towels (Kimberley Clark Corporation) were laid over the membrane followed by a glass plate and a heavy book were placed on the stack as a weight. The transfer was left at room temperature overnight. Then, the nucleic acid was fixed to the membrane by UV crosslinking to the membrane with 120 milijoules.cm$^{-2}$ using a BLX crosslinker (Bio-Link).

### *2.6 Membrane Hybridization and Chemiluminescent detection of DIG-labelled nucleotides*

The Hybond-NX membrane was placed inside a hybridisation bottle (Hybaid Ltd) and pre-hybridized with Southern hybridization buffer (0.5M sodium phosphate buffer (pH7), 7% (w/v) SDS) in the hybridization oven (Hybaid Ltd) at 62ºC with rotation for at least 30 min. Next, buffer was removed and replaced with the probe for overnight incubation at 62 ºC. The digoxigenin-(DIG) labelled probes were generated by PCR using Phusion® High-Fidelity DNA polymerase and DIG DNA labelling mix (Roche Applied Science) (5 µl per 50 µl reaction). The amplified fragment was fractionated by gel electrophoresis, purified and added to 50ml of Southern hybridization buffer. Before, the hybridisation step of the Hybond-NX membranes, the probe was boiled in a water bath at 100ºC for at least 10 min to denaturalise the DNA. The probe can be re-used and kept at -20ºC. After, hybridization, the membrane was washed twice with Southern wash buffer (0.1M of sodium phosphate buffer (pH7), 1% (w/v) SDS) in the hybridization tube at 62ºC for 15 min.

The membrane was equilibrated in DIG wash buffer (150mM NaCl, 01.M maleic acid, pH to 7.5 with NaOH, 0.3% (v/v) Tween 20) at room temperature for 5 min, then to quench background signal DIG was buffer was replaced with with DIG blocking solution (150mM NaCl, 01.M maleic acid, pH to 7.5 with NaOH, 1% milk powder). After, the membrane was incubated with 40 ml antibody solution (0.0001% (v/v) Anti-Digoxigenin-AP, Fab fragments (Roche) subjected to centrifugation for 20 min at 16000 x *g* prior to addition to prevent inclusion of small antibody aggregated, 150 mM NaCl, 0.1 maleic acid, pH to 7.5 with NaOH, 1% (w/v) milk powder) for 30 min. The membrane was next washed twice with DIG wash buffer for 15 min, followed by being equilibrated in 20ml DIG buffer (0.1Tris/HCl (pH9.5), 0.1M NaCl, 50mM magnesium chloride) for 5 min. For the

chemiluminescent reaction, 2 ml of the CDP-Star Solution (Roche) was pipetted onto the membrane and incubated for 5 min at room temperature. The membrane was further incubated at 37ºC for 15 min. DIG-labelled nucleic acids were detected through a chemiluminescent reaction with a chemiluminescent Substrate CDP-star® (Sigma). This reaction was performed by transferring the membrane onto a polypropylene sheet with 1ml CDP-Star® and covered by another polypropylene sheet and incubating for 30 min at 37 ºC. The membrane was exposed to X-ray film (Fuji Medical X-ray film, Fuji Photo Film UK Ltd.) for 30 sec to 30 min at room temperature in an X-ray film cassette and developed in a OptiMax X-ray Processor (Protec).

### *2.7 Assay for examining intracellular infection related development on rice leaves*

The assay to visualize *M. oryzae* cell colonization was adapted from Kankanala e*t al.,* 2007. The assay consists of leaf sheaths inoculation with *M. oryzae* conidial suspensions, prepared at concentration of $10^5$ conidia $ml^{-1}$ in 0.2% gelatine solution, injected in the leaf vein. Leaf sheaths were incubated placed horizontally in a moist chamber and incubated at 24°C.

To visualize by microscopy, leaf sheaths were prepared in a thin section of three to four cell layers.

### *2.8 Epifluorescence and Laser Confocal Microscopy*

For epifluorescence microscopy was used an Olympus IX81 inverted microscope (Olympus, Hamburg, Germany) with X100/1.4 or X60/1.35 oil objectives. A Photometrics CoolSNAP HQ2 camera system (Roper Scientific, Germany) under the control of MetaMorph software package (MDS Analytical Technologies, Winnersh, UK) was used to capture images from the microscope.

Confocal laser scanning fluorescence microscopy was performed on a Leica TCS SP8 microscope using a X63/1.4 oil immersion objective lens. Images were acquired using Leica LAS AF software (Leica Macrosystems Inc., Buffalo Grove, IL, USA). Fluorescence was observed using HyD detectors and white laser. The filter sets used were: GFP, excitation wave length 488 nm and emission 525 and RFP, excitation wave length 543 nm and emission 584.

# Chapter 3. Defining an experimental program to investigate the regulation of effector gene expression

## *3.1 Introduction*

Plant pathogens can be broadly classified according the manner in which they infect their host plant. Necrotrophic pathogens deliver enzymes to degrade plant cell components and are able to complete their life cycle in dead plant tissue. By contrast, biotrophic fungi require their host to be alive throughout their life cycle and many biotrophic fungi develop haustoria that are used to invade living plant cells. Hemibiotrophic fungi also invade the plant tissue using haustoria or similar intracellular hyphal structures and proliferate initially within living plant tissue, but they they switch to a necrotrophic life style and kill plant cells in order to complete their life cycle. *M.oryzae*, *Colletotrichum spp* and *Phytophthora spp* are examples of hemibiotrophic fungi and oomycete pathogens, respectively (Giraldo and Valent, 2013).

There are several growth habits that biotrophic and hemibiotrophic filamentous fungi adopt inside the host. Some pathogens form highly specialized intracellular invasive hyphae like those observed in *M. oryzae,* while others are exclusively extracellular, like the tomato leaf mould pathogen *Cladosporium fulvum*, which grows in the apoplastic spaces between cells. Other fungi and oomycetes develop specialized feeding structures inside the plant host such as haustoria, which can take on a variety of forms (Yi and Valent, 2013). It is becoming clear, however, that invasive hyphae and haustoria-like structures are important structures not only for sequestering nutrients from host cells, but also for delivering effectors to suppress the plant immunity responses enabling the pathogen to rapidly grow in plant tissue.

In *M.oryzae*, the apoplastic space between the pathogen and the host has been called the extrainvasive hyphal matrix (Kankanala et al., 2007) because it is a compartment between the fungal cell wall and the extrainvasive hyphal membrane which is bounded by the plant plasma membrane. The interface between the extrainvasive hyphal membrane and the blast fungus cell wall is, however, separated by a neckband at the penetration site from the rest of the apoplastic space (Giraldo and Valent, 2013). The apoplastic space between the host cell cytoplasm and the fungal cell wall is a site of secretion for both the

fungus and the plant (Yi and Valent, 2013). It has been shown that, for example, plants deliver small RNAs that can be taken-up by pathogens. The function of these sRNA is to silence pathogen virulence genes (Cai et al., 2018). Conversely, the fungus delivers many proteins into the apoplast, such as Slp1 an effector that suppresses chitin-triggered immunity (Mentlak et al., 2012). Therefore, the extra-invasive hyphal matrix is an important site where secretion of host and pathogen proteins occurs, which either activate or suppress the plant immune system (Giraldo and Valent, 2013). There is significant interest in the interplay that occurs at this host-pathogen interface (Giraldo and Valent, 2013) (Dangl and Jones, 2001; Stergiopoulos and de Wit, 2009; Djamei and Kahmann, 2012). However, very little is currently known about the secretion mechanism of fungal effectors into host plant cells.

To explore effector diversity, comparative genomic and transciptomic analyses have been carried out in a number of plant pathogenic fungi. An analysis of *Colletotrichum higginisianum* and *Colletotrichum graminola* has revealed, for example, that infection-related genes are deployed at different time points through the infection process corresponding to the switch from biotrophic to necrotrophic growth. Effectors and other proteins related to biotrophic growth, are expressed in the appressorium before penetration. Interestingly, expression of these genes, may involve a plant signal, because effectors are not expressed in appressoria *in vitro* (O'Connell et al., 2012). This is also the case for other effectors in *U. maydis* and *M. oryzae,* suggesting that effector gene expression involves perception and response to plant signals (Yi and Valent, 2013).

In *C. higginisianum*, the ChEC effectors localise at the appressorium pore at the time that isotropic expansion of the appressorium switches to polarised growth, forming the penetration peg (Kleemann et al., 2012). Expression of ChEC6 and ChEC36 mCherry fusion constructs was observed at the appressorium pore even before penetration, suggesting that the appressorium is not only the infection structure that breaks the plant cuticle, but is also a site of effector secretion. This study also demonstrated that the host is able to detect the pathogen even before penetration occurs. Only one of the ChEC effectors is expressed *in vitro* in the appressorium pore. Such patterns have also been observed for the *ACE1* avirulence gene of *M. oryzae* which is expressed independently of plant signals (Kleemann et al., 2012) (Fudal et al., 2007).

In *M. oryzae* effector delivery has been associated with formation of a specific structure that appears at invasive hyphae shortly after penetration. This structure is known as the biotrophic interfacial complex (BIC). The BIC is a plant structure between the fungal cell wall and the cell membrane of the plant in the extra invasive hyphal matrix (Khang et al., 2010). Fluorescence recovery after photobleaching (FRAP) experiments suggest that the BIC is the site of active translocation of effectors from *M. oryzae* to rice cells (Giraldo et al., 2013). Characterised cytoplasmic effectors such as Pwl2, AvrPia, AvrPita localize at the BIC (Giraldo et al., 2013) (Khang et al., 2010) (Ortiz et al., 2017), while apoplastic effectors such as Slp1, Bas4 and Bas113 localise instead around invasive hyphae (Mentlak et al., 2012) (Mosquera et al., 2009). In spite of the observation of two classes of effectors being delivered to two distinct sub cellular localisations, no translocation motifs have been identified in the corresponding effector-encoding genes. This is in marked contrast to oomycete effectors that can be readily identified by the RXLR (Whisson et al., 2007). This study set out to gain more fundamental knowledge regarding how effectors from the rice blast fungus are secreted from invasive hyphae and how they are then taken up by the plant.

Khang and co-workers previously reported that BIC localisation of AvrPita requires the *AVRPITA* promoter and the predicted signal peptide sequence (Khang et al., 2010). The major objective of this project was to determine whether this observation was of more general significance and conserved in many effector-encoding genes.

In this chapter, I report experiments designed to test whether the promoter sequence of a given effector gene is necessary for its correct secretion, and whether the signal peptide region is also associated with delivery of an effector protein to host cells. To test this idea, I constructed a set of chimeric effector gene constructs that had promoter and signal peptide swaps between genes encoding either cytoplasmic or apoplastic effectors, respectively, as shown in Figure 3.1. My aim was to generate a set of chimeric constructs that encoded fluorescent effector fusion proteins that were expressed in *M. oryzae* under control of different promoter and signal peptide combinations. In this way I aimed to rigorously test whether specific regions at the 5'end of effector genes are required for effector protein secretion from the rice blast fungus during plant infection and tissue invasion.

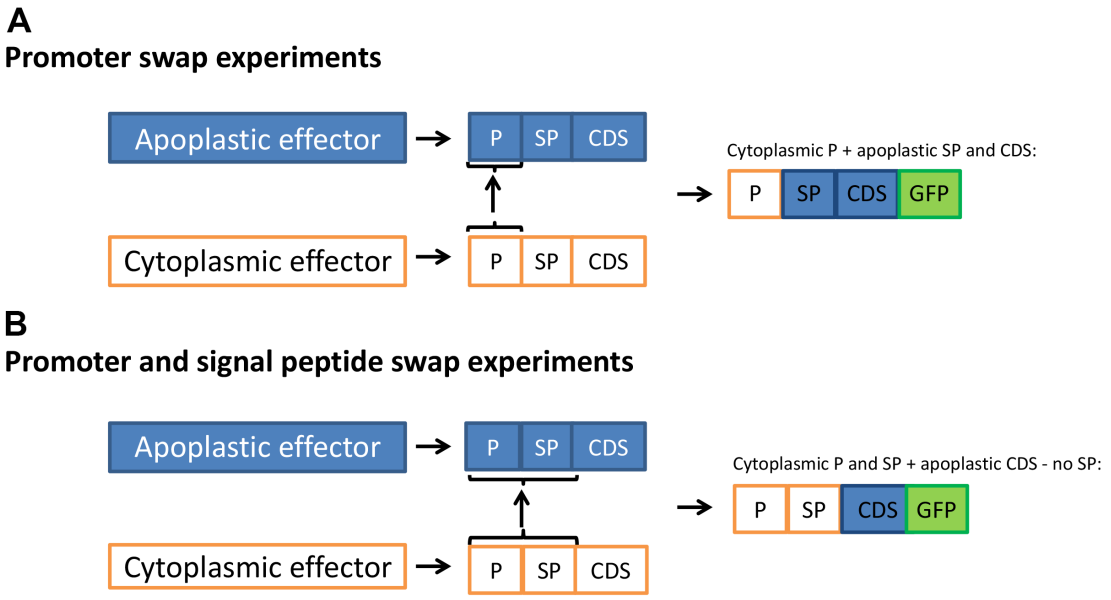


Figure 3.1 **Schematic representation of the strategy followed for design of chimeric effector gene constructs.** A) Promoter swap experiments: this involved a change of the promoter region from the native promoter of an apoplastic effector-encoding gene to the promoter region of a cytoplasmic effector gene. The chimera is also fused to GFP to be enable observation by microscopy after expression in *M. oryzae*. B) Promoter and signal peptide swap: change of the promoter and signal peptide regions of an apoplastic effector-encoding gene for the promoter and signal peptide regions of a cytoplasmic effector gene. P:promoter; SP: signal peptide; CDS: coding region.

## *3.2 Methods*

### 3.2.1 Generation of C-terminal GFP fusion constructs using the promoter region of cytoplasmic effector-encoding genes

To generate *PWL2p:GFP* and *AVRPIAp:GFP* transfomation vectors, primers in Table 3.1 were used to amplify from total genomic *M.oryzae* DNA from strain Guy11 for *PWL2* (MGG_04301) and from strain INA168 for *AVRPIA* (AB498873). *M. oryzae* promoter regions were routinely defined as a 2 kb region upstream of the start codon of the gene. Forward primers always included a 15bp overhang with the *BAR* resistance cassette conferring glufosinate resistance. The reverse primer contained a 15bp overhang at 5'end, which is complementary in nucleotide sequence to the Green Fluorescent Protein *GFP* DNA sequence: The resistance cassette *BAR* gene and *GFP:trpC* terminator fragments were amplified using primers with 15bp overhangs complementary to *Hin*dIII linearised pNEB-1284 plasmid (Figure 3.2). The polymerase enzymes used were Phusion® high fidelity DNA Polymerase (New England Biolabs, Thermo Scientific®) and Q5® High-Fidelity DNA Polymerase (New England Biolabs). The PCR consisted of an initial denaturation step at 98°C for 30 sec followed by 35 cycles of PCR cycling parameters of: denaturation at 98°C for 10 sec, annealing 58°C for 30 sec and extension 72°C for 30 sec/kb target length, followed by a final extension at 72°C for 10 min. Amplified products were analysed by gel electrophoresis. The purified fragments were used for In-fusion Cloning method (Clontech). The fragments were integrated into a *Hin*dIII pNEB-1284 digested plasmid (Figure 3.2). The resulting *PWL2p:GFP* and *AVRPIAp:GFP* plasmids were subsequently introduced into *M. oryzae* by transformation of the *M. oryzae* Guy11 strain.

Table 3.1 Primers used in this study

| Primer name | DNA sequence (5'-3') |
|---|---|
| PWL2F | GAGATTTAGGTCGACTTCGAGGTCCTCCACCAAAC |
| PWL2Revp | ATTAAAAACTTTCAAAATGCAGTTCGCTACC |
| Slp1Forf | ATGCAGTTCGCTACCATCAC |
| Slp1R | CAACATCCCCATCTGCAAGAACATGGTGAGCAAGGGC |
| Slp1F | GAGATTTAGGTCGACAAGATAGCCCAGCCCAAATG |
| Slp1Revp | CCGTCTCTCAAACCGTCAAA |
| PWL2Forf | TCTCAAACCGTCAAAATGAAATGCAACAACATC |
| PWL2R | GAAGAGGGCTGCAATATTATGATGGTGAGCAAGGGC |
| Bas4Forf | ATGCAGCTCTCATTCTCAG |
| Bas4R | CGTCTATCCCCCCTGCTATGGTGAGCAAGGGC |
| Bas4F | GAGATTTAGGTCGACTCCTGCCAAGTAGACTTGAG |
| Bas4Revp | CACAACGAATCTTTTCACA |
| AVR-PiaF | GAGATTTAGGTCGACCAACGCTGGCGTTGTAATTG |
| AVR-Pia_1 | CCATACACGAAAATTCTCAAAATGCAGCTCTCATTC |
| Bas4_2 | ACGAAAATTCTCAAAATGCAGCTCTCATTCTCAG |
| Bas4_1 | CACAACGAATCTTTTCACAATGCATTTTTCGACA |
| AVR-Pia_2 | ACGAATCTTTTCACAATGCATTTTTCGACAATTTTC |
| AVR-PiaR | CTTGCTGCCGAGCCTTACATGGTGAGCAAGGGC |
| Bas4pR | GCCCTTGCTCACCATTGTGAAAAGATTCGTTGTG |
| Bas4spR | GCCCTTGCTCACCATGTCGGCCGTAGCGTGGTTG |
| Slp1pR | GCCCTTGCTCACCATTTTGACGGTTTGAGAGACGG |
| Slp1spR | GCCCTTGCTCACCATGGCGGCGGCAACGCCGGCAA |
| AvrPiapR | GCCCTTGCTCACCATTTTGAGAATTTTCGTGTATG |
| AvrpiaspR | GCCCTTGCTCACCATCGCAGCGCTTACTTTTAGAG |
| AvrPia_01 | TCTCAAACCGTCAAAATGCATTTTTCGACAATTTTC |
| AvrPia_02 | GGTAGCGAACTGCATTTTGAGAATTTTCGTGTATGG |
| AvrPia_03 | GCCGGCGTTGCCGCCGCGCCAGCTAGATTTTGC |
| Slp1_01 | GCCATGCCTGTAAGCAGAG |
| AvrPia_04 | GCTTACAGGCATGGCAGCGCTTACTTTTAGAGCAG |
| Pwl2_01 | ACGAATCTTTTCACAATGAAATGCAACAACATC |
| Pwl2_02 | GAATGAGAGCTGCATTTTGAAAGTTTTTAATTTTA |
| Pwl2_03 | ATTCTGGTGCGAGTCGGCGGTTACAGTGGTCGAA |
| Pwl2_04 | AACCACGCTACGGCCGGTGGCGGGTGGACTAAC |
| Bas4_11 | GACTCGCACCAGAATCTTG |
| AvrPia_10 | ATTCTGGTGCGAGTCAGCGCTTACTTTTAGAGCAG |
| AvrPia_14 | AACCACGCTACGGCCGCGCCAGCTAGATTTTGC |
| Bas4_13 | GGCCGTAGCGTGGTTGAC |
| Slp1_1 | AGCTTGGACTTTCATTTTGACGGTTTGAGAGACGGTG |
| Slp1_2 | TTGAAAGAGCCCACAATGCAGTTCGCTACCATCAC |
| PWL2_4 | GCCGGCGTTGCCGCCGGTGGCGGGTGGACTAACAAAC |
| Slp1_3 | AGTCCACCCGCCACCGGCGGCAACGCCGGCAAAG |
| Slp1_4 | ACCACTGTAACCGCCGCCATGCCTGTAAGCAGAG |
| PWL2_3 | GCTTACAGGCATGGCGGCGGTTACAGTGGTCGAAA |
| Pwl2_6 | GGCGGTTACAGTGGTCGAAA |
| Inv1_7 | ACCACTGTAACCGCCGTGACGACGACTCTCCCC |
| Inv1_R | CTACCAGCGTCAGGAGTAACTGCATGGTGAGCAAGGGCGAG |
| Pwl2_9 | GTAGGCTGCGTGCATTTTGAAAGTTTTTAATTTTA |
| Inv1_10 | ATGCACGCAGCCTACCTC |
| Slp1_7 | GGCGGCAACGCCGGCAAAG |
| Pwl2_7 | GCCCTTGCTCACCATACCGGCGGTTACAGTGG |
| AvrPia_1 | GAATGAGAGCTGCATTTTGAGAATTTTCGTGTATGG |
| AvrPia_2 | ACGAATCTTTTCACA |
| BASTA_3 | GCAGGCATGCAAGCTGTCGACAGAAGATGATATTGAAG |
| BASTA_4 | GTCGACCTAAATCTCGGTGAC |
| GFP_1 | ATGGTGAGCAAGGGCGAG |
| TrC_1 | TGATTACGCCAAGCTAGTGGAGATGTGGAGTGG |

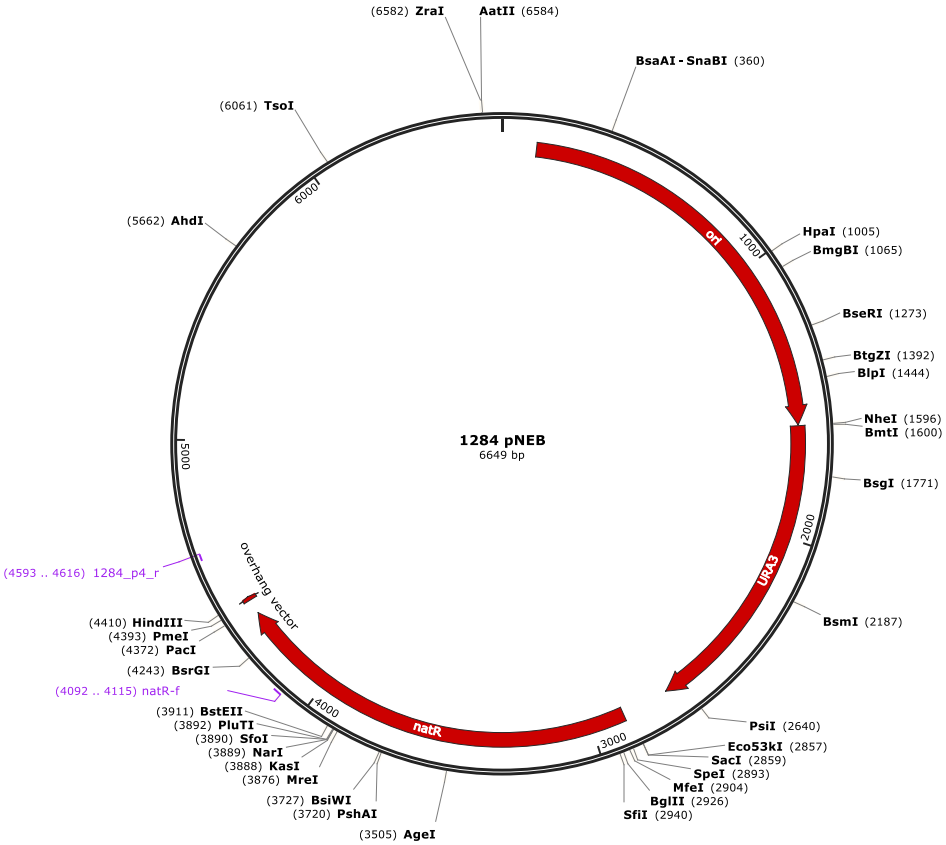


Figure 3.2 **Map of pNEB-1284 plasmid**. This vector was linearized by *Hind*III restriction enzyme and used as a backbone vector for In-fusion cloning experiments (Map from New England BioLabs).

### 3.2.2 Generation of C-terminal GFP fusion constructs using the promoter and signal peptide of cytoplasmic effector-encoding genes

To generate *PWL2p+sp:GFP* and *AVRPIAp+sp:GFP*, primers in Table 3.1 were used to amplify from *M.oryzae* total genomic DNA. A forward primer was designed 2kb upstream of the cleavage site at the end of the predicted signal peptide of *PWL2* and *AVRPIA*. Forward primers always included a 15bp overhang with the *BAR* resistance cassette conferring glufosinate resistance. The reverse primer also had a 15bp overhang, which is complementary in nucleotide sequence to the *GFP* gene sequence: The *BAR* resistance cassette and GFP:*trp*C terminator fragments were also amplified using primers with 15bp overhangs complementary to the vector pNEB-1284. The polymerase enzymes used were Phusion® high fidelity DNA Polymerase (New England Biolabs, Thermo Scientific®) and Q5® High-Fidelity DNA Polymerase (New England Biolabs). The PCR was performed using an initial denaturation step at 98°C for 30 sec followed by 35 cycles of PCR cycling parameters of: denaturation at 98°C for 10 sec, annealing 58°C for 30 sec and extension 72°C for 30 sec/kb target length, followed by a final extension at 72°C for 10 min. PCR products were analysed by gel electrophoresis. The fragments were used to generate chimeras using the In-fusion Cloning method (Clontech). The fragments were integrated into a *Hin*dIII pNEB-1284 digested plasmid (Figure 3.2). The resulting *PWL2p+sp:GFP* and *AVRPIAp+sp:GFP* plasmids were subsequently introduced into *M. oryzae* by transformation of strain Guy11.

### 3.2.3 Generation of chimeric constructs to express apoplastic effectors under control of promoter gene regions of cytoplasmic effector genes

To generate *PWL2p:SLP1:GFP*, *AVRPIAp:SLP1:GFP*, *PWL2p:BAS4:GFP* and *AVRPIAp:BAS4:GFP* chimeric constructs, primers in Table 3.1 were used to amplify a 2 kb fragment containing the active promoter of each gene from genomic DNA of *M. oryzae* Guy11 strain for *PWL2*, from Ina168 for *AVRPIA* gene. Forward primers always included a 15bp overhang with the *BAR* resistance cassette conferring glufosinate resistance. The reverse primer was designed at the 3' end of promoter, before the start codon and included a 15bp overhang complementary in sequence to the coding region of the apoplastic effector *SLP1*

or *BAS4*. The coding sequence of *BAS4* and *SLP1*, including the predicted signal peptide, were also amplified from *M. oryzae* Guy11 total genomic DNA. The forward primer for the coding sequence region was designed at the beginning of the start codon, the reverse primer, was designed at the 3' end of the coding region to exclude the predicted translational stop codon. The reverse primer always had a 15bp overhang, which is complementary in nucleotide sequence to GFP DNA sequence (Table 3.1). The resistance marker *BAR* gene and GFP:*trp*C fragments were also amplified using primers with 15bp overhangs complementary to the pNEB-1284 plasmid. The polymerase enzymes used were Phusion® high fidelity DNA Polymerase (New England Biolabs, Thermo Scientific®) and Q5® High-Fidelity DNA Polymerase (New England Biolabs). The PCR was performed using an initial denaturation step at 98°C for 30 sec followed by 35 cycles of PCR cycling parameters of: denaturation at 98°C for 10 sec, annealing 58°C for 30 sec and extension 72°C for 30 sec/kb target length, followed by a final extension at 72°C for 10 min. PCR products were analysed by gel electrophoresis. The fragments were used to generate the chimeras using the In-fusion Cloning method (Clontech). The fragments became integrated into a *Hin*dIII-digested pNEB-1284 plasmid (Figure 3.2). The resulting *PWL2p:SLP1:GFP*, *AVRPIAp:SLP1:GFP*, *PWL2p:BAS4:GFP* and *AVRPIAp:BAS4:GFP* plasmids were subsequently introduced into *M. oryzae* by transformation of *M. oryzae* Guy11.

### 3.2.4 Generation of apoplastic chimeric constructs with promoter and signal peptide gene regions of cytoplasmic effectors

To generate *PWL2p+sp:SLP1:GFP*, *AVRPIAp+sp:SLP1:GFP*, *PWL2p+sp:BAS4:GFP* and *AVRPIAp+sp:BAS4:GFP*, primers in Table 3.1 were used to amplify a 2 kb fragment containing the promoter region of each gene from genomic DNA of *M. oryzae* Guy11 for *PWL2*, and Ina168 for *AVRPIA*. Forward primers always included a 15bp overhang with the *BAR* resistance cassette conferring glufosinate resistance. The reverse primer was designed at the end of the predicted signal peptide and included a 15bp overhang complementary in sequence to the coding region of the apoplastic effector *SLP1* or *BAS4* without its predicted signal peptide. The coding sequence of *BAS4* and *SLP1*, excluding the predicted signal peptide, were also amplified from Guy11 total genomic DNA. The forward primer for the coding sequence region was designed at the end of

the predicted signal peptide, and the reverse primer was designed at the 3' end of the coding region to exclude the predicted translational stop codon. The reverse primer always had a 15bp overhang, which is complementary in nucleotide sequence to GFP DNA sequence (Table 3.1). The *BAR* resistance cassette and GFP:*trp*C fragments were also amplified using primers with 15bp overhangs complementary to the pNEB-1284 plasmid. The polymerase enzymes used were Phusion® high fidelity DNA Polymerase (New England Biolabs, Thermo Scientific®) and Q5® High-Fidelity DNA Polymerase (New England Biolabs). The PCR was performed using an initial denaturation step at 98°C for 30 sec followed by 35 cycles of PCR cycling parameters of: denaturation at 98°C for 10 sec, annealing 58°C for 30 sec and extension 72°C for 30 sec/kb target length, followed by a final extension at 72°C for 10 min. PCR products were analysed by gel electrophoresis. The fragments were used to generate the chimeras using the In-fusion Cloning method (Clontech). The fragments became integrated into a *Hin*dIII-digested pNEB-1284 plasmid (Figure 3.2). The resulting *PWL2p+sp:SLP1:GFP*, *AVRPIAp+sp:SLP1:GFP*, *PWL2p+sp:BAS4:GFP* and *AVRPIAp+sp:BAS4:GFP* plasmids were subsequently introduced into *M. oryzae* by transformation of *M. oryzae* Guy11.

### 3.2.5 Determination of GFP copy number in GFP fusion constructs

Putative transformants showing GFP fluorescence were grown in CM medium for 12 days. Genomic DNA extraction was then performed, as described in materials and methods section 2.2.1. Quantitative real-time PCR (qPCR) was performed to determine the GFP copy number from a series of dilutions, in blind test performed by iDNA Genetics Ltd (Norwich Research Park). A *M. oryzae* strain (AJF5) containing a single copy number ectopic insertion of the *GFP* gene was used as a positive control and the isogenic strain Guy11 as a negative control. Strain AJF5 was produced in the laboratory by Dr. Andrew Foster.

## *3.3 Results*

### 3.3.1 Construction of *M. oryzae* strains expressing GFP under control of promoter and signal peptide of cytoplasmic effector genes

To study the role of the promoter and signal peptide regions of cytoplasmic effector genes in the control of effector protein secretion, I generated *M. oryzae* strains expressing a series of GFP reporter gene fusions . Cytoplasmic effectors

used in this study were Pwl2 (MGG_04301) and AvrPia (AB498873), both of which have previously been reported to localise to the BIC during plant infection and to be taken up by plant cells. A C-terminal translational fusion of the *PWL2* and *AVRPIA* promoter gene regions or both promoter and signal peptide gene regions, were fused to the GFP reporter gene to generate the following constructs *PWL2p:GFP*, *AVRPIAp:GFP, PWL2p+sp:GFP* and *AVRPIAp+sp:GFP*.

The signal peptide region of each gene was predicted using SIGNALP.4.1 software as shown in Figure 3.3. A 2 kb genomic fragment containing *PWL2* and *AVRPIA* promoter and promoter and signal peptide gene regions was PCR amplified and cloned into *Hin*dIII-digested vector pNEB-1284. The constructs carry the BAR gene conferring resistance to glufosinate (30 µg $ml^{-1}$) thereby allowing selection of putative positive transformants. A diagrammatic representation of the cloning strategy using In-Fusion cloning to generate the vectors is shown in Figure 3.4 A, with the corresponding PCR amplifications, shown in Figure 3.4 B. In-Fusion generated vectors were then transformed into Stellar™ Competent Cells. Bacteria colonies were grown overnight and screened for insertion of the vector using the BAR gene forward and reverse primers. Transformants were then confirmed by cutting extracted plasmids with three different digestion enzymes. *PWL2p:GFP* was digested by *Bam*HI, *Psi*I, *Nde*I (Figure 3.5). *Nde*I,*Pst*I and *Nco*I were used to digest *PWL2p+sp:GFP* (Figure 3.6) and *Psi*I, *Pci*I and *Bgl*II to digest *AVRPIAp:GFP* and *AVRPIAp+sp:GFP* (Figure 3.7). The constructs were then independently confirmed and checked for errors by DNA sequencing. The resulting GFP C-terminal fusions were subsequently introduced into *M. oryzae* Guy11 strain by protoplast-mediated transformation (Talbot et al., 1993). Putative transformants were selected based on glufosinate resistance. GFP positive transformants were screened using the Olympus IX81 inverted microscope. Single copy transformants were confirmed by qPCR blind test (Table 3.2). Single copy transformants for *PWL2p:GFP*, *AVRPIAp:GFP, PWL2p+sp:GFP* and *AVRPIAp+sp:GFP* are in Table 3.3. For *PWL2p+sp:GFP*, we could not identify a single copy transformant *PWL2p+sp:GFP* has 2 GFP copies (Table 3.2).

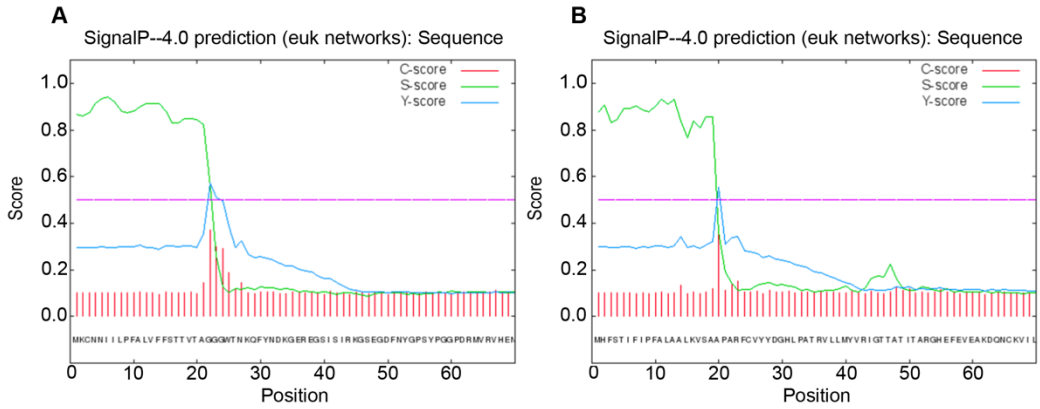


Figure 3.3 **Identification of predicted signal peptide on cytoplasmic effectors genes *PWL2* and *AVRPIA*.** A) Pwl2 signal peptide is from 1-20 amino acids. B) AvrPia having a signal peptide between 1-19 amino acids.

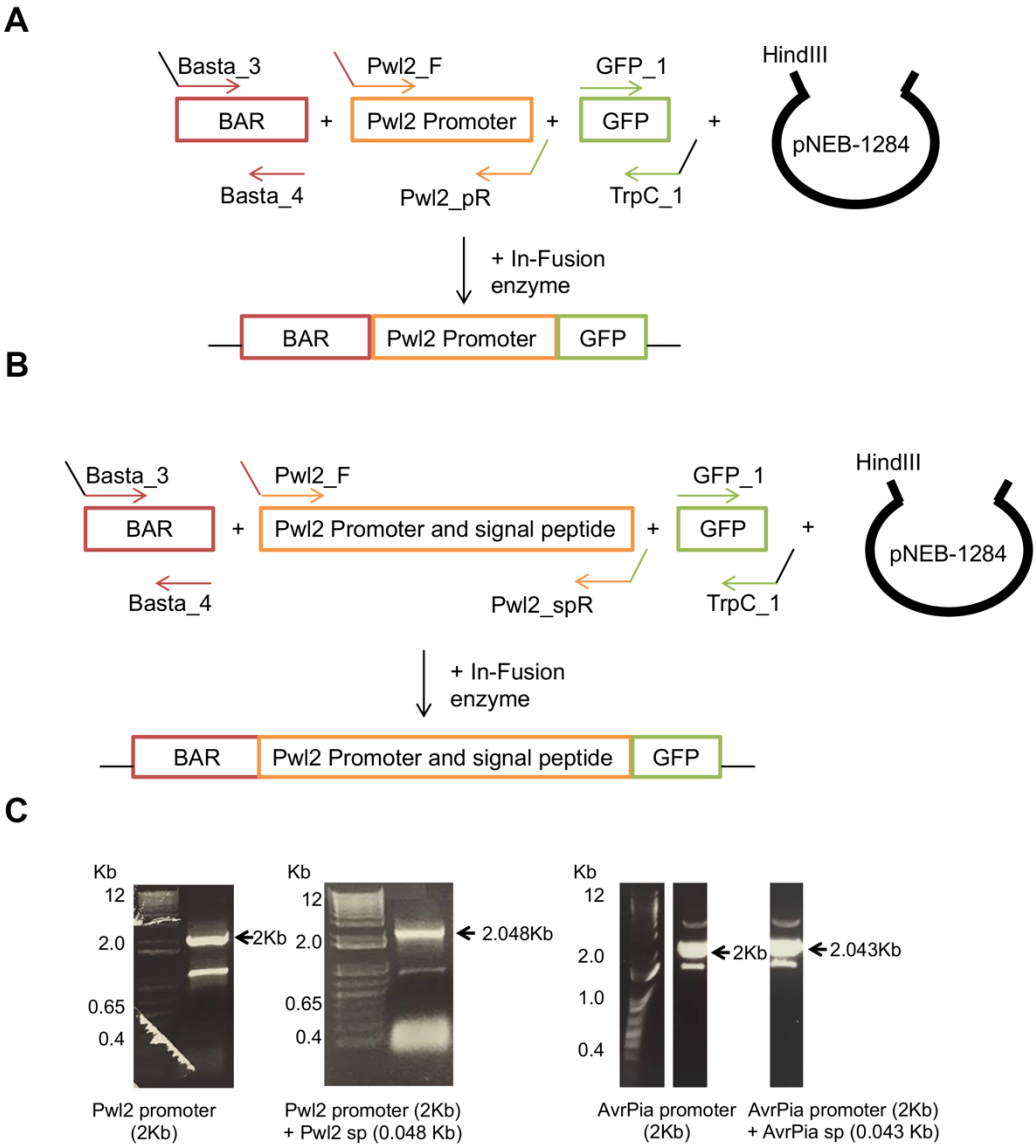


Figure 3.4 **In-Fusion cloning strategy and PCR amplification** A) Scheme of the cloning strategy followed for the construction of effector promoters driving GFP protein. B) Scheme of the cloning strategy followed for the construction of effector promoters driving GFP. C) PCR amplification of 2kb *PWL2* promoter sequence, 2.048kb *PWL2* promoter and signal peptide sequences, 2kb *AVRPIA* promoter sequence and 2.043 *AVRPIA* promoter and signal peptide sequences.

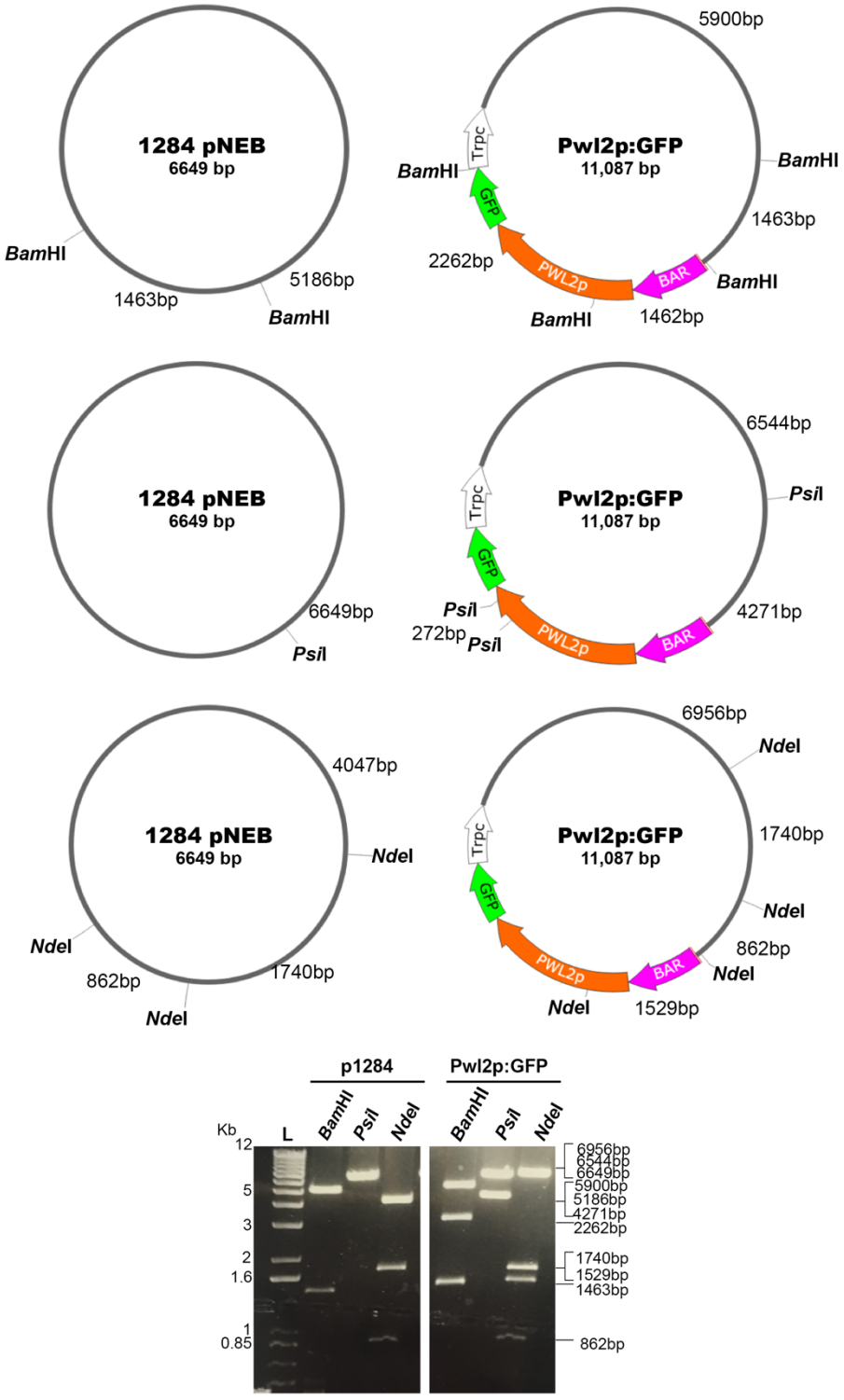


Figure 3.5 ***PWL2p:GFP* plasmid confirmation by restriction enzyme digestion.** Predicted specific size fragments were generated with SnapGene software (from GSL Biotech; available at snapgene.com). Positive bacteria colony PCR *PWL2p:GFP* transformants and pNEB-1284 empty vector were digested with *Bam*HI, *Psi*I and *Nde*I. *Bam*HI displays a specific band size pattern of 1463 bp and 5186 bp for pNEB-1284 and 1463 bp, 1462 bp (not able to distinguish), 2262 bp and 5900 bp for *PWL2p:GFP*. *Psi*I linearised the empty pNEB-1284 vector and has a band size pattern of 4271bp, 212 bp (not seen) and 8544 bp for *PWL2p:GFP*. *Nde*I cuts pNEB-1284 in three fragments 1740bp, 862 bp and 4047 bp. *Nde*I cuts *PWL2p:GFP* in 4 fragments 1740 bp, 862 bp, 1529 bp and 6956 bp. Gene regions in colours: Pink = BAR gene, Blue = apoplastic effector, Orange = cytoplasmic effector, Green = GFP and White = TrpC terminator.

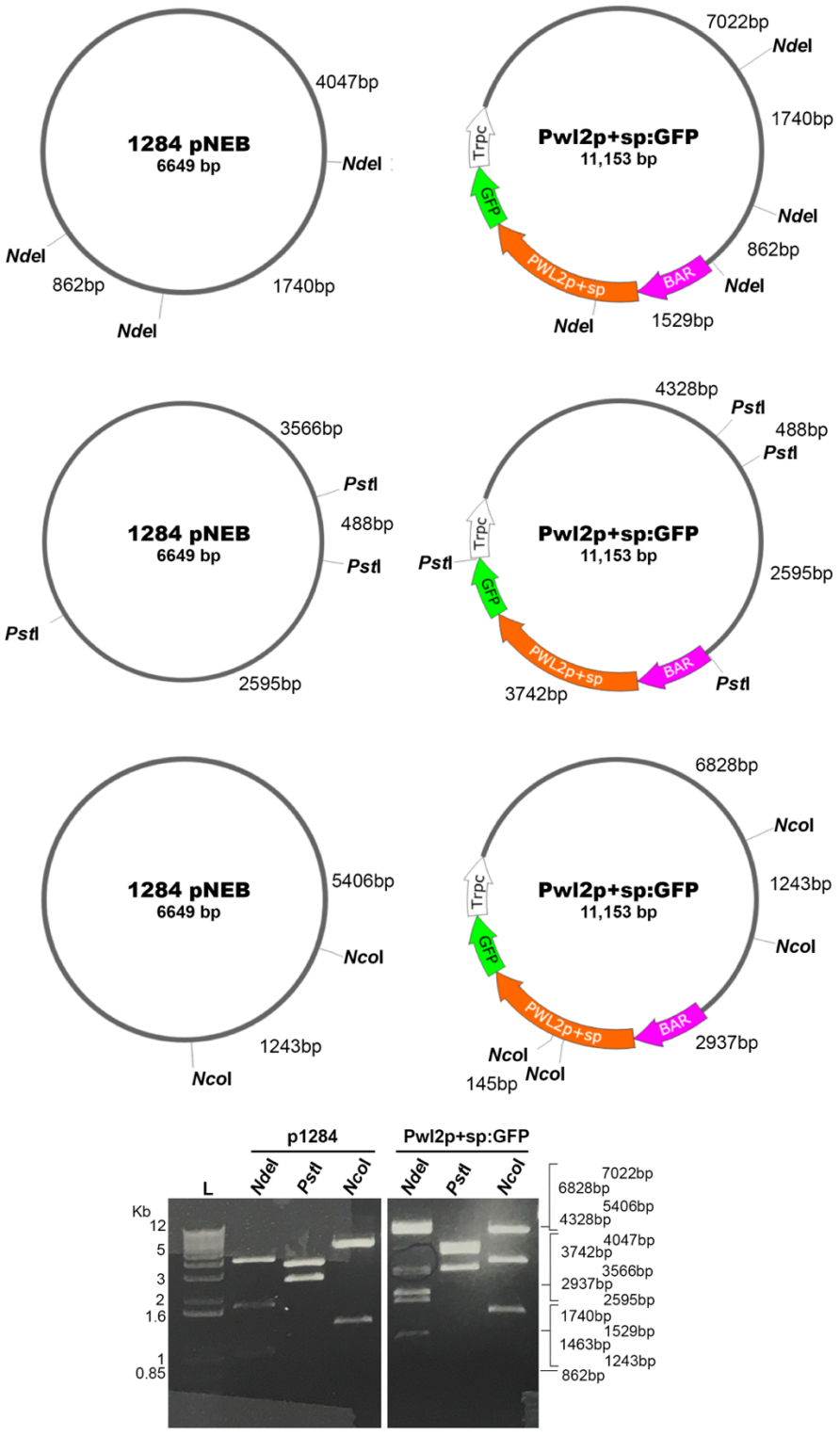


Figure 3.6 ***PWL2p+sp:GFP* plasmid verified by restriction enzymes digestions.** SnapGene software (from GSL Biotech; available at snapgene.com) was used to predict the fragment sizes. *PWL2p+sp:GFP* and pNEB1284 were digested with *Nde*I, *Pst*I and *Nco*I. *Nde*I cuts pNEB-1284 in three fragments 1740bp, 862 bp and 4047 bp. *Nde*I cuts *PWL2p+sp:GFP* in 4 fragments 1740 bp, 862 bp, 1529 bp and 7022 bp. *Pst*I displays a specific band size pattern of 488 bp (not seen), 2595 bp and 3566 bp for pNEB-1284 and 488 bp (not seen), 2595 bp, 3742 bp and 4328 bp for *PWL2p+sp:GFP*. *Nco*I presents 1243 bp and 5406 bp fragments for pNEB-1284 and has a band size pattern of 1243 bp, 2937 bp, 145 bp (not seen) and 6828 bp for *PWL2p+sp:GFP*. Gene regions in colours: Pink = BAR gene, Blue = apoplastic effector, Orange = cytoplasmic effector, Green = GFP and White = TrpC terminator.

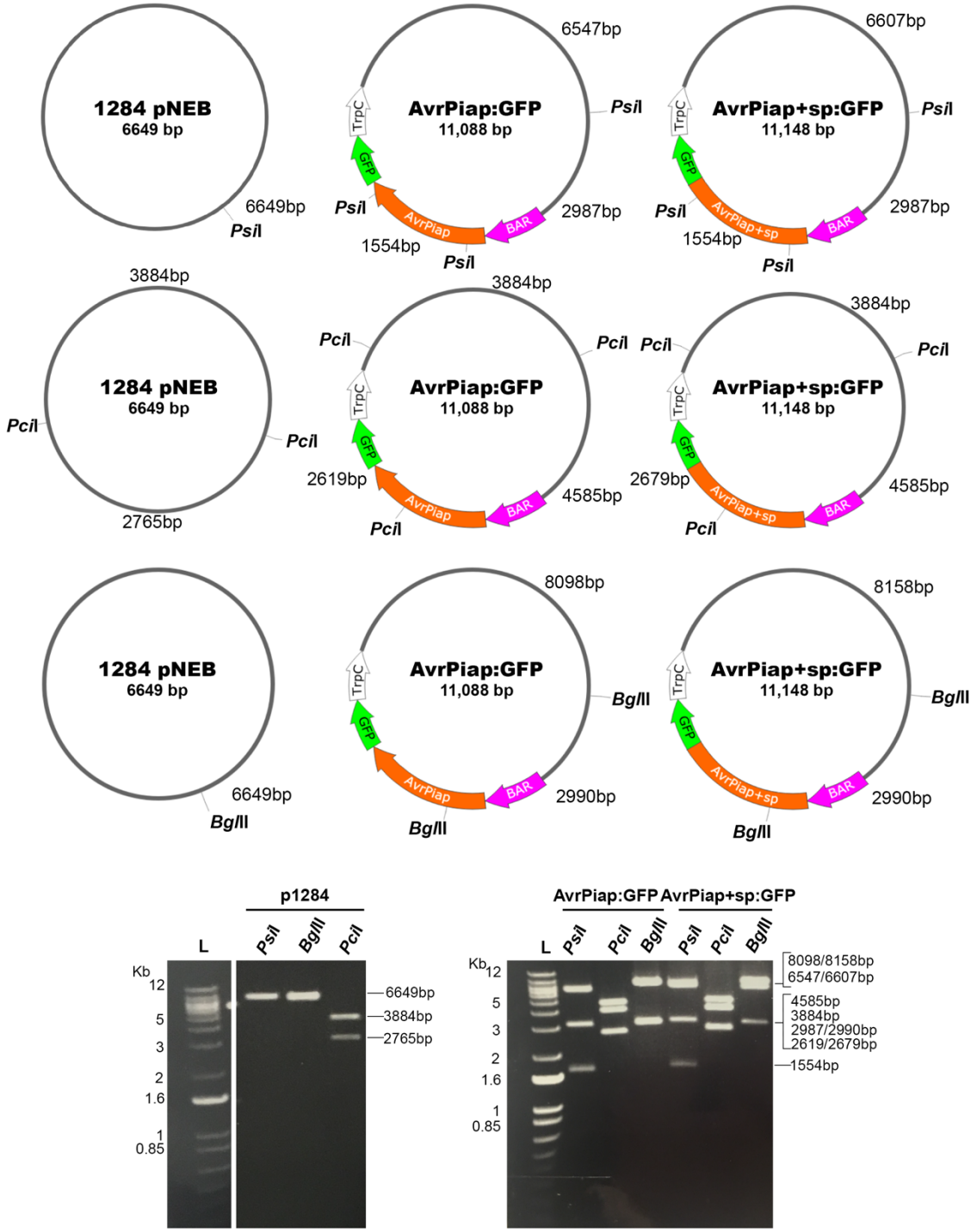


Figure 3.7 ***AVRPIAp:GFP* and *AVRPIAp+sp:GFP* plasmid verification by restriction digestion.** SnapGene software (from GSL Biotech; available at snapgene.com) was used to predict the expected fragment sizes. Positive bacteria colony PCR for *AVRPIAp:GFP* and *AVRPIAp+sp:GFP* transformants and pNEB-1284 empty vector were digested with *Psi*I, *Bgl*II and *Pci*I. *Psi*I linearised the empty pNEB-1284 vector, has a band size pattern of 2987 bp, 1554 bp and 6547 bp for *AVRPIAp:GFP* and 2987 bp, 1554 bp and 6607 bp for *AVRPIAp+sp:GFP*. *Bgl*II linearised pNEB-1284 and cuts *AVRPIAp:GFP* and *AVRPIAp+sp:GFP* in 2990 bp, 8098 bp and 2990 bp, 8158 bp, respectively. *Pci*I displays a specific band size pattern of 2765 bp and 3884 bp for pNEB-1284, 4585 bp, 2619 bp and 3884 bp for *AVRPIAp:GFP* and 4585 bp, 2679 bp and 3884 bp for *AVRPIAp+sp:GFP*. Gene regions in colours: Pink = BAR gene, Blue = apoplastic effector, Orange = cytoplasmic effector, Green = GFP and White = TrpC terminator.

Table 3.2 Determination of GFP copy number by qPCR analysis for *PWL2p:GFP, PWL2p+sp:GFP*, *AVRPIAp:GFP* and *AVRPIAp+sp:GFP*.

| Sample | GFP Copy Number[1] | Sample | GFP Copy Number[1] |
|---|---|---|---|
| Guy11 | 0 | Pwl2p+sp#1 | 2 |
| Control | 1 | AvrPiap#3 | 2 |
| Pwl2p#2 | 2 | AvrPiap#5 | 1 |
| Pwl2p#3 | 8 | AvrPiap#7 | 1 |
| Pwl2p#5 | 1 | AvrPiap#8 | 1 |
| Pwl2p#6 | 114 | AvrPiap#12 | 2 |
| Pwl2p#8 | 25 | AvrPiap+sp#2 | 1 |
| Pwl2p#7 | 1 | AvrPiap+sp#7 | 1 |
| Pwl2p#9 | 3 | AvrPiap+sp#9 | 16 |

[1]Blind qPCR test performed by iDnaGENETICS Ltd (Norwich Research Park).

Table 3.3 Transformants used in Chapter 3

| Name of the construct | Number 1 | Number 2 |
|---|---|---|
| Pwl2p:GFP | 5 | 7 |
| Pwl2p+sp:GFP | 1 | - |
| AvrPiap:GFP | 5 | 7 |
| AvrPiap+sp:GFP | 2 | 7 |
| AvrPiap:Bas4:GFP | 1 | 2 |
| AvrPiap+sp:Bas4:GFP | 3 | 9 |
| AvrPiap:Slp1:GFP | 6 | 12 |
| AvrPiap+sp:Slp1:GFP | 1 | 11 |
| Pwl2p:Slp1:GFP | 8 | 6 |
| Pwl2p+sp:Slp1:GFP | 5 | 6 |
| Pwl2p:Bas4:GFP | 3 | 6 |
| Pwl2p+sp:Bas4:GFP | 5 | 3 |

### 3.3.2 The promoter and signal peptide regions of cytoplasmic effectors are sufficient for BIC localisation

To test whether the promoter and signal peptide regions of the *PWL2* and *AVRPIA* gene are important for secretion, I expressed free GFP under control of the promoter, or the promoter and signal peptide gene regions, of both genes Pwl2 and AvrPia are BIC-localised, cytoplasmic effectors (Khang et al., 2010; Sornkom et al., 2017). Strains of *M. oryzae* expressing promoter fusions Pwl2p:GFP, Pwl2p+sp:GFP, AvrPiap:GFP and AvrPiap+sp:GFP were inoculated onto epidermal leaf tissue of the blast susceptible rice cultivar Mokoto.

After 30 hours post inoculation (hpi), infected tissue was prepared and observed by epifluorescence microscopy, as shown in Figure 3.8. Pwl2p:GFP and AvrPiap:GFP were observed to localise inside invasive hyphae and in the appressorium. GFP fluorescence appeared in large vesicles inside the cytoplasm of the invasive hyphae. Interestingly, when strains expressing Pwl2p+sp:GFP and AvrPiap+sp:GFP promoter and signal peptide fusions were visualized, BIC localisation was restored, as shown in Figure 3.8. The BIC has been proposed to be the site of translocation of *M. oryzae* cytoplasmic effectors into the rice cytoplasm, and can therefore be described as a specific domain for secretion of cytoplasmic effectors, as apoplastic effectors do not normally accumulate in the structure. I conclude that the native promoter and the signal peptide region of a cytoplasmic effector gene are sufficient to enable secretion of GFP into the BIC. The promoter region alone, however, is not able to enable this delivery. The initial results therefore suggest there is a region at the 5'end of *M. oryzae* cytoplasmic effector genes that may be necessary sorting fungal effector proteins into the correct secretory domain.

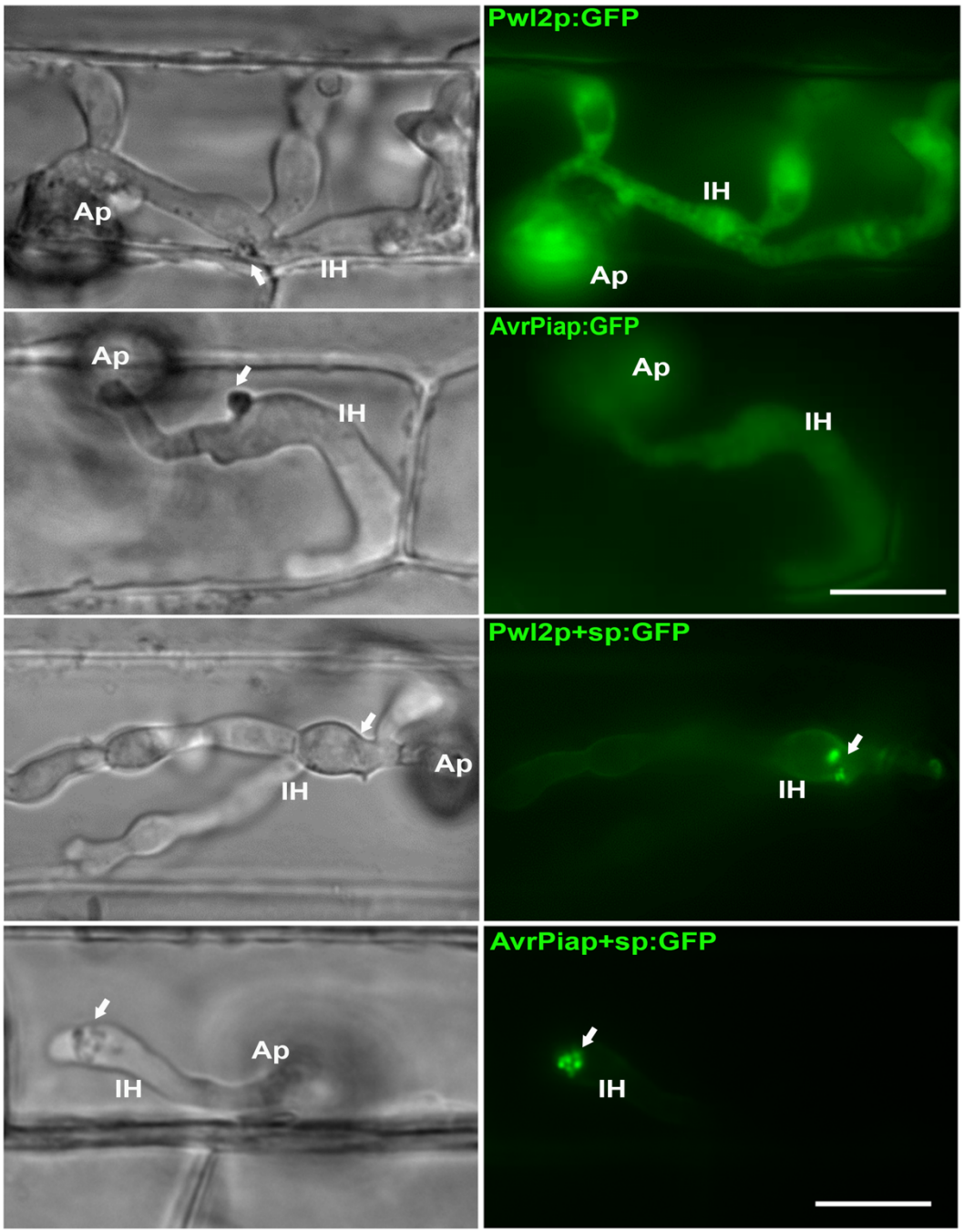


Figure 3.8 **The promoter and signal peptide of cytoplasmic effectors gene *PWL2* and *AVRPIA* are both necessary for BIC localisation.** Micrographs obtained by live cell imaging from leaf sheaths of *M. oryzae* infection of rice by epifluorescence microscopy of promoter gene regions of *PWL2* and *AVRPIA* driving free GFP and promoter and signal peptide gene regions of *PWL2* and *AVRPIA* driving free GFP. All the strains were excited at 488nm for 200 ms. Scale bars represent 10 µm. Arrow marks the BIC, Ap marks the appressorium and invasive hyphae marks *M. oryzae* invasive hyphae.

### 3.3.3 Construction of apoplastic chimeric fungal constructs driven by promoter or promoter and signal peptide gene regions of cytoplasmic effector genes

To test whether the promoter and signal peptide regions of each different class of effector, were required for their correct secretion, I generated the chimeric constructs shown in Figure 3.9. The cytoplasmic effector genes used in this study were *PWL2* (MGG_04301) and *AVRPIA* (AB498873), while the apoplastic effector genes used in this study are *SLP1* (MGG_10097) and *BAS4* (MGG_10914).

A 2 kb fragment containing the promoter of either *PWL2* and *AVRPIA* and the coding sequence of *SLP1* and *BAS4* including the predicted signal peptide DNA fragments were cloned into *Hin*dIII-digested vector pNEB-1284 to generate the constructs shown in Figure 3.9. A diagrammatic representation of the cloning strategy using In-Fusion cloning to generate the vectors in Figure 3.10 with PCR amplifications. Positive bacteria colonies from the In-Fusion cloning were confirmed by restriction digestion. *PWL2p:SLP1:GFP* plasmids was digested with *Hin*dIII, *Eco*RV and *Bsr*GI (Figure 3.11). *PWL2p+sp:SLP1:GFP* plasmids was digested with *Hin*dIII, *Nco*I and *Bam*HI (Figure 3.12). *AVRPIAp:SLP1:GFP* and *AVRPIAp+sp:SLP1:GFP* plasmids were digested with *Psi*I, *Sal*I and *Pci*I (Figure 3.13). *PWL2p:BAS4:GFP* and *PWL2p+sp:BAS4:GFP* transformants were digested with *Bam*HI, *Xma*I and *Xmn*I (Figure 3.14). *AVRPIAp:BAS4:GFP* was digested with *Pst*I, *Bam*HI and *Eco*RV (Figure 3.15). *AVRPIAp:BAS4:GFP* was digested with *Bgl*II, *Bam*HI and *Pst*I (Figure 3.16). The constructs were independently confirmed and checked for errors by DNA sequencing. The resulting C-terminal GFP fusions were subsequently introduced into *M. oryzae* Guy11 strain by protoplast-mediated transformation (Talbot et al., 1993). Putative transformants were selected based on their resistance to glufosinate and GFP fluorescence.

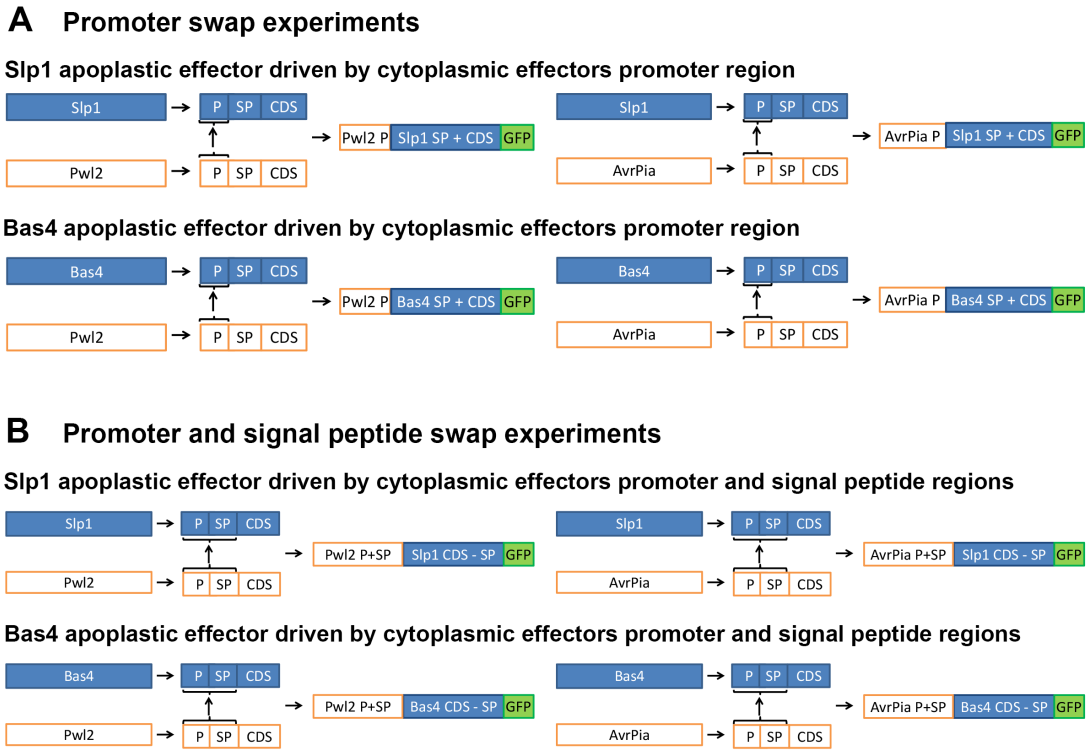


Figure 3.9 **Chimeric constructs used in Chapter 3.** Schematic representation of the strategy to generate each chimeric construct used to test the role of the promoter and signal peptide regions of effector-encoding genes in their secretion. Blue: Apoplastic effector; White: Cytoplasmic effector; P:promoter; SP: signal peptide; CDS: coding region.

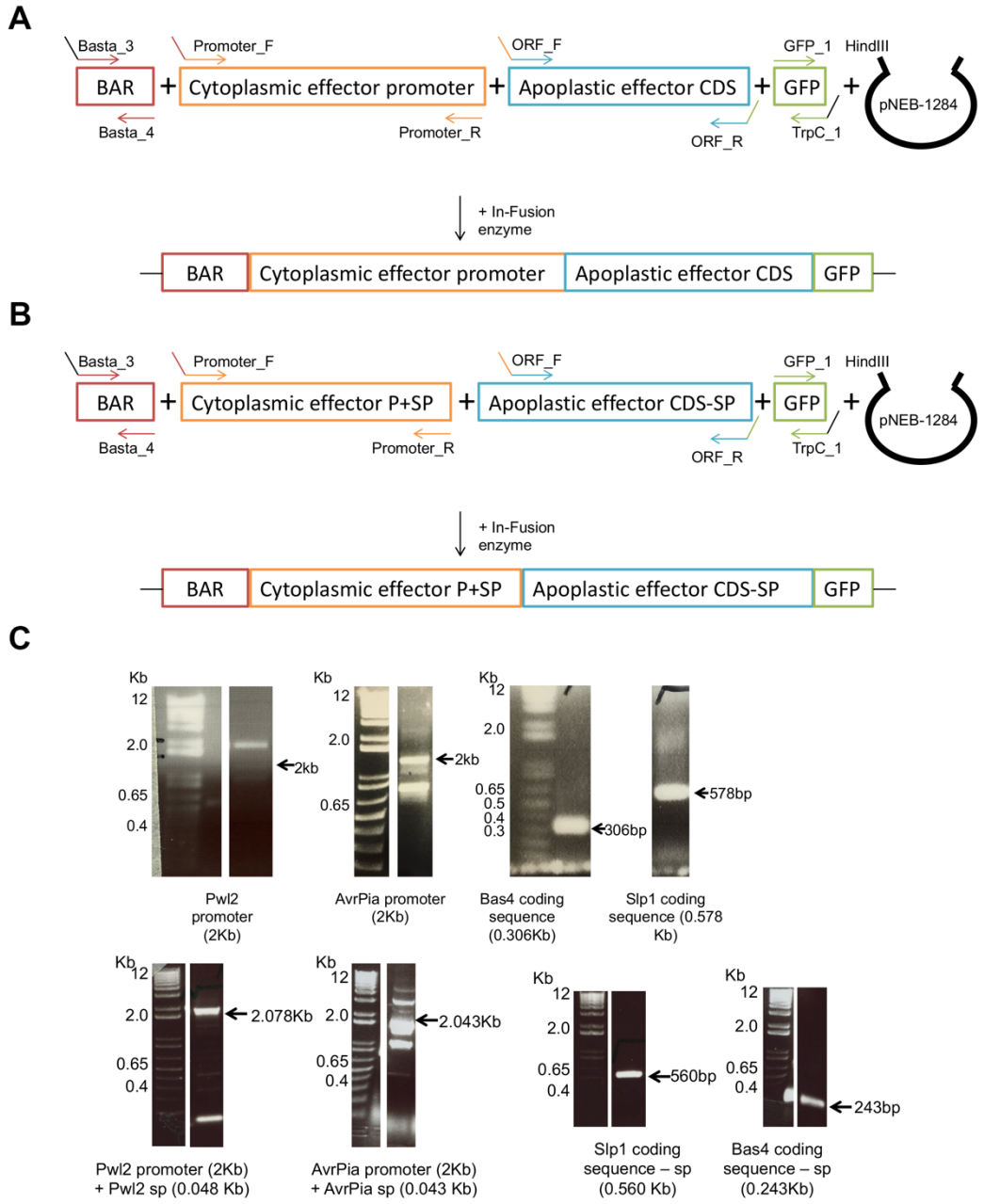


Figure 3.10 **Schematic representation of cloning strategy for each chimeric effector gene construct and associated PCR amplifications** A) Cloning strategy for the chimeric constructs using the promoter gene region of cytoplasmic effectors to drive the apoplastic effector genes *BAS4* and *SLP1*. B) Cloning strategy for each chimera constructs using the promoter and signal peptide gene regions of cytoplasmic effectors and the coding gene regions without its predicted signal peptide of apoplastic effectors *BAS4* and *SLP1*. C) PCR amplification of the fragments 2kb *PWL2* promoter, 2kb *AVRPIA* promoter, 2.078 kb *PWL2* promoter and signal peptide, 2.043 kb *AVRPIA* promoter and signal peptide, 306 bp of *BAS4* coding sequence, 578 bp *SLP1* coding sequence, 243 bp of *BAS4* coding sequence without its predicted signal peptide and 560 bp *SLP1* coding sequence without its predicted signal peptide.

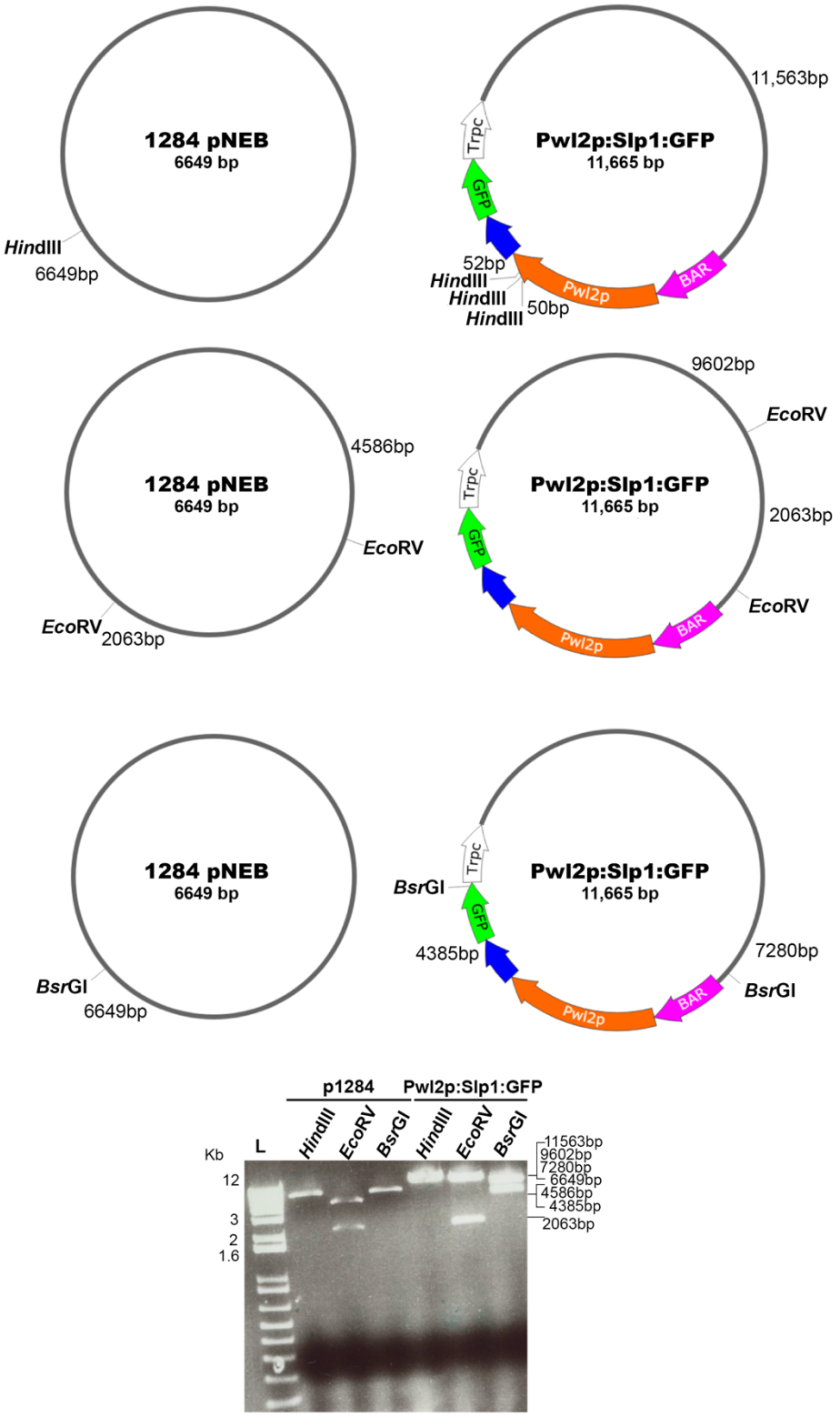


Figure 3.11 ***PWL2p:SLP1:GFP* plasmid verification by restriction digestion.** SnapGene software (from GSL Biotech; available at snapgene.com) was used to predict the expected fragment sizes. Positive PCR for *PWL2p:SLP1:GFP* and pNEB-1284 empty vector were digested with *Hin*dIII, *Eco*RV and *Bsr*GI. *Hin*dIII linearised pNEB-1284 and has pattern of 50 bp, 52 bp (not seen) and 11563 bp for *PWL2p:SLP1:GFP*. *Eco*RV cuts pNEB-1284 into 2063 bp and 4586 bp and cuts *PWL2p:SLP1:GFP* in 2063 bp and 9602 bp. *Bsr*GI linearises pNEB-1284 and cuts *PWL2p:SLP1:GFP* into 4385 bp and 7280 bp. Gene regions: Pink = BAR gene, Blue = apoplastic effector, Orange = cytoplasmic effector, Green = GFP and White = TrpC terminator.

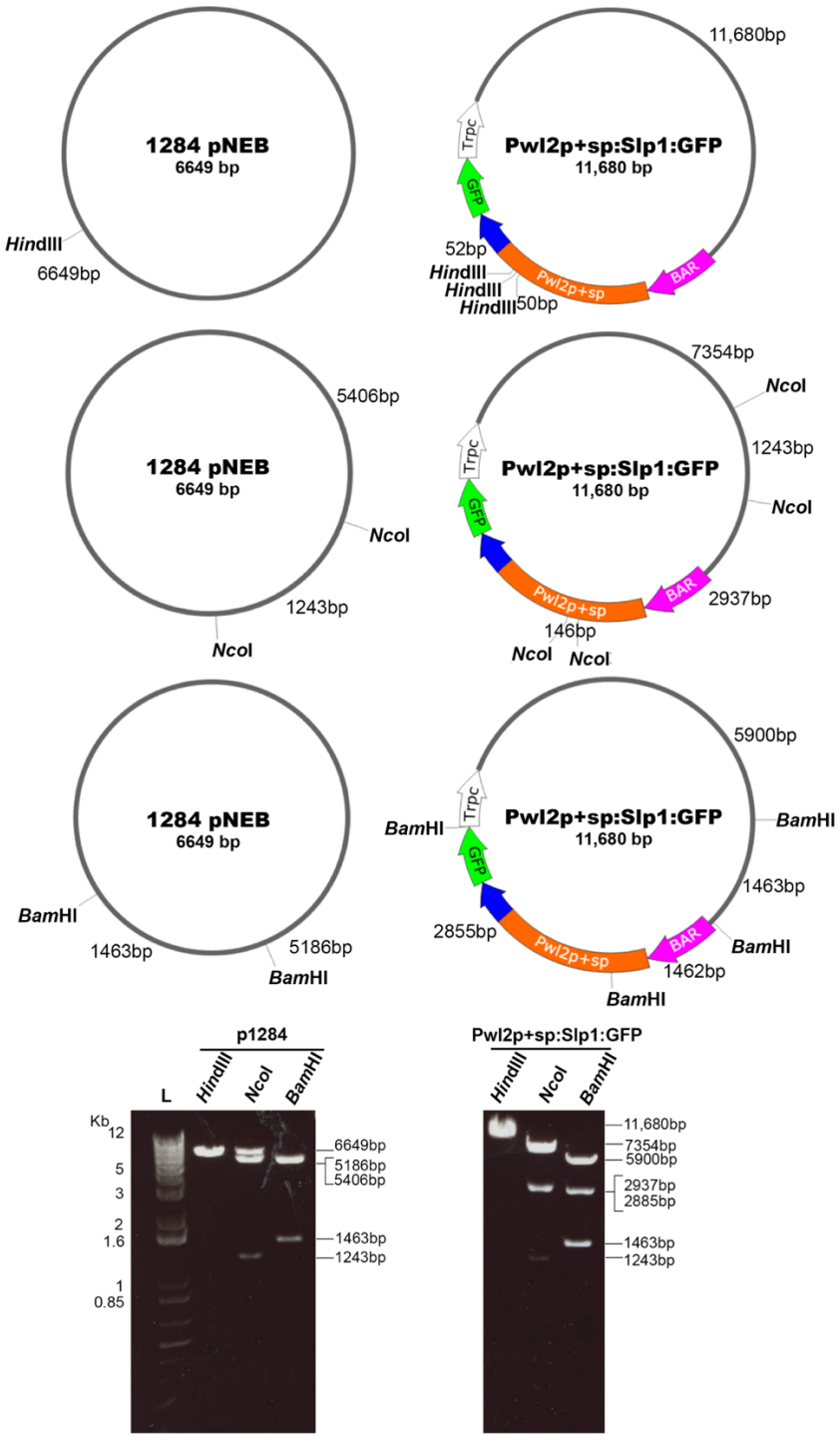


Figure 3.12 ***PWL2p+sp:SLP1:GFP* plasmid verification by restriction digestion.** SnapGene software (from GSL Biotech; available at snapgene.com) was used to predict fragment sizes. *PWL2p+sp:SLP1:GFP* and pNEB1284 were digested with *Hin*dIII, *Nco*I and *Bam*HI. *Hin*dIII linearised pNEB-1284 and cuts 50 bp, 52 bp (not seen) and 11680 bp for *PWL2p+sp:SLP1:GFP*. *Nco*I cuts pNEB-1284 into 1463 bp and 5406 bp and *PWL2p+sp:SLP1:GFP* in 1243 bp, 2937 bp, 146 bp (not seen) and 7354 bp. *Bam*HI cuts pNEB-1284 into 1463 bp and 5186 bp and *PWL2p+sp:SLP1:GFP* into 1463 bp, 1462 (not seen), 2855 bp and 5900 bp. Gene regions in colours: Pink = BAR gene, Blue = apoplastic effector, Orange = cytoplasmic effector, Green = GFP and White = TrpC terminator.

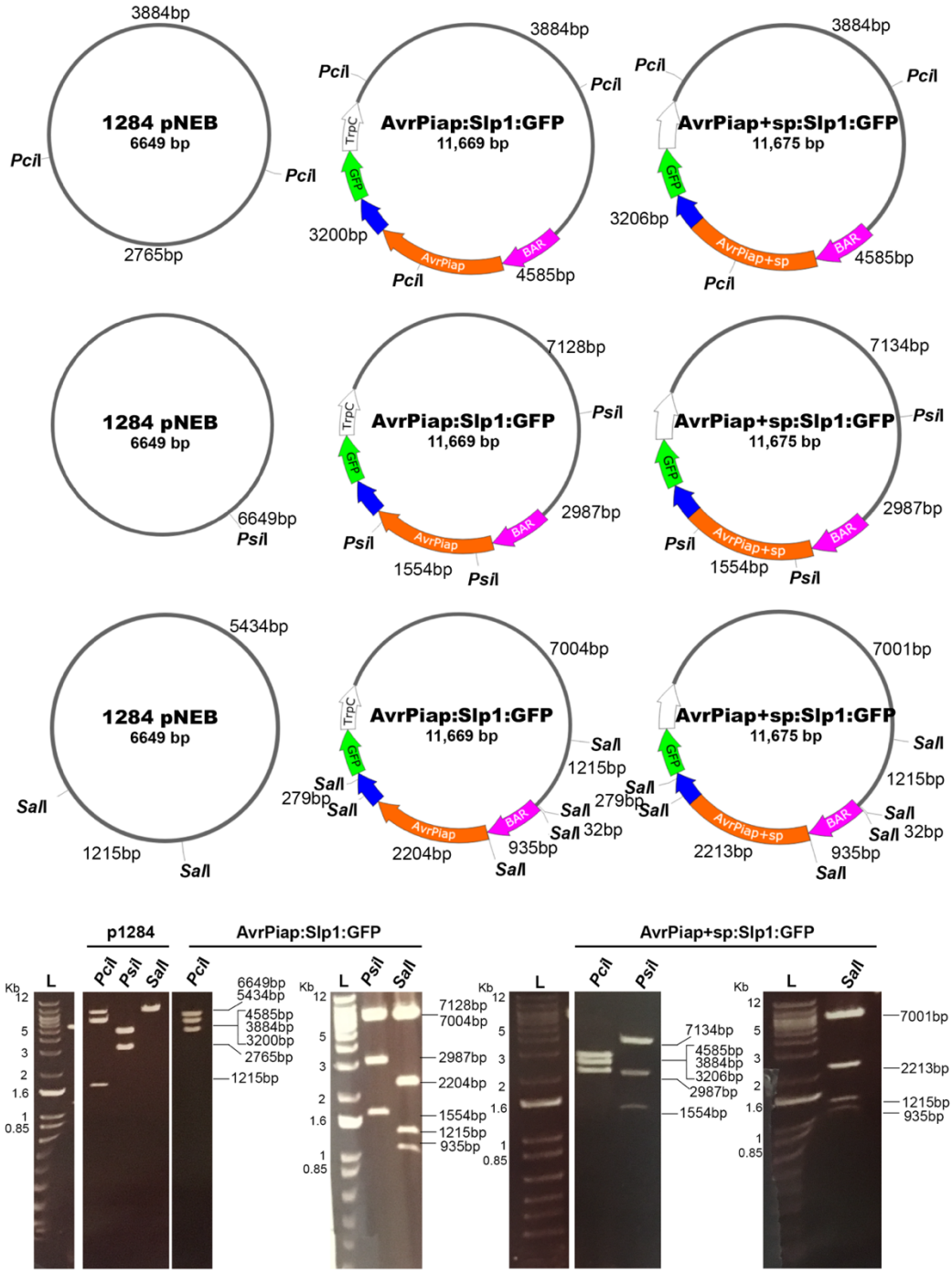


Figure 3.13 ***AVRPIAp:SLP1:GFP* and *AVRPIAp+sp:SLP1:GFP* plasmid verification by restriction digestion.** SnapGene software (from GSL Biotech; available at snapgene.com) was used to predict the fragment sizes. *AVRPIAp:SLP1:GFP*, *AVRPIAp+sp:SLP1:GFP* and pNEB-1284 were digested with *Psi*I, *Sal*I and *Pci*I and fractionated by gel electrophoresis. *Pci*I displays a specific band size pattern of 2765 bp and 3884 bp for pNEB-1284, 4585 bp, 3200 bp and 3884 bp for *AVRPIAp:SLP1:GFP* and 4585 bp, 3206 bp and 3884 bp for *AVRPIAp+sp:SLP1:GFP*. *Psi*I linearised the empty pNEB-1284 vector and has a band size pattern of 2987 bp, 1554 bp and 7128 bp for *AVRPIAp:SLP1:GFP* and 2987 bp, 1554 bp and 7134 bp for *AVRPIAp+sp:SLP1:GFP*. *Sal*I cuts pNEB-1284 into 2 fragments 1215 bp and 5434 bp, whereas *Sal*I cuts *AVRPIAp:SLP1:GFP* and *AVRPIAp+sp:SLP1:GFP* into 6 fragments 1215 bp, 32 bp (not seen), 935 bp, 2204 bp, 279 bp (not seen) and 7004 bp for *AVRPIAp:SLP1:GFP* and 1215 bp, 32 bp (not seen), 935 bp, 2213 bp, 279 bp (not seen) and 7001 bp for *AVRPIAp+sp:SLP1:GFP*. Gene regions in colours: Pink = BAR gene, Blue = apoplastic effector, Orange = cytoplasmic effector, Green = GFP and White = TrpC terminator.

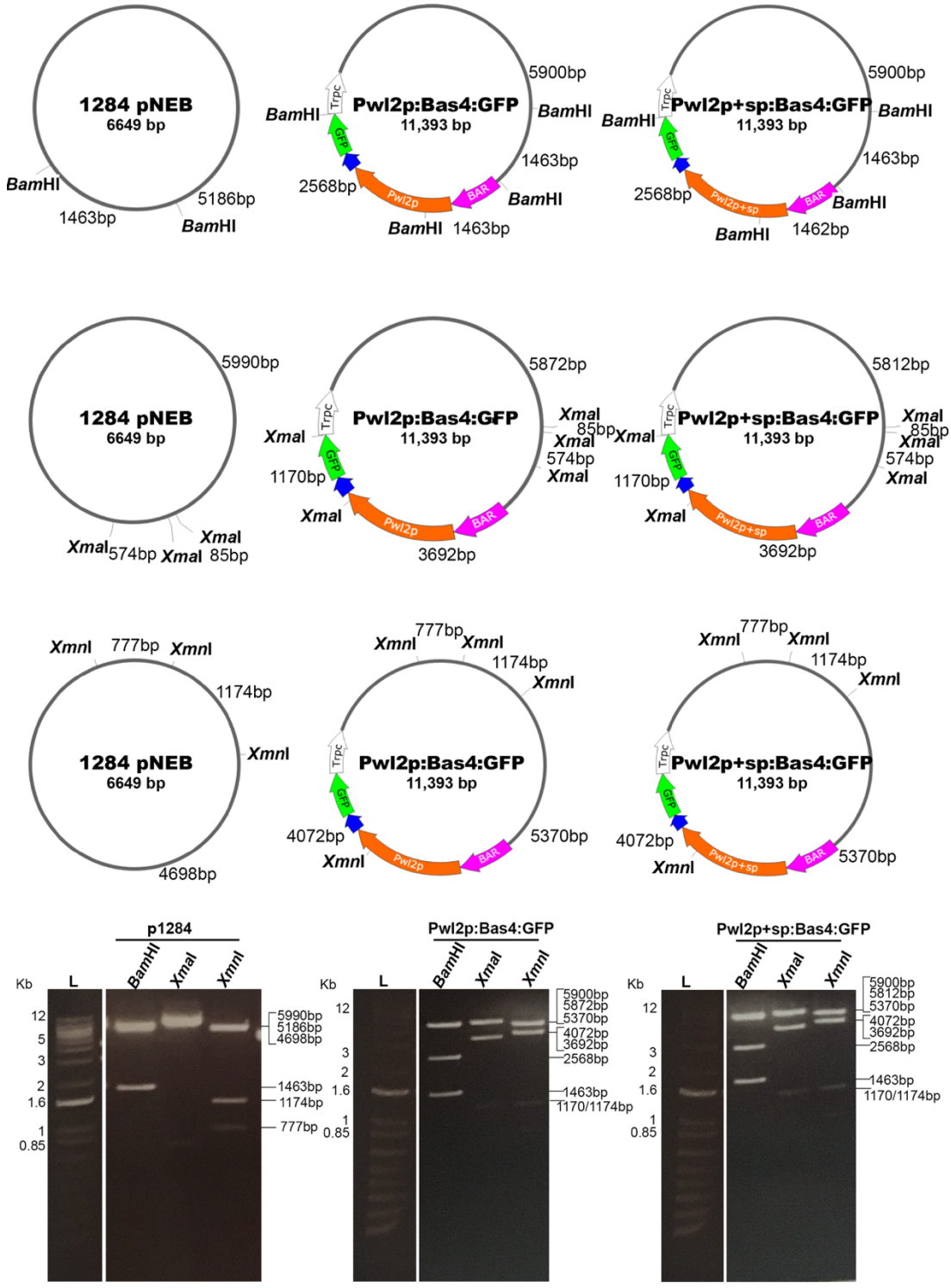


Figure 3.14 ***PWL2p:BAS4:GFP* and *PWL2p+sp:BAS4:GFP* plasmid verification by restriction digestion.** SnapGene software (from GSL Biotech; available at snapgene.com) was used to predict the fragment sizes. *PWL2p:BAS4:GFP*, *PWL2p+sp:BAS4:GFP* and pNEB-1284 were digested with *Bam*HI, *Xma*I and *Xmn*I. *Bam*HI cuts pNEB-1284 into 1463 bp and 5186 bp. *Bam*HI cuts *PWL2p:BAS4:GFP* and *PWL2p+sp:BAS4:GFP* into 1463 bp, 1462 bp, 2568 bp and 5900 bp. *Xma*I cuts into 85 bp, 574 bp (not seen) and 5990 bp pNEB-1284 and 85 bp, 574 bp (not seen) 2987 bp, 3692 bp, 1170 bp and 5872 bp or 5812 for *PWL2p:BAS4:GFP* and *PWL2p+sp:BAS4:GFP*, respectively. *Xmn*I cuts pNEB-1284 into 777 bp, 1174 bp and 4698 bp, whereas *Xmn*I cuts *PWL2p:BAS4:GFP* and *PWL2p+sp:BAS4:GFP* into 777 bp (not seen), 1174 bp, 5370 bp and 4072 bp. Gene regions in colours: Pink = BAR gene, Blue = apoplastic effector, Orange = cytoplasmic effector, Green = GFP and White = TrpC terminator.

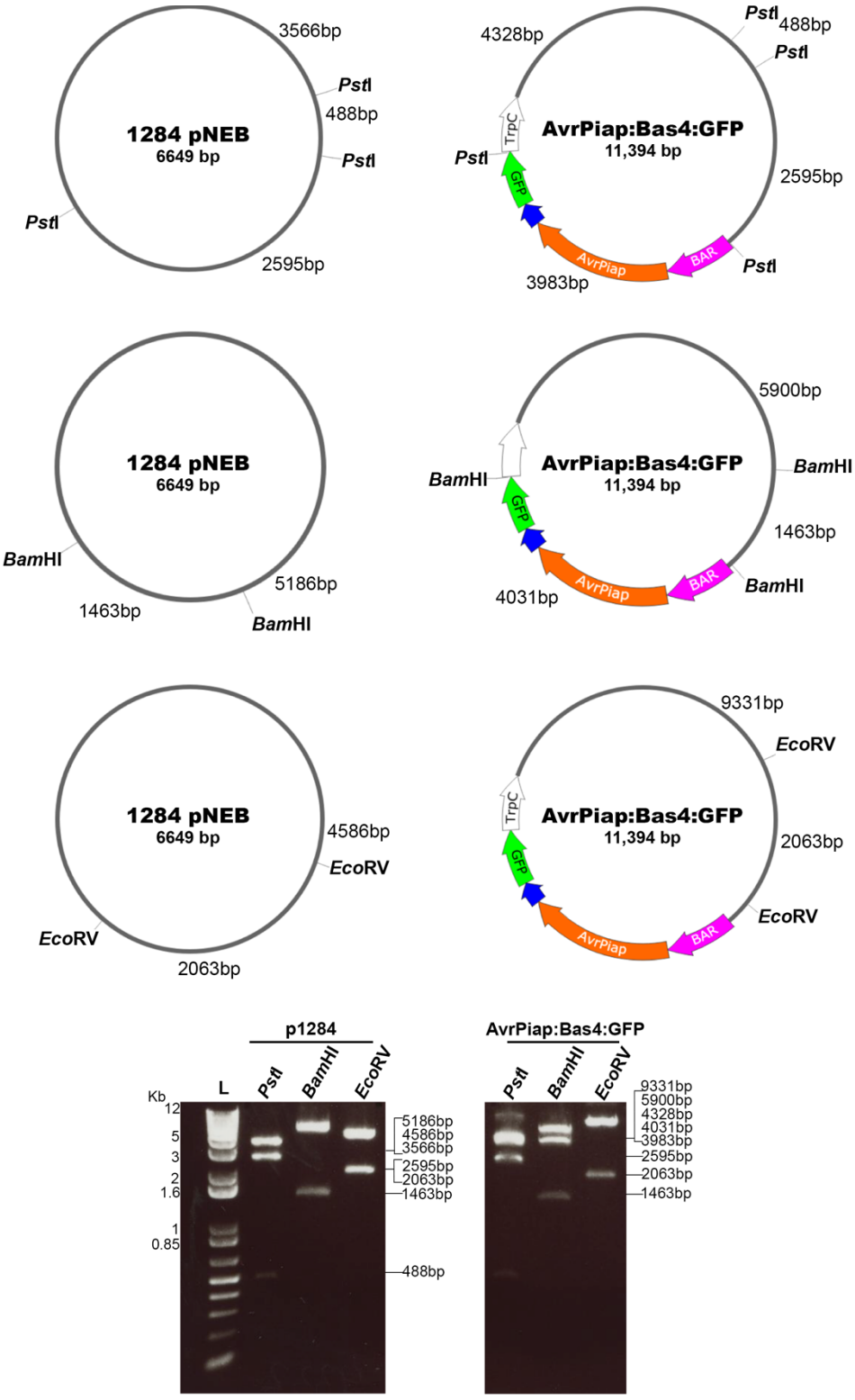


Figure 3.15 ***AVRPIAp:BAS4:GFP* plasmid verification by restriction digestion.** SnapGene software (from GSL Biotech; available at snapgene.com) was used to predict fragment sizes. Positive PCR for *AVRPIAp:BAS4:GFP* and pNEB-1284 were digested with *Pst*I, *Bam*HI and *Eco*RV. *Pst*I cuts 488 bp (not seen), 2595 bp and 3566 bp for pNEB-1284, whereas for *AVRPIAp:BAS4:GFP* is 488 bp (not seen), 2595 bp, 3983 bp and 4328 bp. *Bam*HI cuts pNEB-1284 into 1463 bp and 5186 bp and *AVRPIAp:BAS4:GFP* into 1463 bp, 4031 bp and 5900 bp. *Eco*RV cuts pNEB-1284 into fragments 2063 bp and 4586 bp and cuts *AVRPIAp:BAS4:GFP* in 2063 bp and 9331 bp. Gene regions in colours: Pink = BAR gene, Blue = apoplastic effector, Orange = cytoplasmic effector, Green = GFP and White = TrpC terminator.

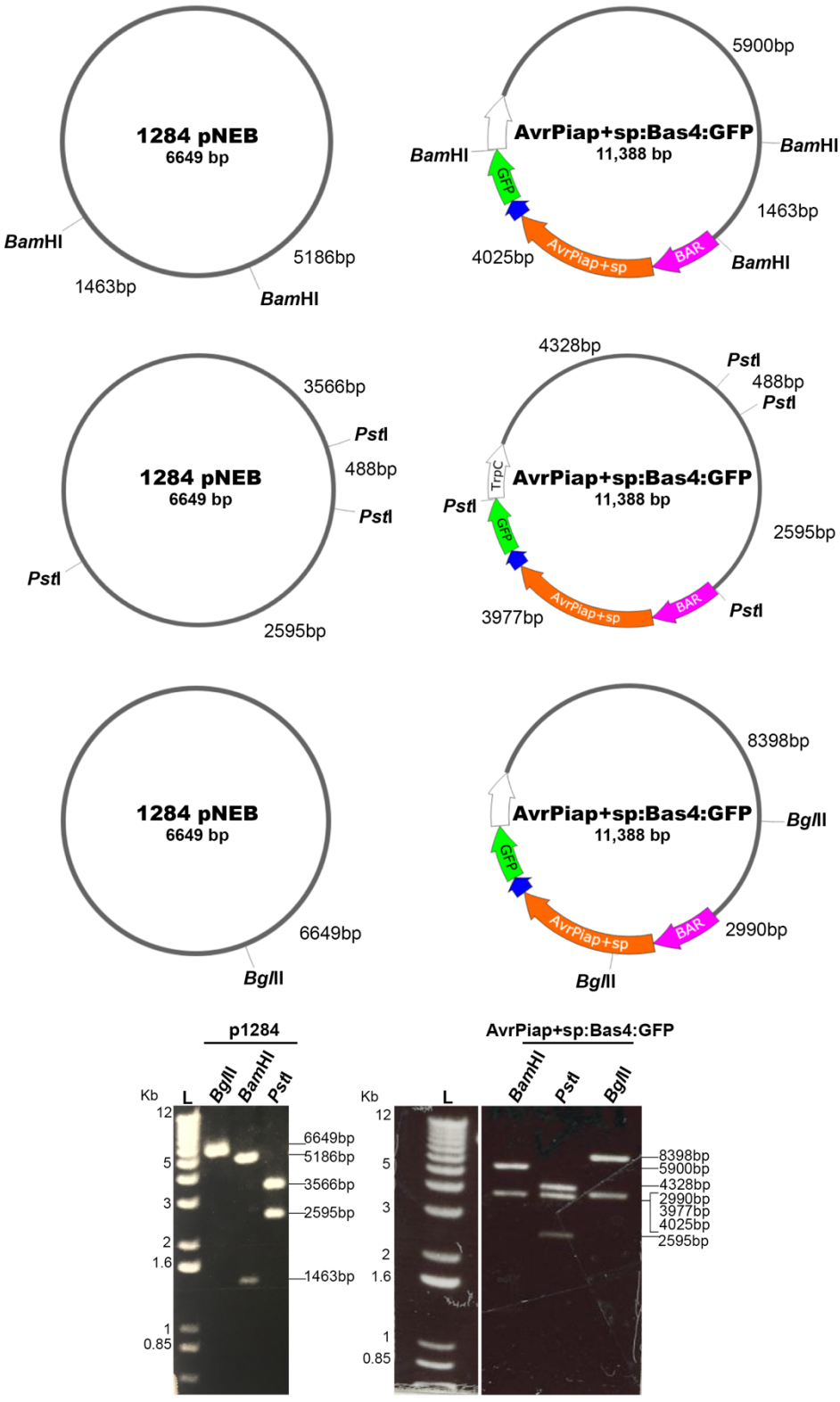


Figure 3.16 ***AVRPIAp+sp:BAS4:GFP* plasmid verification by restriction digestion.** SnapGene software (from GSL Biotech; available at snapgene.com) was used to predict fragment sizes. Positive PCR for *AVRPIAp+sp:BAS4:GFP* and pNEB-1284 were digested with *Bgl*II, *Bam*HI and *Pst*I. *Bgl*II linearised pNEB-1284 and cuts *AVRPIAp+sp:BAS4:GFP* into, 1463 bp (very faint), 4025 bp and 5900 bp. *Pst*I cuts of 488 bp (not seen), 2595 bp and 3977 bp for pNEB-1284, whereas for *AVRPIAp+sp:BAS4:GFP* is 488 bp (not seen), 2595 bp, 3983 bp and 4328 bp. *Bam*HI cuts pNEB-1284 into 1463 bp and 5186 bp and AvrPiap+sp:Bas4:GFP into 2990 bp and 8398 bp. Gene regions in colours: Pink = BAR gene, Blue = apoplastic effector, Orange = cytoplasmic effector, Green = GFP and White = TrpC terminator.

Confirmation of single copy transformants was initially carried out routinely by Southern blot analysis (Sambrook and Russell, 2006). The probe used was a 1kb GFP:*trp*C fragment. An example of a Southern blot used to analysis *M.oryzae* transformants expressing AvrPiap:Bas4:GFP and Bas4p:AvrPia:GFP, is shown in Figure 3.17. Southern blot analysis cannot, however, easily distinguish when the plasmid is inserted in multiple tandem copies. For this reason, we subsequently used a qPCR method to determine GFP copy number of plasmid insertion, as shown in Table 3.4. This was eventually contracted in blind tests to iDNA Genetics Ltd (Norwich Research Park) to enable rigorous independent analysis of all transformants generated in the study.

In the Southern blot analysis shown in Figure 3.17, transformant AvrPiap:Bas4:GFP#1 and AvrPiap:Bas4:GFP#2 both show single copy insertions, which were subsequently corroborated by qPCR in Table 3.4. The single copy transformants used in this study are in Table 3.3. For Pwl2p:Bas4:GFP and Pwl2p+sp:Bas4:GFP, we could not find more than one single copy transformant. Pwl2p:Bas4:GFP#6 and Pwl2p+sp:Bas4:GFP#3 (2 and 8 GFP copies) were used as the second pair of chimera transformants to analyse for mislocalisation of Bas4.

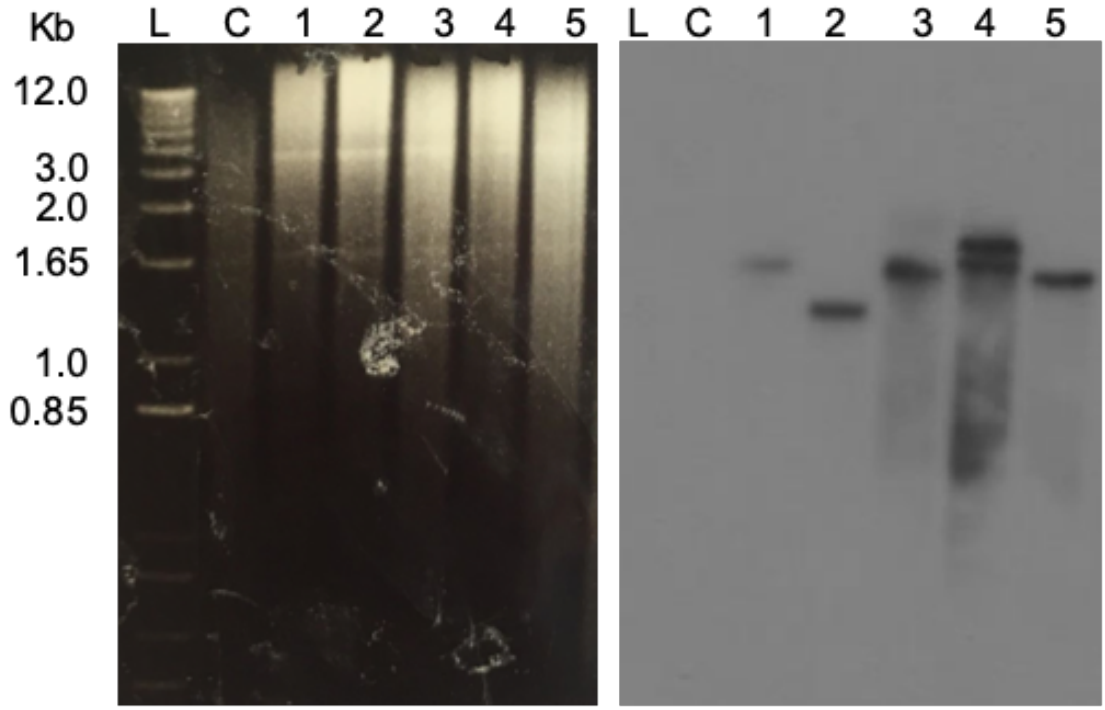


Figure 3.17 **Southern Blot analysis.** Genomic DNA was digested with *Pml*I restriction enzyme. The DNA was transferred to a Hybond-XN membrane (Amesham) and probed with 1kb probe of GFP:*trp*C fragment. As a control Guy 11 DNA was used. Lane 1 is AvrPiap:Bas4:GFP#1. Lane 2 is AvrPiap:Bas4:GFP#2. Lane 3 is Bas4p:AvrPia:GFP#1. Lane 4 is Bas4p:AvrPia:GFP#3. Lane 5 is Bas4p:AvrPia:GFP#4. Single copy transformants AvrPiap:Bas4:GFP#1, AvrPiap:Bas4:GFP#2, Bas4p:AvrPia:GFP#1, Bas4p:AvrPia:GFP#4 were used for subsequent analysis.

Table 3.4 Determination of GFP copy number by qPCR for chimeric constructs

| Sample | Copies GFP[1] | Sample | Copies GFP[1] |
|---|---|---|---|
| Control | 1 | Pwl2pSlp1#2 | 4 |
| Guy11 | 0 | Pwl2pSlp1#3 | 1 |
| AvrPiapBas4#1 | 1 | Pwl2pSlp1#6 | 1 |
| AvrPiapBas4#2 | 1 | Pwl2pSlp1#8 | 1 |
| AvrPiap+spBas4#1 | 2 | Pwl2pSlp1#9 | 2 |
| AvrPiap+spBas4#3 | 1 | Pwl2p+spSlp1#5 | 1 |
| AvrPiap+spBas4#4 | 6 | Pwl2p+spSlp1#6 | 1 |
| AvrPiap+spBas4#5 | 5 | Pwl2pBas4#1 | 2 |
| AvrPiap+spBas4#6 | 7 | Pwl2pBas4#3 | 1 |
| AvrPiap+spBas4#7 | 2 | Pwl2pBas4#6 | 2 |
| AvrPiap+spBas4#8 | 1 | Pwl2pBas4#7 | 4 |
| AvrPiap+spBas4#9 | 1 | Pwl2pBas4#9 | 2 |
| AvrPiapSlp1#1 | 4 | Pwl2pBas4#21 | 5 |
| AvrPiapSlp1#3 | 4 | Pwl2pBas4#24 | 4 |
| AvrPiapSlp1#5 | 22 | Pwl2pBas4#29 | 3 |
| AvrPiapSlp1#6 | 1 | Pwl2p+spBas4#3 | 8 |
| AvrPiapSlp1#12 | 1 | Pwl2p+spBas4#5 | 1 |
| AvrPiap+spSlp1#1 | 1 | Pwl2p+spBas4#22 | 14 |
| AvrPiap+spSlp1#11 | 1 | Pwl2p+spBas4#23 | 2 |
| AvrPiap+spSlp1#15 | 1 | | |

[1] Blind qPCR test were performed by iDnaGENETICS Ltd (Norwich Research Park).

### 3.3.4 Promoter and signal peptide regions of cytoplasmic effectors are involved in localisation pattern of apoplastic effector Slp1

I next set out to investigate whether the localisation pattern of an apoplastic effector is affected when it is expressed under control of the promoter region of a cytoplasmic effector gene, or the promoter and signal peptide combination of a cytoplasmic effector gene. To do this, a series of chimeric constructs were made and expressed in *M. oryzae.*

The Slp1 effector protein has been reported to localize around *M. oryzae* invasive hyphae, in the EIHM (Mentlak et al., 2012). Single copy transformants expressing AvrPiap:Slp1:GFP, AvrPiap+sp:Slp1:GFP, Pwl2p:Slp1:GFP and Pwl2p+sp:Slp1:GFP (Table 3.3) were therefore used to test whether Slp1 localisation around the invasive hyphae is maintained when *SLP1* is expressed under the control of *AVRPIA* and *PWL2* promoter gene region, or *AVRPIA* and *PWL2* promoter and predicted signal peptide regions combined. The Slp1:GFP construct from the lab strains collection generated by T. Mentlak (Mentlak et al., 2012) was used as a control for Slp1 protein localisation, as it is driven under the control of its native promoter (Figure 3.18 A).

*M. oryzae* Guy11 strains Pwl2p:Slp1:GFP, Pwl2p+sp:Slp1:GFP, and Slp1:GFP (Mentlak et al., 2012) were grown on CM plates. After 9 days, spores were collected and resuspended in $dH_2O$. The resulting spore suspension was inoculated into epidermal leaf tissue, as previously described (section 2.6.1). Then, 30 hours post inoculation (hpi) the infected rice leaf sheaths were visualised by epifluorescence light microscopy. I observed and recorded every cell in which *M. oryzae* was growing. At 30hpi, most *M. oryzae* appressoria had penetrated cells and developed invasive hyphae, with a BIC always observed in the first bulbous invasive hypha. From every infection recorded, the number of infections in which Slp1 protein localisation was observed around invasive hyphae, and those that showed mislocalisation of Slp1 to the BIC, were recorded.

Slp1 is an apoplastic effector and normally observed to localise around *M. oryzae* invasive hyphae, when expressed under control of it native promoter, as shown in Figure 3.18 A. When Slp1 was driven by the promoter of *PWL2,* in *M. oryzae* strain Pwl2p:Slp1:GFP, localisation was also observed around invasive hyphae (Figure 3.18 A). However, when I observed Slp1 driven by both the promoter and

signal peptide region of *PWL2*, the fusion protein was observed at the BIC Figure 3.18 A. The localisation of Pwl2p+sp:Slp1:GFP was significantly different to that of Slp1:GFP (*P<0.05)* as shown in Figure 3.18 B. I conclude that the promoter and signal peptide region of *PWL2* is sufficient to enable secretion of a proportion of the Slp1 effector protein into the BIC.

To investigate whether this effect was specific to the *PWL2* promoter and signal peptide regions, or a more general characteristic of cytoplasmic effector genes, I generated *M. oryzae* strains expressing *SLP1* under control of the promoter, or promoter and signal peptide, of *AVRPIA*. Microscopy observation for each strain was recorded in the same way, as above. *M. oryzae* strains expression AvrPiap:Slp1:GFP, AvrPiap+sp:Slp1:GFP and Slp1:GFP were grown in CM plates. Spore suspensions were then used to infect epidermal rice leaf tissue and observed after 30h.

The Slp1:GFP control showed fluorescence around invasive hyphae, as expected. Transformants expressing AvrPiap:Slp1:GFP showed localisation to invasive hyphae with a small (non-significant *P>0.05)* proportion also showing BIC localisation (Figure 3.19 A). Transformants expressing AvrPiap+sp:Slp1:GFP showed an increased frequency of BIC fluorescence. There was a significance difference between localisation patterns of AvrPiap:Slp1:GFP, AvrPiap+sp:Slp1:GFP and Slp1:GFP (*P<0.05)* as shown in Figure 3.19 B. I conclude that the promoter and signal peptide region of *AVRPIA* are also able to facilitate delivery of the Slp1 effector into the BIC.

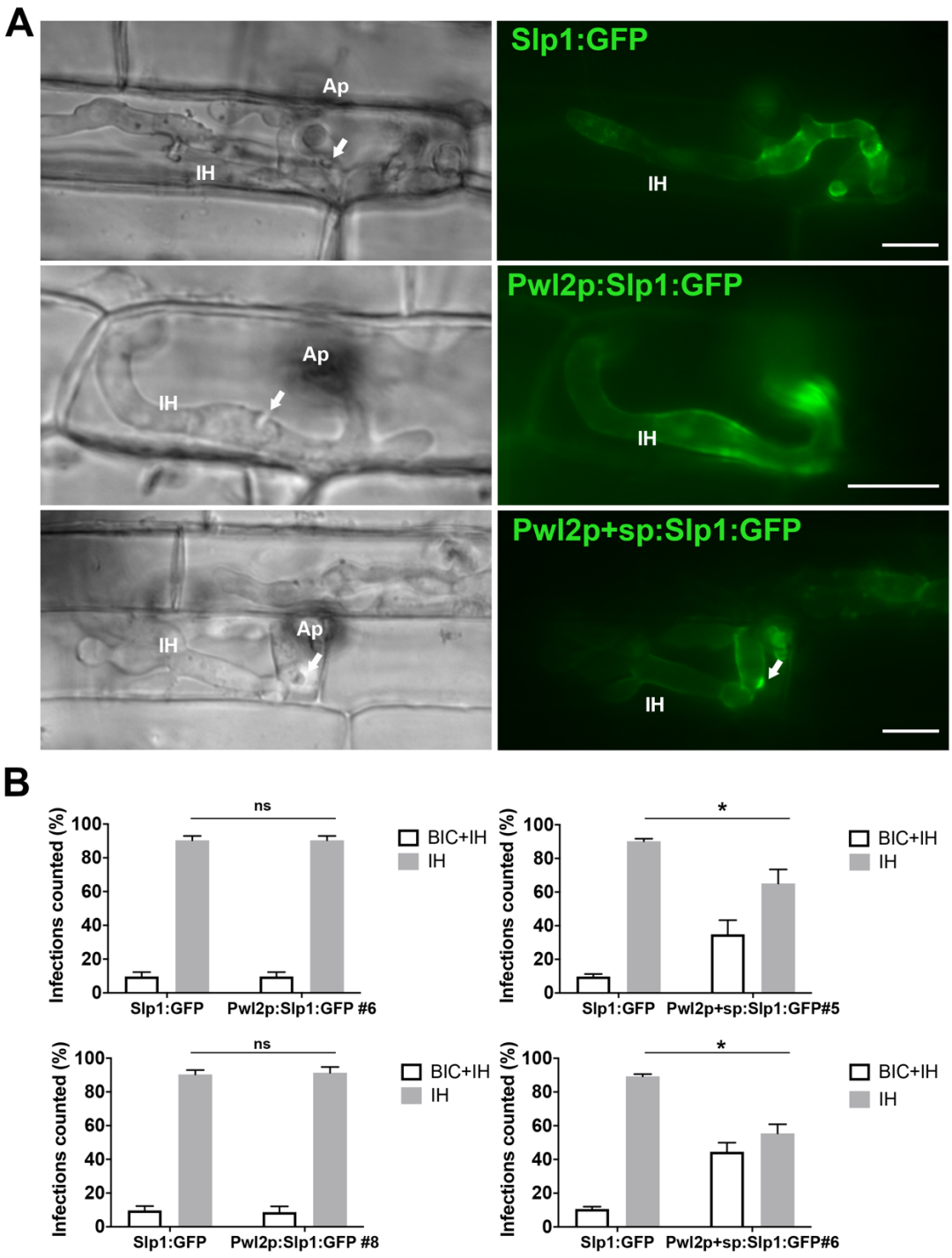


Figure 3.18 **The promoter and signal peptide of cytoplasmic effector gene *PWL2* drive Slp1 effector protein into the BIC.** Micrographs from live cell imaging of leaf sheaths of *M. oryzae* infection of rice by epifluorescence microscopy. A) Localisation of Slp1-GFP, Pwl2p:Slp1-GFP and Pwl2p+sp:Slp1-GFP. B) Bar charts to show proportion of BIC structures showing fluorescence. From transformants Pwl2p:Slp1:GFP#6 and Pwl2p:Slp1:GFP#8, a total of 3 replicates were made with 80 infections observed. An unpaired t-test with a two-tailed distribution gave a *P*-value of 0.99 for Pwl2p:Slp1:GFP#6 and a *P*-value of 0.86 for Pwl2:Slp1:GFP#8. From the Pwl2p+sp:Slp1:GFP#5 and Pwl2p+sp:Slp1:GFP#6 constructs a total of 4 replicates was made with 130 infections observed. An unpaired t-test with a two-tailed distribution gave a *P*-value of 0.03 for Pwl2p+sp:Slp1:GFP#5 and a *P*-value of 0.02 for Pwl2p+sp:Slp1:GFP#6. All the strains were excited at 488nm for 200 ms. Scale bars represent 10 µm. Arrow marks the BIC, Ap marks the appressorium and IH marks *M. oryzae* invasive hyphae.

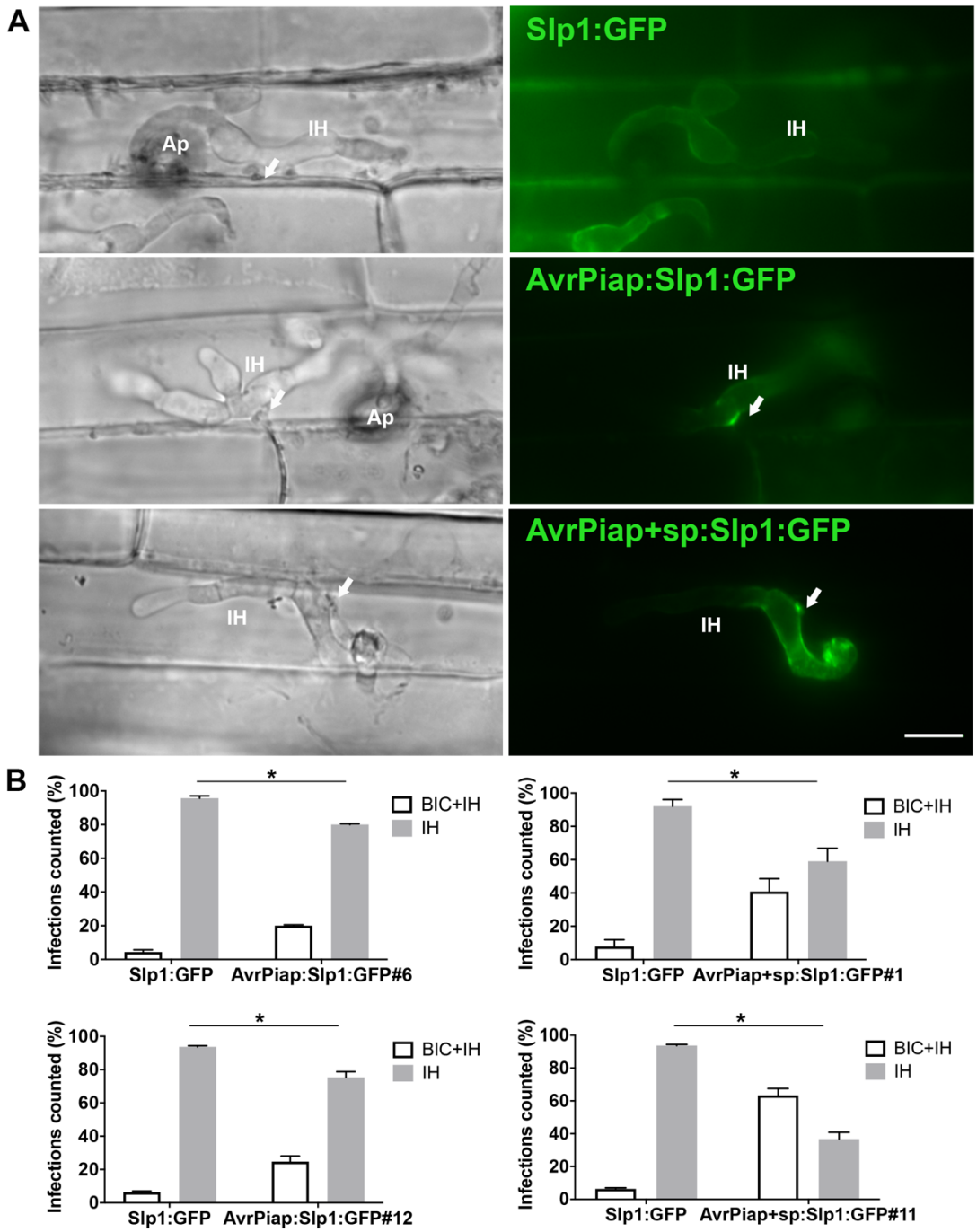


Figure 3.19 **The promoter and signal peptide of cytoplasmic effector gene *AVRPIA* drive Slp1 effector protein into the BIC.** Micrographs of live cell imaging of leaf sheaths of *M. oryzae* infection of rice. A) Localisation of Slp1:GFP, AvrPiap:Slp1:GFP and AvrPiap+sp:Slp1:GFP. B) Bar charts to show proportion of BIC structures with fluorescence. From AvrPiap:Slp1:GFP#6 and AvrPiap:Slp1:GFP#12 a total of 3 replicates was made with 89 infections counted. An unpaired t-test with a two-tailed distribution gave a *P*-value of 0.004 for AvrPiap:Slp1:GFP#6 and a *P*-value of 0.006 for AvrPiap:Slp1:GFP#12. From the AvrPiap+sp:Slp1:GFP#1 and AvrPiap+sp:Slp1:GFP#11 3 replicates was made with 94 infections counted. An unpaired t-test with a two-tailed distribution gave a *P*-value of 0.031 for AvrPiap+sp:Slp1:GFP#1 and a *P*-value of 0.002 for AvrPiap+sp:Slp1:GFP#11. All the strains were excited at 488nm for 200 ms. Scale bars represent 10 µm. Arrow marks the BIC, Ap marks the appressorium and IH marks *M. oryzae* invasive hyphae.

### 3.3.5 Promoter and signal peptide regions of cytoplasmic effectors are involved in localisation pattern of apoplastic effector Bas4

Having determined that the promoter and signal peptide regions of a cytoplasmic effectors were sufficient to direct the apoplastic Slp1 effector to the BIC, I decided to investigate whether this effect could be reproduced using a second apoplastic effector. To do this, I used the Bas4 apoplastic effector, which surrounds the invasive hyphae at the EIHM. This effector does, however, also show some localisation to the BIC when expressed under its native promoter (Mosquera et al., 2009). However, plasmolysis assays have demonstrated that Bas4 is not internalised by the host cytoplasm, even though some BIC localisation is apparent (Kankanala et al., 2007; Giraldo et al., 2013). It is possible that high level expression of *BAS4* causes a proportion of the effector to accumulate in the BIC (Mosquera et al., 2009; Giraldo et al., 2013). In view of this localisation pattern, it became clear that I could not use the same quantification strategy used for the *SLP1* chimeric constructs. I therefore used a line scan analysis in MetaMorph (Molecular Devices) to quantify the maximum fluorescence intensity at the BIC and the maximum intensity in the first bulbous hyphae. This was recorded as a ratio defined as maximum intensity BIC/ maximum intensity invasive hyphae ($GFP^{BIC}/GFP^{IH}$). This allowed me to compare a transformant expressing Bas4:GFP under expression of its own promoter, with a series of *M. oryzae* strains, expressing *BAS4* chimeras, in which the promoter, or promoter- and signal peptide regions, we used to drive *BAS4* expression. My hypothesis was that the proportion of Bas4 directed to the BIC would increase when driven by the alternative cytoplasmic effector gene promoter and signal peptide. The fluorescence intensity at the BIC cannot be compared directly between strains because the C-terminal GFP fusion constructs were inserted ectopically in Guy11 *M. oryzae*, such that position effects on expression levels cannot be ruled out. However, I reasoned that the $GFP^{BIC}/GFP^{IH}$ ratio could be compared between strains.

First, *M. oryzae* transformants expressing *BAS4* under the control of the *PWL2* promoter, or promoter and signal peptide, were observed. A Bas4:GFP transformant (Giraldo et al., 2013) was used as a control. *M. oryzae* Guy11 Pwl2p:Bas4:GFP, Pwl2p+sp:Bas4 and Bas4:GFP transformants were grown in

CM plates for 9 days. Spore suspensions were collected and used to inoculate epidermal leaf tissue. After 30 h post inoculation (hpi) leaf sheaths were viewed by epifluorescence light microscopy. Every cell with *M. oryzae* growing as a bulbous invasive hypha was recorded, as previously described, using the line scan method.

I observed that the localisation of Pwl2p:Bas4:GFP (Figure 3.20 A) was similar to Bas4:GFP, surrounding invasive hyphae, and the $GFP^{BIC}/GFP^{IH}$ ratio showed no significant difference between Pwl2p:Bas4:GFP and Bas4:GFP as shown in Figure 3.20 B.

Localisation of Pwl2p+sp:Bas4:GFP was also observed around invasive hyphae and at the BIC (Figure 3.20 A). However, the $GFP^{BIC}/GFP^{IH}$ ratio showed a significant difference ($P$<0.001*)* between Pwl2p+sp:Bas4:GFP and Bas4:GFP (Giraldo et al., 2013) (Figure 3.20 B). This indicates that the fusion protein Pwl2p+sp:Bas4:GFP preferably accumulates at the BIC, compared to Bas4:GFP (Giraldo et al., 2013).

I then repeated the same analysis using an alternative cytoplasmic effector gene to drive *BAS4* expression. For this, *M. oryzae* transformants expressing Bas4 under the control of the *AVRPIA* promoter, or promoter and signal peptide sequence, were observed. Spore suspensions of transformants expressing AvrPiap:Bas4:GFP, AvrPiap+sp:Bas4 and Bas4:GFP constructs were collected. and used to inoculate rice leaf sheath tissue. Every cell with *M. oryzae* growing as a bulbous invasive hypha was recorded, as previously described using the line scan method.

I observed AvrPiap:Bas4:GFP localisation around *M. oryzae* invasive hyphae (Figure 3.21 A) and a Mann-Whitney test showed there no significant difference the $GFP^{BIC}/GFP^{IH}$ ratio between AvrPiap:Bas4:GFP and Bas4:GFP transformants (Giraldo et al., 2013) as shown in Figure 3.21 B. By contrast, there was a significant difference in the $GFP^{BIC}/GFP^{IH}$ ratio between AvrPiap+sp:Bas4:GFP and Bas4:GFP transformants (Giraldo et al., 2013). The AvrPiap+sp:Bas4:GFP transformants showed a $GFP^{BIC}/GFP^{IH}$ ratio similar to that observed with Pwl2p+sp:Bas4:GFP infections. I conclude that when the *BAS4* apoplastic effector gene is expressed under control of the *AVRPIA* promoter and signal peptide sequence, the Bas4 effector protein preferably accumulates at the

BIC. When considered together, these results provide evidence that the promoter together with the signal peptide gene regions of *PWL2* and *AVRPIA,* are able to re-direct apoplastic effectors to the BIC.

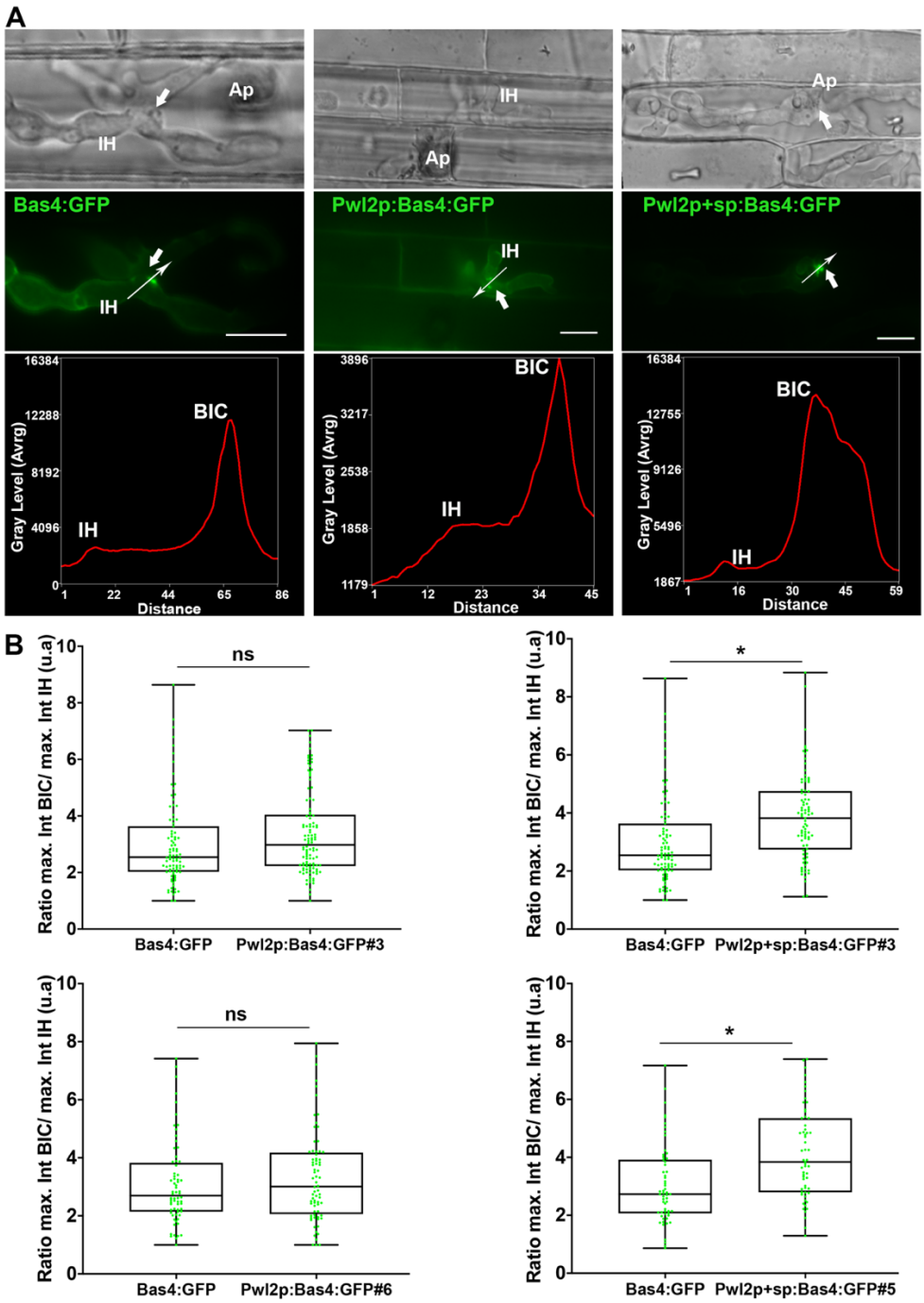


Figure 3.20 The promoter and signal peptide of cytoplasmic effector gene *PWL2* are sufficient to re-direct the Bas4 effector protein into the BIC. Micrographs from live cell imaging of rice leaf sheaths infected by *M. oryzae*. A) Localisation of Bas4:GFP, Pwl2p:Bas4:GFP and Pwl2p+sp:Bas4:GFP. B) Box and whiskers plots showing the $GFP^{BIC}/GFP^{IH}$ ratio for Pwl2p:Bas4:GFP#3, Pwl2p:Bas4:GFP#6 and Bas4:GFP control. From the constructs Pwl2p:Bas4:GFP#3 and Pwl2p:Bas4:GFP#6 a total of 3 replicates was made from 108 infections observed. A Mann-Whitney test gave a *P*-value of 0.05 for Pwl2p:Bas4:GFP#3 and a *P*-value 0.4 for Pwl2p:Bas4:GFP#6. Box and whisker plots showing the $GFP^{BIC}/GFP^{IH}$ ratio for Pwl2p+sp:Bas4#5, Pwl2p+sp:Bas4:GFP#3 and Bas4:GFP control. From the Pwl2p+sp:Bas4:GFP#5 and Pwl2p+sp:Bas4:GFP#3 constructs a total of 3 replicates was made with 59 infections observed. A Mann-Whitney test gave a *P*-value of 0.0001 for Pwl2p+sp:Bas4:GFP#5 and a *P*-value of 0.001 for Pwl2p+sp:Bas4:GFP#3. All the strains were excited at 488nm for 200 ms. Scale bars represent 10 µm. Arrow marks the BIC, Ap marks the appressorium and IH marks *M. oryzae* invasive hyphae.

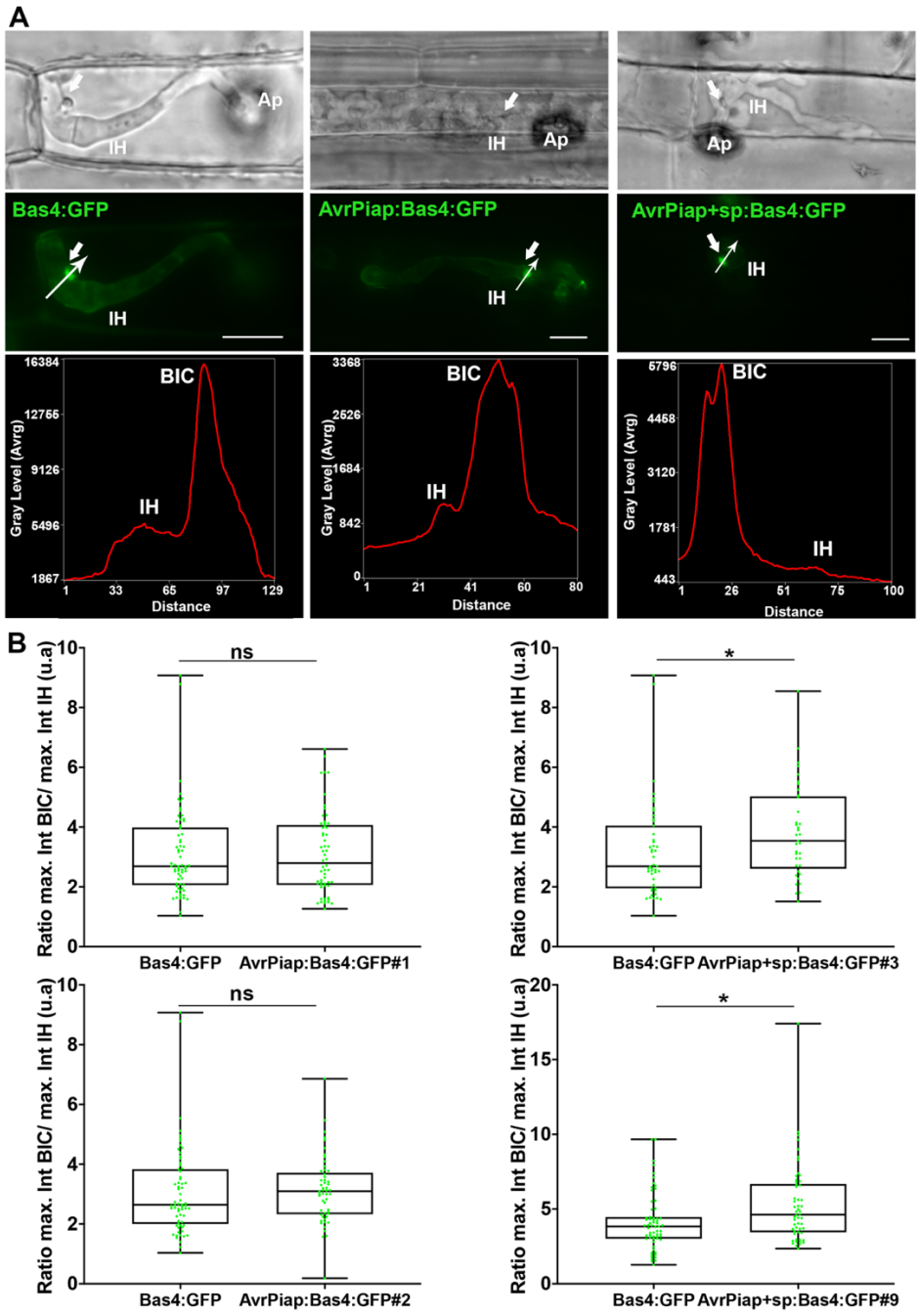


Figure 3.21 The promoter and signal peptide of cytoplasmic effector gene *PWL2* are sufficient to re-direct the Bas4 effector protein into the BIC. Micrographs of live cell imaging from leaf sheaths infected by *M. oryzae* observed by epifluorescence microscopy. A) Localisation of Bas4:GFP, AvrPiap:Bas4:GFP and AvrPiap+sp:Bas4:GFP. B) Box and whiskers plots showing $GFP^{BIC}/GFP^{IH}$ ratio for AvrPiap:Bas4:GFP#1, AvrPiap:Bas4:GFP#2 and Bas4:GFP control. From the constructs AvrPiap:Bas4:GFP#1 and AvrPiap:Bas4:GFP#2 a total of 3 replicates was made with 66 infections observed. A Mann-Whitney test gave a *P*-value of 0.9 for AvrPiap:Bas4:GFP#1 and a *P*-value of 0.3 for AvrPiap:Bas4:GFP#2. Box and whiskers plots showing $GFP^{BIC}/GFP^{IH}$ ratio for AvrPiap+sp:Bas4:GFP#3, AvrPiap+sp:Bas4:GFP#9 and Bas4:GFP control. From the AvrPiap+sp:Bas4:GFP#3 and AvrPiap+sp:Bas4:GFP#9 constructs a total of 3 replicates was made with 63 infections observed. A Mann-Whitney test gave a *P*-value of 0.03 for AvrPiap+sp:Bas4#3 and a *P*-value of 0.007 for AvrPiap+sp:Bas4:GFP#9. All the strains were excited at 488nm for 200 ms. Scale bars represent 10 µm. Arrow marks the BIC, Ap marks the appressorium and IH marks *M. oryzae* invasive hyphae.

### *3.4 Discussion*

In this chapter, I reported my initial investigations of the role of the promoter and signal peptide regions of effector-encoding genes in guiding the secretion of effector proteins. Promoters are normally associated with regulating the level of expression of a gene, in terms of the quantity of mRNA produced during transcription (Clancy, 2008). The role of this region to regulate localisation is therefore very unusual. Previous published reports had suggested, however, that the promoter region of a *M. oryzae* effector may be important in determining the manner in which it is secreted (Khang et al., 2010). I therefore set out to see if these observations were reproducible and then to systematically characterise the relative contribution of sequences at the 5' end of effector genes in guiding the secretory route of the associated effector protein.

The strategy I adopted was to generate a series of chimeras in which I swapped the promoters and signal peptide regions from cytoplasmic effector-encoding genes and placed these upstream of either the GFP fluorescent reporter gene or an apoplastic effector-encoding gene. First, I was able to show that GFP could be directed to the BIC when the *GFP* gene was expressed in *M. oryzae* under control of the promoter and signal peptide regions of either *PWL2* or *AVRPIA*. This is consistent with previous reports that the promoter and signal peptide regions of the cytoplasmic effector gene *Avr-PITA*, demonstrating the importance of these 5' sequences.

To test this idea further, I then generated a series of chimeric constructs to see whether localisation of apoplastic effectors was re-directed when Bas4 and Slp1 were expressed under the control of the promoter, or the promoter and signal peptide sequences of *PWL2* and *AVRPIA*, respectively. I observed that when the promoter and signal peptide region of either of the cytoplasmic effector genes *PWL2* or *AVRPIA* was used to control expression of Slp1-GFP a significant proportion of the fluorescent signal accumulated in the BIC. For the same constructs using Bas4 effector protein, I quantified a much larger number of observed infection sites and these too showed more accumulation at the BIC, when expressed under control of *PWL2* or *AVRPIA* promoter-signal peptide combinations. When considered together, these results highlighted the importance of both the promoter region and signal peptide sequence to the spatial control of effector secretion. However, I also observed some limited BIC

localisation in transformants of the fungus expressing AvrPiap:Slp1:GFP, which has only the 2 kb upstream promoter sequence of *AVRPIA* driving expression of the *SLP1* gene. This suggested that if there is a potential signal for effector localisation in the 5' end of effector-encoding genes then it may not reside exclusively in the signal peptide region, but also at the 3'end of the promoter region proximal to the site of transcription initiation. The relevance of this observation can be compared to a published study of the AvrCO39 effector in *M. oryzae*. AvrCO39 is a cytoplasmic effector, that is known to be translocated inside the host, because it is recognized by resistance gene products inside the plant. The intracellular NLR immune receptor pair Rga5 and Rga4 are necessary for its perception during an incompatible interaction (Cesari et al., 2013). Based on this information, AvrCO39 would be predicted to be localised at the BIC. However, in the study from Ribot and co-workers, AvrCO39 localisation was observed to surround invasive hyphae rather than accumulating at the BIC. This could, however, be explained because the fluorescent protein fusion construct was expressed under control of the P27 promoter and not the native promoter sequence. P27 is a constitutive high-level expression promoter from *M oryzae* (Ribot et al., 2013). Ribot and co-workers proposed that after entering the secretory pathway (in a rice protoplast assay) the effector is able to re-enter the plant cell causing hypersensitive cell death in protoplasts expressing *RGA4/RGA5*. They tested this idea by introducing an ER retention signal (HDEL), and their results suggested that effectors might enter the plant cell without using any fungal factors (Ribot et al., 2013). However, the cell re-entry assay used by Ribot and co-workers and Rafiqi and co-workers used has been claimed not to be reliable in recent reports (Petre et al., 2016). Petre and co-workers state the assay can be a source of false positives, because in their experiments expressing AvrM and AVR3a effectors in *Phytophthora infestans*, some molecules with signal peptides stayed in the cytoplasm and did not enter the secretory system.

Based on the experiments reported in this Chapter, I decided to carry out reciprocal experiments in which I would attempt to express cytoplasmic effector genes under control of promoter and signal peptide combinations from apoplastic effector-encoding genes. In this way, I reasoned that it would be possible to define the significance of the 5' sequences of effectors in guiding the secretory route in a more rigorous manner than has been carried out to date.

# Chapter 4. Defining the significance of the promoter and signal peptide sequence of an apoplastic effector-encoding gene in guiding effector protein secretion

## *4.1 Introduction*

In this chapter I report the results of experiments designed to test whether the promoter of an apoplastic effector-encoding gene and its corresponding signal peptide sequence is sufficient to guide the secretion of a cytoplasmic effector protein into the apoplast. *M.* oryzae effectors have been broadly divided into two groups based on the destination to which they are delivered. Cytoplasmic effectors are those that have a function inside host plant cells (Giraldo and Valent, 2013), while apoplastic effectors are extracellular and accumulate within the gap between the fungal cell wall and the EIHM. Both classes of effector have been implicated in suppressing host immunity, but the number of effectors that has been characterised to date in *M. oryzae* and, indeed, in any plant pathogenic fungus, remain very small. This is in contrast to the very large repertoires of effector-encoding genes that have been predicted in plant pathogenic fungi based on comparative genome studies.

In oomycete pathogens cytoplasmic effectors have been more readily predicted because they contain the RXLR motif which has been shown to be present in all effectors that have been demonstrated to be translocated to plant host cells (Petre and Kamoun, 2014). In fungi there have only been reported four translocation motifs. In the wheat tan spot fungus *Pyrenophora tritici-repentis*, the ToxA gene contains a solvent-exposed loop containing an RGD cell attachment motif that appears to acts as a translocation signal (Manning et al., 2008). In the poplar rust *Melampsora larici-populina,* an effector protein Ctp1 contains an N-terminal peptide domain necessary for its translocation into the chloroplast (Plett et al., 2011). While the AvrL567 and AvrM effectors from the flax rust fungus *Melampsora lini* (Manning et al., 2008) (Rafiqi et al., 2010) are known to be translocated into the host cytoplasm because they are recognised by immune receptors inside the plant cell. They have unrelated N–terminal motifs which appear to be both necessary and sufficient for entering host cells (Rafiqi et al., 2010). The signal peptide of both AvrL567 and AvrM was, furthermore, found to

be functional in plants, which suggests that in order to enter the plant cell AvrL567 and AvrM do not require a specific fungal mechanism, but that this is likely to be a plant-directed process (Rafiqi et al., 2010). In all of these studies, however, the means by which the effectors are secreted from invasive hyphae or haustoria remain unknown.

Most studies to date investigating fungal effector delivery have relied on advances in live cell imaging to visualize fluorescent effector gene fusions during pathogen colonisation of the plant. However, not all pathogens can be manipulated to generate transformants expressing a fluorescent marker (Khang et al., 2010; Djamei et al., 2011; Giraldo and Valent, 2013). In these cases, researchers have instead relied upon transient expression of the effector, normally by *Agrobacterium*-mediated infiltration in the model plant species *Nicotiana benthamiana*. Some examples of where localisation of effectors by transient expression has been explored are AVRblb2 and the CRN effectors from the oomycete *P. infestans*. AVRblb2 is an RXLR effector, which suggests it is going to be translocated inside the host plant, and based on transient expression experiments AVRblb2 was observed to accumulate around haustoria and at the periphery of uninvaded cells (Bozkurt et al., 2011). CRN effectors were localised to plant cell nuclei (Schornack et al., 2010). Other transient expression experiments have been carried out for the Hpa RxLR effector candidates from the oomycete downy mildew pathogen *Hyaloperonospora arabidopsidis*. These effectors have been shown to target different plant compartments. Even though, these examples cannot be used to understand effector delivery, it is important to mention that because the expression of the effectors was carried out using a high level constitutive plant promoter, it is therefore possible that localisation patterns might be different to those expressed under native promoters. (Caillaud et al., 2012; Giraldo and Valent, 2013). This was observed for example with the constitutive promoter 35S (Pumplin et al., 2012), which reinforces the idea for testing the promoter regions in this thesis.

Some *U. maydis* and *M. oryzae* cytoplasmic effectors localisation has been characterised in electron microscopy and live cell imaging experiments during

pathogen host colonisation (Khang et al., 2010; Djamei et al., 2011; Giraldo and Valent, 2013; Kemen et al., 2013). RTP1p cytoplasmic effector, from the bean rust fungus *Uromyces fabae*, for example, localises at the interface between haustoria and the plasma membrane and inside the host cytoplasm (Kemen et al., 2013). Djamei and co-workers characterised Cmu1, a cytoplasmic effector in *U. maydis*. They found it encoded a chorismate mutase, an enzyme of the shikimate pathway that down-regulates the plant phenylproanoid pathway necessary for phytoalexin production and host defence responses. It is required for full virulence of the pathogen. Electron microscopy showed that Cmu1, expressed under the control of its native promoter, accumulates at the periphery of fungal hyphae, at the interface between the fungus, and importantly inside the plant cytoplasm. Transient expression of Cmu1, without its signal peptide, was observed inside plant cells and it was also able to be observed in adjacent cells (Djamei et al., 2011). This was also reported for one of *M. oryzae* cytoplasmic effectors Pwl2-mCherry expressing a nuclear localisation signal (NLS) and this is explored in more detail directly in Chapter 5 (Khang et al., 2010). BIC localisation has also been reported for the *M. oryza*e cytoplasmic effectors, AvrPia, AvrPiz-t, AvrPita and AvrPik, based on expression in *M.oryzae*, but cytoplasmic accumulation has also been shown for all of these effectors based on transient expression studies (Khang et al., 2010; Park et al., 2012; Cesari et al., 2013; Sornkom et al., 2017).

These studies (Khang et al., 2010; Park et al., 2012; Cesari et al., 2013; Sornkom et al., 2017) have investigated the interactions between cytoplasmic effectors and cognate immune receptors NLRs. In *M. oryzae* the most studied pairs of NLRs are RGA4/RGA5, Pik-1/Pik-2 and Pik-m (Jia et al., 2000; Cesari et al., 2013). Interestingly, the RGA4/RGA5 NLR pair confer resistance to two different *M. oryzae* effectors, AvrPia and AvrCO39. RGA5 has a small heavy metal-associated (HMA) domain integrated into the leucine rich repeat (LRR) domain of the NLR. This acts as a decoy that binds to AvrPia and AvrCO3, which normally target sHMA proteins in rice as their virulence target to suppress PAMP-triggered immunity (PTI) pathways. Without the presence of RGA5, RGA4 initiates a cell death response in *N. bentamiana*. This provides evidence that RGA4 is the NLR sensor and RGA5 is not only responsible for recognition of the effector but also

suppresses RGA4 from initiating the cell death response until Avr perception has occured (Cesari et al., 2014a). Cesari and co-workers also established that the interaction between RGA4 and RGA5 occurred between their CC domain (Cesari et al., 2014a).

Research on fungal effectors to date has therefore largely been restricted to functional studies based on transient expression analyses, which have provided key insights into their interaction with virulence targets and with cognate NLRs, when they are perceived during effector-triggered immunity (ETI). These have provided the first real insight into effector biology, so have been extremely valuable. However, these studies have not provided evidence concerning effector secretion and delivery. This is in marked contrast to the studies in oomycete pathogens which, driven by the discovery of the RXLR motif, have focused far more on effector delivery mechanisms, although so far with some conflicting and controversial results. The aim of the work presented here is to carry out a detailed analysis of effector secretion in the rice blast fungus, which can test hypotheses concerning the mechanisms by which exocytosis from invasive hyphae may occur. This is likely to be separate from, but a pre-requisite to take-up of effectors by host plant cells.

In this Chapter, I report the reciprocal experiments in which I attempted to determine whether cytoplasmic effectors from *M. oryzae* could be re-directed to apoplastic secretion based on the promoter and signal peptide regions from apoplastic effector genes. Chimeric constructs were designed to test this idea as shown in the schematic representation, shown in Figure 4.1. These constructs were expressed in *M. oryzae* and live cell imaging, coupled with quantitative analysis, used to determine the fate of the fungal effector protein fusions in plant infections

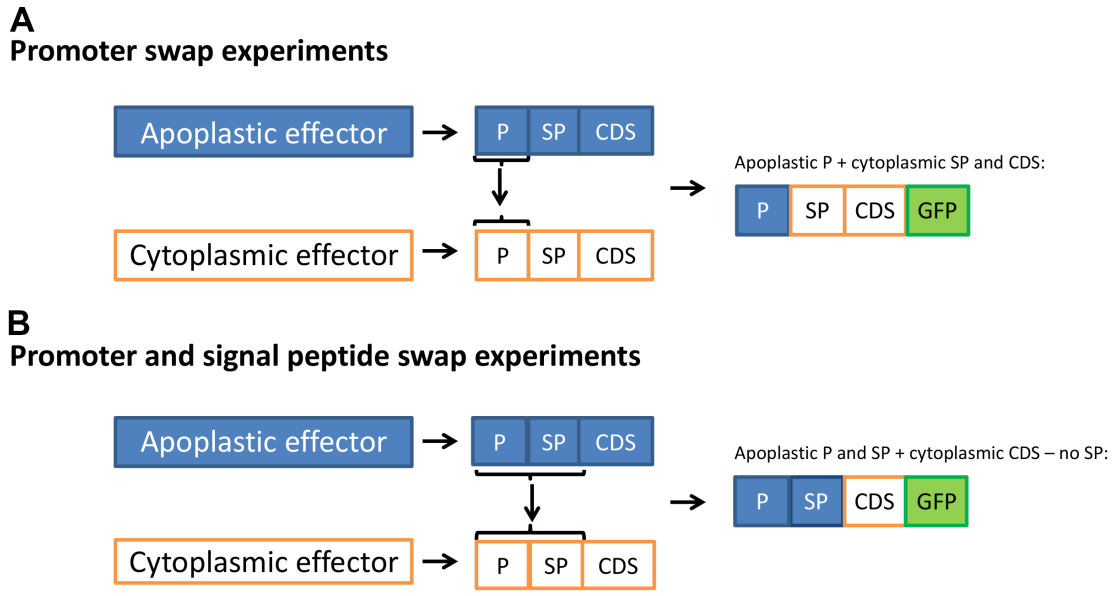


Figure 4.1 **Schematic representation of the strategy followed to generate chimeras to mis-regulate cytoplasmic effector genes**. Promoter swap experiments were undertaken in which a substitution of the promoter region from an apoplastic effector gene was used to drive expression of a cytoplasmic effector. The construct was fused to GFP to be able to observe it by epifluorescence microscopy. Promoter and signal peptide swaps involved substitution of the promoter and signal peptide regions of an apoplastic effector gene to drive expression of a cytoplasmic effector. P:promoter; SP: signal peptide; CDS: coding region.

## *4.2 Methods*

### 4.2.1 Generation of *M. oryzae* transformants expressing apoplastic effector gene-GFP fusions

To generate *SLP1p:GFP* and *BAS4p:GFP* vectors, primers in Table 3.1 were used to amplify *SLP1* (MGG_10097) and *BAS4* (MGG_10914) from genomic DNA. Promoter sequences were defined as 2 kb upstream of the start codon of the corresponding gene. Forward primers always included a 15bp overhang with the *BAR* resistance cassette. The reverse (3') primer also had a 15bp overhang, complementary to the GFP DNA sequence. The *BAR* gene and GFP:*trp*C fragments were amplified using primers with 15bp overhangs complementary to the pNEB-1284 plasmid. The polymerase enzymes used were Phusion® high fidelity DNA Polymerase (New England Biolabs, Thermo Scientific®) and Q5® High-Fidelity DNA Polymerase (New England Biolabs). The PCR was performed using an initial denaturation step at 98°C for 30 sec followed by 35 cycles of PCR cycling parameters of: denaturation at 98°C for 10 sec, annealing 58°C for 30 sec and extension 72°C for 30 sec/kb target length, followed by a final extension at 72°C for 10 min and hold at 4°C. PCR products were analysed by gel electrophoresis. The fragments were used to generate chimeric constructs using the In-fusion Cloning method (Clontech). Fragments became integrated into a *Hin*d*III*-digested pNEB-1284 plasmid (Figure 3.2). The resulting *SLP1p:GFP* and *BAS4p:GFP* plasmids were subsequently introduced into *M. oryzae* by transformation of *M. oryzae* Guy11.

### 4.2.2 Generation of *M. oryzae* transformants expressing cytoplasmic effector gene-GFP fusions

To generate *SLP1p+sp:GFP* and *BAS4p+sp:GFP* vectors, primers in Table 3.1 were used to amplify gene sequences from total genomic *M.oryzae* DNA. *M. oryzae* promoter regions were defined as described in 4.2.1. Forward primers always included a 15bp overhang with the *BAR* resistance cassette. The reverse primer also had a 15bp overhang, which is complementary in nucleotide sequence to the *GFP* DNA sequence. The polymerase enzymes used were

Phusion® high fidelity DNA Polymerase, as described in 4.2.1. PCR products were analysed by gel electrophoresis. The fragments were used to generate the chimeric constructs using In-fusion Cloning (Clontech). Fragments became integrated into a *Hin*dIII-digested pNEB-1284 plasmid (Figure 3.2). The resulting *SLP1p+sp:GFP* and *BAS4p+sp:GFP* plasmids were subsequently introduced into *M. oryzae* by transformation of *M. oryzae* Guy11.

### 4.2.3 Generation of *M. oryzae* transformants expressing cytoplasmic effector genes under control of promoter gene regions from apoplastic effector-encoding genes

To generate *SLP1p:PWL2:GFP*, *BAS4p:PWL2:GFP*, *SLP1p:AVRPIA:GFP* and *BAS4p:AVRPIA:GFP*, strategy described in 3.2.2 was followed. Primers in Table 3.1 were used to amplify a 2 kb fragment containing a promoter sequence from each gene from genomic DNA. The coding sequences of *PWL2* and *AVRPIA,* including the predicted signal peptide, were also amplified from genomic DNA of *M. oryzae* Guy11 strain for *PWL2*, from Ina168 for *AVRPIA* gene. The polymerase enzymes used were Phusion® high fidelity DNA Polymerase (New England Biolabs, Thermo Scientific®) and Q5® High-Fidelity DNA Polymerase (New England Biolabs), as described in 4.2.1. PCR products were analysed by gel electrophoresis. The fragments were used to generate the chimeric constructs using the In-fusion Cloning method (Clontech). The fragments became integrated into a *Hin*d*III*-digested pNEB-1284 plasmid (Figure 3.2). The resulting *SLP1p:PWL2:GFP*, *BAS4p:PWL2:GFP*, *SLP1p:AVRPIA:GFP* and *BAS4p:AVRPIA:GFP* plasmids were subsequently introduced into *M. oryzae* by transformation into Guy11.

### 4.2.4 Generation of *M. oryzae* transformants expressing cytoplasmic effector genes under control of promoter and signal peptide gene regions from apoplastic effector-encoding genes

To generate *SLP1p+sp:PWL2:GFP*, *BAS4p+sp:PWL2:GFP*, *SLP1p+sp:AVRPIA:GFP* and *BAS4p+sp:AVRPIA:GFP*, strategy described in 3.2.3 was followed. Primers in Table 3.1 were used to amply the promoter and

signal peptide region from *SLP1 and BAS4*. The coding regions of cytoplasmic effectors *PWL2* or *AVRPIA,* respectively without its predicted signal peptide were also amplified from genomic DNA of *M. oryzae* Guy11 strain for *PWL2*, from Ina168 for *AVRPIA* gene. The polymerase enzymes used were Phusion® high fidelity DNA Polymerase (New England Biolabs, Thermo Scientific®) and Q5® High-Fidelity DNA Polymerase (New England Biolabs), as previously described 4.2.1. PCR products were analysed by gel electrophoresis. The fragments were used to generate the chimeric constructs using In-fusion Cloning (Clontech). The fragments became integrated into a *Hin*dIII-digested pNEB-1284 plasmid (Figure 3.2). The resulting *SLP1p+sp:PWL2:GFP*, *BAS4p+sp:PWL2:GFP*, *SLP1p+sp:AVRPIA:GFP* and *BAS4p+sp:AVRPIA:GFP* plasmids were subsequently introduced into *M. oryzae* by transformation of the Guy11.

### *4.2.5* Generation of the *AVRPIA:GFP* gene fusion vector

To generate the *AVRPIA:GFP* vector, primers were designed (Table 3.1) to amplify a 2 kb *AVRPIA* fragment from INA168 total genomic DNA. The forward primer was designed 2 kb upstream of the *AVRPIA* start codon to include the promoter sequence of the *AVRPIA* gene and contained a 15 bp overhang with *BAR* gene resistance cassette. The reverse primer was designed at the 3' end of the *AVRPIA* coding sequence to exclude the predicted *AVRPIA* translational stop codon. The reverse primer also included a 15 bp overhang complementary in nucleotide sequence to *GFP*. The polymerase enzymes used were Phusion® high fidelity DNA Polymerase (New England Biolabs, Thermo Scientific®) and Q5® High-Fidelity DNA Polymerase (New England Biolabs), as previously described in 4.2.1. PCR products were analysed by gel electrophoresis. The fragments were used to generate *AVRPIA:GFP* using In-fusion Cloning method (Clontech). The fragments became integrated into a *Hin*d*III*-digested pNEB-1284 plasmid (Figure 3.2). The resulting *AVRPIA:GFP* plasmid was subsequently introduced into *M. oryzae* by transformation of the *M. oryzae* Guy11 strain.

### 4.2.6 Generating the *SLP1*p:*PWL2*sp:*SLP1*:GFP fusion vector

To generate the *SLP1*p:*PWL2*sp:*SLP1*:GFP vector, a 2 kb fragment containing the promoter region of *SLP1* was amplified and a 15 bp overhang with *BAR* gene resistance cassette. The nucleotide coding region for the Pwl2sp:Slp1 peptide

was synthesised (GENEWIZ, UK), designed with a forward 15 bp overhang for Slp1 promoter fragment and a reverse 15 bp overhang for *GFP* sequence. A 1ul aliquot was used in the In-fusion reaction. The polymerase enzymes used were Phusion® high fidelity DNA Polymerase (New England Biolabs, Thermo Scientific®) and Q5® High-Fidelity DNA Polymerase (New England Biolabs), as previously described 4.2.1. PCR products were analysed by gel electrophoresis. The resulting *SLP1p*:*PWL2sp: SLP1:GFP* plasmid was subsequently introduced into *M. oryzae* by transformation of *M. oryzae* Guy11.

## *4.3 Results*

### 4.3.1 Construction of *M. oryzae* strains expressing apoplastic effector genes promoter and promoter/signal peptide GFP fusions

Apoplastic effectors used in this study are Slp1 (MGG_10097) and Bas4 (MGG_10914). A C-terminal translational fusion of the *SLP1* and *BAS4* promoter gene, or the promoter-signal peptide combination were fused to the reporter gene *GFP*. The following constructs were generated: *SLP1p:GFP*, *SLP1p+sp:GFP*, *BAS4p:GFP* and *BAS4p+sp:GFP*. The signal peptides were predicted using SIGNALP.4.1 software (Figure 4.2). The cloning strategy followed is shown in Figure 4.3 and followed the same logic as for constructs described in Chapter 3. After *E. coli* transformation using competent cells, bacterial colonies were confirmed by PCR analysis. Constructs were then digested with three different restriction enzymes. *SLP1p:GFP* and *SLP1p+sp:GFP* were digested with *Pci*I, *Eco*RV and *Nco*I (Figure 4.4). *BAS4p:GFP* and *BAS4p+sp:GFP* were digested with *Xmn*I*, Hin*dIII*, Bgl*II and restriction digestion to confirm cloning(Figure 4.5). The constructs were independently confirmed and checked for errors by DNA sequencing of the entire inserts. The resulting GFP fusions were subsequently introduced into *M. oryzae* by DNA-mediated transformation (Talbot et al., 1993) of Guy11. Putative transformants were selected based on resistance to glufosinate. Transformants were screened for fluorescence using the Olympus IX81 inverted microscope and single copy transformants confirmed by qPCR in a blind test (Table 4.1). *SLP1p:GFP*, *SLP1p+sp:GFP*, *BAS4p:GFP* and *BAS4p+sp:GFP* single copy transformants used are in Table 4.2.

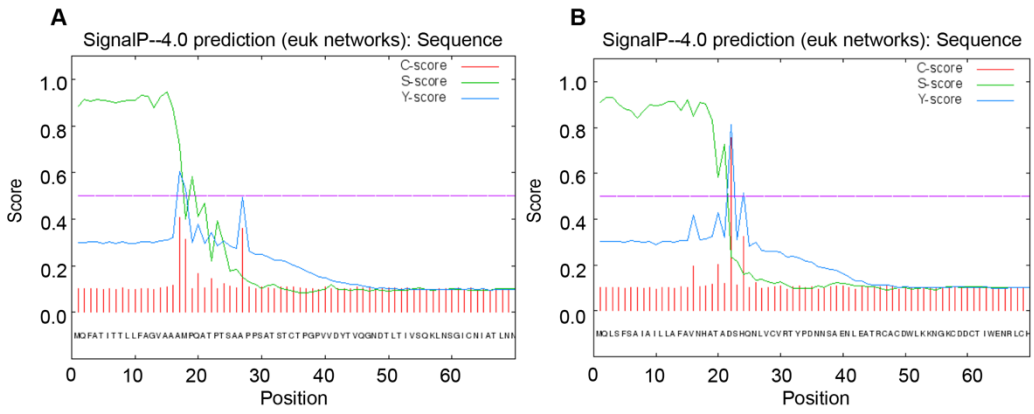


Figure 4.2 **Identification of predicted signal peptide on apoplastic effector genes *BAS4* and *SLP1.*** A) Slp1signal peptide is from 1-16 amino acids. B) Bas4 having a signal peptide between 1-22 amino acids.

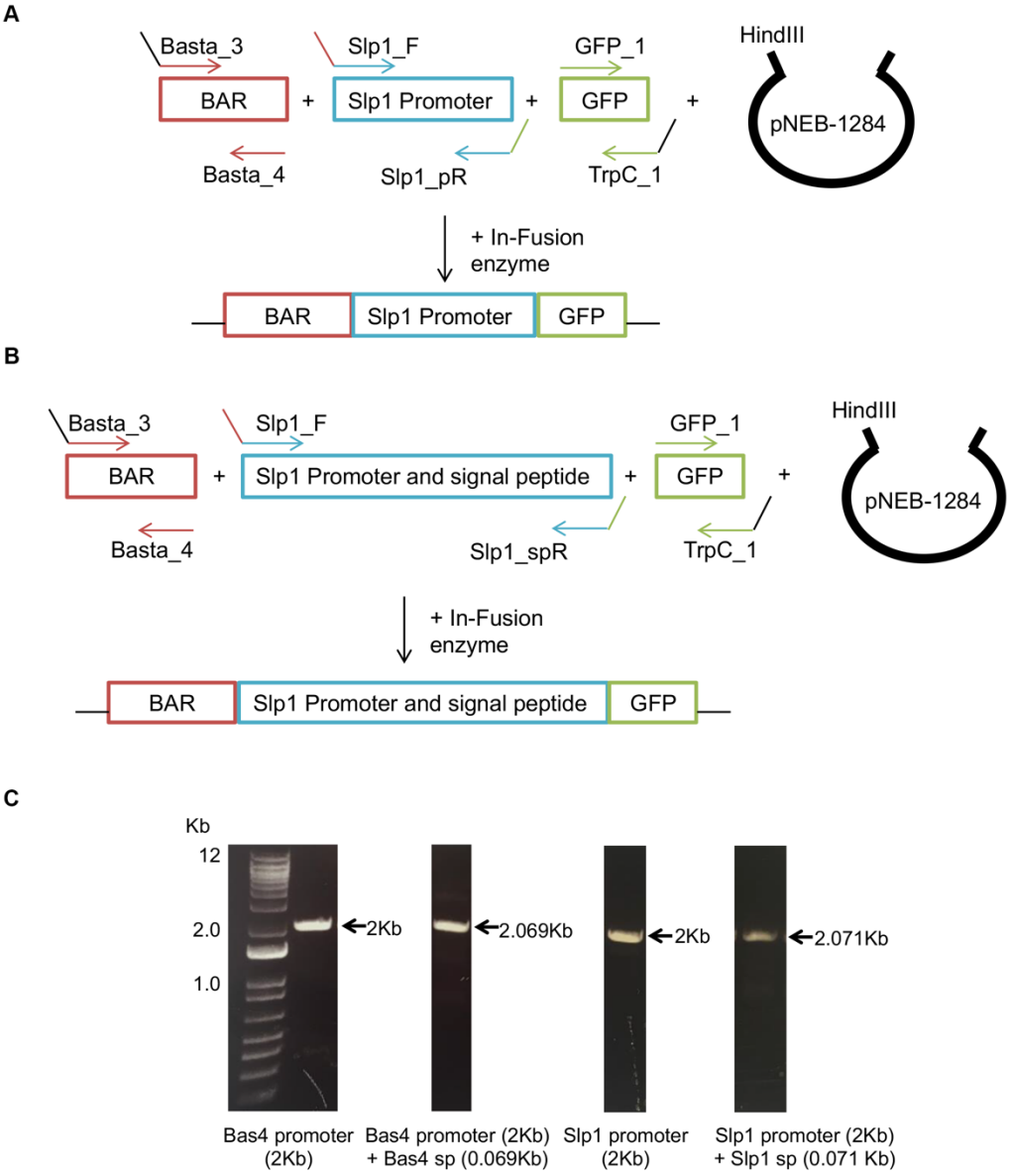


Figure 4.3 **In-Fusion cloning strategy and associated PCR amplifications** A) Schematic representation of the cloning strategy followed for generation of C-terminal GFP constructs with the promoter of the apoplastic effector gene *SLP1*. B) Scheme of the cloning strategy followed for construction of *SLP1* promoter and signal peptide regions driving GFP expression. C) PCR amplification of 2kb *BAS4* promoter, 2.069kb *BAS4* promoter and signal peptide, 2kb *SLP1* promoter and 2.071kb *SLP1* promoter and signal peptide.

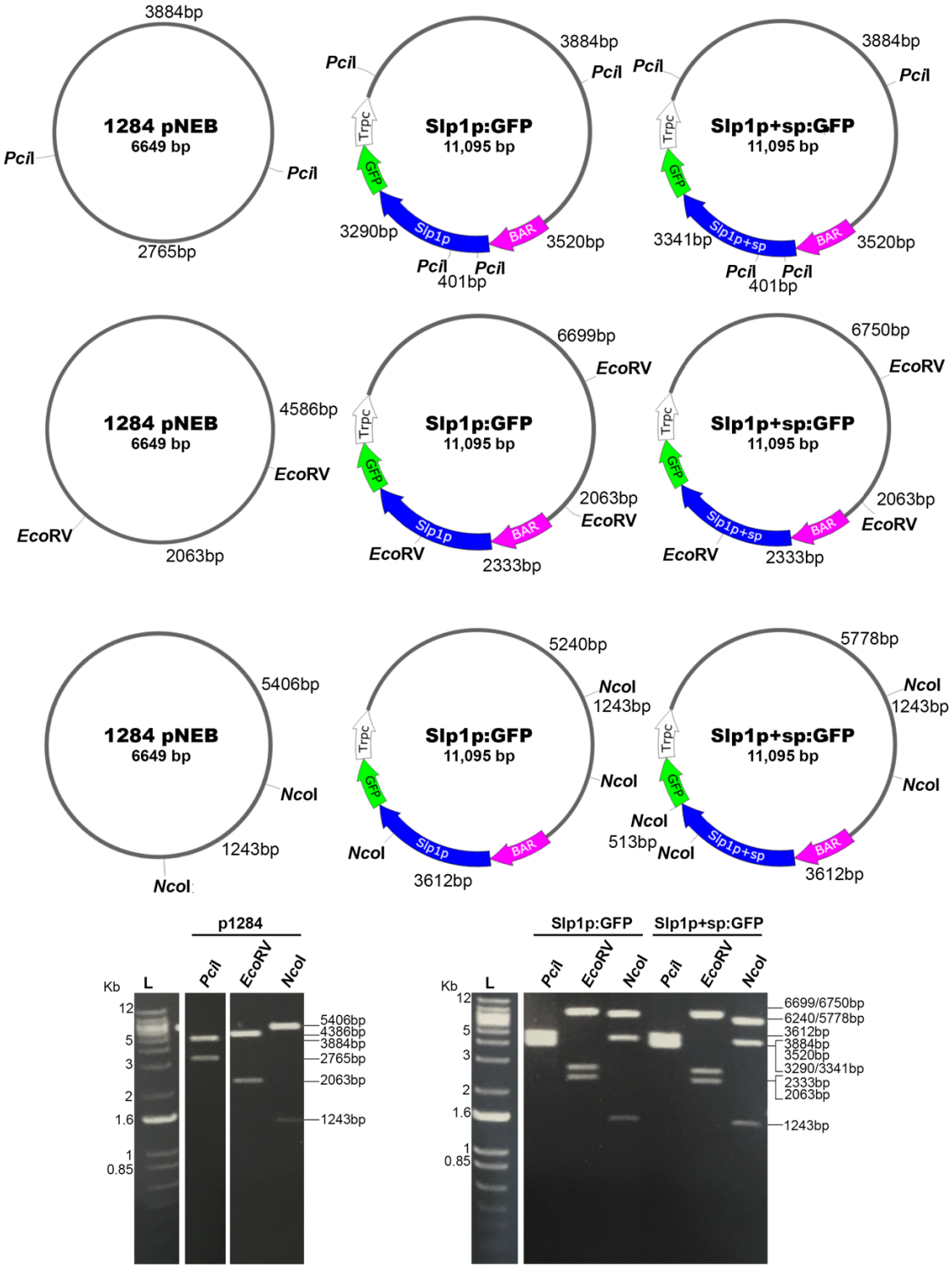


Figure 4.4 ***SLP1p:GFP* and *SLP1p+sp:GFP* plasmid verification by restriction digestion.** SnapGene software (from GSL Biotech; available at snapgene.com) was used to predict fragment sizes. Positive PCR for *SLP1p:GFP, SLP1p+sp:GFP* and pNEB1284 were digested with *Pci*I, *Eco*RV and *Nco*I. *Pci*I cuts pNEB1284 into 2765 bp and 3884 bp, *SLP1p:GFP,* 3520 bp, 401 bp (not seen), 3290 bp and 3884 bp and *SLP1p+sp:GFP* , 3520 bp, 401 bp (not seen), 3341 bp and 3884 bp. *Eco*RV cuts pNEB-1284 into 2063 bp and 4586 bp. *Eco*RV cuts *SLP1p:GFP and SLP1p+sp:GFP* into 2063 bp, 2333 bp and 6699bp; and 2063 bp, 2333 bp and 6750 bp. *Nco*I cuts pNEB1284 into 1243 bp and 5406. *Nco*I digests *SLP1p:GFP* 1243 bp, 3612 bp and 5240 bp. *Nco*I cuts *SLP1p+sp:GFP* 1243 bp, 3612 bp, 513 bp (not seen) and 5778 bp. Gene regions in colours: Pink = BAR gene, Blue = apoplastic effector, Orange = cytoplasmic effector, Green = GFP and White = TrpC terminator

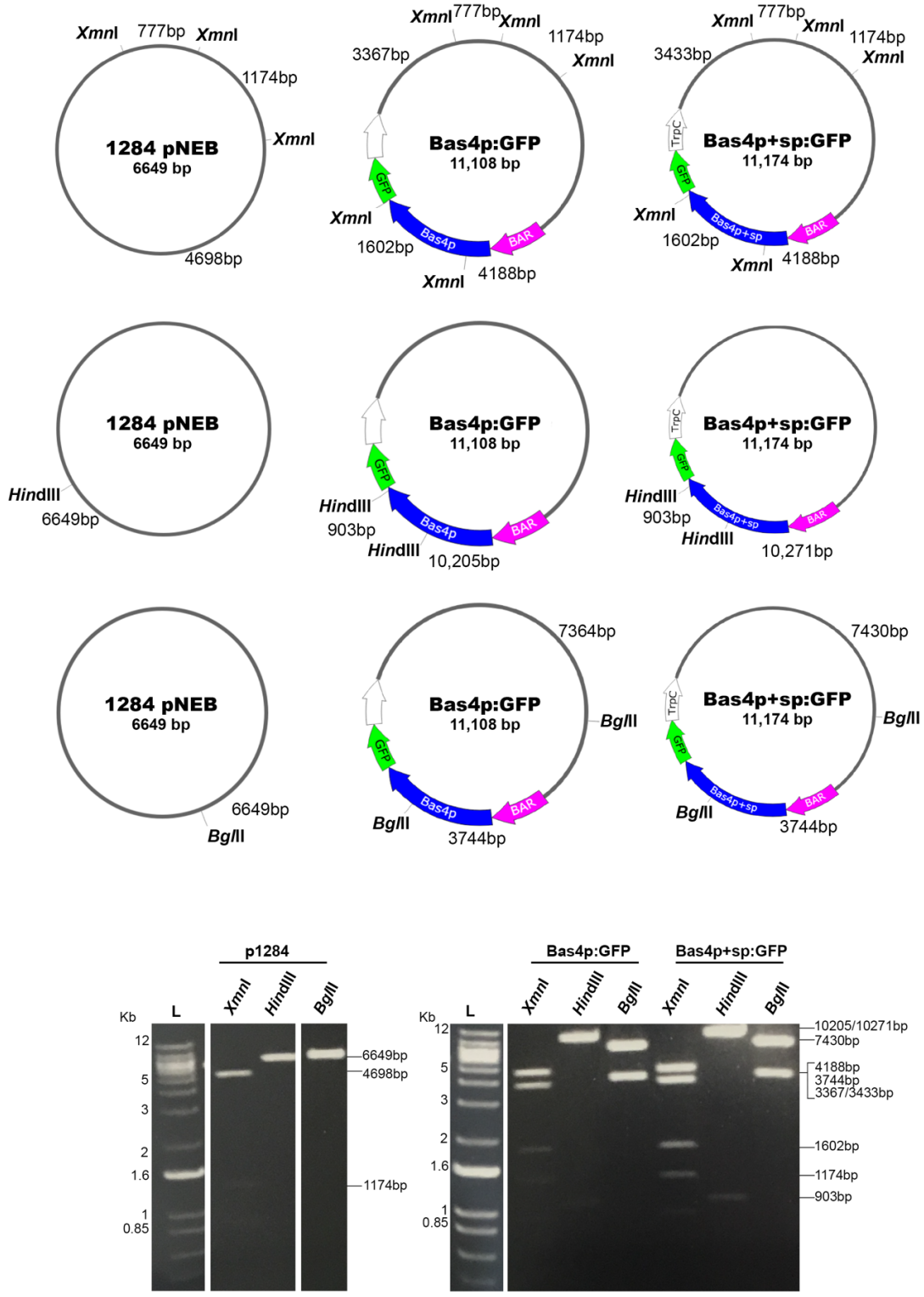


Figure 4.5 ***BAS4p:GFP* and *BAS4p+sp:GFP* plasmid verification by restriction digestion.** SnapGene software (from GSL Biotech; available at snapgene.com) was used to predict fragment sizes. Positive bacteria colony PCR for *BAS4p:GFP*, *BAS4p+sp:GFP* and pNEB1284 were digested with *Xmn*I, *Hin*dIII, *Bgl*II. *Xmn*I cuts pNEB-1284 into 777 bp (not seen), 1174 bp and 4698 bp. *Xmn*I cuts *BAS4p:GFP* and *BAS4p+sp:GFP* into 777 bp (not seen), 1174 bp, 4188 bp, 1602 bp and 3433/3367 bp. *Hin*dIII digest pNEB-1284 once. *BAS4p:GFP* and *BAS4p+sp:GFP* digested with *Hin*dIII show a pattern, 903 bp (very faint) and 10,205 bp or 10,271 bp. *Bgl*II linearises pNEB-1284 and cuts *BAS4p:GFP* and *BAS4p+sp:GFP* into 3744 bp and 7364 bp or 7430 bp in size. Gene regions in colours: Pink = BAR gene, Blue = apoplastic effector, Orange = cytoplasmic effector, Green = GFP and White = TrpC terminator.

Table 4.1 Determination of GFP copy number by qPCR for *SLP1p:GFP,* SLP1p+sp:GFP, BAS4p:GFP and BAS4p+sp:GFP.

| Sample | GFP Copy Number[1] |
|---|---|
| Guy11 | 0 |
| Control | 1 |
| Slp1p#1 | 8 |
| Slp1p#3 | 2 |
| Slp1p#4 | 1 |
| Slp1p#6 | 5 |
| Slp1p#9 | 2 |
| Slp1p#11 | 7 |
| Slp1p+sp#1 | 4 |
| Slp1p+sp#8 | 1 |
| Slp1p+sp#9 | 5 |
| Slp1p+sp#10 | 1 |
| Slp1p+sp#11 | 1 |
| Bas4p#5 | 3 |
| Bas4p#6 | 1 |
| Bas4p#10 | 2 |
| Bas4p#12 | 2 |
| Bas4p#13 | 5 |
| Bas4p#14 | 3 |
| Bas4p#16 | 2 |
| Bas4p+sp#1 | 1 |
| Bas4p+sp#2 | 1 |
| Bas4p+sp#3 | 3 |
| Bas4p+sp#4 | 13 |
| Bas4p+sp#5 | 12 |
| Bas4p+sp#6 | 6 |

[1]Blind qPCR test performed by iDnaGENETICS Ltd (Norwich research park).

Table 4.2 Transformants used in Chapter 4

| Name of the construct | Number 1 | Number 2 |
|---|---|---|
| Slp1p:GFP | 4 | - |
| Slp1p+sp:GFP | 8 | 10 |
| Bas4p:GFP | 6 | - |
| Bas4p+sp:GFP | 1 | 2 |
| Slp1p:Pwl2:GFP | 37 | - |
| Slp1p+sp:Pwl2:GFP | 25 | - |
| Bas4p:Pwl2:GFP | 1 | 12 |
| Bas4p+sp:Pwl2:GFP | 1 | 8 |
| Slp1p:AvrPia:GFP | 47 | - |
| Slp1p+sp:AvrPia:GFP | 23 | - |
| Bas4p:AvrPia:GFP | 4 | 5 |
| Bas4p+sp:AvrPia:GFP | 4 | 8 |
| Slp1p:Pwl2sp:Slp1:GFP | 10 | 11 |

### 4.3.2 Promoter and signal peptide regions of apoplastic effectors restores their localisation pattern

My initial experimental observation in chapter 3 provided evidence that the promoter and signal peptide gene regions of cytoplasmic effector genes in *M. oryzae* were sufficient for BIC localisation of GFP or an apoplastic effector. I therefore decided to perform the reciprocal experiment to ask whether the corresponding promoter and signal peptide sequences from apoplastic effector genes were sufficient to direct free GFP or a cytoplasmic effector protein to the apoplast. First, I used the promoter and signal peptide regions of the apoplastic effectors *SLP1* and *BAS4* to express GFP.

*M. oryzae* strains expressing *SLP1p:GFP, SLP1p+sp:GFP, BAS4p:GFP* and *BAS4p+sp:GFP* were inoculated onto epidermal leaf tissue of the blast susceptible rice cultivar Mokoto. After 30 hpi infected tissue was prepared for microscopy. Representative observations of infected cells are shown in Figure 4.6. The Slp1p:GFP and Bas4p:GFP signals could be observed inside and surrounding invasive hyphae. This was identical to the localisation pattern of Pwl2p:GFP and AvrPiap:GFP promoter fusion constructs reported in Figure 3.8. *M. oryzae* strains expressing Slp1p+sp:GFP and Bas4p+sp:GFP showed localisation surrounding *M. oryzae* invasive hyphae, although for Bas4p+sp:GFP GFP accumulation was also observed at the BIC. The localisation patterns of Slp1p+sp:GFP and Bas4p+sp:GFP localisation were therefore similar to the patterns observed when Slp1 and Bas4 effector GFP fusion proteins are expressed (Chapter 3 Figure 3.8). These results provide further evidence that the sorting mechanism for effectors must be associated with the 5’ regions of the genes, rather than their mature peptide coding sequences.

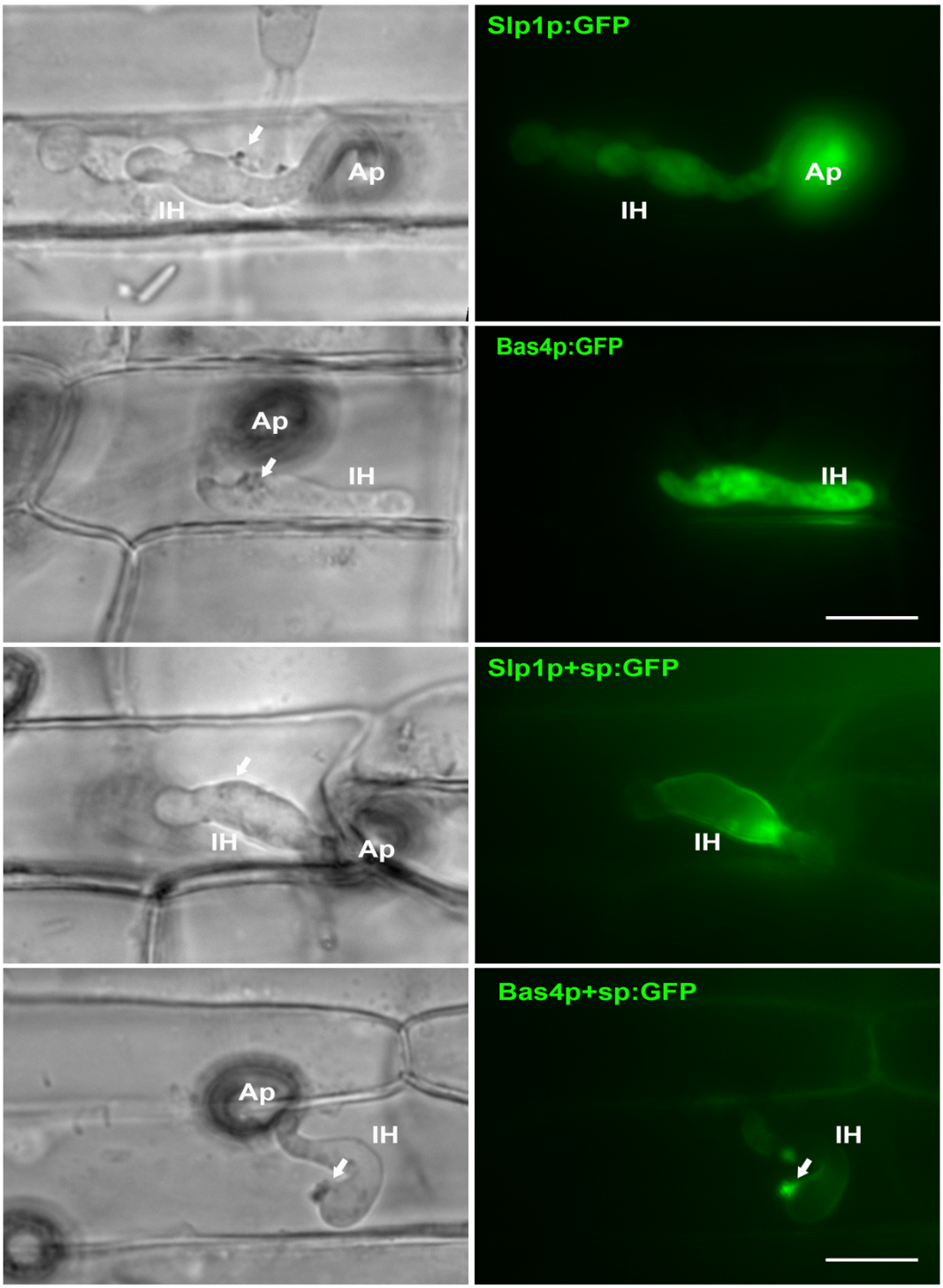


Figure 4.6 **The promoter and signal peptide of the apoplastic effector genes *SLP1* and *BAS4* are both necessary for BIC localisation.** Micrographs obtained by live cell imaging from leaf sheaths of *M. oryzae* infection of rice by epifluorescence microscopy of promoter gene regions of *SLP1* and *BAS4* driving free GFP and promoter and signal peptide gene regions of *SLP1* and *BAS4* driving free GFP. All the strains were excited at 488nm for 200 ms. Scale bars represent 10 µm. Arrow marks the BIC, Ap marks the appressorium and IH marks *M. oryzae* invasive hyphae.

### 4.3.3 Construction of the cytoplasmic chimeric construct driven by promoter or the promoter and signal peptide gene regions apoplastic effectors

To continue studying the promoter and signal peptide regions of apoplastic effectors, the reciprocal promoter swap experiments were generated as shown in Figure 4.7.

The cloning strategy (Figure 4.8) followed for these constructs was always the same as in chapter 3. The PCR positive transformant from competent cells transformation were confirmed by restriction enzymes. *PWL2p:SLP1:GFP* was digested with *Hin*dIII, *Eco*RV and *Bsr*GI (Figure 4.9). *SLP1p+sp:PWL2:GFP* was digested with *Nco*I, *Pst*I and *Psi*I (Figure 4.10). *SLP1p:AVRPIA:GFP* was digested with *Eco*RI, *Pst*I and *Pci*I (Figure 4.11). *SLP1p+sp:AVRPIA:GFP* was digested with *Eco*RI, *Not*I and *Pst*I (Figure 4.12). *BAS4p:PWL2:GFP* and *BAS4p+sp:PWL2:GFP* were digested with *Sac*II*, Pci*I *and Psi*I (Figure 4.13). *BAS4p:AVRPIA:GFP* was digested with *Pst*I, *Bam*HI and *Eco*RV (Figure 4.14). *BAS4p+sp:AVRPIA:GFP* was digested with *Pst*I, *Bam*HI and *Bgl*II (Figure 4.15). The constructs were independently confirmed and checked for errors by DNA sequencing. The resulting GFP C-terminal fusions were subsequently introduced into *M. oryzae* by protoplast-mediated transformation (Talbot et al., 1993) of Guy11. Putative transformants were selected based on their resistant cassette *BAR* gene with glufosinate (30 µg $ml^{-1}$). GFP positive transformants were screened for fluorescence by using Olympus IX81 inverted microscope. Single copy transformants were confirmed by qPCR blind test (Table 4.3). The single copy transformants used in this study are in Table 4.2. All of these are single copy with the exception of Slp1p+sp:Pwl2:GFP#25, Bas4p:Pwl2:GFP#1 and Bas4p+sp:Pwl2:GFP#8, where single copy transformants could not be generated.

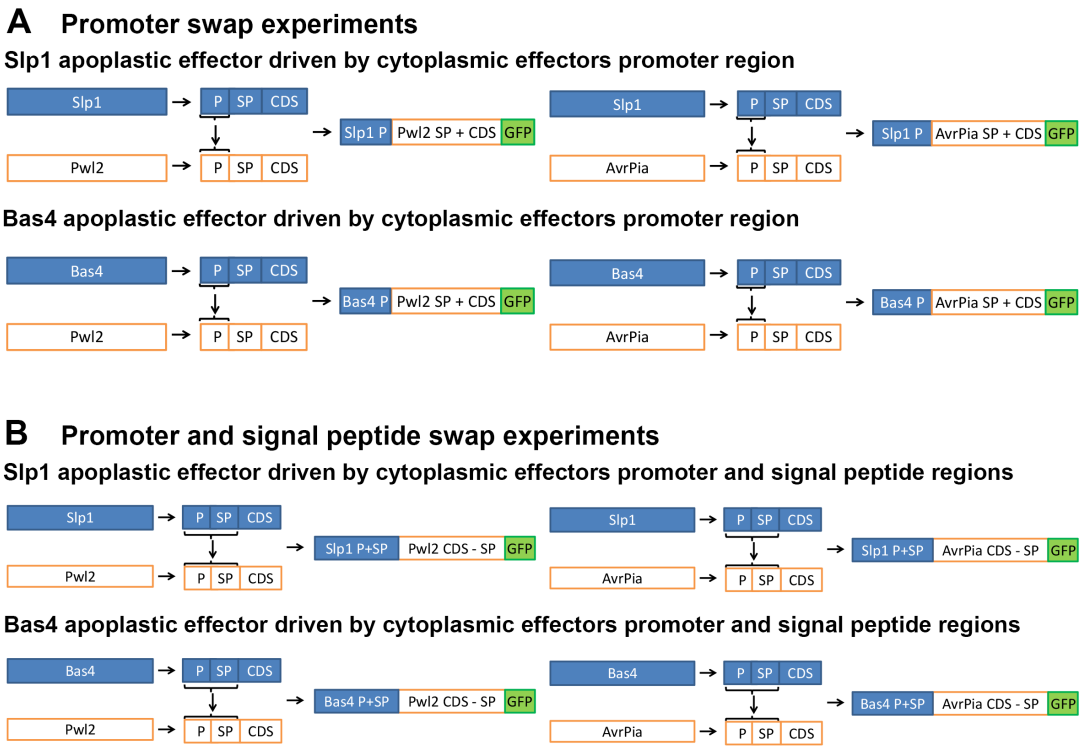


Figure 4.7 **Chimeric constructs used in Chapter 4.** Scheme of the promoter and signal pdeptid swap strategy used to generate each chimeric construct reported in Chapter 4.

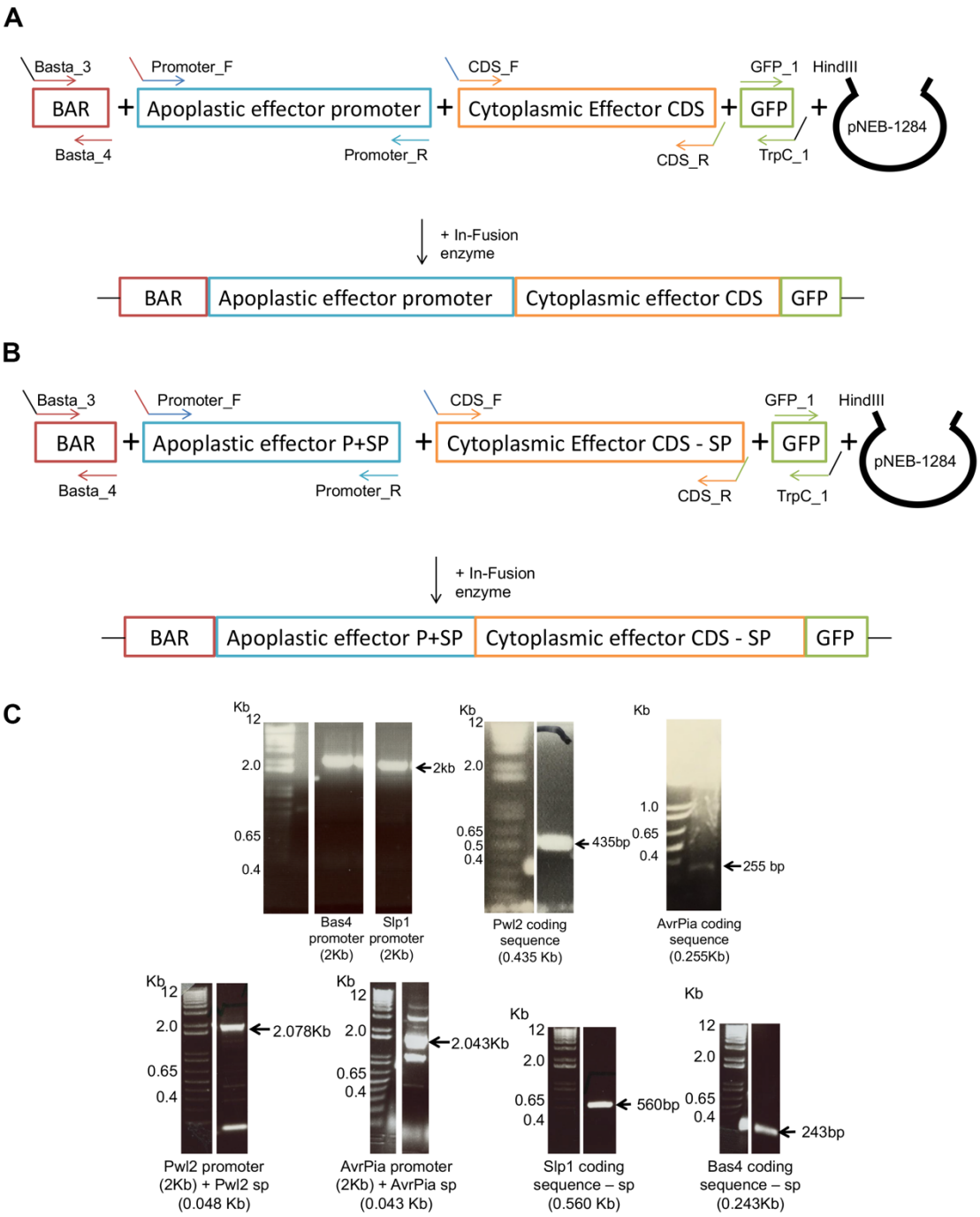


Figure 4.8 **Schematic representation of cloning strategy for chimeric constructs and associated PCR amplifications.** A) Cloning strategy for the chimeric constructs using the promoter region of apoplastic effectors driving cytoplasmic effectors *PWL2* and *AVRPIA* genes. B) Cloning strategy for the chimeric constructs using the promoter and signal peptide regions of apoplastic effectors driving the coding gene regions of *PWL2* and *AVRPIA* without its predicted signal peptide. C) PCR amplification of the fragments 2kb *BAS4* promoter, 2kb *SLP1* promoter, 2.071 kb *SLP1* promoter and signal peptide, 2.069 kb *BAS4* promoter and signal peptide, 435 bp of *PWL2* coding sequence, 255 bp *AVRPIA* coding sequence, 402 bp of *PWL2* coding sequence without its predicted signal peptide and 198 bp *SLP1* coding sequence without its predicted signal peptide.

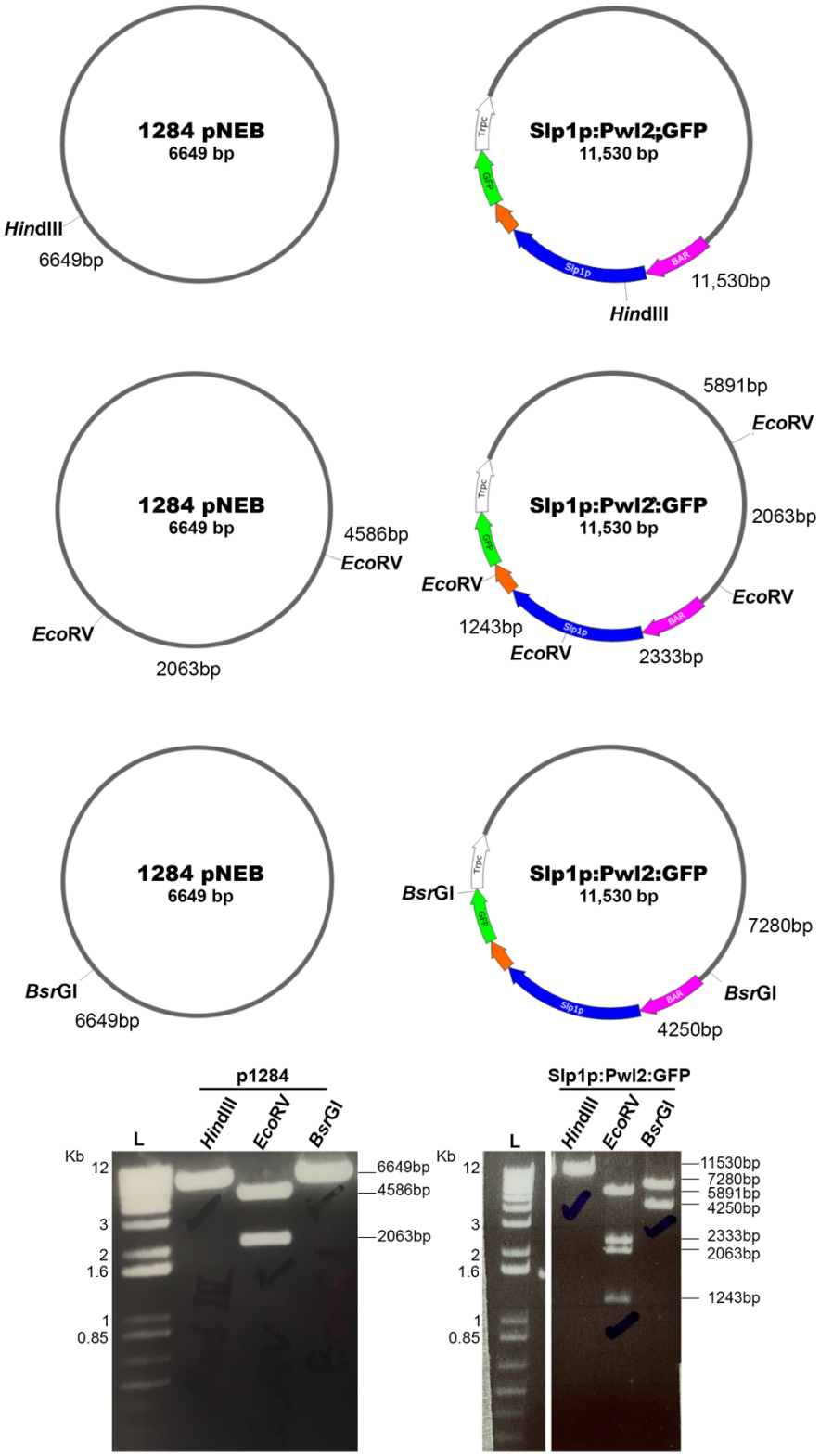


Figure 4.9 ***SLP1p:PWL2:GFP* plasmid verification by restriction digestion**. SnapGene software (from GSL Biotech; available at snapgene.com) was used to predict the expected fragment sizes. Positive bacteria colony PCR for *SLP1p:PWL2:GFP* transformants and pNEB-1284 empty vector were digested with *Hin*dIII, *Eco*RV and *Bsr*GI. *Hin*dIII linearised the empty pNEB-1284 vector and has a band size pattern of 50 bp, 52 bp (not seen) and 11530 bp for *SLP1p:PWL2:GFP*. *Eco*RV cuts pNEB-1284 into fragments 2063 bp and 4586 bp and cuts *SLP1p:PWL2:GFP* in 2063 bp, 2333 bp, 1243 bp and 5891 bp. *Bsr*GI linearises pNEB-1284 and cuts *SLP1p:PWL2:GFP* into 4250 bp and 7280 bp. Gene regions in colours: Pink = BAR gene, Blue = apoplastic effector, Orange = cytoplasmic effector, Green = GFP and White = TrpC terminator.

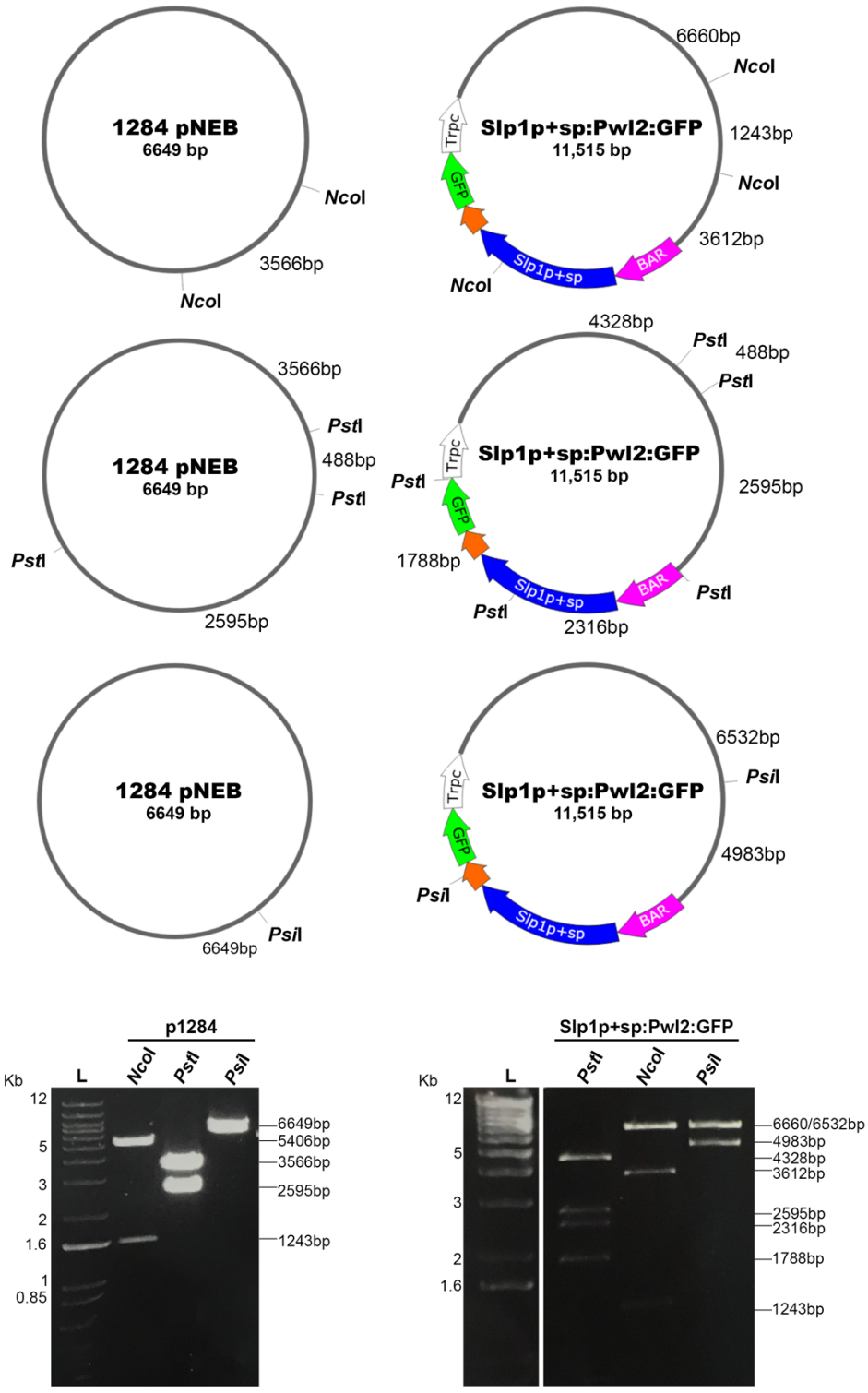


Figure 4.10 ***SLP1p+sp:PWL2:GFP* plasmid verification by restriction digestion.** SnapGene software (from GSL Biotech; available at snapgene.com) was used to predict the expected fragment sizes. Positive bacteria colony PCR for *SLP1p+sp:PWL2:GFP* transformants and pNEB-1284 empty vector were digested with *Nco*I, *Pst*I and *Psi*I and fractionated by gel electrophoresis. *Nco*I cuts pNEB-1284 into fragments 1463 bp and 5406 bp and cuts *SLP1p+sp:PWL2:GFP* in 1243 bp, 3612 bp, and 6660 bp. *Pst*I digests pNEB-1284 in 3 fragments sizes: 488 bp, 2595 bp and 3566 bp. *Pst*I digests *SLP1p+sp:PWL2:GFP* in 5 fragments sizes: 488 bp (not seen), 2595 bp, 2316 bp, 1788 bp and 4328 bp. *Psi*I linearises the empty vector and cuts into 2 fragments *SLP1p+sp:PWL2:GFP*; 4983 bp and 6532 bp. Gene regions in colours: Pink = BAR gene, Blue = apoplastic effector, Orange = cytoplasmic effector, Green = GFP and White = TrpC terminator

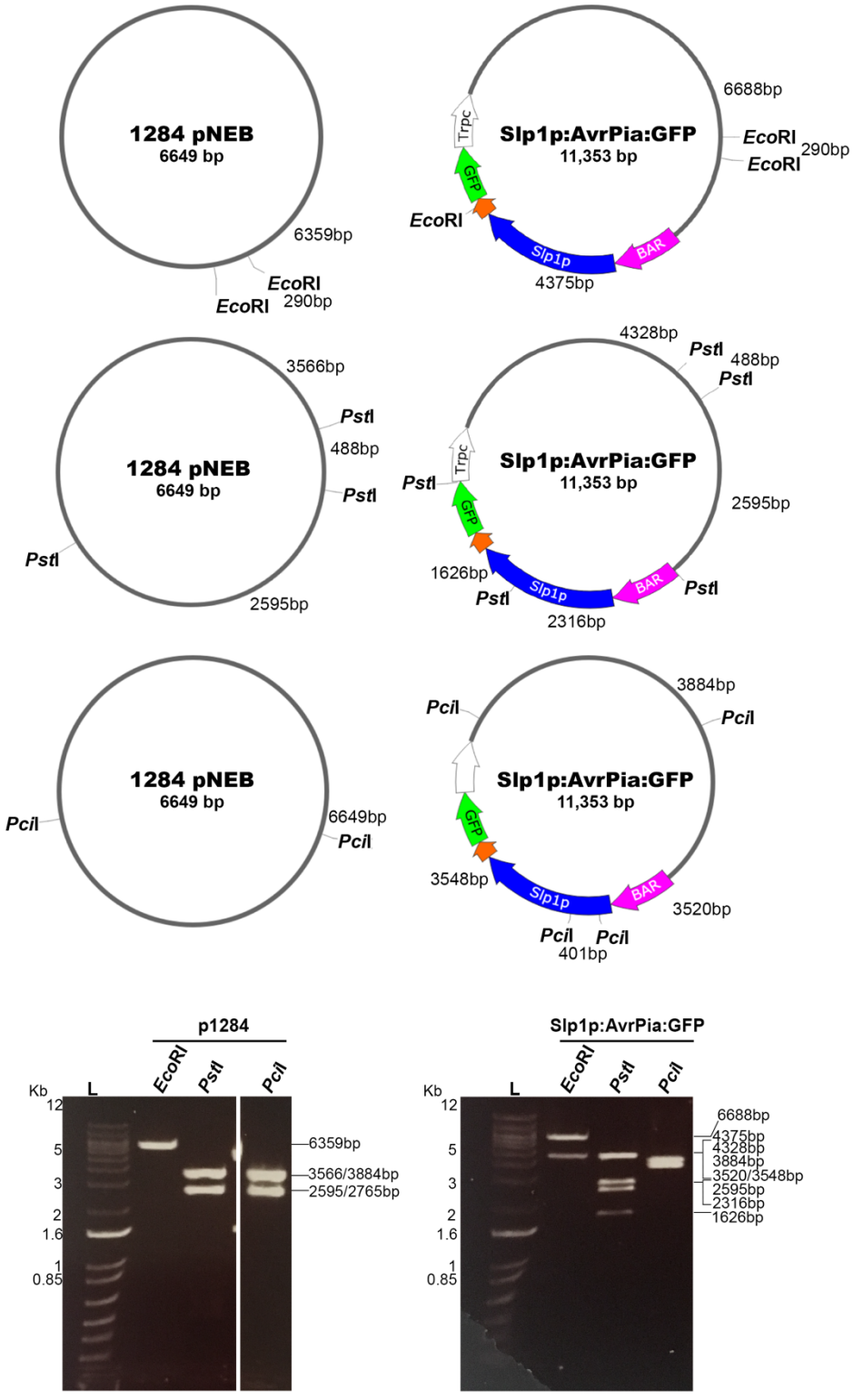


Figure 4.11 ***SLP1p:AVRPIA:GFP* plasmid verification by restriction digestion.** SnapGene software (from GSL Biotech; available at snapgene.com) was used to predict fragment sizes. *SLP1p:AVRPIA:GFP* and pNEB-1284 were digested with *Eco*RI, *Pst*I and *Pci*I. *Eco*RI cuts the empty vector in two fragments 290 bp (not seen) and 6359 bp and *SLP1p:AVRPIA:GFP* into 3 fragments 290 bp (not seen), 4375 bp and 6888 bp. *Pst*I displays a specific band size pattern of 488 bp (not seen), 2595 bp and 3566 bp for pNEB-1284 and 488 bp (not seen), 2595 bp, 2316 bp, 1626 bp and 4328 bp for *SLP1p:AVRPIA:GFP*. *Pci*I band size pattern from cutting empty vector pNEB-1284 is 2765 bp and 3884 bp. For *SLP1p:AVRPIA:GFP* is 3520 bp, 401 bp (not seen), 3548 bp and 3884 bp. Gene regions in colours: Pink = BAR gene, Blue = apoplastic effector, Orange = cytoplasmic effector, Green = GFP and White = TrpC terminator

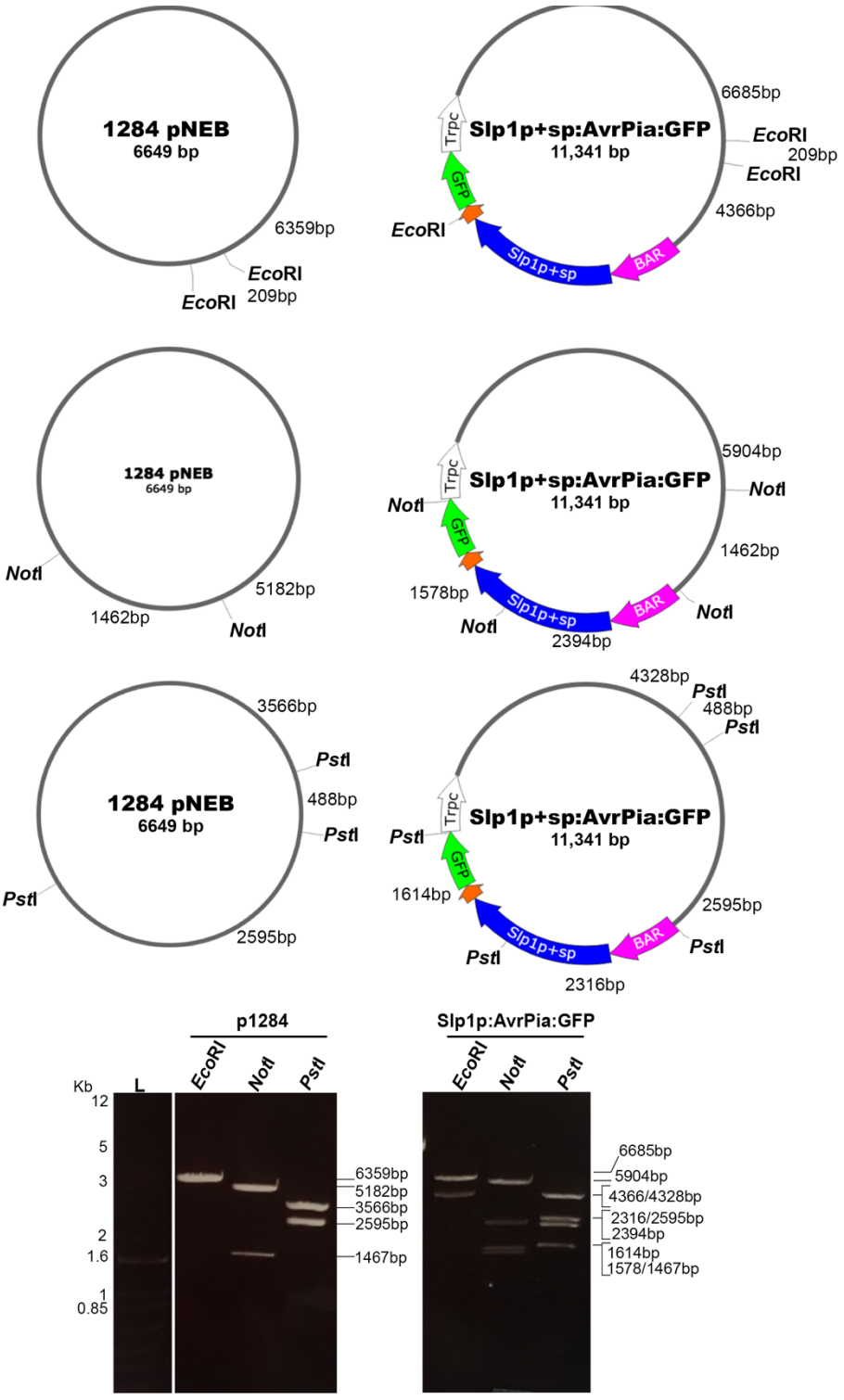


Figure 4.12 ***SLP1p+sp:AVRPIA:GFP* plasmid verification by restriction digestion.** SnapGene software (from GSL Biotech; available at snapgene.com) was used to predict the expected fragment sizes. Positive bacteria colony PCR for *SLP1p+sp:AVRPIA:GFP* transformants and pNEB-1284 empty vector were digested with *Eco*RI, *Not*I and *Pst*I and fractionated by gel electrophoresis. *Eco*RI cuts the empty vector in two fragments 290 bp (not seen) and 6359 bp and *SLP1p+sp:AVRPIA:GFP* into 3 fragments 290 bp (not seen), 4366 bp and 6685 bp. NotI cuts empty vector pNEB-1284 into 1426 bp and 5182 bp. NotI cuts *SLP1p+sp:AVRPIA:GFP* into 1462 bp, 2394 bp, 1578 bp and 5904 bp. *Pst*I displays a specific band size pattern of 488 bp (not seen), 2595 bp and 3566 bp for pNEB-1284 and 488 bp (not seen), 2595 bp, 2316 bp, 1624 bp and 4328 bp for *SLP1p+sp:AVRPIA:GFP*. Gene regions in colours: Pink = BAR gene, Blue = apoplastic effector, Orange = cytoplasmic effector, Green = GFP and White = TrpC terminator.

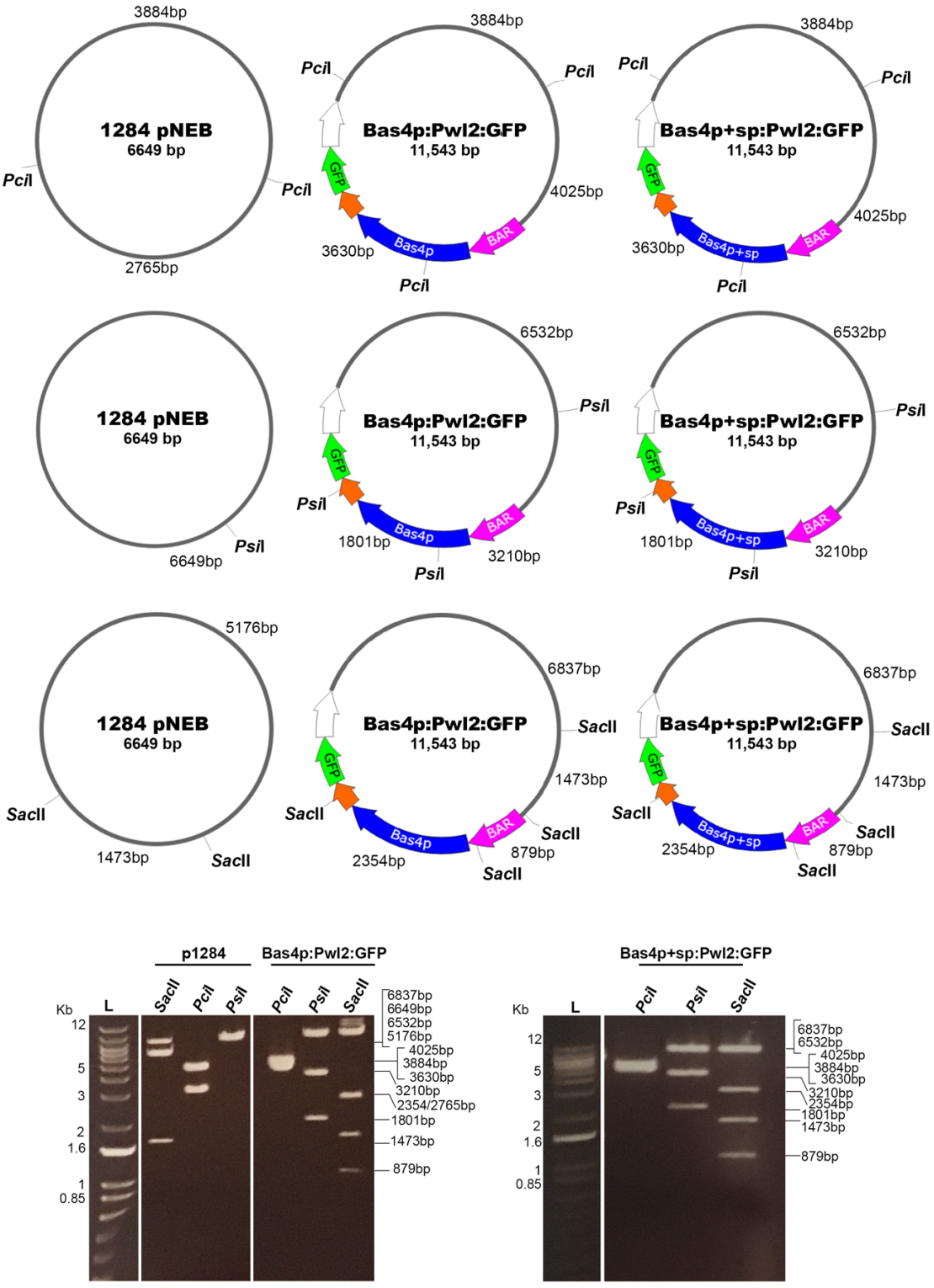


Figure 4.13 ***BAS4p:PWL2:GFP* and *BAS4p+sp:PWL2:GFP* plasmid verification by restriction digestion.** SnapGene software (from GSL Biotech; available at snapgene.com) was used to predict the fragment sizes. *BAS4p:PWL2:GFP*, *BAS4p+sp:PWL2:GFP* and pNEB-1284 were digested with *Sac*II, *Pci*I *and Psi*I. *Pci*I band size pattern for pNEB-1284 is 2765 bp and 3884 bp. For *BAS4p:PWL2:GFP* and *BAS4p+sp:PWL2:GFP* is 4025 bp, 3630 bp and 3884 bp. *Psi*I digests pNEB-1284 as a linearised fragment and cuts *BAS4p:PWL2:GFP* and *BAS4p+sp:PWL2:GFP* into: 3210 bp, 1801 bp and 6532 bp. *Sac*II cuts pNEB-1284 into 1473 bp and 5176 bp. *Sac*II cuts *BAS4p:PWL2:GFP* and *BAS4p+sp:PWL2:GFP* into 1473 bp, 879 bp, 2354 bp and 6837 bp. Gene regions in colours: Pink = BAR gene, Blue = apoplastic effector, Orange = cytoplasmic effector, Green = GFP and White = TrpC terminator.

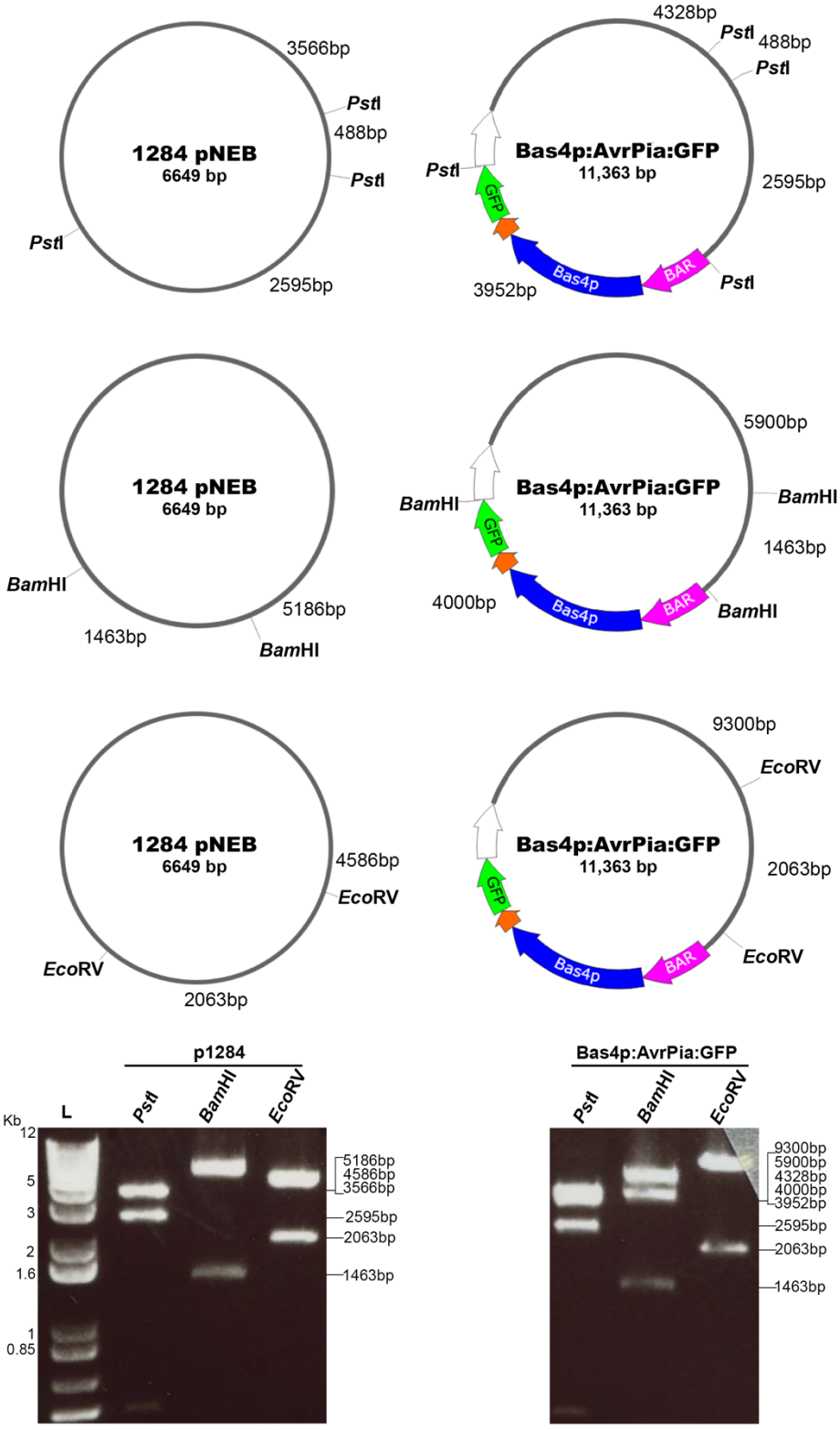


Figure 4.14 ***BAS4p:AVRPIA:GFP* plasmid verification by restriction digestion.** SnapGene software (from GSL Biotech; available at snapgene.com) was used to predict the expected fragment sizes. *BAS4p:AVRPIA:GFP* and pNEB-1284 were digested with *Pst*I, *Bam*HI and *Eco*RV. *Pst*I displays a specific band size pattern of 488 bp (not seen), 2595 bp and 3566 bp for pNEB-1284 and 488 bp (not seen), 2595 bp, 3952 bp and 4328 bp for *BAS4p:AVRPIA:GFP*. *Bam*HI cuts pNEB-1284 into 1463 bp and 5186 bp and *BAS4p:AVRPIA:GFP* into 1463 bp, 4000 bp and 5900 bp. *Eco*RV cuts pNEB-1284 into fragments 2063 bp and 4586 bp and cuts *BAS4p:AVRPIA:GFP* in 2063 bp and 9300 bp. Gene regions in colours: Pink = BAR gene, Blue = apoplastic effector, Orange = cytoplasmic effector, Green = GFP and White = TrpC terminator.

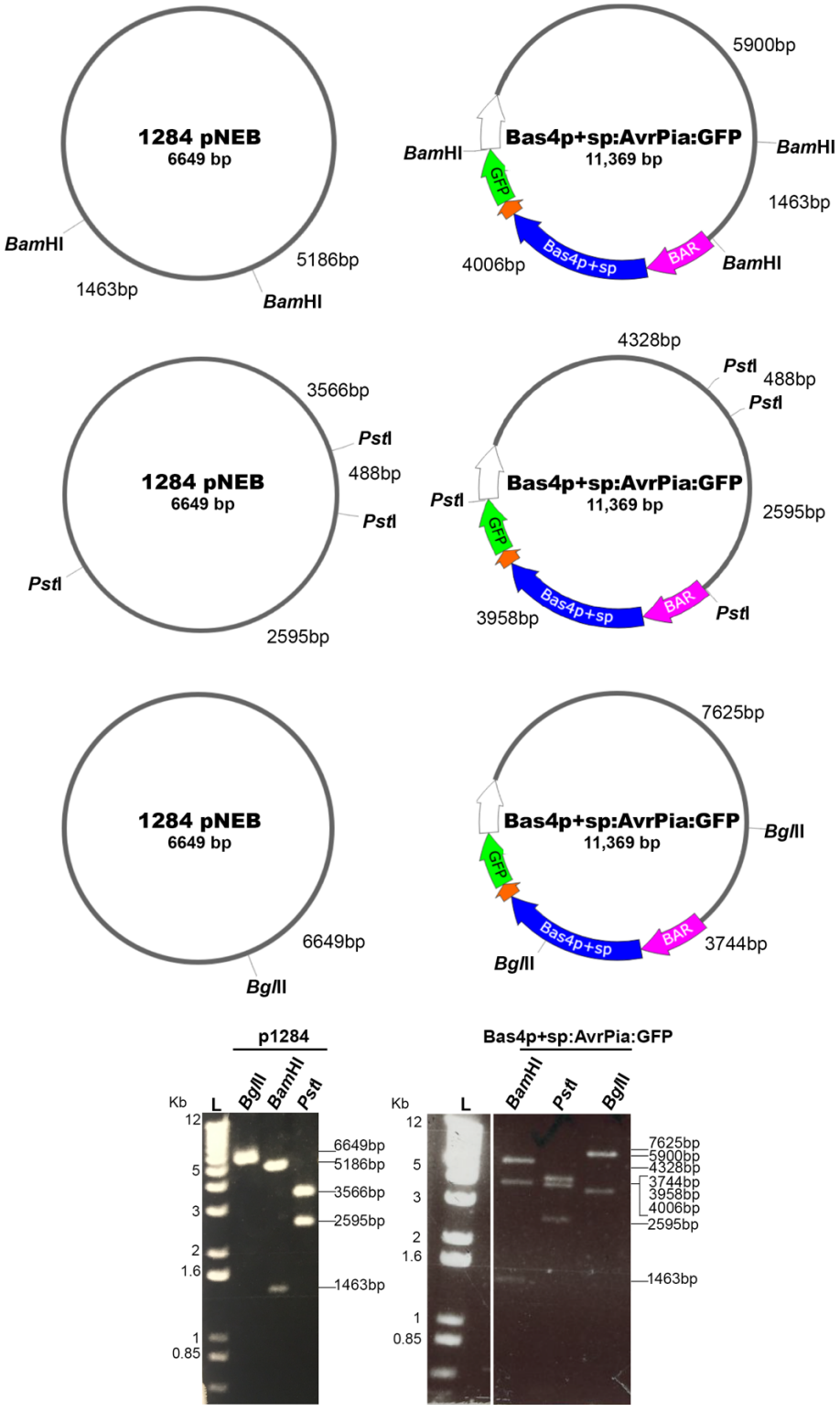


Figure 4.15 ***BAS4p+sp:AVRPIA:GFP* plasmid verification by restriction digestion.** SnapGene software (from GSL Biotech; available at snapgene.com) was used to predict the expected fragment sizes. *BAS4p+sp:AVRPIA:GFP* and pNEB-1284 were digested with *Pst*I, *Bam*HI and *Bgl*II. *Bam*HI cuts pNEB-1284 into 1463 bp and 5186 bp and *BAS4p+sp:AVRPIA:GFP* into 1463 bp, 4006 bp and 5900 bp. *Pst*I displays a specific band size pattern of 488 bp (not seen), 2595 bp and 3566 bp for pNEB-1284 and 488 bp (not seen), 2595 bp, 3958 bp and 4328 bp for *BAS4p+sp:AVRPIA:GFP*. *Bgl*II linearises the empty vector and cuts *BAS4p+sp:AVRPIA:GFP* into 2 fragments, 3744 bp and 7625 bp. Gene regions in colours: Pink = BAR gene, Blue = apoplastic effector, Orange = cytoplasmic effector, Green = GFP and White = TrpC terminator.

Table 4.3 Determination of GFP copy number by qPCR for chimeric constructs *SLP1p:AVRPIA:GFP, SLP1p+sp:AVRPIA:GFP, SLP1p:PWL2:GFP, SLP1p+sp:PWL2:GFP, BAS4p:PWL2:GFP*, *BAS4p+sp:PWL2:GFP BAS4p:AVRPIA:GFP* and *BAS4p+sp:AVRPIA:GFP.*

| Sample | GFP Copy Number[1] | Sample | GFP Copy Number[1] |
|---|---|---|---|
| Control | 1 | Bas4pAvrPia#4 | 1 |
| Guy11 | 0 | Bas4pAvrPia#3 | 12 |
| Slp1pAvrPia#1 | 2 | Bas4pAvrPia#1 | 4 |
| Slp1pAvrPia#6 | 2 | Bas4pAvrPia#5 | 1 |
| Slp1pAvrPia#8 | 1 | Bas4p+spAvrPia#4 | 1 |
| Slp1pAvrPia#15 | 3 | Bas4p+spAvrPia#8 | 1 |
| Slp1pAvrPia#47 | 1 | Bas4p+spAvrPia#3 | 2 |
| Slp1p+spAvrPia#8 | 7 | Bas4pPwl2#12 | 1 |
| Slp1p+spAvrPia#23 | 1 | Bas4pPwl2#13 | 3 |
| Slp1p+spAvrPia#24 | 2 | Bas4pPwl2#3 | 4 |
| Slp1p+spAvrPia#25 | 4 | Bas4pPwl2#1 | 4 |
| Slp1pPwl2#37 | 1 | Bas4pPwl2#4 | 8 |
| Slp1pPwl2#38 | 33 | Bas4pPwl2#5 | 11 |
| Slp1pPwl2#52 | 5 | Bas4p+spPwl2#1 | 1 |
| Slp1p+spPwl2#25 | 4 | Bas4p+spPwl2#4 | 4 |
| Slp1p+spPwl2#31 | 3 | Bas4p+spPwl2#6 | 4 |
| | | Bas4p+spPwl2#8 | 8 |
| | | Bas4p+spPwl2#12 | 3 |

[1]Blind qPCR test performed by iDnaGENETICS Ltd (Norwich research park).

### 4.3.4 The promoter and signal peptide region of an apoplastic effector is sufficient to direct Pwl2 secretion to the apoplast

Having generated the appropriate constructs, I then investigated the pattern of localisation of the cytoplasmic effector protein Pwl2 when driven by the promoter, or promoter and signal peptide regions, of the apoplastic effector genes, *SLP1* or *BAS4*. Pwl2 is a cytoplasmic effector that normally localizes to the BIC (Khang et al., 2010; Giraldo et al., 2013) as shown in Chapter 3. *M oryzae* strains expressing Slp1p:Pwl2:GFP, Slp1p+sp:Pwl2:GFP (Table 4.2) were used to infect rice leaf sheath preparations with a Pwl2:mCh transformant (Giraldo et al., 2013) as the control. Spore suspensions were inoculated into epidermal leaf tissue, as previously described in (Section 2.6.1). After 30 h, leaf sheaths were examined by epifluorescence microscopy.

I recorded the frequency of infected cells in which apoplastic localisation was observed around invasive hyphae and BIC (labelled IH+BIC) or at the BIC alone (BIC), or when a strong signal was observed within invasive hyphae (labelled inside the IH), as shown in Figure 4.16 A. *M. oryzae* transformants expressing Slp1p:Pwl2:GFP predominantly showed BIC localisation (Figure 4.16) and there was no significant difference in localisation patterns observed between transformants expressing Slp1p:Pwl2:GFP and Pwl2:mCh (Giraldo et al., 2013), as shown in Figure 4.16 B. By contrast, transformants expressing Slp1p+sp:Pwl2:GFP localisation showed fluorescence signal both surrounding and inside *M. oryzae* invasive hyphae (Figure 4.16 A). Slp1p+sp:Pwl2:GFP secretion was impaired ($P<0.05$) and BIC localisation was sometimes observed in the leaf sheaths (Figure 4.16 B). The promoter and predicted signal peptide gene region of *SLP1* are therefore sufficient to mis-direct Pwl2, so that some apoplastic delivery of the protein appears to take place, as well as impairment in its secretion, such that the effector can be observed within fungal hyphae.

I then observed secretion of Pwl2 under control of the *BAS4* apoplastic effector-encoding gene. I observed Bas4p:Pwl2:GFP and Bas4p+sp:Pwl2:GFP

localisation both at the BIC and surrounding invasive hyphae, when infections of transformants expressing these constructs were viewed by epifluorescence microscopy (Figure 4.17). This pattern is consistent with the localisation of the Bas4 effector protein and distinct from the exclusive BIC localisation normally observed for Pwl2 (Figure 4.17 A). Quantitative analyses revealed that the Bas4p:Pwl2:GFP and Bas4p+sp:Pwl2:GFP localisation pattern was significantly different (*P<0.05)* from that observed for Pwl2:mCh (Figure 4.17 B). Interestingly, the Bas4p+sp:Pwl2:GFP construct also displays impaired secretion like Slp1p+sp:Pwl2:GFP, providing further evidence that the signal peptide and the 3'end of the promoter are involved in effector secretion.

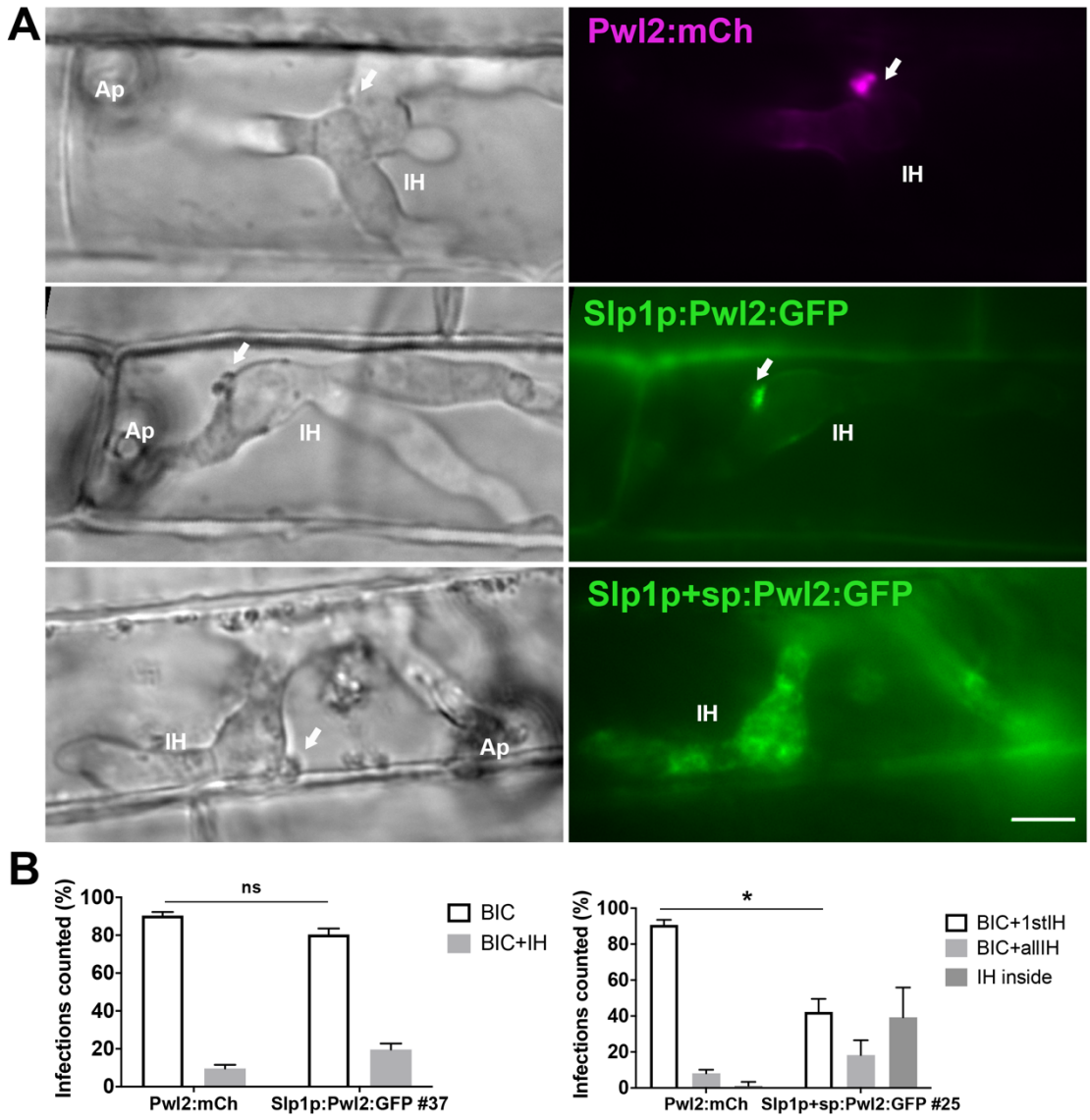


Figure 4.16 **The promoter and signal peptide of apoplastic effector gene *SLP1* does not drive Pwl2 effector protein into the BIC.** Micrographs of live cell imaging of leaf sheath infections by *M. oryzae* viewed by obtained epifluorescence microscopy. A) Localisation of Pwl2:mCh, Slp1p:Pwl2:GFP#37 and Slp1p+sp:Pwl2:GFP#25. B) Bar charts to show proportion of BIC structures showing fluorescence. For Slp1p:Pwl2:GFP#37 and Slp1p+sp:Pwl2:GFP#25 *M. oryzae* expressing strains a total of 3 replicates were made with 94 infections observed. An unpaired parametrical t-test with a two-tailed distribution gave a *P*-value of 0.05 for Slp1p:Pwl2:GFP#37 and a *P*-value of 0.003 for Slp1p+sp:Pwl2:GFP#25. All the strains were excited at 488nm for 200 ms. Scale bars represent 10 µm. Arrow marks the BIC, Ap marks the appressorium and IH marks *M. oryzae* invasive hyphae. BIC+1stIH means fluorescence observed at the BIC and first invasive hyphae. BIC+allIH means fluorescence observed at the BIC and around all the invasive hyphae.

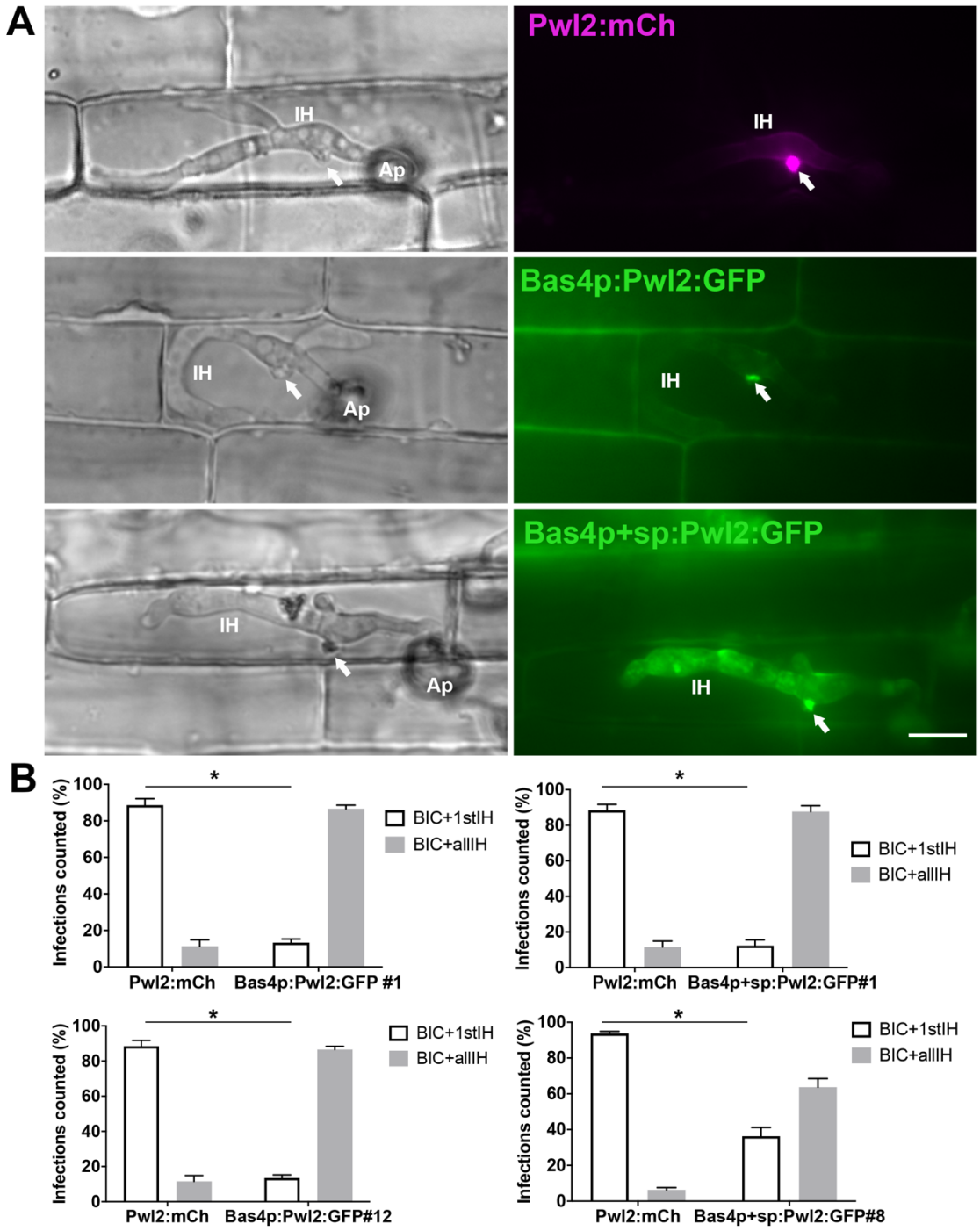


Figure 4.17 The promoter and signal peptide of apoplastic effector gene *BAS4* driving Pwl2 effector protein has an apoplastic localisation pattern. Micrographs obtained on conventional epifluorescence of live cell imaging from leaf sheaths of M. oryzae infection in rice. A) Localisation of Pwl2:mCh, Bas4p:Pwl2-GFP and Bas4p+sp:Pwl2-GFP. B) Bar charts to show proportion of *M. oryzae* whole invasive hyphae fluorescence. For constructs Bas4p:Pwl2:GFP#1, Bas4p:Pwl2:GFP#12, Bas4p+sp:Pwl2:GFP#1 and Bas4p+sp:Pwl2:GFP#8 a total of 3 replicates was done, with 91 infections observed. An unpaired parametrical t-test with a two-tailed distribution gave a *P*-value of 0.00004 for Bas4p:Pwl2:GFP#1, a *P*-value of 0.00005 for Bas4p:Pwl2:GFP#12, a *P*-value of 0.00009 for Bas4p+sp:Pwl2:GFP#1 and a *P*-value of 0.0003 for Bas4p+sp:Pwl2:GFP#8. All the strains were excited at 488nm for 200 ms. Scale bars represent 10 µm. Arrow marks the BIC, Ap marks the appressorium and IH marks *M. oryzae* invasive hyphae. . BIC+1stIH means fluorescence observed at the BIC and first invasive hyphae. BIC+allIH means fluorescence observed at the BIC and around all the invasive hyphae.

### 4.3.5 The promoter and signal peptide regions of apoplastic effectors are sufficient to re-direct the secretion of AvrPia

I decided to extend the study to see if a further cytoplasmic effector, Avr-Pia, could be re-directed based on expression by the promoter and signal peptide sequences of an apoplastic effector-encoding gene. For this, I selected single copy transformants expressing Slp1p:AvrPia:GFP and Slp1p+sp:AvrPia:GFP and used a *M. oryzae* strain expressing *AVRPIA:GFP* (Section 4.2.5) as a control was made in the laboratory. Infection of leaf sheath tissue were carried out as described previously and then viewed by epifluorescence microscopy.

I observed Slp1p:AvrPia:GFP localisation (Figure 4.18 A) around *M. oryzae* invasive hyphae and at the BIC and no significant difference was apparent between the localisation patterns of Slp1p:AvrPia:GFP and AvrPia:GFP (*P>0.05)* (Figure 4.18 B). By contrast, when both promoter and signal peptide sequences were present in Slp1p+sp:AvrPia:GFP transformants , then localisation (Figure 4.18 A) was observed around *M. oryzae* invasive hyphae and a significant number of infections (*P<0.05)* were observed not have BIC fluorescence (Figure 4.18 B). These results are consistent with the promoter and signal peptide regions of *SLP1* being sufficient to re-direct the secretion of a proportion of AvrPia to the apoplast.

In order to provide for a consistent study, I then expressed AvrPia under control of the *BAS4* apoplastic effector gene promoter or promoter and signal peptide regions and selected single copy transformants. In order to quantify if there was a significant difference between *M. oryzae* strains expressing *AVRPIA* under the control of its own promoter, the *BAS4* promoter or the *BAS4* promoter and signal peptide sequence, respectively, I quantified the maximum intensity at the BIC and divided this the maximum intensity in the first invasive hypha ($GFP^{BIC}/GFP^{IH}$), as described in Chapter 3.

I observed localisation of Bas4p:AvrPia:GFP around the invasive hyphae and at the BIC, as shown in Figure 4.19 A, with an example of a line scan analysis and

the quantification of the $GFP^{BIC}/GFP^{IH}$ ratio between Bas4p:AvrPia:GFP and AvrPia:GFP. The results showed no significant difference (*P>0.05)*. The *BAS4* promoter does not therefore have an effect on AvrPia effector protein localisation (Figure 4.19 B). However, when Bas4p+sp:AvrPia:GFP transformants were observed localisation was observed both outlining invasive hyphae and at the BIC, as shown in Figure 4.19 A. The $GFP^{BIC}/GFP^{IH}$ ratio between Bas4p+sp:AvrPia:GFP and AvrPia:GFP showed a significant difference *(P*<0.001) *(*Figure 4.19 B). The comparisons were always recorded between the control and one of the chimeric constructs. The comparisons between the chimeric constructs would need to be done apart. I conclude that the *BAS4* promoter and signal peptide regions are able to affect the secretion of the AvrPia effector directing a proportion of the protein to the apoplast rather than the BIC. This is consistent with the observation that when the promoter and signal peptide regions are used together then they are sufficient to affect the secretion patterns of cytoplasmic or apoplastic effectors, based on the 16 different chimeric constructs I have presented in Chapters 3 and 4.

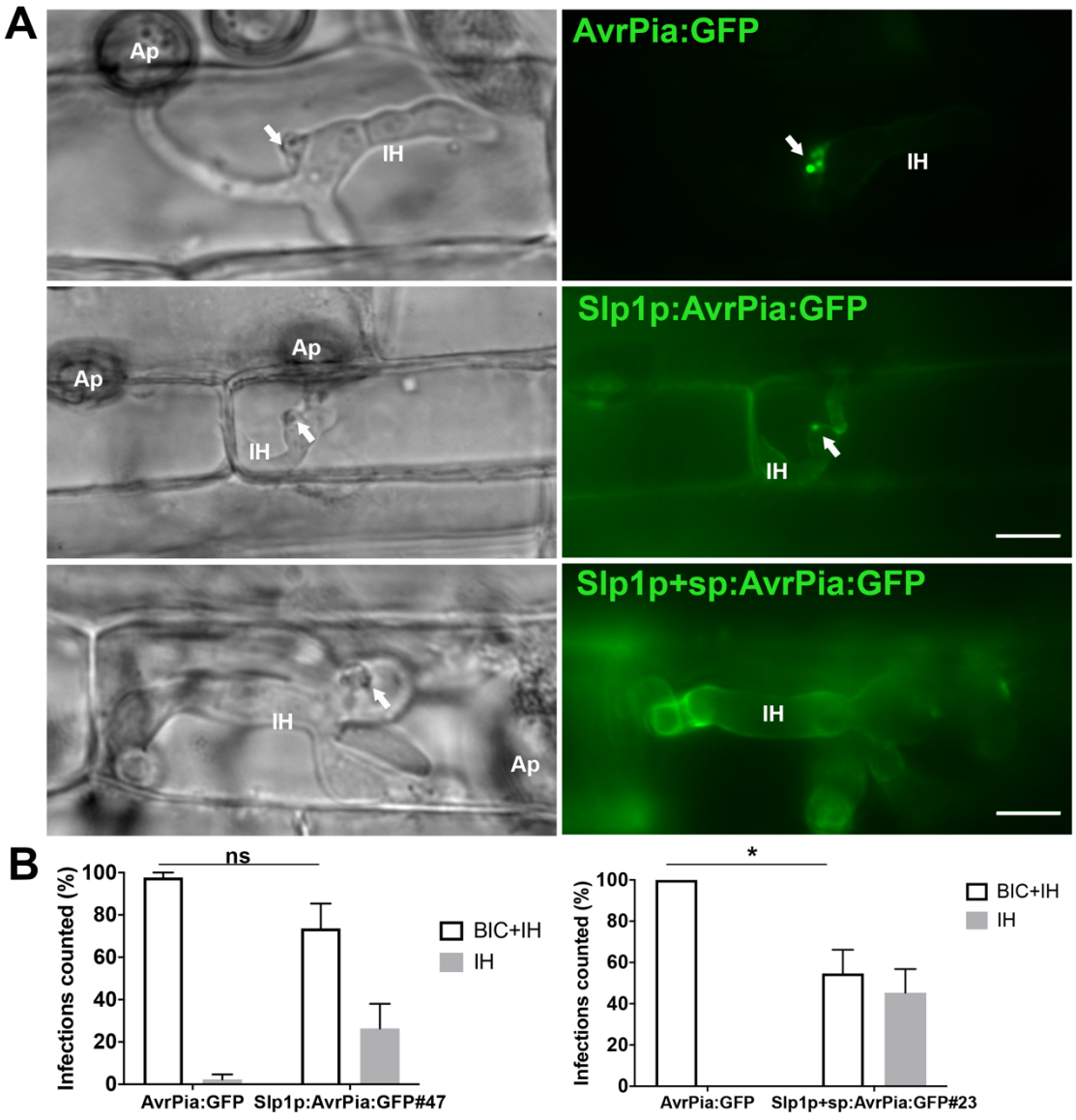


Figure 4.18 The promoter and signal peptide of apoplastic effector gene *SLP1* is sufficient to re-direct secretion of the AvrPia effector protein. Micrographs of live cell imaging of leaf sheath infections by *M. oryzae* viewed by obtained epifluorescence microscopy. A) Localisation of AvrPia-GFP, Slp1p:AvrPia:GFP#47 and Slp1p+sp:AvrPia:GFP#23. B) Bar charts to show proportion of BIC structures showing fluorescence. For Slp1p:AvrPia:GFP#47 and Slp1p+sp:AvrPia:GFP#23 *M. oryzae* expressing strains a total of 3 replicates were made with 96 infections observed. An unpaired parametrical t-test with a two-tailed distribution gave a *P*-value of 0.06 for Slp1p:AvrPia:GFP#47 and a *P*-value of 0.016 for Slp1p+sp:AvrPia:GFP#23. All the strains were excited at 488nm for 200 ms. Scale bars represent 10 µm. Arrow marks the BIC, Ap marks the appressorium and IH marks *M. oryzae* invasive hyphae.

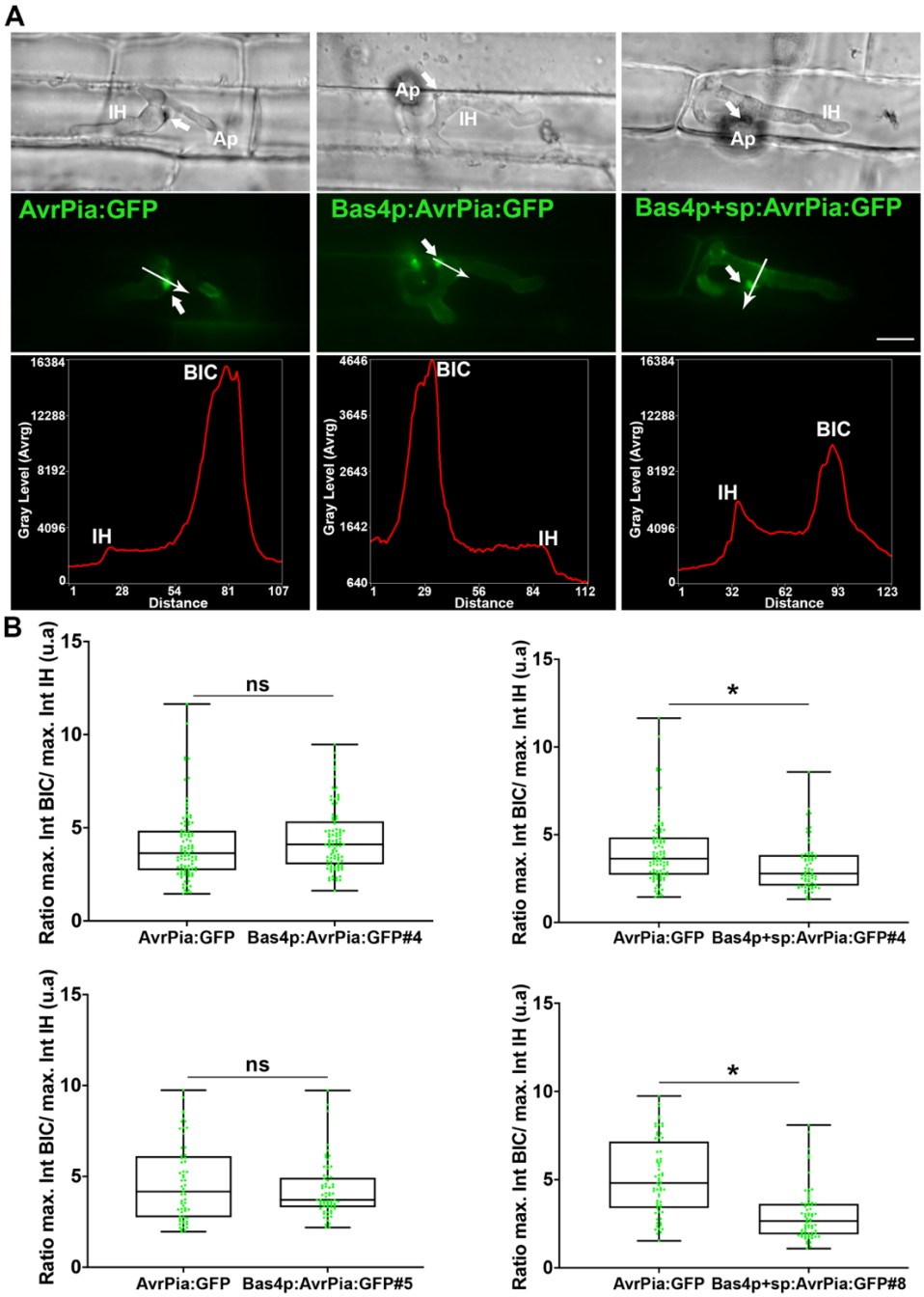


Figure 4.19 **The promoter and signal peptide of the apoplastic effector *BAS4* re-directs the secretion of the cytoplasmic effector AvrPia.** Micrographs of live cell imaging of leaf sheath infections by *M. oryzae* viewed by obtained epifluorescence microscopy. A) Localisation of AvrPia:GFP, Bas4p:AvrPia:GFP and Bas4p+sp:AvrPia:GFP. B) Box and whiskers plots showing the ratio $GFP^{BIC}/GFP^{IH}$ for Bas4p:AvrPia:GFP#4, Bas4p:AvrPia:GFP#5 and AvrPia:GFP control. From the constructs Bas4p:AvrPia:GFP#4 and Bas4p:AvrPia:GFP#5 a total of 3 replicates was made with 94 number of infections observed. A Mann-Whitney test gave a *P*-value of 0.07 for Bas4p:AvrPia:GFP#4 and a *P*-value of 0.6 for Bas4p:AvrPia:GFP#5. Box and whiskers plots showing the ratio $GFP^{BIC}/GFP^{IH}$ for Bas4p+sp:AvrPia:GFP#4, Bas4p+sp:AvrPia:GFP#8 and Bas4:GFP control. From the Bas4p+sp:AvrPia:GFP#4 and Bas4p+sp:AvrPia:GFP#8 constructs a total of 3 replicates was made with 94 infections observed. A Mann-Whitney test gave a *P*-value of 0.001 for Bas4p+sp:AvrPia:GFP#4 and a *P*-value of 0.0001 for Bas4p+sp:AvrPia:GFP#8. All the strains were excited at 488nm for 200 ms. Scale bars represent 10 µm. Arrow marks the BIC, Ap marks the appressorium and IH marks *M. oryzae* invasive hyphae.

### 4.3.6 Generation of single copy *M. oryzae* strains expressing *SLP1p:PWL2sp:SLP1:GFP* construct

In this chapter and chapter 3 we demonstrate that the promoter and signal peptide gene sequences of effectors are partially responsible for directing effectors to the correct secretion domain, either the apoplast or the BIC. To investigate whether it was only the signal peptide, I constructed *SLP1p:PWL2sp:SLP1:GFP* vector (Figure 4.20). The predicted signal peptide of Pwl2 was fused to the mature Slp1 without its native signal peptide to create Pwl2sp:Slp1 oligo fragment. This fragment was subsequently fused to GFP DNA sequence. Expression of this vector was driven by the native 2.0 kb *SLP1* promoter fragment. To do this, a 593 bp DNA fragment encoding Pwl2sp:Slp1 peptide was synthesised (GENEWIZ). The fragment was engineered to contain 15 bp overhangs at the 3' end of the 2.0 kb *SLP1* promoter and at the beginning of the GFP sequence. This fragment together with 2.0 kb Slp1 promoter fragment, Bar gene sequence fragment and GFP fragment were used to transform in bacteria using In-Fusion system. The *SLP1p:PWL2sp:SLP1:GFP* construct was independently confirmed by restriction digestion (Figure 4.21) and checked for errors by DNA sequencing. The resulting vector was subsequently introduced into *M. oryzae* by protoplast-mediated transformation (Talbot et al., 1993) of Guy11. Putative transformants were selected based on their resistant cassette *BAR* gene with glufosinate (30 µg $ml^{-1}$). GFP positive transformants were screened for fluorescence by using Olympus IX81 inverted microscope. Single copy transformants were confirmed by qPCR blind test (Table 4.4). Single copy Slp1p:Pwl2sp:Slp1:GFP *M. oryzae* transformants used in this study are in Table 4.2.

Table 4.4 Determination of GFP copy number by qPCR for *SLP1p:PWL2sp:SLP1:GFP*

| Sample | GFP Copy Number[1] |
|---|---|
| Guy11 | 0 |
| Control | 1 |
| Slp1pPwl2spSlp1#1 | 1 |
| Slp1pPwl2spSlp1#2 | 0 |
| Slp1pPwl2spSlp1#4 | 1 |
| Slp1pPwl2spSlp1#6 | 12 |
| Slp1pPwl2spSlp1#8 | 1 |
| Slp1pPwl2spSlp1#10 | 1 |
| Slp1pPwl2spSlp1#11 | 1 |
| Slp1pPwl2spSlp1#12 | 2 |
| Slp1pPwl2spSlp1#14 | 5 |
| Slp1pPwl2spSlp1#15 | 1 |
| Slp1pPwl2spSlp1#17 | 12 |
| Slp1pPwl2spSlp1#18 | 12 |

[1]Blind qPCR test performed by iDnaGENETICS Ltd (Norwich research park).

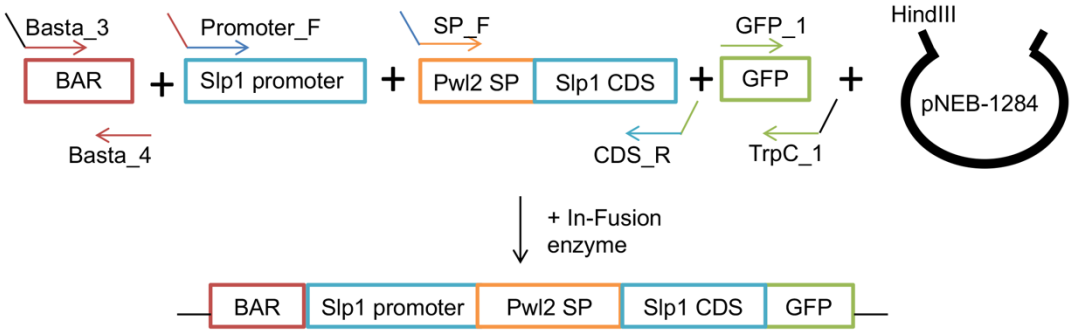


Figure 4.20 **Schematic representation of the cloning strategy**. Cloning strategy for the *SLP1p:PWL2sp:SLP1:GFP* construct with the signal peptide region of apoplastic effector *SLP1* was replaced with the signal peptide region of cytoplasmic effector *PWL2*.

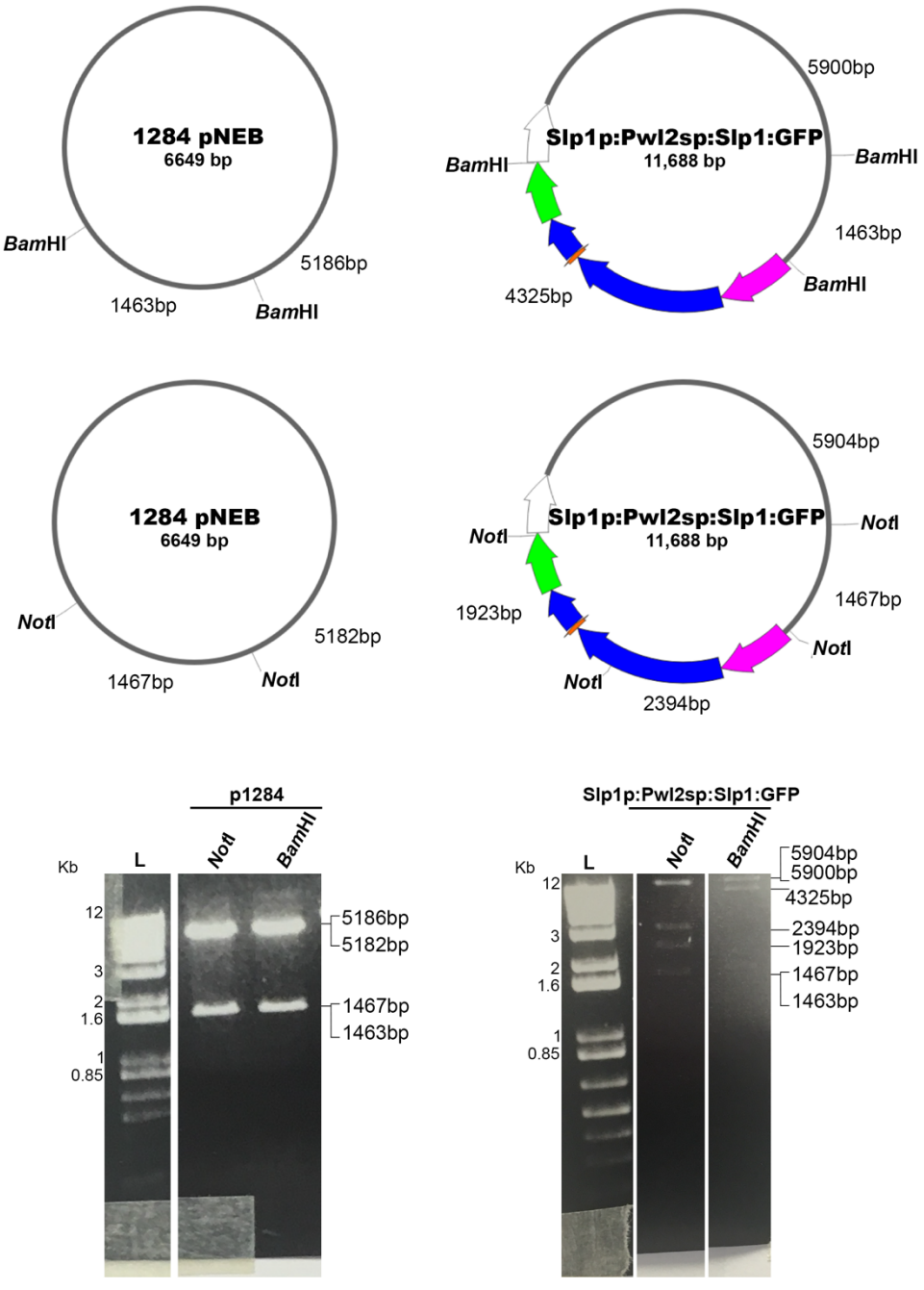


Figure 4.21 ***SLP1p:PWL2sp:SLP1:GFP* plasmid verification by DNA digestion.** SnapGene software (from GSL Biotech; available at snapgene.com) was used to predict the expected fragment sizes. Positive bacteria colony PCR for *SLP1p:PWL2sp:SLP1:GFP* transformants and pNEB-1284 empty vector were digested with *Bam*HI and *Not*I and fractionated by gel electrophoresis. *Bam*HI cuts pNEB-1284 into 1463 bp and 5186 bp and *SLP1p:PWL2sp:SLP1:GFP* into 1463 bp, 4325 bp and 5900 bp. *Not*I displays a specific band size pattern of 1467 bp and 5182 bp for pNEB-1284 and 1467 bp, 2394 bp, 1923 bp and 5904 bp for *SLP1p:PWL2sp:SLP1:GFP*. Gene regions in colours: Pink = BAR gene, Blue = apoplastic effector, Orange = cytoplasmic effector, Green = GFP and White = TrpC terminator

### 4.3.7 Investigating the role of a signal peptide sequence alone to re-direct effector secretion

All of the results obtained from analysis of 16 chimeric constructs provided a consistent picture that the promoter and signal peptide sequence of each class of effector was vital to its correct secretion. Thus, when the promoter and signal peptide sequence of a cytoplasmic effector gene was used to drive expression of an apoplastic effector, then the apoplastic effector would be re-directed to the BIC. Conversely, when the promoter and signal peptide of an apoplastic effector was used to drive expression of a cytoplasmic effector, then less of the protein was directed to the BIC with some re-direction to the apoplast observed and, in some combinations, impairment in secretion. An overriding conclusion from this work was the significance of the signal peptide region, in addition to the promoter, as the re-direction of secretion was never observed when the promoter was used on its own.

I therefore decided to investigated whether it was possible to re-direct the secretion of the apoplastic effector Slp1 when driven by its native promoter but replacing the predicted signal peptide of Slp1 with the Pwl2 signal peptide. In this way, I reasoned that the role of the signal peptide operating separately, could be determined.

*M.* oryzae transformants expressing Slp1p:Pwl2sp:Slp1:GFP were used to inoculated rice leaf tissue and 30 hpi, leaf sheaths were observed by microscopy. The pattern of localisation of Slp1p:Pwl2:Slp1:GFP was, however, very similar to that observed in Slp1:GFP transformants with fluorescence very predominantly localised to the apoplast (Figure 4.22 A). This localisation pattern was analysed in two single copy transformants of Slp1p:Pwl2:Slp1:GFP, and no significant difference ($P$>0.05) was observed with the control Slp1:GFP (Figure 4.22 B). In conclusion, the signal peptide of *PWL2* is not sufficient to re-direct the Slp1 effector into the BIC. When considered together with all the observation of the effector chimeras generated, it appears that the important signal for control of secretion must, therefore lie towards the 3' end of the promoter and the 5' end of the signal peptide, with neither sequence on their own being sufficient for re-directing effector secretion.

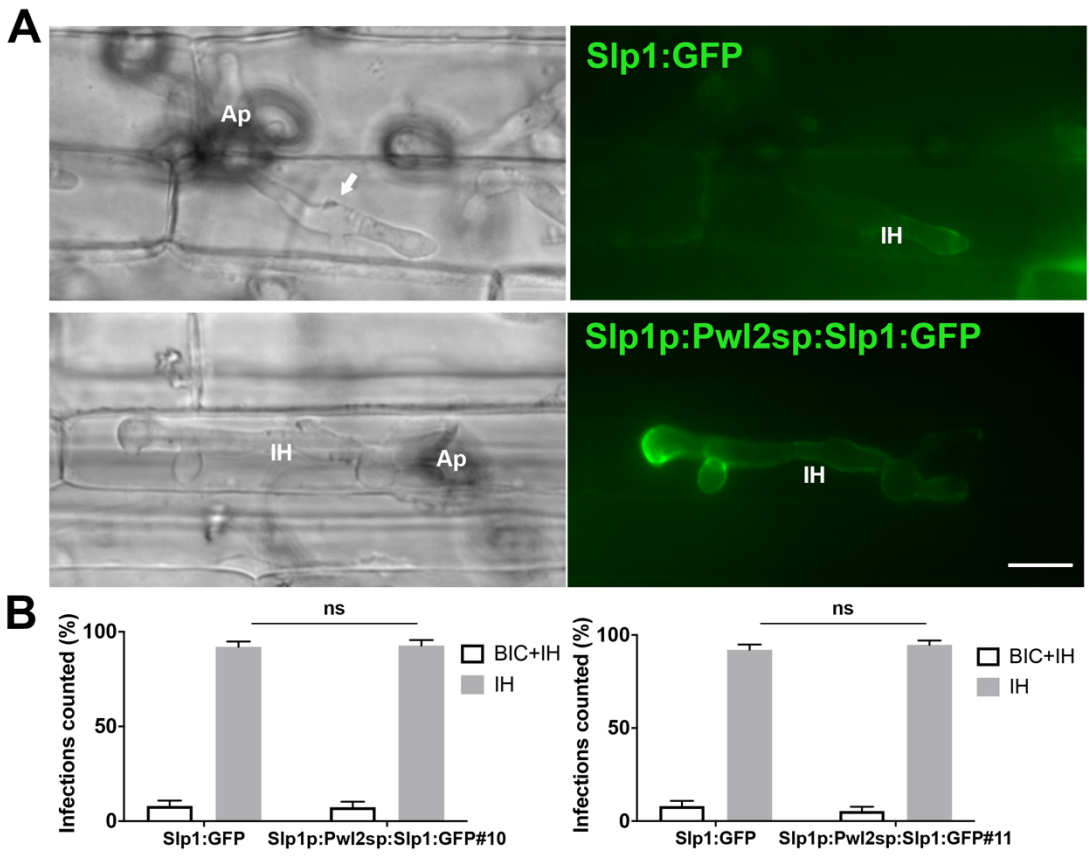


Figure 4.22 **The signal peptide of cytoplasmic effector gene *PWL2* does not drive Slp1 effector protein into the BIC.** Micrographs of live cell imaging of leaf sheath infections by *M. oryzae* viewed by obtained epifluorescence microscopy. A) Localisation of Slp1:GFP. B) Slp1p:Pwl2sp:Slp1:GFP *M. oryzae* strains localisation. C) Bar charts to show proportion of BIC structures showing fluorescence. For Slp1p:Pwl2sp:Slp1:GFP#10 and Slp1p:Pwl2sp:Slp1:GFP#11 *M. oryzae* expressing strains a total of 3 replicates were made with 102 infections observed. An unpaired parametrical t-test with a two-tailed distribution gave a *P*-value of 0.9 for Slp1p:Pwl2sp:Slp1:GFP#10 and a *P*-value of 0.5 for Slp1p:Pwl2sp:Slp1:GFP#11. All the strains were excited at 488nm for 200 ms. Scale bars represent 10 µm. Arrow marks the BIC, Ap marks the appressorium and IH marks *M. oryzae* invasive hyphae.

## *4.4 Discussion*

In this Chapter, I have reported experiments to test whether the promoter of an apoplastic effector-encoding gene and its corresponding signal peptide sequence is sufficient to guide the secretion of a cytoplasmic effector protein into the apoplast. Results from Chapter 3 provided evidence that when the promoter and signal peptide combination from a cytoplasmic effector-encoding gene was used to drive expression of an apoplastic effector, then it could be re-direct secretion into the BIC. I therefore wanted to see if the reciprocal was true: Is it possible to re-direct effector localisation simply by changing the promoter and signal peptide sequence?

To test this idea, I first needed to test whether *BAS4* and *SLP1* promoter and signal peptide sequences could direct free GFP to the apoplast, as normally observed when these genes are expressed natively as C-terminal GFP fusions. This provided a test of sufficiency, as it would determine whether any sequences within the coding region of either *BAS4* or *SLP1* were necessary for correct secretion. I observed that the localisation of Slp1p+sp:GFP was identical to that observed previously for a C-terminal Slp1-GFP translational fusion (Mentlak et al., 2012) with fluorescence surrounding invasive hyphae, consistent with the apoplastic secretion of the effector, where it fulfils its role in suppression of chitin-triggered immunity (Mentlak et al., 2012). I carried out the same experiments to investigate whether the promoter and signal peptide of *BAS4* were sufficient to drive expression of free GFP to the correct location. This analysis was, however, complicated by the fact that Bas4, which is an apoplastic effector (Mosquera et al., 2009), also shows some localisation to the BIC, as previously reported (Khang et al., 2010) and shown in Chapter 3. For this reason, it became necessary to use the quantitative method introduced in Chapter 3 to quantify all effects using *BAS4.*

Localisation of Bas4p+sp:GFP showed the same apoplastic localisation pattern as Bas4-GFP with some BIC localisation observed too. These results are consistent with the results with *SLP1*, and therefore support the hypothesis that the promoter and signal peptide gene regions of *M. oryzae* effectors are sufficient to regulate the final secretory location of the protein.

It is important to underline the unusual nature of this conclusion. Promoter sequences regulate the expression of genes, leading to temporal and spatial patterns of mRNA production during development, or in response to environmental signals (Kleemann et al., 2012; Dutt et al., 2014; Xu et al., 2017). This is one of the most basic rules associated with gene expression. Signal peptides, meanwhile, are necessary for directing newly synthesized proteins to the secretory pathway. This normally directs them to the ER and then to their target organelle, or to the Golgi and via secretory vesicles to the plasma membrane for exocytosis. These sequences do not, however, normally determine any further sorting of the destination of a given protein, which is instead determined by post-translational modifications, such as glycosylation, interaction with other proteins, such as chaperones, or by the action of other signalling pathways (Konig et al., 2009; Goldberg and Cowman, 2010; Pantazopoulou, 2016; Steinberg, 2016; Zheng et al., 2016; Rico-Ramirez et al., 2018).

I therefore prepared the reciprocal chimeric constructs to those analysed in Chapter 3 in order to rigorously test whether there really were signals associated with these regions, that were sufficient to re-direct effectors of both classes. For these experiments, I used the cytoplasmic effector proteins Pwl2 and AvrPia and expressed them under control of the promoter, or promoter-signal peptide regions of the apoplastic effector genes *BAS4* and *SLP1*. When the Pwl2 effector protein-encoding genes were expressed without their predicted signal peptide, but under the control of *SLP1* promoter and corresponding signal peptide regions, BIC localisation was not observed. Most infections observed for Slp1p+sp:Pwl2:GFP showed some impairment in secretion with fluorescence observed inside *M. oryzae* invasive hyphae. This pattern of fluorescence inside the invasive hyphae, with less BIC fluorescence was also observed for Bas4p+sp:Pwl2:GFP, suggesting the *PWL2* promoter and signal peptide are important for its normal delivery to the BIC, and may therefore also be necessary for translocation of the Pwl2 effector protein to host cells. Pwl2 is known to be delivered into host cells because when a nuclear signal (NLS) was fused to the C-terminus of a Pwl2-mCherry fusion protein, the fluorescent protein was observed in the nucleus of the infected cells, and in adjacent plant cells (Khang et al., 2010). Using the *BAS4* promoter and signal peptide to drive Pwl2 effector protein led to a significant

reduction in BIC localisation and more accumulation around invasive hyphae in the apoplast.

Live cell imaging of the Arbuscular Mycorrhizal symbiosis between *Medicago truncatula* and *Rhizophagus irregularis* has shown that localisation of the periarbuscular plant host protein MtPT4, which encodes a predicted phosphate transporter, an arbuscule branch domain membrane protein, and MtBcp1, an arbuscule trunk domain protein that encodes a blue copper-binding protein was also dependent on their native promoters (Pumplin and Harrison, 2009; Pumplin et al., 2012). pMtPT4:MtPT4-GFP localises to the periarbuscular membrane surrounding the branches of mid-size and mature arbuscules, but there was no GFP signal on the membrane surrounding trunk arbuscules. The pMtBcp1:GFP-MtBcp1 signal localised in the plasma membrane and the periarbuscular membrane around the arbuscule trunk (Pumplin and Harrison, 2009). When driven by the high level constitutive 35S promoter or the MtBcp1 promoter, MtPT4 was retained in the ER (Pumplin and Harrison, 2009). It has been suggested that this is because these promoters regulate expression at different time points during infection. Pumplin and co-workers therefore used MtPT1 and the 35S promoter to generate different chimeric constructs. MtPT1 is another phosphate transporter that localises to the plasma membrane when expressed under the control of its native promoter, but at the periarbuscular membrane under the control of MtPT4 promoter. MtPT1 has 61% amino acid identity with MtPT4 but the 5' sequences are different. These 5' untranslated leader sequences were therefore exchanged in swap experiments, but revealed not to play a role in localisation of these proteins. It has therefore been proposed that the generation of different domains that form the periarbuscular membrane is mediated by precise temporal expression of membrane-protein encoding genes (Pumplin et al., 2012). It is therefore possible that results reported here might be affected by precise temporal regulation of each promoter although infection experiments and observations were all carried out across a time course and recorded at exactly the same times. This is something that will need to be explored in detail in future.

I observed very similar results when the cytoplasmic AvrPia effector protein was expressed under the control of *SLP1* or *BAS4* promoter and signal peptide gene sequences, with a clear reduction in the amount of BIC localisation observed and

a more predominant localisation pattern around invasive hypha. These results are therefore consistent with the original observations reported in Chapter 3.

Interestingly, however, the replacement of the *SLP1* signal peptide with the *PWL2* signal peptide was not sufficient to re-direct Slp1 into the BIC. This provides important information that suggests that the signal for control of the secretory destination does not reside solely in the signal peptide region of an effector.

This result led us to speculate that the signal may well reside in the 3'end of the promoter and the very 5' end of the gene. Given that all of the promoter fusions reported here were made at the start codon, rather than the putative transcriptional start site, it is possible that the region associated with secretory destination of the protein might be in the 5' untranslated region of the effector gene transcript. This would suggest that some of the sorting mechanism might occur at the mRNA level, directing an effector gene transcript into a distinct domain for translation that might ultimately determine the secretory pathway that the resulting effector then entered. In such a model, the 5'end of the transcript would therefore be important for determining if an apoplastic effector entered the conventional secretion pathway, or a cytoplasmic effector entered the Brefeldin A-insensitive pathway that directs their entry to the BIC.

In Chapter 5 I report experiments to test this idea by expressing the chimeric constructs generated in this study in the presence or absence of Brefeldin A. I also set out to determine whether the promoter-signal peptide combinations necessary for re-direction to the BIC actually facilitate translocation of proteins into host plant cells.

# Chapter 5. Investigating the delivery and translocation of effectors in the rice blast fungus *M. oryzae*

## *5.1 Introduction*

Evidence of effector protein delivery into host plants has been obtained to date by immunofluorescence microscopy (Kemen et al., 2005; Rafiqi et al., 2010; Plett et al., 2011), live cell imaging using fluorescent markers (Khang et al., 2010) and by electron microscopy (Djamei et al., 2011) (Kemen et al., 2005; Kankanala et al., 2007). Electron microscopy was used, for example, to demonstrate effector translocation inside the plant for the RTP1p and Cmu1 cytoplasmic effectors (Djamei et al., 2011; Kemen et al., 2013). Using immunolocalization, Rafiqi and co-workers demonstrate that the flax rust AvrM protein is secreted from haustoria and detected in the plant cytoplasm (Rafiqi et al., 2010). Rust transferred protein 1 from *Uromyces fabae* (Uf-RTP1p) and homolog Us-RTP1p in *Uromyces striatus* were detected inside plant cells by immunofluorescence and immunogold electron microscopy.

The translocation of effectors into host plants by *M. oryzae* has been visualised using two different techniques to date (Kankanala et al., 2007; Khang et al., 2010). First, the addition of a nuclear localisation sequence (NLS) at the C-terminus of the effector protein, Pwl2, was used to visualise the effector within plant nuclei, which concentrated the effector sufficiently for observation to be possible, overcoming the dilution effect that occurs when the effector is delivered normally into the cytoplasm (Khang et al., 2010). Secondly, plasmolysis has been used as a means of concentrating effector proteins to allow visualisation in *M. oryzae* infected leaf sheaths. The leaf sheath preparations are exposed to hyperosmotic sucrose solution that cause the cell to shrink so the plant plasma membrane withdraws from the cell wall, allowing concentration of the diffused signal of the translocated effector inside the cytoplasm of the host to accumulate and therefore observation by laser confocal microscopy (Kankanala et al., 2007). Both of these methods were used to demonstrate that Pwl2, not only accumulates in infected rice cells, but also diffuses to adjacent non-infected cells (Khang et al., 2010). This plasmolysis assay in *M. oryzae* also demonstrated that the EIHM

forms a sealed unit with the rice blast fungus (Kankanala et al., 2007). The cytoplasmic membrane shrinks around *M. oryzae* invasive hyphae and FM4-64 staining localised to the plant cell membrane but not the fungal cell membrane, showing the inaccessibility of the sealed compartment (Kankanala et al., 2007).

Previous work in the rice blast fungus has demonstrated that apoplastic and cytoplasmic effectors appear to be secreted from fungal invasive hyphae using two different secretion pathways (Giraldo et al., 2013). In this chapter, I presented experiments to explore the operation of these pathways. Apoplastic effectors, which are only secreted at the interface between the fungus and the host, have been previously reported to follow the ER-Golgi conventional pathway, whereas cytoplasmic effectors, which are secreted and translocated inside the plant from the BIC structure, follow an unconventional, Golgi-independent secretion pathway (Giraldo et al., 2013). It seems likely that the octameric exocyst complex and associated RabGTPases are involved in this unconventional secretory mechanism, as exocyst mutants are also impaired in cytoplasmic effector delivery (Giraldo et al., 2013) (Zheng et al., 2016).

Interestingly, it has recently been shown that cytoplasmic effectors follow an unconventional secretory pathway in the oomycete pathogen *P. infestans.* Here, the cytoplasmic effector Pi04314 and apoplastic effector EPIC1 have been shown to be secreted by different routes (Wang et al., 2017b). Pi04314 interacts with plant host protein phosphatase 1 catalytic (PP1c) isoforms in the plant nucleus, where it localises, causing their re-localisation from the nucleolus to the nucleoplasm (Boevink et al., 2016; Wang et al., 2017b). EPIC1, meanwhile, is a cysteine protease inhibitor (Song et al., 2009). The secretion of EPIC1 was shown to be BFA sensitive, indicating that it follows the ER-Golgi secretion pathway in the same way as apoplastic effectors of *M. oryzae*. Pi04314, however, showed BFA in-sensitive secretion, suggesting that it follows an alternative secretion route, in the same as observed for cytoplasmic effectors of *M. oryzae* (Wang et al., 2017b). It is therefore possible that diverse pathogens have evolved alternative secretory routes for effector proteins designated for translocation into host cells. However, clearly not all delivered effectors follow this rule. MiSSP7 a

*Laccaria bicolor* cytoplasmic effector, for example, is secreted in a BFA sensitive manner (Plett et al., 2011), suggesting that differences in secretory route may not be conserved across all pathogens (Plett et al., 2011). It has also been proposed that trafficking of effectors could require chaperone complexes rather than secretory vesicles (Alfano and Collmer, 2004; Knuepfer et al., 2005; Yi et al., 2009; Bozkurt et al., 2012). Interestingly, some pathogenic bacteria that employ Hrp type III secretion system use cytoplasmic chaperones along with other export components to deliver effectors. These chaperones are proposed to interact with effector residues as a second secretion signal (Alfano and Collmer, 2004).

In this chapter, I report experiments in which I investigated how chimeric effector constructs and the localisation of different components of the secretory pathway during live imaging of *M. oryzae* host colonisation. Additionally, I study the role of the promoter and signal peptide regions of *PWL2* in the translocation of a non-effector secreted protein.

## *5.2 Methods*

### 5.2.1 Generation of C-terminal GFP fusion vector expressing the promoter gene region of *PWL2* driving Invertase protein

To generate the *PWL2p:INV1:GFP* vector, the oligonucleotide primers in Table 3.1 were used to amplify a 2 kb fragment containing the promoter sequence of *PWL2* from *M. oryzae* strain Guy11. The forward primer was designed to include a 15bp overhang complementary in sequence to the *BAR* resistance gene cassette. The reverse primer was designed to include a 15bp overhang with the beginning of the *INV1* invertase-encoding coding sequence. The *INV1* coding sequence was amplified from Guy11 *M. oryzae* genomic DNA. The forward primer was the beginning of *INV1* coding sequence. The reverse primer was designed to exclude the predicted stop codon from the *INV1* gene and to include a 15bp overhang complementary in nucleotide sequence to the *GFP* DNA sequence. The thermotolerant DNA polymerase enzymes used were Phusion® high fidelity DNA Polymerase (New England Biolabs, Thermo Scientific®) and

Q5® High-Fidelity DNA Polymerase (New England Biolabs), as previously described in 3.2.1. PCR products were analysed by gel electrophoresis. The fragments were used to generate the chimeric constructs using the In-fusion Cloning method (Clontech). The fragments became integrated into a *Hin*d*III*-digested pNEB-1284 plasmid. The resulting plasmid *PWL2p:INV1:GFP* was then introduced into *M. oryzae* by PEG-mediated fungal transformation.

### 5.2.2 Generation of C-terminal GFP fusion vector expressing the promoter and signal peptide gene region of *PWL2* driving the Invertase gene coding sequence

To generate *PWL2p+sp:INV1:GFP*, oligonucleotide primers in Table 3.1 were used to amplify approximately a 2 kb fragment containing the promoter and predicted signal peptide sequence of *PWL2* from *M. oryzae* strain Guy11. The forward primer was designed to include a 15bp overhang complementary in sequence to the *BAR* resistance cassette. The reverse primer was designed to include a 15bp overhang with the beginning of the *INV1* coding sequence excluding the *INV1* predicted signal peptide. The *INV1* coding sequence without its predicted signal peptide was the amplified from Guy11 *M. oryzae* genomic DNA. The forward primer was positioned at the end of *INV1* predicted signal peptide. The reverse primer was designed to exclude the predicted stop codon from *INV1* and to include a 15bp overhang complementary in nucleotide sequence to the *GFP* gene sequence. The polymerase enzymes used were Phusion® high fidelity DNA Polymerase (New England Biolabs, Thermo Scientific®) and Q5® High-Fidelity DNA Polymerase (New England Biolabs), as previously described in 3.2.1. PCR products were analysed by gel electrophoresis. The fragments were used to generate the chimeric constructs using the In-fusion Cloning method (Clontech). The fragments were integrated into a *Hin*d*III*-digested pNEB-1284 plasmid. The resulting plasmid *PWL2p+sp:INV1:GFP* was then introduced into *M. oryzae* by PEG-mediated fungal transformation.

### 5.2.3 Brefeldin A treatment

Brefeldin A (BFA) treatment was performed, as previously described by (Giraldo et al., 2013). A BFA stock solution was prepared at a concentration of 10 mgml$^{-1}$

in dimethyl sulphoxide (DMSO, Sigma) as described by Bourett & Howard, (1996). Rice leaf sheaths were inoculated with *M. oryzae* strains, expressing apoplastic and cytoplasmic effector chimeric constructs. After 27 h post inoculation, leaf sheaths were submerged in Brefeldin A (BFA) (Sigma) solution (50µg/ml) or 0.1 % DMSO, as a control. After 3h, leaf sheath preparations were observed by laser confocal microscopy.

### 5.2.4 Plasmolysis assay

Leaf sheaths were inoculated with *M. oryzae* strains expressing effector gene constructs with a fluorescent marker. After 30h post inoculation, leaf sheaths were submerged in 0.75 M sucrose solution for 5 min. Then, leaf sheaths were trimmed and prepared for observation by epifluorescence microscopy.

## *5.3 Results*

### 5.3.1 Bas4 is Brefeldin A-insensitive when it is driven by the AVRPIA promoter and signal peptide

Cytoplasmic and apoplastic effectors in *M. oryzae* have previously been reported to be secreted by two different secretion pathways (Giraldo et al., 2013). Apoplastic effectors are BFA-sensitive, indicating those follow the conventional endoplasmic reticulum to Golgi secretion pathway, whereas cytoplasmic effectors are BFA-insensitive, suggesting they follow an unconventional Golgi-independent secretion pathway. I therefore first decided to repeat experiments to investigate these two distinct pathways. BFA treatment on strains expressing Bas4 and Pwl2 effector proteins was therefore carried out. The Bas4:GFP Pwl2:mCh:NLS *M. oryzae* strain from (Giraldo et al., 2013) was prepared and after 9 days spores were collected. Leaf sheaths from rice cultivar CO-39 were inoculated with the spore suspension and treated with BFA, as described in 5.2.3. When BFA treated samples were observed in confocal microscopy, Bas4-GFP localisation was observed around and inside invasive hyphae, while Pwl2-mCh:NLS localisation was observed at the BIC and plant nucleus, as shown in Figure 5.1. Samples treated with 0.1% DMSO, showed Bas4-GFP localisation around invasive hyphae, with Pwl2-mCh:NLS localisation observed at the BIC and plant nucleus (Figure 5.1). The quantification of infections observed between the control and

BFA-treatment resulted in a significant difference in Bas4-GFP localisation, but not for Pwl2:mCh:NLS, as shown in Figure 5.1. After BFA exposure, Bas4 secretion was significantly impaired with more infections observed to show fluorescence inside invasive hyphae, whereas Pwl2 was always observed to be secreted at the BIC or in the plant nucleus, due to the NLS. These results are therefore consistent with (Giraldo et al., 2013), with Bas4:GFP secretion affected by BFA treatment but Pwl2:mCh:NLS not affected.

Next, I expressed a chimeric construct of the Bas4 effector-encoding gene under the control of the promoter and signal peptide of *AVRPIA*, in order to investigate BFA-sensitivity. The AvrPiap+sp:Bas4:GFP chimeric construct was generated, as described in Chapter 3 and, as a control, the Bas4:GFP Pwl2:mCh strain (Giraldo et al., 2013) was used. AvrPiap+sp:Bas4:GFP, Bas4:GFP Pwl2mCh:NLS *M. oryzae* expressing strains were also grown in culture plates for 9 days, from which spores were collected and inoculated into leaf sheaths of the blast-susceptible rice cultivar Mokoto. Leaf sheath preparations were treated with BFA (50 µg/ml) or 0.1% DMSO. Results are shown in Figure 5.2. The Pwl2-mCh:NLS fusion protein localised at the BIC and plant nucleus when exposed to either BFA (50 µg/ml) or 0.1% DMSO, and no difference was therefore observed in Pwl2-mCh:NLS localisation. By contrast, Bas4-GFP localised around and inside *M. oryzae* invasive hyphae after treatment with BFA, whereas after exposure to just 0.1% DMSO, the Bas4-GFP fusion protein localised around *M. oryzae* invasive hyphae. The AvrPiap+sp:Bas4-GFP fusion was observed around *M. oryzae* invasive hyphae when treated with BFA (50 µg/ml) or in 0.1% DMSO. Quantitative analysis of observed infections showed that AvrPiap+sp:Bas4:GFP infections observed were not significantly different from infections observed in the control with 0.1% DMSO, whereas Bas4-GFP driven by the *BAS4* native promoter was observed to be BFA-sensitive compared to exposure to 0.1% DMSO in the control experiment (Figure 5.2).

I conclude that BFA sensitivity of the Bas4 apoplastic effector secretion is inhibited by expression under control of the *AVRPIA* promoter and associated signal peptide sequence. This suggests that *AVRPIA* promoter and signal peptide may be sufficient to drive the Bas4 apoplastic effector protein into the un-conventional secretion pathway.

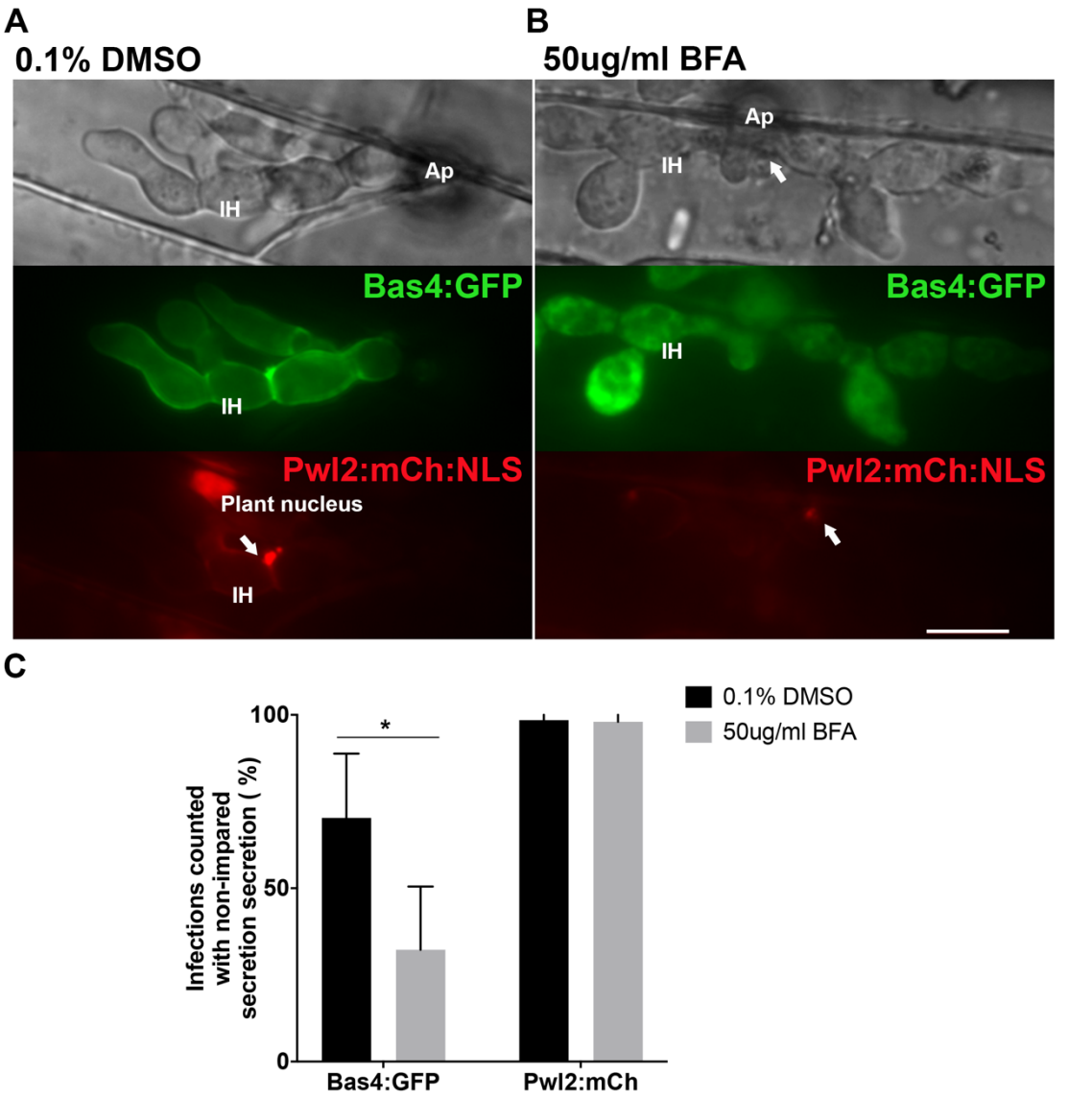


Figure 5.1 **Cytoplasmic effectors are secreted via an unconventional secretory pathway.** Micrographs obtained by laser confocal microscopy of live cell imaging from leaf sheath preparations of *M. oryzae* infection in rice. A) Bas4:GFP shows apoplastic localisation surrounding invasive hyphae, Pwl2:mCh:NLS localises at the BIC and after secretion is translocated into the rice nucleus. B) In the presence of BFA, Bas4:GFP is observed inside and outlining *M. oryzae* invasive hyphae, while Pwl2:mCh:NLS remains at the BIC. C) Bar chart showing quantification of infections observed with non-impaired secretion in Bas4:GFP and Pwl2:mCh samples treated with 0.1% DMSO and BFA (50 µg/ml). For the Bas4:GFP Pwl2:mCh:NLS *M. oryzae* expressing strain, a total of 4 replicates were made with 90 infections observed. An unpaired parametrical t-test with a two-tailed distribution showed a *P*-value of 0.04 for Bas4:GFP and 0.7 for Pwl2:mCh:NLS. All the strains were excited at 488nm and 561nm with an argon laser. Scale bars represent 10 µm. Arrow marks the BIC, Ap marks the appressorium, IH marks *M. oryzae* invasive hyphae and plant nucleus marks the rice cell nucleus.

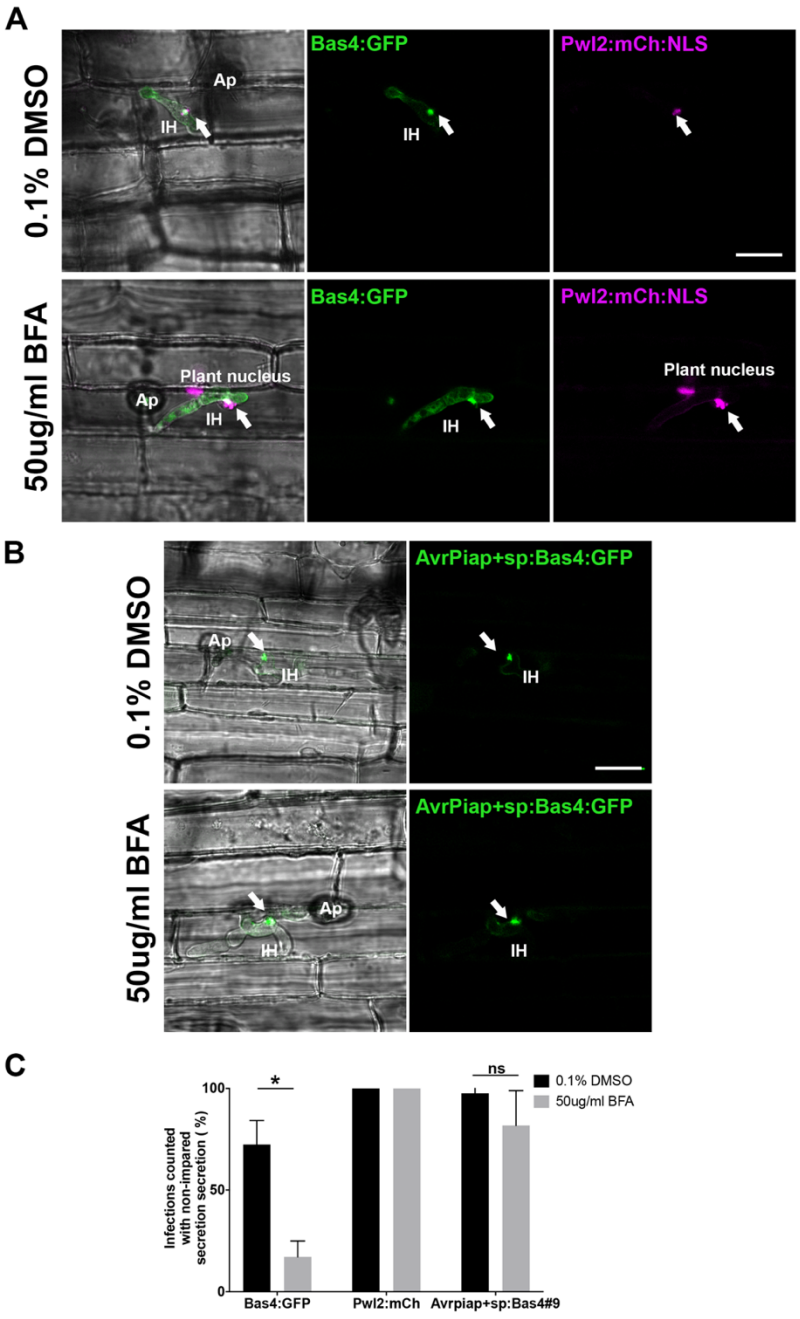


Figure 5.2 **Bas4 secretion is Brefeldin A insensitive when expression is driven by the *AVRPIA* promoter and signal peptide.** Micrographs of confocal microscopy of live cell imaging from leaf sheaths of *M. oryzae* infection in rice. A) Bas4-GFP shows apoplastic localisation surrounding invasive hyphae, Pwl2-mCh:NLS localises at the BIC and after secretion is translocated into the rice nucleus. In the presence of BFA, Bas4:GFP is observed inside and outlining *M. oryzae* invasive hyphae, while Pwl2:mCh:NLS. B) AvrPiap+sp:Bas4-GFP localises at the BIC and outlines invasive hyphae when treated with Brefeldin A AvrPiap+sp:Bas4:GFP remains at the BIC. C) Bar chart showing quantification of infections observed with non-impaired secretion in Bas4:GFP and Pwl2:mCh samples, treated with 0.1 DMSO and BFA (50 µg/ml), respectively. For Bas4:GFP Pwl2:mCh:NLS and AvrPiap+sp:Bas4:GFP *M. oryzae* expressing strains, a total of 5 replicates were made with 63 infections observed. An unpaired parametrical t-test with a two-tailed distribution showed a *P*-value of 0.00002 for Bas4:GFP, a *P*-value of 1 for Pwl2:mCh:NLS and a *P*-value of 0.08 for AvrPiap+sp:Bas4:GFP. All strains were excited at 488nm and 561nm with argon laser. cale bars represent 10 µm. Arrow marks the BIC, Ap marks the appressorium, IH marks *M. oryzae* invasive hyphae and plant nucleus marks the rice cell nucleus. RFP signal is shown in magenta.

### 5.3.2 MoRab5B GTPase during *M. oryzae* rice colonisation

Several secretory components are predicted to be part of the un-conventional secretion pathway for cytoplasmic effectors (Giraldo et al., 2013). I first repeated previously reported analysis of *M. oryzae* Sec5 and Exo70 mutants expressing Pwl2:mCh, to observe BIC localisation. Sec5 and Exo70 are components of the exocyst complex that are also involved in plant infection (Giraldo et al., 2013; Gupta et al., 2015). The Δ*sec5* and Δ*exo70* strains expressing *PWL2*:mCh showed internal retention of Pwl2:mCh inside *M. oryzae* invasive hyphae, confirmed by line scan analysis (Figure 5.3). I also replicated the observation of myosin light chain protein Mlc1 and Exo70 mutant strains published in (Giraldo et al., 2013). Giraldo and co-workers showed that Spitzenkorper markers, such as Mlc1 and Snc1, the exocyst complex markers, Exo70 and Sec5 and the t-SNARE marker Sso1 could be observed in the BIC-associated cell, whereas the polarisome marker Spa2 was only visualised at the bulbous hyphal tip (Giraldo et al., 2013). The Exo70-GFP marker always localised to the BIC associated cell (Figure 5.4). Mlc1-GFP localises to the BIC-associated cell and at septa of *M. oryzae* invasive hyphae (Figure 5.4).

I then observed further proteins involved in intracellular trafficking in *M. oryzae* infections. RabGTPases are a family of G proteins that regulate membrane trafficking. In *M. oryzae,* MoRab5A and MoRab5B have been characterised to be necessary for fungal development and pathogenicity (Yang et al., 2017). The Rab5B:mCh plasmid was generated by Dr Magdalena Martin-Urdiroz and transformed into *M. oryzae* Guy11 expressing *AVRPIA:GFP*, as described in Chapter 4. The Rab5B-mCh localised as small vesicles that move bi-directionally from the appressorium to the hyphal tip as shown in Figure 5.5. Interestingly, the Rab5 vesicles also moved towards the BIC inside the BIC-associated cell. This suggests a potential role for RabGTPases in the unconventional secretion pathway.

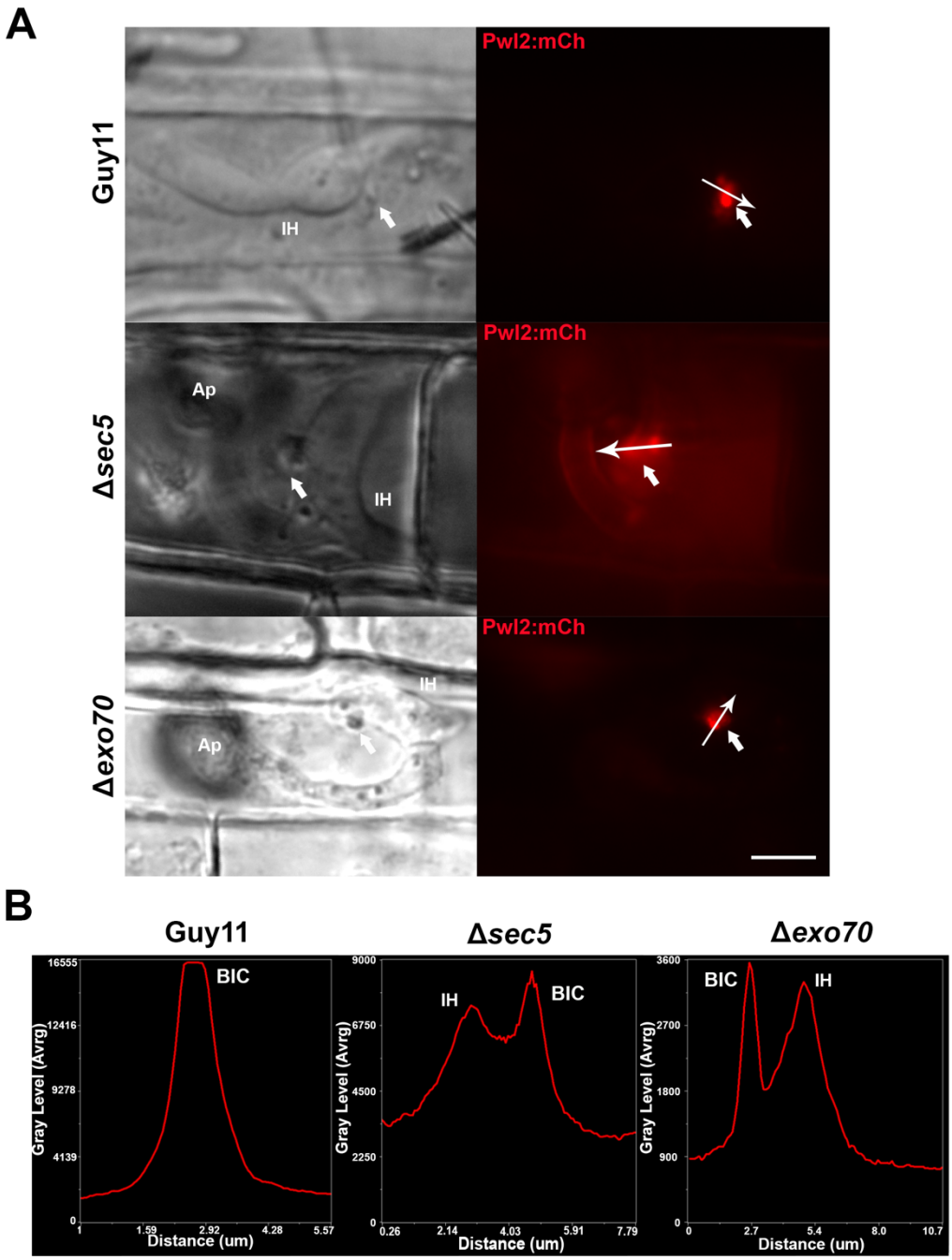


Figure 5.3 **BIC localisation of Pwl2 is impaired in Δsec5 and Δexo70 mutants.** Micrographs obtained by epifluorescence microscopy of live cell imaging from leaf sheath preparations of *M. oryzae* infection of rice. A) Pwl2-mCh localises to the BIC. Pwl2-mCh is observed at the BIC and retained in invasive hyphae in Δsec5 and Δexo70 mutants. B) Line scans showing Pwl2:mCh fluorescence in Guy11, Δsec5 and Δexo70 mutants. Scale bars are 10 um. Arrow marks the BIC, Ap marks the appressorium and IH marks *M. oryzae* invasive hyphae. All strains were excited at 561nm for 100 ms.

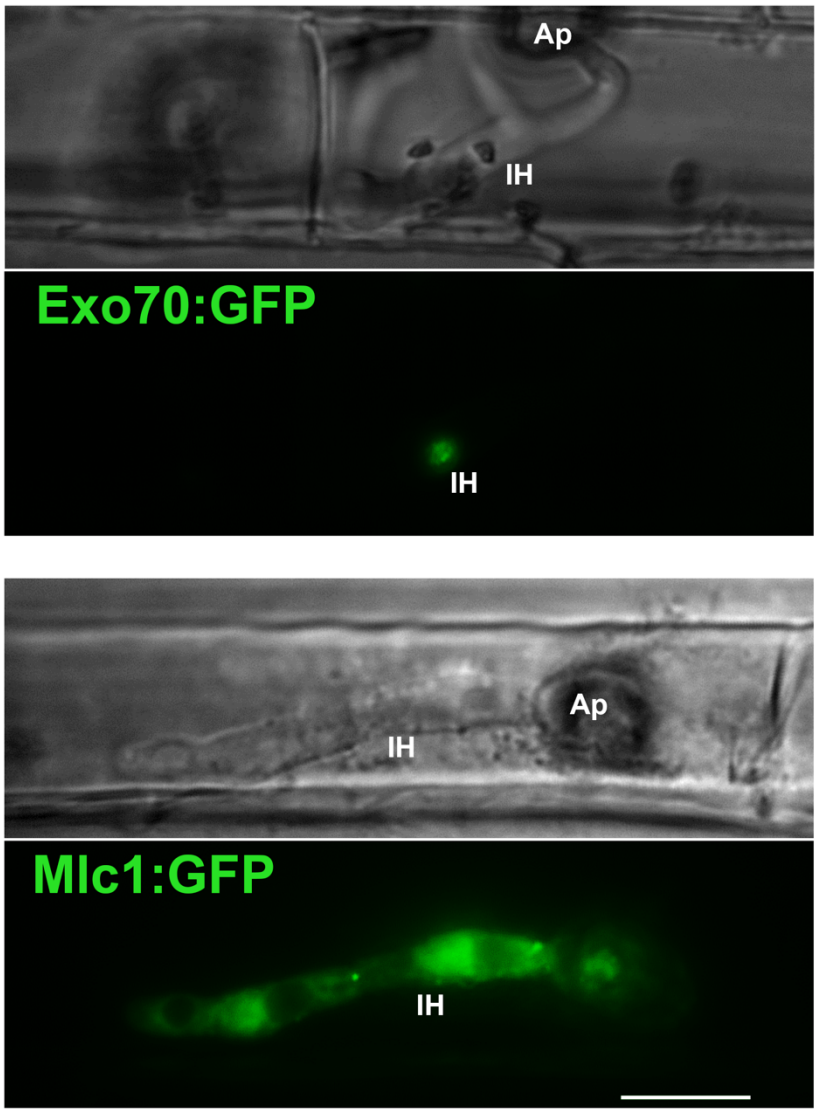


Figure 5.4 **Exo70 and Mlc1 localisation during rice colonisation by *M. oryzae*.** Micrographs obtained by epifluorescence microscopy of live cell imaging from leaf sheath infections of *M. oryzae* in rice. Exo70-GFP localises to the BIC-associated cell. Mlc1-GFP localises to the BIC associated cell and invasive hyphae septa. Scale bars represent 10 µm. Ap marks the appressorium and IH marks *M. oryzae* invasive hyphae. All strains were excited at 488nm for 200 ms.

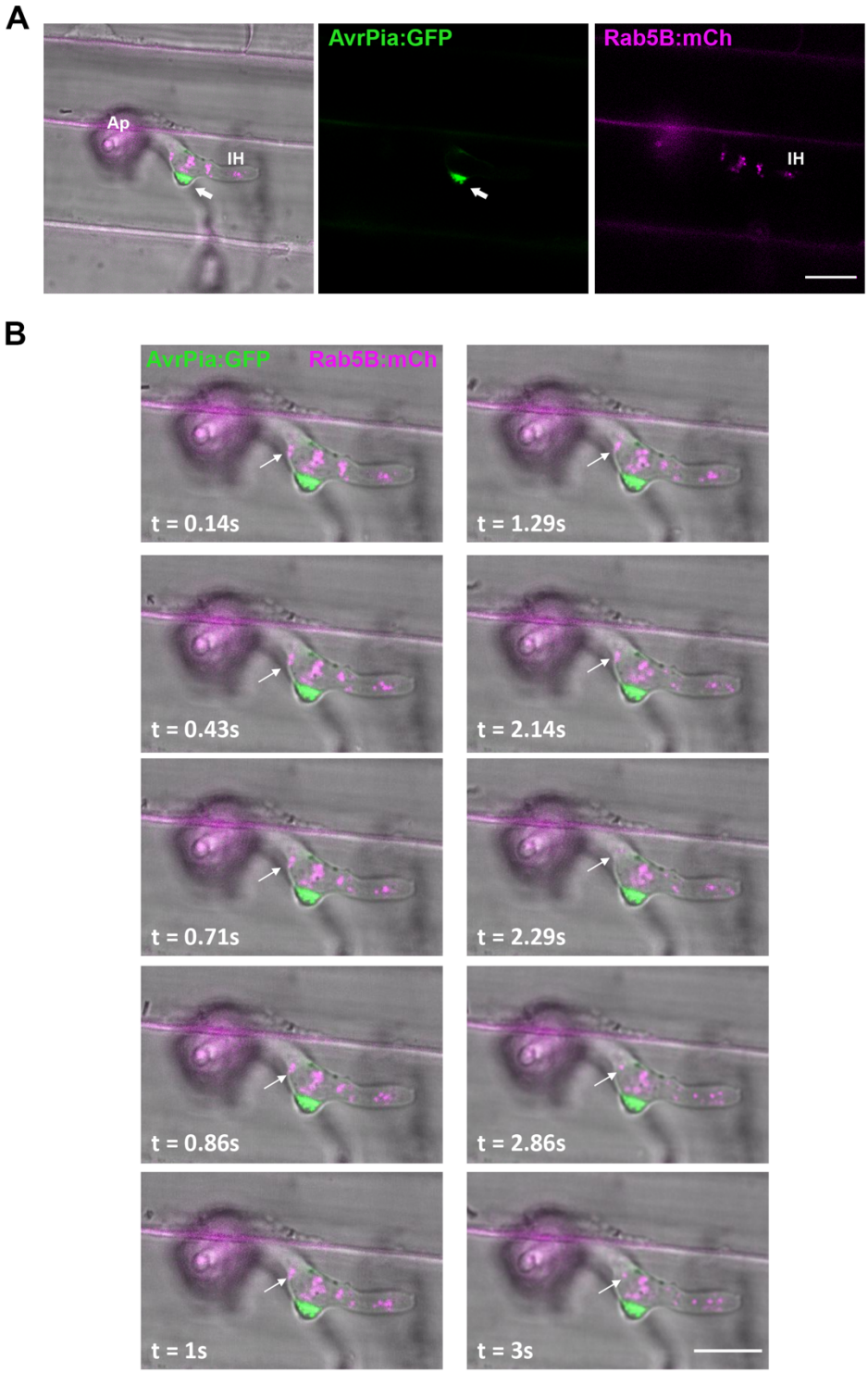


Figure 5.5 **MoRab5B localisation during rice blast fungus rice tissue colonisation.** Micrographs obtained by confocal microscopy of live cell imaging from leaf sheaths of *M. oryzae* infections of rice. A. Overlay of AvrPia:GFP and Rab5B:mCh. AvrPia-GFP localises to the BIC. Rab5B-mCh localises around the BIC. B. Time lapse imaging over a period of 3 seconds of Rab5B movement from and into the appressorium. All strains were excited at 488nm and 561nm with argon laser. Scale bars represent 10 µm. Arrow marks the BIC, Ap marks the appressorium, IH marks *M. oryzae* invasive hyphae, plant cytoplasm or Cyt marks the rice cell membrane and plant nucleus marks the rice cell nucleus. RFP signal is false-colour imaged to magenta.

### 5.3.3 Plasmolysis assay to visualise effector translocation using a plasma membrane-marked rice transgenic line

A plasmolysis assay, described in 5.2.4 and consisting of submerging infected leaf sheaths in a 0.75M sucrose solution, was used to investigate effector translocation. In this assay, plant cells shrink due to the hyperosmotic conditions outside the cell, causing the plant plasma membrane to recede from the rigid plant cell wall. It is important to mention that plasmolysis is reversible and a characteristic of living plant cells, so live cell imaging of infections could still be carried out (Cheng et al., 2017) (Kankanala et al., 2007). Additionally, Cheng and co-workers have shown that during the plasmolysis assay in *Arabidopsis* plants organelle movement still occurs throughout the process (Cheng et al., 2017).

#### *5.3.3.1 Development of a transgenic rice line expressing a plasma membrane marker*

To study membrane dynamics *in planta*, a transgenic rice line was used to investigate *M. oryzae* intracellular growth. To visualise the plant plasma membrane an LTi6B:GFP *sasanishiki* rice cultivar was used. The LTi6B gene encodes a 67 amino acid, salt responsive protein (T. Mentlak, 2012), and expression of the LTi6B:GFP vector, under the control of the 35S constitutive promoter has been shown to localise GFP to the plant cell membrane in *Arabidopsis thaliana* (Kurup et al., 2005) (T. Mentlak 2012). To confirm localisation of LTi6B:GFP to the plant membrane, leaf sheaths of LTi6B:GFP transgenic plants were observed by confocal microscopy. The GFP signal was retained at the cell cortex confirming that LTi6B:GFP localises to the plant plasma membrane (Figure 5.6).

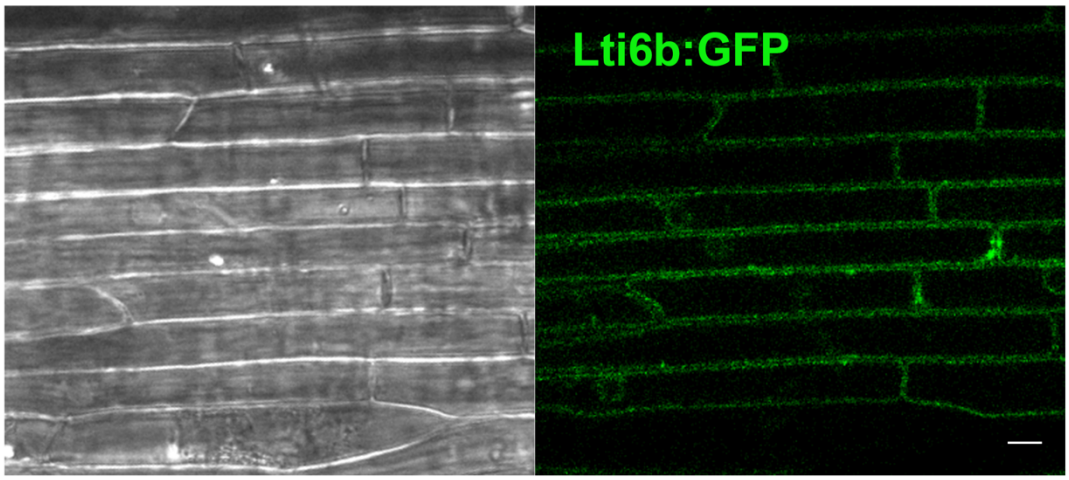


Figure 5.6 **Plants expressing the LTi6B:GFP vector localise GFP to the plant plasma membrane.** Transgenic rice lines expressing LTi6B:GFP visualised under the Leica SP5 laser confocal microscope. All the strains were excited at 488nm with argon laser. Scale bars represent 10 μm.

#### *5.3.3.2 Plant plasma membrane outlines M. oryzae invasive hyphae during tissue invasion*

As soon as *M. oryzae* enters the rice cell, the host plama membrane becomes invaginated around the invading fungus, as reported by (Kankanala et al., 2007; Khang et al., 2010; Mentlak et al., 2012). The plasma membrane outlining *M. oryzae* invasive hyphae is referred to as the EIHM (Kankanala et al., 2007). The EIHM has been visualised by electron microscopy (Kankanala et al., 2007) and by observing the rice transgenic line LTi6B:GFP during host colonisation (Mentlak et al., 2012). *M. oryzae* strains expressing Pwl2:mCh were used to visualise the BIC during host cell colonisation of rice transgenic lines LTi6B:GFP. The observations were consistent with the work of Mentlak and co-workers LTi6B:GFP re arranges and accumulates at the BIC, labelled with Pwl2:mCh (Figure 5.7 A) (Mentlak et al., 2012). Linescan analysis (Figure 5.7 B) showed that the BIC is a plant membrane-rich structure in between the fungal cell wall and the plant plasma membrane. Interestingly, Mentlak and co-workers also found that the BIC structure was also partly composed of host-derived ER (T. Mentlak, thesis).

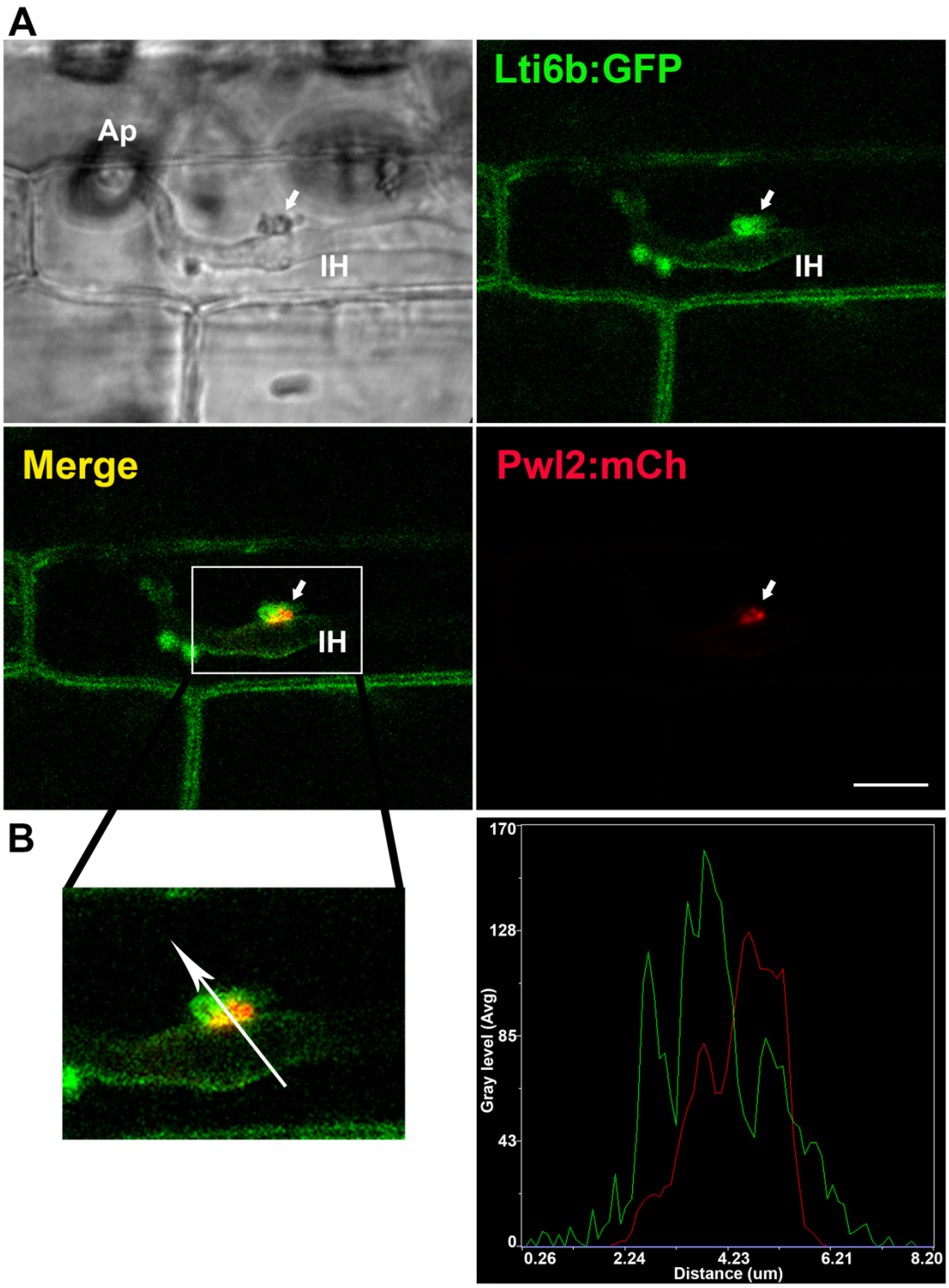


Figure 5.7 **The plant plasma membrane accumulates at the BIC.** A. A transgenic rice line expressing the LTi6B:GFP membrane marker (Green) was inoculated with a *M.oryzae* Pwl2:mCh (Red) strain. At 30 hpi co-localisation was observed between the plant plasma membrane and Pwl2 at the BIC. B. Co-localisation was demonstrated by linescan analyses. All the strains were excited at 488nm and 561nm with argon laser. Scale bars represent 10 µm. Arrow marks the BIC, Ap marks the appressorium and IH marks *M. oryzae* invasive hyphae.

#### *5.3.3.3 Transgenic rice lines expressing endosomal marker Ara6*

After observing localisation of LTi6B:GFP in transgenic rice plants, we decided to investigate gene Ara6 fusions as plant membrane markers to understand the BIC structure (Khang et al., 2010). Because it is thought that the BIC is the site for cytoplasmic effector to enter the plant cell, we set out to investigate plant endosomal movement during *M. oryzae* tissue invasion. Ara6 is a marker of early endosomes, and is reported to act in the fusion of endosomes with the plasma membrane (Ebine et al., 2011). The putative Ara6 sequence in *Oryza sativa* was identified by a search with the respective protein sequence from *Arabidopsis thaliana* (provided by Dr D. Soanes and Dr G. Littlejohn). The plasmid was generated by Dr. Magdalena Martin-Urdiroz. Transformed rice of cultivar Nippobare was made by the tissue culture service in The Sainsbury Laboratory (UK). The gene fusion was expressed under control of the constitutive 35S promoter. Plants were grown for 3-4 weeks and epidermal leaf tissue prepared for laser confocal microscopy. As shown in Figure 5.8 A, Ara6-GFP localisation appeared close to the plant plasma membrane, where the trafficking of vesicles and SNARE proteins has been reported to occur (Ebine et al., 2011). There is also a dynamic movement of endosomes, as seen in Figure 5.8 B.

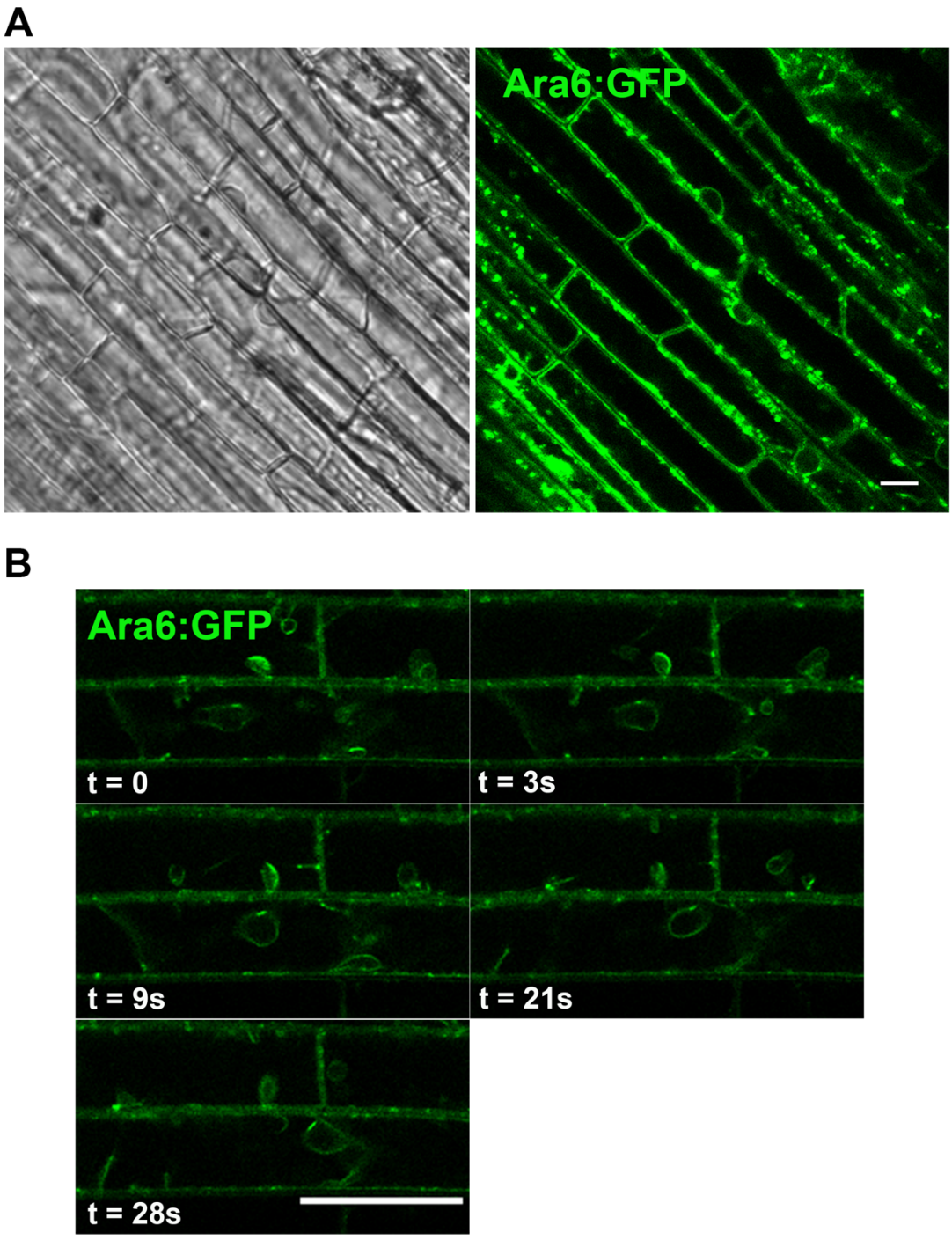


Figure 5.8 **Epidermal plant cells expressing Ara6:GFP enables the observation of dynamic network in the rice plant cell**. A. Micrographs obtained with Leica SP8 confocal microscopy, Ara6:GFP localises at the plant plasma membrane and through microtubules inside the rice cell. B. Time lapse imaging over a period of 28 seconds of endosomal trafficking in rice cells. All the strains were excited at 488nm with argon laser at 20%. Scale bars represent 10 μm.

#### *5.3.3.4 Early endosomes outline the BIC structure during M. oryzae host colonisation*

Plants expressing Ara6:GFP were used to examine the structure of the BIC. A Pwl2:mCh *M. oryzae* strain was first used to label the BIC. The secretory machinery from the rice plant has not yet been reported during *M. oryzae* intracellular growth so this is an exciting opportunity. As shown in Figure 5.9, the Ara6:GFP gene fusion shows a re-organisation and accumulation at the BIC, that was also observed with the plant plasma membrane and endoplasmic reticulum (T. Mentlak, thesis). Additionally, Ara6:GFP localises to the outline of the BIC (Figure 5.9). This is consistent with endocytotic trafficking from the plant occurring at the BIC. Additionally, most of the infections observed with fully developed invasive hyphae showed similar accumulation of Ara6-GFP, reinforcing the idea that there is active secretion and uptake of effector proteins at the BIC, occurring through an alternative pathway to apoplastic effector secretion at the hyphal tip. It would be interesting to study plants expressing Ara6:GFP during BFA treatment as a manner to control how the drug affects the plant secretion system. I have showed that cytoplasmic effectors secretion to the BIC is BFA independent. I used Pwl2 cytoplasmic effector fused to a nuclear signal (NLS) and I could observe nucleus fluorescence suggesting uptake from the BIC is still taking place. Therefore, I would hypothesise that plants might be affected by BFA, however, we might not see a significantly effect with current methodology.

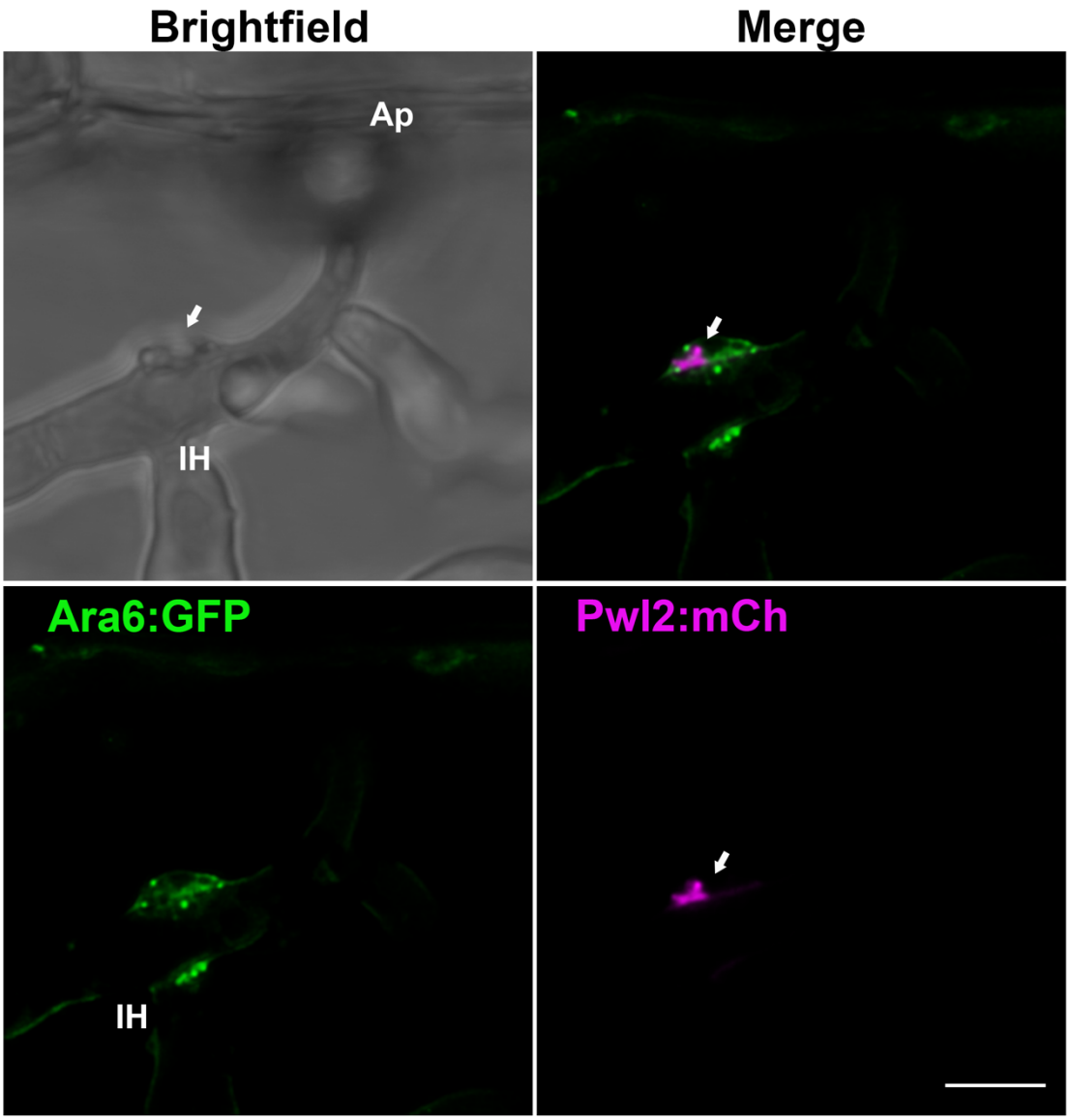


Figure 5.9 **Rice early endosomes accumulate at the BIC.** Rice plants expressing Ara6:GFP were inoculated with Guy11 Pwl2:mCh and incubated in a moist chamber. At 30 hpi, early endosomes (Ara6:GFP) were observed to re-organise and accumulate outlining the BIC (BIC). All material was excited at 488nm and 561nm with argon laser at 20%. Scale bars represent 10 µm. Arrow marks the BIC, Ap marks the appressorium and IH marks *M. oryzae* invasive hyphae. RFP signal is false-colour imaged to magenta.

#### *5.3.3.5 During M. oryzae intracellular growth the plant plasma membrane is not disrupted*

To observe whether plant plasma membrane integrity was preserved throughout infection, I carried out a plasmolysis assay on *sasanishiki* rice cultivar transgenic line expressing the plant plasma membrane marker LTi6B:GFP (Kurup et al., 2005; Mentlak et al., 2012). When cell shrinkage occurred fluorescently labelled effector proteins accumulate allowing their visualisation (Kankanala et al., 2007). Apoplastic effectors are not translocated inside the host plant and therefore, remain at the interface between the plant and *M. oryzae* invasive hyphae. A schematic drawing of this process is shown in Figure 5.10.

Leaf sheath preparations of the LTi6B:GFP transgenic line were infected with *M. oryzae* strain expressing the cytoplasmic effector *PWL2*:mCh (Khang et al., 2010). After 30hpi, leaf sheaths were treated with 0.75M sucrose solution, as described in 5.2.4. Plasmolysed rice cells were then checked by confocal microscopy (Figure 5.11 A), and fluorescence from the LTi6B:GFP plasma membrane marker was observed at the plasma membrane, suggesting that the cells were still intact. The Pwl2-mCh signal was localised to the BIC, surrounding *M. oryzae* invasive hyphae and surrounding the shrunken plant cell. Line scan analysis was used to visualise this distribution, as shown in Figure 5.11 B. From the infections observed (n=56), 20% of the Pwl2-mCh signal was observed in the apoplast, suggesting that the EIHM suffered breakage and there was spillage of Pwl2-mCh into the apoplast, while 80% of infections showed Pwl2-mCh localisation at the BIC, outlining *M. oryzae* invasive hyphae consistent with maintenance of cell integrity. Additionally, it could be possible I could not observe minor damage in the plasma membrane with Lti6b:GFP fluorescent marker for the plasma membrane. This could also explain the 20% Pwl2:mCh fluorescence EIHM leakage.

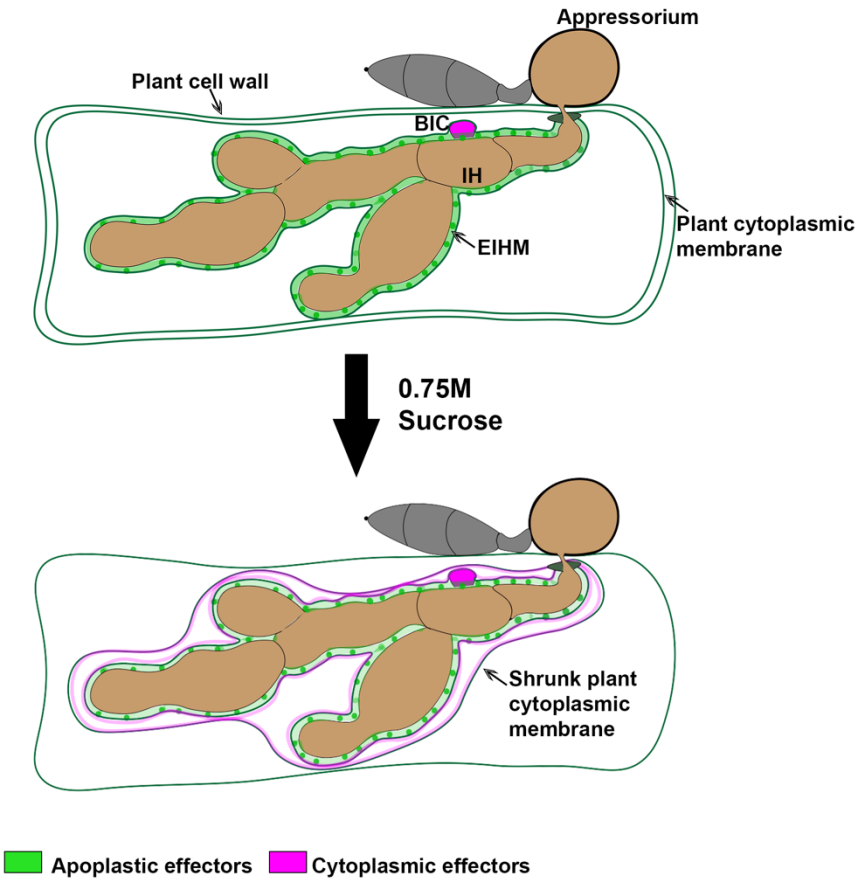


Figure 5.10 **Schematic representation of plasmolysis assay.** Drawing of a *M. oryzae* model of colonisation inside the rice plant cell before and after plasmolysis of the rice cell. The localisation of apoplastic and cytoplasmic effectors during cell colonisation are indicated, as observed by confocal microscopy.

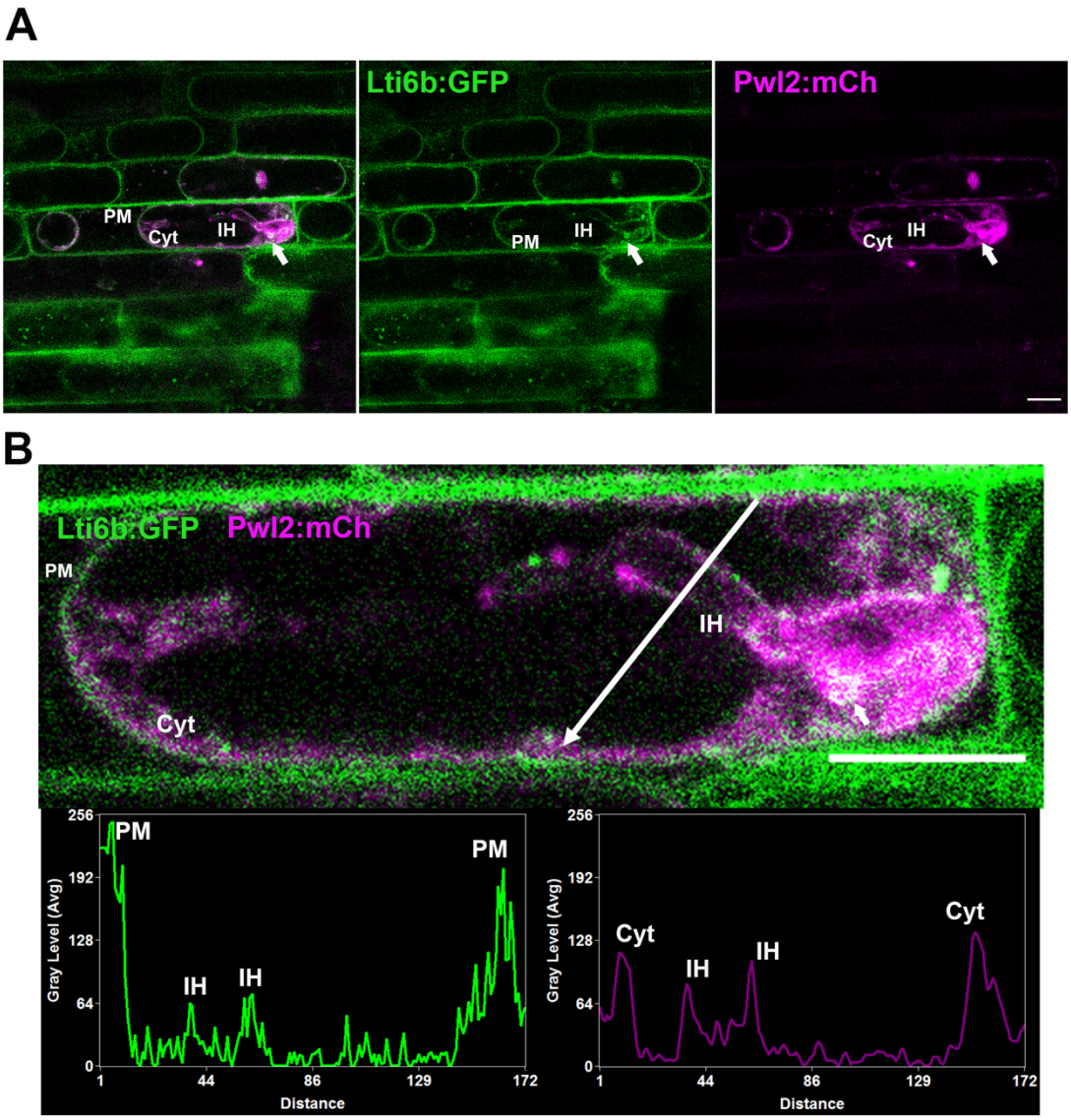


Figure 5.11 **Plasmolysis assay with transgenic rice lines expressing LTi6B plasma membrane marker.** Micrographs obtained by confocal microscopy of live cell imaging of leaf sheaths of *M. oryzae* infection in rice. A) Overlay of LTi6B:GFP and Pwl2:mCh. LTi6B:GFP outlines the plant cell membrane and the Pwl2:mCh cytoplasmic effector is at the BIC, and cytoplasm of the rice cell. B) Overlay of LTi6B:GFP and Pwl2:mCh and line scan graphs for each channel. All strains were excited at 488nm and 561nm with the argon laser at 20%. Scale bars represent 10 µm. Arrow marks the BIC, Ap marks the appressorium, IH marks *M. oryzae* invasive hyphae, plant cytoplasm or Cyt marks the rice cell membrane and plant nucleus marks the rice cell nucleus. RFP signal is shown as magenta.

### 5.3.4 Plasmolysis assay with PWL2 promoter and signal peptide C-terminal GFP fusion

In Chapter 3, I observed that the promoter and signal peptide regions of *PWL2* were able to deliver GFP into the BIC. The BIC is thought to be the active site of translocation from the fungus to the host, suggesting that these gene regions might be involved secretion. Here, I report a series of experiments to investigate whether these regions are also able to translocate GFP into the host when assayed by plasmolysis of host cells.

*M. oryzae* strains expressing Bas4:GFP Pwl2:mCh:NLS (Giraldo et al., 2013) and Pwl2p+sp:GFP were grown for 9 days, and spores then collected. The resuspended spore suspension in $dH_2O$ was used to inoculate rice cultivar CO39. After 30h, leaf sheaths were submerged in 0.75M sucrose, as described in 5.2.4, and prepared for microscopy. I quantified the number of infections which showed fluorescence inside the plant cytoplasm for Bas4:GFP Pwl2:mCh:NLS (Giraldo et al., 2013) and Pwl2p+sp:GFP (Figure 5.12 B). Bas4-GFP was mostly seen surrounding *M. oryzae* invasive hyphae at the EIHM, while some infections also showed fluorescence of Bas4:GFP inside the rice cytoplasm. It is possible that this is due to breakage in the EIHM. Breakage of the EIHM could result from sucrose treatment but also because the fungus could be ready to move to the adjacent cells. Pwl2-mCh:NLS was localised at the BIC, and the plant cytoplasm and because of the nuclear localisation signal Pwl2:mCh:NLS was also observed in the plant nucleus. A significant number of infections for Pwl2p+sp:GFP also showed localisation to the BIC and inside the plant cell cytoplasm (Figure 5.12 A). Interestingly, Pwl2p+sp:GFP was also observed in the receding plant cell membrane of the non-infected adjacent cells, consistent with Pwl2:mCh:NLS that can also be visualised in adjacent non-infected cells, as shown in Figure 5.13.

The promoter and signal peptide regions of cytoplasmic effector PWL2 are not only sufficient to drive GFP into the correct domain for cytoplasmic effectors, the BIC, but these regions are also sufficient to observe the translocation of GFP inside the cytoplasm of the rice cell.

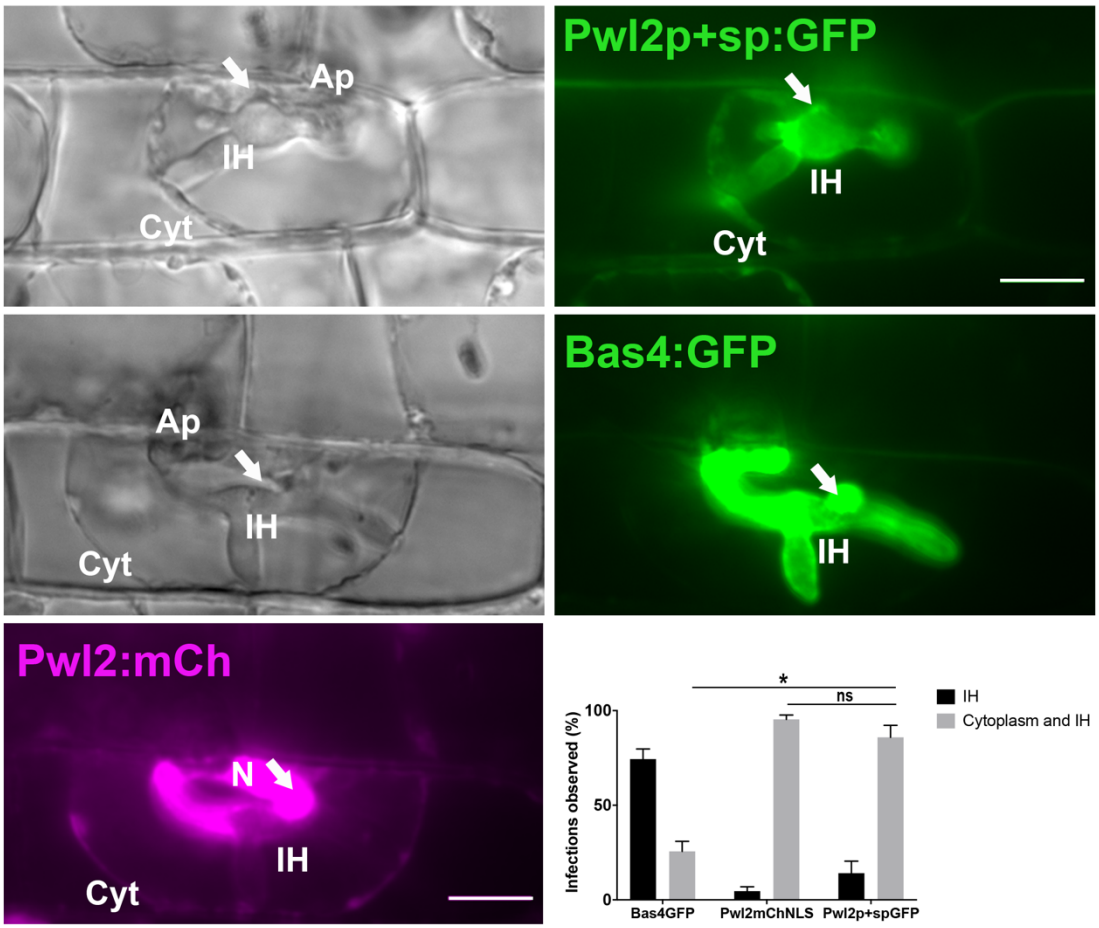


Figure 5.12 **The promoter and signal peptide regions of *PWL2* were observed to translocate GFP inside the rice cell cytoplasm.** A) Micrographs obtained on epifluorescence microscopy of live cell imaging from plasmolysed leaf sheaths of *M. oryzae* infection in rice by exposure to 0.75M sucrose solution. Bas4-GFP localises outlining *M. oryzae* invasive hyphae, Pwl2-mCh:NLS at the BIC, cytoplasm of the rice cell and plant nucleus. Pwl2P+sp-GFP localises at the BIC and rice cell cytoplasm. Bar charts showing quantification of the plasmolysed infections observed with or without fluorescence inside the rice cell cytoplasm. For Bas4:GFP Pwl2:mCh and Pwl2p+sp:GFP *M. oryzae* expressing strains a total of 3 replicates were made with 95-94 infections observed. An unpaired parametrical t-test with a two-tailed distribution of a p-value of 0.002 for Bas4:GFP vs Pw2p+sp:GFP, a p-value of 0.2 for Pwl2:mCh:NLS vs Pw2p+sp:GFP. Scale bars represent 10 um. Arrow marks the BIC, Ap marks the appressorium, IH marks *M. oryzae* invasive hyphae, plant cytoplasm or Cyt marks the rice cell membrane and N marks the rice cell nucleus. All the strains were excited at 488nm and 561nm for 200 ms and 100ms, respectively. RFP signal is shown as magenta.

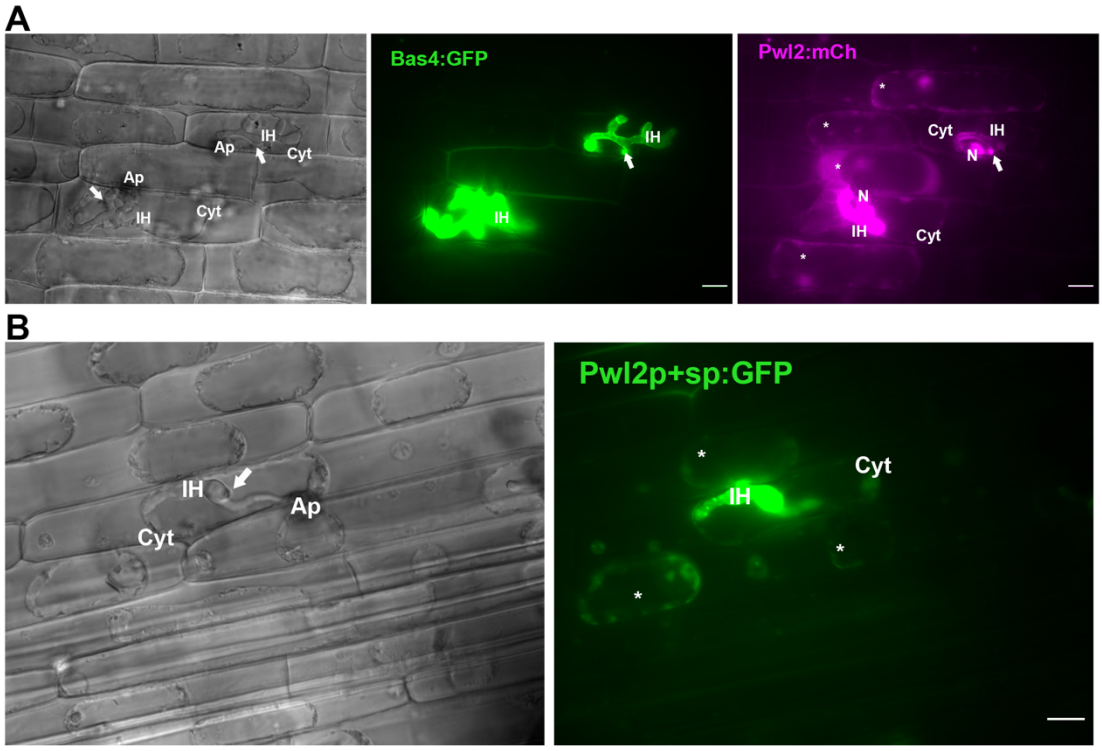


Figure 5.13 **The promoter and signal peptide regions of *PWL2* were observed to translocate GFP inside non-infected rice cell cytoplasm.** Micrographs obtained on epifluorescence microscopy of live cell imaging from plasmolysed leaf sheaths of *M. oryzae* infection in rice by exposure to 0.75M sucrose solution. Bas4-GFP localises outlining *M. oryzae* invasive hyphae, Pwl2-mCh:NLS and Pwl2p+sp-GFP at the BIC, cytoplasm of the rice cell infected and adjacent non-infect cells. Scale bars represent 10 um. Arrow marks the BIC, Ap marks the appressorium, IH marks *M. oryzae* invasive hyphae, asterisk marks fluorescent rice cells non-infected, plant cytoplasm or Cyt marks the rice cell membrane and N marks the rice cell nucleus. All the strains were excited at 488nm and 561nm for 200 ms and 100ms, respectively. RFP signal is shown as magenta.

### 5.3.5 Plasmolysis assay with BAS4 promoter and signal peptide C-terminal GFP fusion

The promoter and signal peptide regions of *BAS4* fused to GFP were observed in the BIC in Chapter 4. Even though, Bas4 is an apoplastic effector it is also observed in the BIC. However, plasmolysis assays (Khang et al., 2010) demonstrate that it is not translocated inside the host cytoplasm. Here, I study whether these regions are able to translocate GFP into the host in a similar way as the promoter and signal peptide regions of *PWL2*.

*M. oryzae* strains expressing Bas4:GFP Pwl2:mCh:NLS (Giraldo et al., 2013) and Bas4p+sp:GFP were grown in culture plates for 9 days, then spores were collected and resuspended in $dH_2O$. The spore solution was inoculated into CO39 rice cultivar leaf sheaths, as described in materials and methods 2.7.1. After 30h leaf sheaths were submerged in 0.75M of sucrose, and prepared for microscopy. I quantified how many infections were observed showing fluorescence in the plant cytoplasm for Bas4:GFP Pwl2:mCh:NLS (Giraldo et al., 2013) and Bas4p+sp:GFP. From n=26, 20% of Bas4-GFP were observed surrounding *M. oryzae* invasive hyphae, 88% of Pwl2-mCh:NLS were observed in the rice cytoplasm and 31% of Bas4p+sp-GFP infections were observed in the host cell cytoplasm (Figure 5.14). Therefore, the promoter and signal peptide regions of *BAS4* apoplastic effector are not sufficient to translocate GFP inside the host as it could be specific for the promoter and signal peptide regions of *PWL2* cytoplasmic effector.

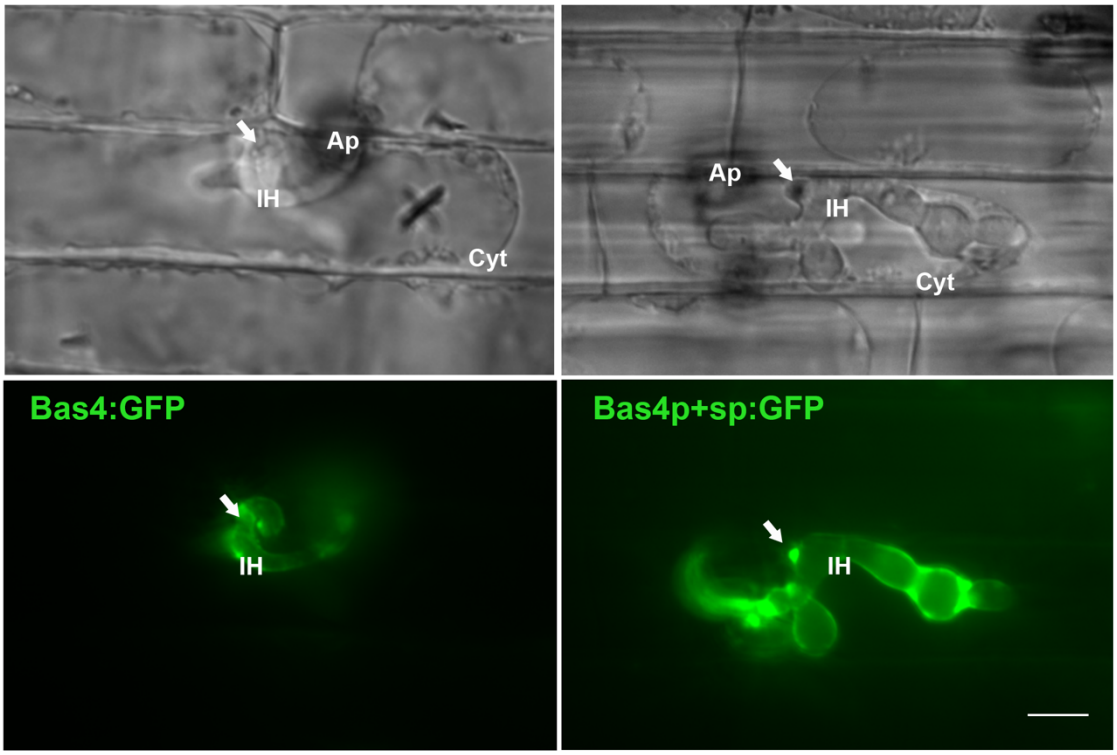


Figure 5.14 **The promoter and signal peptide regions of *BAS4* do not translocate GFP inside rice cell cytoplasm.** Micrographs obtained on epifluorescence microscopy of live cell imaging from plasmolysed leaf sheaths of *M. oryzae* infection in rice by exposure to 0.75M sucrose solution. Bas4-GFP and Bas4p+sp:GFP remain outlining *M. oryzae* invasive hyphae, Pwl2-mCh:NLS localises at the BIC, cytoplasm of the rice cell infected and rice cell nucleus. Scale bars represent 10 um. Arrow marks the BIC, Ap marks the appressorium, IH marks *M. oryzae* invasive hyphae, plant cytoplasm or Cyt marks the rice cell membrane and plant nucleus marks the rice cell nucleus. All the strains were excited at 488nm and 561nm for 200 ms and 100ms, respectively.

### 5.3.6 Construction of C-terminal GFP fusion vector expressing the promoter or promoter and signal peptide gene region of PWL2 driving Invertase protein

In this chapter I studied the promoter and signal peptide region of Pwl2 driving a non-effector secreted protein, the metabolic enzyme invertase. A C-terminal translational fusion of the *PWL2* promoter gene or the promoter and signal peptide gene regions were fused to the coding sequence of Invertase gene, with or without is predicted signal peptide. The following constructs were generated: Pwl2p:Inv1:GFP and Pwl2p+sp:Inv1:GFP.

The signal peptide was predicted using SIGNALP.4.1 software (Figure 5.15). The cloning strategy followed (Figure 5.16) for these constructs was always as described in chapter 3 and chapter 4. The constructs were independently confirmed and checked for errors by DNA sequencing. The resulting GFP C-terminal fusions were subsequently introduced into *M. oryzae* by protoplast-mediated transformation (Talbot et al., 1993) of Guy11. Putative transformants were selected based on their resistant cassette *BAR* gene with glufosinate (30 µg $ml^{-1}$). GFP positive transformants were screened for fluorescence by using Olympus IX81 inverted microscope. Single copy transformants were confirmed by qPCR blind test (Table 5.1). For subsequent analyses single copy transformant Pwl2p:Inv1:GFP#2 was used. It was not possible to generate a positive single copy transformant for Pwl2p+sp:Inv1:GFP, in this chapter Pwl2p+sp:Inv1:GFP#1 transformant was used.

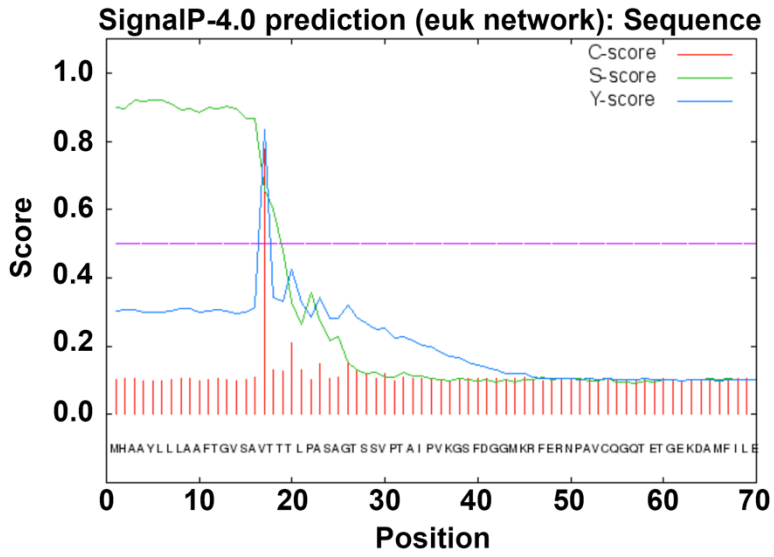


Figure 5.15 **Identification of predicted signal peptide of *INV1* gene of *M. oryzae*.** Inv1 signal peptide is from 1-16 amino acids.

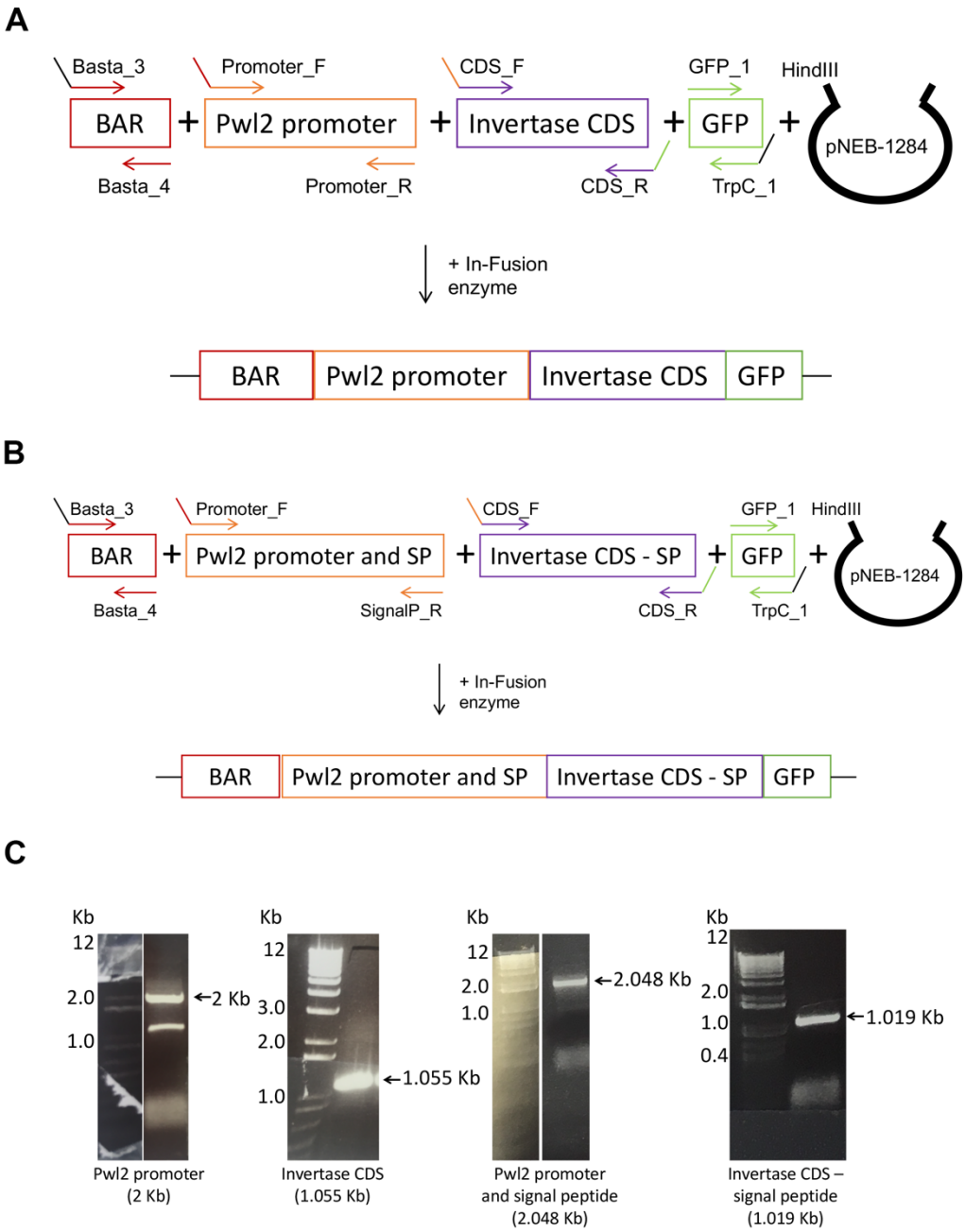


Figure 5.16 **In-Fusion cloning strategy and PCR amplifications** A) Scheme to show the cloning strategy followed for generation of GFP C-terminal constructs with the promoter of cytoplasmic effector *PWL2* driving the invertase metabolic enzyme-encoding gene *INV1*. B) Scheme of the cloning strategy followed for construction of *PWL2* promoter and signal peptide regions driving *INV1*. C) PCR amplification of 2kb *PWL2* promoter, 2.048kb *PWL2* promoter and signal peptide, 1.055kb *INV1* coding sequence and 1.019kb *INV1* coding sequence without its predicted signal peptide.

Table 5.1 Determination of GFP copy number by qPCR for Pwl2p:Inv1:GFP and Pwl2p+sp:Inv1:GFP

| Sample | Copies GFP[1] |
|---|---|
| Control | 1 |
| Guy11 | 0 |
| Pwl2p+spInv1#1 | 4 |
| Pwl2pInv1#11 | 1 |
| Pwl2pInv1#15 | 1 |
| Pwl2pInv1#13 | 1 |
| Pwl2pInv1#4 | 1 |
| Pwl2pInv1#9 | 1 |
| Pwl2pInv1#2 | 1 |

[1] Blind qPCR test were performed by iDnaGENETICS Ltd (Norwich Research Park).

### 5.3.7 Plasmolysis assay with *PWL2* promoter and its signal peptide gene regions driving *INV1*

In order to investigate the role of the promoter and signal peptide regions of *PWL2* in the translocation of a non-effector protein, I visualised translocation of proteins into the plant cytoplasm using a plasmolysis assay. For this investigation I used *INV1* which encodes invertase an enzyme secreted by fungi to catalyse the metabolism of sucrose into fructose and glucose (Talbot, 2010; Lindsay et al., 2016).

First, I generated a vector containing the promoter and signal peptide regions of *PWL2* driving *INV1*, called Pwl2p+sp:Inv1:GFP, and also used Inv1:mCh as a control (previously generated by Dr. Richard Lindsay - University of Exeter). Culture plates were grown for 9 days and spores collected. The resuspended spore suspension was inoculated onto rice leaf sheaths of cultivar CO39. After 30h, infected leaf sheaths were prepared for epifluorescence microscopy. Inv1-mCh localises at the interface outlining *M. oryzae* when driven by its native promoter and signal peptide gene sequences (Figure 5.17 A). When *INV1* is expressed under control of the promoter and signal peptide of *PWL2* it localised to *M. oryzae* invasive hyphae and a significant proportion was observed at the BIC (Figure 5.17 A and B). I conclude that the promoter and signal peptide sequence of *PWL2* is not only able to drive a significant proportion of the apoplastic effectors Bas4 and Slp1 proteins into the BIC, but also a secreted protein unrelated to effectors. The ability to direct proteins to the BIC is therefore not effector-specific.

I then carried out a plasmolysis assay to observe whether translocation of Invertase to the host cells could be observed. *M.*oryzae strains expressing Pwl2p:Inv1:GFP, Pwl2p+sp:Inv1:GFP and Inv1:mCh were observed. In addition, the Bas4:GFP and Pwl2:mCh:NLS (Giraldo et al., 2013) strains of *M. oryzae* were also used as controls. This allowed any EIHM breakage and Bas4-GFP spillage

into the cytoplasm to be observed. Spore suspensions were inoculated into CO39 rice leaf sheaths. After 30h, infected leaf sheaths were then submerged in 0.75M sucrose solution and prepared for epifluorescence microscopy.

After plasmolysis, Pwl2:mCh:NLS (81-99% n = 92) localises at the BIC, plant cell cytoplasm and plant cell nucleus. Bas4:GFP (75-80%, n =92) and Inv1-mCh (93-100%, n = 87) were observed to remain in the apoplastic space between the fungal cell wall and the EIHM (Figure 5.18 A). When *M. oryzae* expressing Pwl2p+sp:Inv1:GFP or PWL2p:Inv1:GFP were observed, fluorescence signal was observed inside the rice cytoplasm in 75-84% (n = 93) cases for PWL2p+sp:Inv1:GFP compared to 21-33% (n = 88) for PWL2p:Inv1:GFP (Figure 5.18 A). There was a significant difference between the number of infections in which the signal was observed inside host cells between Pw2p:Inv1:GFP, Pwl2p+sp:Inv1:GFP and Inv1:mCh, respectively (Figure 5.18 B). However, frequency with which the Pwl2p:Inv1:GFP occurred inside host cells was similar to that observed for Bas4:GFP. This could mean that a small number of infections by the Pwl2p:Inv1:GFP strain result in signal inside the host cell because of a occasional breakage of the EIHM. By contrast, the frequency of signal observed inside host cells for Pwl2p+sp:Inv1:GFP was similar to that observed for Pwl2:mCh:NLS (Figure 5.18 B). This is consistent with the promoter and signal peptide regions of *PWL2* being sufficient to secrete invertase into the BIC and also translocate the protein into host cells. The result is consistent with secretion to the BIC of any *M. oryzae* protein being sufficient to lead to its uptake by host cells. This provides evidence that uptake itself may be a host-regulated process, perhaps involving endocytosis for instance, that does not require specific signals or motifs present in effector proteins.

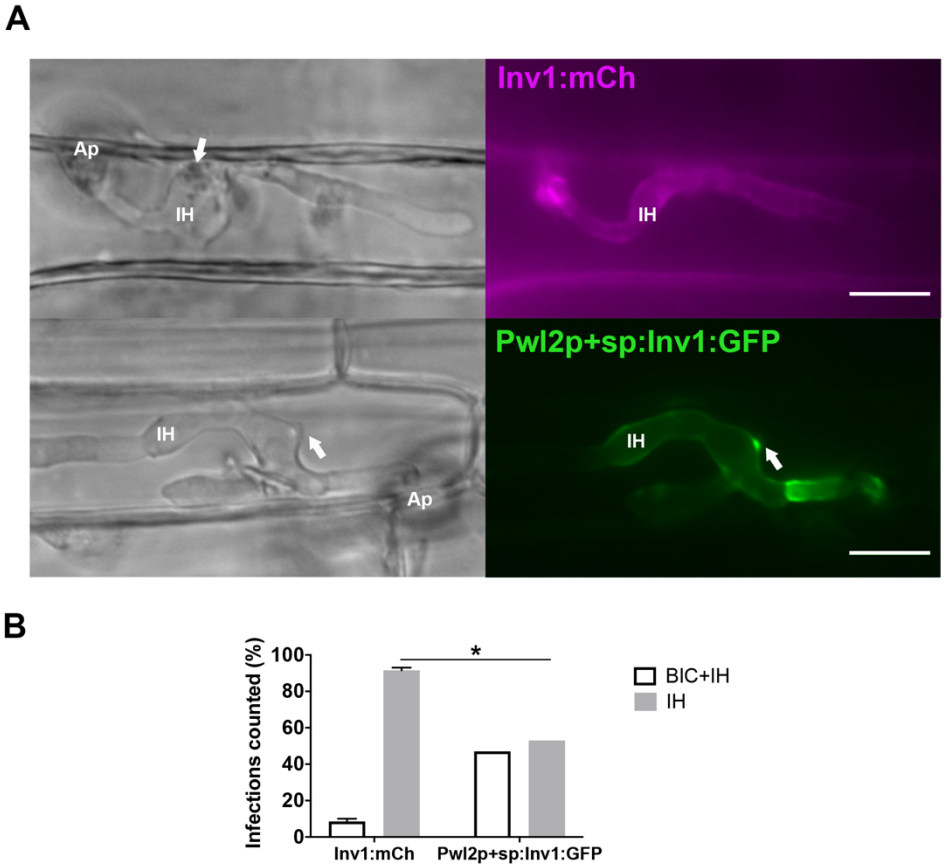


Figure 5.17 **The promoter and signal peptide of *PWL2* drive Inv1 protein into the BIC.** A) Micrographs obtained by epifluorescence microscopy of live cell imaging of *M. oryzae* infection in rice. Inv1:mCh localises outlining *M. oryzae* invasive hyphae, Pwl2p+sp:Inv1:GFP outlining *M. oryzae* invasive hyphae and at the BIC. B) Bar charts showing quantification of infections in which signal at the BIC or non-BIC location was observed. For Inv1:mCh and Pwl2p+sp:Inv1:GFP *M. oryzae* expressing strains a total of 2 replicates were made with 60 infections observed in total. An unpaired parametrical t-test with a two-tailed distribution gave a *P*-value of 0.0015 for Inv1:mCh vs Pw2p+sp:Inv1:GFP. Scale bars represent 10 µm. Arrow marks the BIC, Ap marks the appressorium, IH marks *M. oryzae* invasive hyphae. All the strains were excited at 488nm and 561nm for 200 ms and 100ms, respectively. RFP signal is false-colour imaged to magenta for ease of observation.

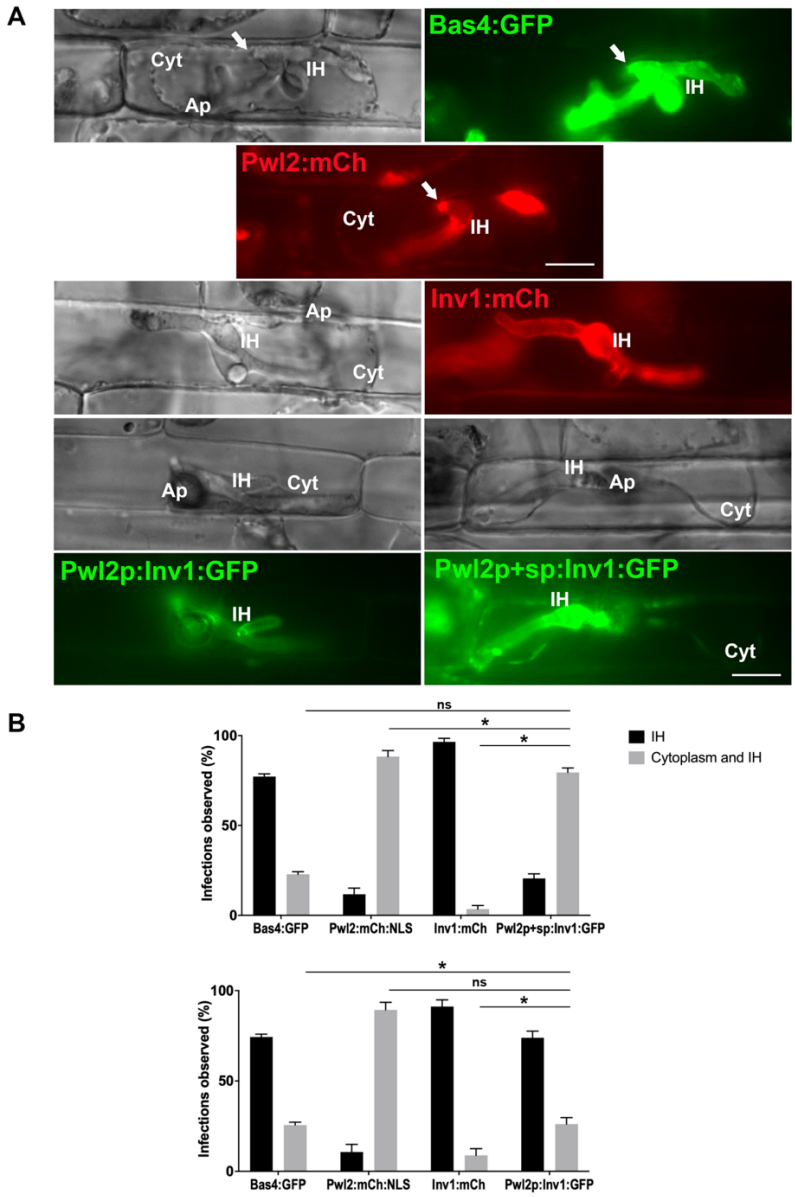


Figure 5.18 Plasmolysis assay to investigate translocation of Invertase 1 protein driven either by its native promoter, the *PWL2* promoter region or *PWL2* promoter and signal peptide sequences. A) Micrographs obtained by epifluorescence microscopy of live cell imaging from plasmolysed leaf sheaths of *M. oryzae* infection in rice following exposure to 0.75M sucrose solution. Pwl2-mCh:NLS was observed at the BIC, cytoplasm of the rice cell and plant nucleus, Bas4-GFP and Inv1:mCh localises outlining *M. oryzae* invasive hyphae. Pwl2p:Inv1-GFP localises surrounding the rice blast fungus while Pwl2p+sp:Inv1-GFP localises around *M. oryzae* invasive hyphae and in the rice cytoplasm. B) Bar charts showing quantification of the frequency in which fluorescence signal was observed inside the rice cell cytoplasm in the plasmolysed infections observed. For Bas4:GFP Pwl2:mCh, Inv1:mCh, Pwl2p:Inv1:GFP and Pwl2p+sp:Inv1:GFP *M. oryzae* expressing strains a total of 3 replicates were made with 82-92 infections observed. An unpaired parametrical t-test with a two-tailed distribution of a *P*-value of 0.9 for Bas4:GFP vs Pw2p:Inv1GFP, a *P*-value of 0.0003 for Pwl2:mCh:NLS vs Pw2p:Inv1GFP, a *P*-value of 0.03 for Inv1:mCh vs Pw2p:Inv1GFP, a p-value of 0.0004 for Bas4-GFP vs Pw2p+sp:Inv1:GFP, a *P*-value of 0.1 for Pwl2:mCh vs Pw2p+sp:Inv1:GFP and a *P*-value of 0.00001 for Pwl2:mCh vs Pw2p+sp:Inv1:GFP. Scale bars represent 10 µm. Arrow marks the BIC, Ap marks the appressorium, IH marks *M. oryzae* invasive hyphae and Cyt marks the rice cell membrane. All the strains were excited at 488nm and 561nm for 200 ms and 100ms, respectively.

### *5.4 Discussion*

The principal aim of experiments reported in this chapter was to investigate *M. oryzae* effector secretion pathways and the translocation of effectors into host cells using the library of chimeric constructs generated and reported in Chapter 4 and Chapter 5. First, I repeated the experiments previously reported that had shown an inhibitory effect of Brefeldin A (BFA) treatment on the secretion of apoplastic effectors, but which had also shown BFA-insensitivity in the secretion of cytoplasmic effectors (Giraldo et al., 2013). My observations of the secretion of Bas4:GFP and Pwl2:mCh were consistent with the previously published report (Giraldo et al., 2013). Bas4, an apoplastic effector protein, was impaired in secretion by the presence of BFA. I observed a significant proportion of *M. oryzae* invasive hyphae in which fluorescence was retained inside the fungus. By contrast, Pwl2, a cytoplasmic effector, was not impaired in its secretion by the presence of BFA. The Pwl2-mCh:NLS fusion protein localised at the BIC, and because of the nuclear localisation signal, it also accumulated in the plant cell nucleus. The conclusion from (Giraldo et al., 2013), and this study, is that Bas4 is BFA-sensitive, which provides evidence that it follows the conventional ER-Golgi secretion pathway, while Pwl2 is BFA-insensitive, which suggests that it is secreted by an unconventional secretion pathway.

I then extended the analysis and used a chimeric construct that expressed Bas4 under control of a cytoplasmic effector promoter and signal peptide. When I expressed the AvrPiap+sp:Bas4-GFP fusion protein in *M. oryzae* in the presence of BFA, I did not observe accumulation within *M. oryzae* invasive hyphae, but instead saw delivery of the fluorescence signal into the BIC. This provides evidence that the promoter and signal peptide gene regions of *AVRPIA* are sufficient to deliver Bas4 into the unconventional secretion pathway. It was also reported in (Giraldo et al., 2013), and reproduced in this study, that in the unconventional secretion pathway, the fungal exocyst components Exo70 and Sec5 play a role in delivery of cytoplasmic effectors. I observed impairment of secretion of Pwl2:mCh in Δ*sec5* and Δ*exo70* mutants. Interestingly, the retention of Pwl2:mCh inside the fungus was associated with the first bulbous invasive hypha, directly adjacent to the BIC. These results suggest that secretion of Pwl2 does not occur at the hyphal tip, but rather from the BIC-associated cell (Giraldo

et al., 2013). It has been reported in *Trichoderma reesei* and *Aspergillus oryzae* that secretion can occur in subapical components (Hayakawa et al., 2011),(Valkonen et al., 2007). It is important to mention that these discoveries were made using advanced live-cell imaging techniques, reinforcing the importance of these techniques to facilitate such observations. Valkonen and co-workers found that exocytosis from subapical hyphal compartments required SNARE proteins (Valkonen et al., 2007) and in *A. oryzae* SNARE proteins are also involved in this subapical secretion along with AoSec3, a protein from the exocyst complex (Hayakawa et al., 2011). In this chapter, I visualised some of the secretory components reported previously (Giraldo et al., 2013) that are involved in cytoplasmic effector secretion, such as Exo70, a protein from the exocyst and Mlc1, a protein normally associated with the Spitzenkörper. Exo70 was visible in the BIC-adjacent cell, while Mlc1-GFP localisation was more uniform inside *M. oryzae* invasive hyphae. I was also interested in observing other intracellular membrane trafficking components, such as MoRab5B (Yang et al., 2017). MoRab5B localises to small vesicles that move in a bi-directional manner between the appressorium to the hyphal tip. Interestingly, these vesicles are observed at the BIC associated cell near the BIC. It would be interesting to observe secretion of a cytoplasmic effector in a ∆morab5 mutant to see if it was necessary for delivery of either class of effector.

I also investigated *M. oryzae* effector translocation using plasmolysis assays in order to visualise effectors within host cells, by effectively concentrating the fluorescent signal within the shrunken cell. This assay was first used by (Kankanala et al., 2007), where it was also reported that there is a seal between the plant plasma membrane and *M. oryzae* fungal cell wall. FM4-64, a lipophilic plasma membrane dye, was unable to be internalised by the fungus and plasmolysis of the plant plasma membrane did not retract the EIHM from *M. oryzae* invasive hyphae. I observed that upon plasmolysis, the plant plasma membrane was intact during fungal infection. Pwl2:mCh was visualised at the BIC and co-localised at the plant cytoplasm where it accumulated after plasmolysis. This indicates that the plasmolysis assay is a good live cell imaging tool for observation of effector translocation to the host. I then used the promoter and signal peptide regions of *PWL2* to study effector translocation under these

conditions. First, I used the promoter and signal peptide regions of *PWL2* fused to GFP. The Pwl2p+sp:GFP localised to the BIC and the host cell in a plasmolysed cell. The promoter and signal peptide regions of *PWL2* are therefore sufficient to translocate free GFP into the host. Additionally, I observed Pwl2p+sp-GFP localisation inside adjacent non-infected rice cells. Khang and co-workers previously reported the ability of Pwl2 to move to adjacent non-infected rice cells (Khang et al., 2010). I also observed this after expression of the Pwl2:mCh:NLS, which was directed to rice cell nuclei. To investigate whether this behaviour was specific to cytoplasmic fungal effectors, I used the apoplastic effector *BAS4* promoter and signal peptide regions fused to GFP in a plasmolysis assay. The majority of signal observed was not delivered to host cells but instead retained in fungal hyphae. Occasionally, Bas4p+sp:GFP was observed in isolated cells, which may be due to breakage of the EIHM. The signal observed with strains expressing Bas4p+sp:GFP was therefore similar to the localisation of Bas4:GFP driven by its own native promoter. Plasmolysis assays have been used to study secretion of the Pep1 effector in *U. maydis*, showing that it accumulates in the apoplastic space (Doehlemann et al., 2009).

To investigate whether the secretion was completely independent of the type of protein being delivered, I carried out a series of experiments in which I studied secretion of a non-effector protein, but expressed under control of an effector gene promoter and signal peptide region. For this series of experiments, I used the *PWL2* promoter and signal peptide sequences fused to the coding sequence of *INV1*. This gene encodes a *M. oryzae* invertase protein that is normally secreted into the apoplast during infection, or by vegetative hyphae during growth on sucrose (Lindsay et al., 2016). Consistent with this the Inv1-mCh fusion protein localised around invasive hyphae when expressed under its native promoter. However, the Pwl2p+sp:Inv1:GFP fusion protein was instead delivered into the BIC. When I observed plasmolysed rice leaf sheath preparations with Pwl2p:Inv1:GFP and Pwl2p+sp:Inv1:GFP, the Pwl2p+sp:Inv1:GFP fusion protein was observed predominantly inside host cells. The promoter and signal peptide regions of *PWL2* were therefore sufficient to translocate free GFP or a non-effector protein into host cells during *M. oryzae* infection.

## Chapter 6. General Discussion

The characterisation of effectors has provided significant insight into the nature of microbial pathogenesis and also the operation of the plant immune system. Effector-driven biology has, for example, led to a much deeper understanding of how NLR immune receptors are activated (Wang et al., 2009; Wang et al., 2019b), how NLRs can operate in networks to mediate immunity (Wu et al., 2017), how NLRs can harbour integrated decoy domains (Cesari et al., 2013; Cesari et al., 2014a; Cesari et al., 2014b; Sarris et al., 2015; Kroj et al., 2016), and how these recognize specific effectors (Maqbool et al., 2015; De la Concepcion et al., 2018).These discoveries are likely to prove pivotal in controlling devastating plant crop diseases, such as rice blast, in future by predictive manipulation of the plant immune system.

There are, however, many significant gaps in our current understanding. We do not know, for example, how effectors from filamentous eukaryotic micro-organisms, such as fungi and oomycetes, are secreted by pathogen and how they are then taken up by plant cells. In bacterial pathogens, a well-known array of secretion systems operates, including the type II secretion system that delivers effectors to the apoplast and the type III secretion system that delivers effector proteins into the cytoplasm of host plant cells (Pfeilmeier et al., 2016). Bacteria, however, possess an even larger array of secretory systems, from Type I to Type IX that are deployed by diverse bacteria, including the type IV and type VI secretion systems used by *Agrobacterium tumefaciens*, for example (Christie, 2019). These secretory systems have been well-characterized and were instrumental in the characterisation of effectors, such as the type III effectors delivered by *Pseudomonas syringae* (Alfano and Collmer, 2004).

In filamentous fungi, it is not at all clear how pathogen effectors are secreted or delivered into plant cells and the absence of a translocation motif has made characterising the delivered effectors much more challenging. By contrast, the identification of the RXLR motif in oomycete pathogens enabled many effectors to be identified and characterised, but the mechanism of delivery has remained controversial, as many of the assays used to monitor effector delivery have not

proven to be reproducible (Kale et al., 2010). It was set against this background, that the current study was planned. The principal aims of the project were to define the necessary pre-requisites for secretion of effectors from the rice blast fungus *Magnaporthe oryzae*. It was known that there are two broad groups of effectors in *M. oryzae* made according to where the effectors localise during host colonisation (Giraldo et al., 2013), but not at all clear how they are secreted precisely and how different effectors are sorted appropriately into the specific secretory pathway for delivery to the host cytoplasm or apoplast.

Apoplastic effectors, including Bas4 and Slp1 used in this study, are localised to the gap between the fungal cell wall and a specific compartment of the plant plasma membrane, called the EIHM (Kankanala et al., 2007; Giraldo et al., 2013). There they are involved in suppressing extracellular immune responses from rice (Zhang and Xu, 2014). Slp1 is the most well-characterised apoplastic effector in *M. oryzae*. It suppresses chitin-triggered immune responses from the plant by competing with the chitin elicitor binding protein (CEBiP) for binding to chitin oligosaccharides (Mentlak et al., 2012). In this way it can competitively inhibit CEBiP and thereby suppress immune responses.

In contrast, cytoplasmic effectors such as Pwl2 and AvrPia, used in this study, accumulate at the biotrophic interfacial complex (BIC) (Khang et al., 2010; Giraldo et al., 2013), which appears to be an active site of secretion by the rice blast fungus and a portal for effector translocation inside the host (Giraldo et al., 2013), where these effectors have their targets. Cytoplasmic effectors have a wide range of activities with Avr-Pik, AvrCo-39 and AvrPia all targeting HMA-containing proteins to suppress immunity. Fungal and oomycete effectors that target plant immune responses are, for example, AvrPizt (Park et al., 2012) and Slp1 (Mentlak et al., 2012) in *M. oryzae*, Avr3a in *P. infestans* (Bos et al., 2010), Ecp6 and Avr4 in *C. fulvum* (de Jonge et al., 2010; Kombrink and Thomma, 2013) and Pep1 in *U. maydis* (Hemetsberger et al., 2012). Slp1, Ecp6 and Avr4 are LysM effectors which bind to chitin receptors to suppress chitin-triggered immunity (de Jonge et al., 2010; Mentlak et al., 2012; Kombrink and Thomma, 2013). Pep1 is an apoplastic effector from *U. maydis* that protects the fungus from ROS burst by

interacting with peroxidase inhibitors (Hemetsberger et al., 2012). AvrPizt and Avr3a target the plant ubiquitination system, that has been shown to regulate the plant immune system (Bos et al., 2010; Park et al., 2012). AvrPtoB an effector from *Pseudomonas syringae* secreted into the host by the type III secretion system has also been reported to inhibit host immune response by mimicking host E3 ubiquitin ligases (Janjusevic et al., 2006). Other effector targets include host metabolic enzymes and pathways (Schornack et al., 2010; Bozkurt et al., 2011; Tanaka et al., 2019). The Tin2 cytoplasmic effector from *U. maydis* has undergone neo-functionalization, in which it is able to redirect host resources into the anthocyanin pathway (Tanaka et al., 2019). To fight pathogen proliferation, plants secrete lytic enzymes such as proteases, glucanases and chitinases into the apoplastic space and therefore, have become effector targets (Rose et al., 2002; Rooney et al., 2005; Damasceno et al., 2008; Song et al., 2009; Mueller et al., 2013; Delaunois et al., 2014). An example of this is the PR2 endoglucanase targeted by GIP1 effector from *P. sojae* (Rose et al., 2002). Other effectors targeting host proteases include *U. maydis* Pit2 (Mueller et al., 2013), *C. fulvum* Avr2 (Rooney et al., 2005) and EPIC1 and EPIC2b from *P. infestans* (Song et al., 2009).

The BIC is a plant membrane-rich structure that appears first at the tip of the primary penetration hypha, a point at which the fungus then forms a bud-like outgrowth differentiating into a bulbous, invasive hyphae, via a budding type growth. The BIC then appears as a sub-apical cell appendage and can be visualised readily by light microscopy (Mentlak et al., 2012). Experiments carried out previously and reported in this study, using a rice transgenic line expressing Lti6b-GFP, provide evidence for the BIC being composed in part of plant plasma membrane. As *M. oryzae* enters the rice cell the plant plasma membrane is always intact (Mentlak et al., 2012) and its integrity is maintained as the fungus moves from one cell to the next (Sakulkoo et al., 2018). This means the rice blast fungus always proliferates in living tissue and effectors are the enablers of this rapid growth.

This study aimed to understand how effector proteins are directed by the rice blast fungus into the correct effector localisation domain, either the apoplast or the BIC. The main objective was to understand the key role of the promoter and the signal peptide regions of effector-encoding genes in guiding this secretion. This was based on a report implicating the promoter of effectors in their sub-cellular localisation pattern (Khang et al., 2010). At the outset of the project, it did not seem likely that the promoter of an effector gene, that would normally be involved in control of transcriptional regulation, could play a role in effector protein secretion. Furthermore, the signal peptide regions of effectors were thought only to play a role in directing newly synthesised proteins to the ER and Golgi for secretion, as for any secreted protein. To test the role of these regions of effector genes, I therefore set out to construct a series of chimeras in which promoter and promoter-signal peptide swaps could be made between genes encoding cytoplasmic and apoplastic effectors, respectively.

Two further questions arose from these studies: Does re-directing an effector to a different destination involve switching the secretory system through which it is exported, and, are the regulatory processes specific to effector-encoding genes? To answer these questions, I also performed chemical inhibition assays, direct visualisation assays of effector translocation, and tested non-effector proteins for their secretion under control of effector promoter and signal peptide combinations.

In this study, I first showed that the promoter and signal peptide gene regions of Pwl2, and AvrPia, which are BIC localised effectors, can deliver free GFP to the BIC, while the promoter/signal peptide of Slp1 and Bas4 direct GFP to the apoplast. This is complicated by the observation that the high-level expression of *BAS4* causes some BIC localisation of the effector, or GFP. To allow for this in my assays, I used a ratiometric analysis of the fluorescence signal to determine the proportion of GFP signal in each compartment and enable statistical analysis of differences in the chimeric constructs made.

I initially made a library of chimeric constructs consisting of promoter swap and promoter/signal peptide swaps. Firstly, I exchanged the promoter gene region between apoplastic and cytoplasmic effectors. Then, I replaced both the promoter and signal peptide gene regions between apoplastic and cytoplasmic effectors. These experiments always used at least two independent transformants per construct that had a single copy insertion. The results provided evidence, reported in Chapters 3 and 4, that the corresponding promoter and signal peptide regions are sufficient to direct effectors into either the BIC or the apoplast. This secretion is therefore independent of the effectors themselves, apart from the very 5' end of the gene, including the signal peptide. I also found that two of the promoter swap constructs, Bas4p:Pwl2:GFP and AvrPiap:Slp1:GFP led to limited re-direction of effector localisation. This suggested that the 3' end of the promoter and the predicted signal peptide region together, may be necessary to guide effector secretion. Based on this observation I then tested what would happen if only the signal peptide sequence was replaced. I discovered that the signal peptide sequence of *PWL2* alone was not sufficient to deliver the apoplastic Slp1 effector into the BIC when linked to the *SLP1* native promoter. When considered together, this strongly suggested that the 5'end of the gene, including the signal peptide region, but also the very 3' end of the promoter sequence are important for guiding effector secretion. This led us to speculate that the 5'UTR region might be involved in re-directing effectors into the correct domain. We envisaged that this might occur at the level of mRNA, given that the gene fusions made were all translational fusions made at the start codon, so the most 3' end of the 'promoter' sequence in our constructs, actually incorporated sequences that would likely be present in the 5'end of the mRNA downstream of the transcription initiation site. Mapping transcription initiation sites effectively in all of the effectors has not been carried out, except by analysis of RNA-seq reads and would require direct analysis using 5'RACE analysis in future.

The significance of the promoter in effector secretion has been proposed in *M. oryzae* by Ribot and co-workers (Ribot et al., 2013). AvrCO39 is known to have a target inside the host, but was reported not to be BIC-localised when expressed under the control of constitutive promoter P27 (Ribot et al., 2013). Khang and co-workers also used P27 and Cutinase 1 signal peptide to drive GFP and found

that these non-effector promoter and signal peptide sequences do not confer BIC localisation (Khang et al., 2010). Promoter specificity in the localisation of a host phosphate transporter has also been shown in the arbuscular mycorrhizal symbiosis (Pumplin et al., 2012).

I next wanted to ask the question of whether the re-direction of effectors to the BIC and apoplast, respectively, was a consequence of them entering the Golgi-dependent and independent pathways previously reported (Giraldo et al., 2013). I therefore performed Brefeldin A (BFA) treatment of *M.oryzae* expressing AvrPiap+sp:Bas4:GFP. BFA treatment prevents Golgi guanine nucleotide exchange factors (GEFs) from activating Arf1(Steinberg et al., 2017), which is an Arf GTPase that regulates GeaA in the early Golgi and Sec7 in the late Golgi. Bas4, is an apoplastic effector, and has been reported to be secreted in a BFA sensitive way (Giraldo et al., 2013). When Bas4 protein is driven by the promoter and signal peptide regions of cytoplasmic effector *AVRPIA*, its secretion becomes BFA insensitive. This suggests that promoter/signal peptide region are sufficient to guide the effector into unconventional Golgi-independent secretory pathway. Golgi independent secretion has also been demonstrated in *N. crassa* for different chitin synthases (Riquelme et al., 2007; Sanchez-Leon et al., 2015), suggesting that unconventional secretory pathways do operate across fungi. However, my analysis needs to be extended in the exocyst secretion mutants that have an effect on cytoplasmic effector secretion (Giraldo et al., 2013).

Interestingly, distinct secretion pathways have been reported for apoplastic and cytoplasmic effectors in the un-related filamentous oomycete pathogen *P. infestans* (Wang et al., 2017b; Wang et al., 2018). These different Brefeldin A (BFA) experiments provide evidence that non-conventional secretion pathways may be deployed by both fungi and oomycetes as a mechanism to deliver translocated effectors. However, in these experiments the expression of cytoplasmic effector Pi04314 and apoplastic effector EPCI1 was controlled by the Ham34p constitutive promoter (Wang et al., 2017b). This would suggest that the 5'UTR of effectors genes are not involved in the unconventional pathway, as appears to be the case for *M. oryzae*. The apoplastic effector EPCI1 and the

cytoplasmic effector Pi04314, both driven by theHam34p constitutive promoter, were secreted from haustoria (Wang et al., 2017b). This is therefore also different from apoplastic and cytoplasmic effectors of *M. oryzae* which seem to have preferred domains for secretion. The most important difference, however, is that the majority of cytoplasmic effectors in *P. infestans* include a translocation motif, whereas in *M. oryzae* no translocation motif has yet been identified (Giraldo et al., 2013). It is also important to mention that Wang and co-workers were able to identify putative apoplastic effectors by using BFA treatment combined with liquid chromatography-tandem mass spectrometry (LC-MS/MS) (Wang et al., 2018). This reveals a new and innovative experiment to identify putative effectors. Interestingly, their study also revealed a possibility that proteolytic cleavage of RXLR motif occurs before secretion (Wang et al., 2018). This was also proposed in another study using Avr3a, another RXLR cytoplasmic effector (Wawra et al., 2013).

I also tested the role of exocyst components in cytoplasmic effector delivery, as previously reported (Giraldo et al., 2013) by using Δ*sec5* and Δ*exo70* mutants expressing Pwl2:mCh. The Δ*sec5* and Δ*exo70* mutants were impaired in Pwl2:mCh secretion, and a proportion of the Pwl2 signal remains inside the BIC associated cell. Interestingly, when the Pwl2p-GFP fusion is expressed in a wild type strain of *M.oryzae*, because there is no signal peptide, the GFP is localised uniformly in all bulbous cells of invasive hyphae, but protein expression of Pwl2-mCh (containing the native promoter and signal peptide region) is only expressed and retained in the BIC-associated cell. It is worth speculating therefore that transcription of *PWL2* occurs in all cells of invasive hyphae, but that translation only happens in the BIC associated cell. Secretion components, such as Spitzenkörper markers Mlc1 and Snc1, the exocyst complex markers, Exo70 and Sec5 and t-SNARE marker Sso1, are also localised to the BIC associated cell as well as the growing hyphal tip (Giraldo et al., 2013). This reinforces the idea that there are two secretory pathways in the rice blast fungus; the ER-Golgi conventional secretion pathway where secretion happens at the hyphal tip (as in vegetative hyphae grown in axenic culture) and the unconventional secretion pathway where secretion happens at the BIC-associated cell. To understand this further, I examined the localisation of the MoRab5B Rab GTPase. It was reported

that MoSec4, a *M. oryzae* homolog of the Sec4p Rab GTPase from yeast, is necessary for normal secretion of cytoplasmic effectors but has no effect on the secretion of apoplastic effectors (Zheng et al., 2016). Sec4p controls trafficking of vesicles from the Golgi to the plasma membrane, and the active Sec4p protein docks to a partial assembled exocyst complex (Zheng et al., 2016). Its reported function in the secretion of cytoplasmic effectors therefore, is consistent with what has been reported for Exo70 and Sec5 (Giraldo et al., 2013).

Recent reports suggest that MoRab5B is necessary for pathogenicity (Yang et al., 2017). MoRab5A and MoRab5B play a role in fungal endocytosis (Qi et al., 2015), and I therefore wanted to observe whether the BIC associated cell is likely to be a site of active endocytosis, as well as exocytosis. This would make sense in terms of ensuring membrane homoeostasis is achieved at this site. The rice blast fungal strain expressing *MoRAB5B:mCh* and *AVRPIA:GFP*, were used to observe endocytosis at the BIC by confocal microscopy. AvrPia-GFP accumulated at the BIC, and MoRab5B-mCh was localised in dynamic punctate structures. MoRab5-mCh moved bi-directionally from the appressorium to the hyphal tip, accumulating near the BIC, demonstrating that the BIC-associated cell is likely to be a site for endocytosis and that the appressorium is still active in the trafficking of vesicles into invasive hyphae. In *M. oryzae* the Mep1 effector is observed at the appressorium pore during host colonisation, indicating that this is an active site of secretion from *M. oryzae* appressorium at the time of cuticle rupture and plant infection (Xia et al., data not published). The *ACE1* is also expressed and localised in the appressorium in vitro. This suggests that the appressorium expresses some effector proteins before host penetration (Fudal et al., 2007).

Having demonstrated that promoter and signal peptide sequences are collectively necessary for the unconventional secretion pathway sorting of effectors into the apoplast or cytoplasmic delivery process, I wanted to know if these were processes specific to effector proteins. To answer this, I visualised the internalisation of effectors inside host cells by performing a plasmolysis assay

to shrink host cells and thereby concentrate the fluorescence signal of delivered effector gene fusions.

I checked the gross integrity of the host cell membrane in these assays by expressing a plasma membrane marker tagged with GFP, LTi6B in transgenic rice lines (Kurup et al., 2005) (Mentlak et al., 2012), which were then infected with a *M. oryzae* strain expressing *PWL2*:mCh. I observed the plant plasma membrane wrapped around *M. oryzae* invasive hyphae and accumulation at the BIC, where it colocalised with Pwl2-mCh, consistent with previous reports (Mentlak et al., 2012). Moreover, when *M. oryzae* invasive hyphae grow into adjacent plant cells, cell integrity is maintained (Mentlak et al., 2012). When I performed plasmolysis assays, the rice plasma membrane retracted from the rice cell wall but remained attached to the rice blast fungus, as previously reported using FM4-64 staining (Kankanala et al., 2007). The GFP signal remained in the plant plasma membrane, demonstrating that the plasmolysis assay did not rupture cells. Pwl2-mCh localised at the BIC and outlined the plant plasma membrane on the inside, which indicated translocation of Pwl2 into the rice cytoplasm. Additionally, I observed transgenic plants expressing the early endosome marker Ara6:GFP during *M. oryzae* infection. During host colonisation of *M. oryzae* Ara6 re-organises around the BIC, demonstrating, that the BIC is an active site of vesicle trafficking from the host plant, consistent with endocytosis occurring at this point.

In the pursuit of studying the role of the promoter and signal peptide regions using the plasmolysis assay, I used Pwl2p+sp:GFP and Bas4p+sp:GFP to visualise whether GFP could be translocated from the BIC. The Pwl2p+sp:GFP signal could be observed inside the rice cell, including non-infected adjacent rice cells after plasmolysis. This is consistent with reports showing Pwl2:mCh:NLS in nuclei of non-infected rices cells (Khang et al., 2010; Giraldo et al., 2013). However, Bas4p+sp:GFP could not be significantly observed inside the rice cytoplasm. providing further evidence that it is an apoplastic effector that does not get translocated inside the rice cell, in spite of its partial localisation to the BIC. This does seem to be a consequence therefore of its high-level expression. The

results in this study therefore suggest that re-direction of effectors to the BIC is sufficient to enable translocation to the cytoplasm of rice cells. Furthermore, all of the evidence provided in this study shows that this secretory guidance is provided by sequences at the 5'end of the effector gene in the region that I have defined in the chimeras generated as the promoter and signal peptide region. However, I cannot completely rule out that the translocation mechanism from the BIC is not a fungal-driven process but instead is driven by the host plant. It might be possible, for instance, that before BIC secretion, the fungus sorts cytoplasmic effectors into different vesicles inside the BIC and these are then recognised by the plant. However, more extensive live plant imaging and appropriate endocytic mutants in rice would be required to answer these questions.

To test if the processes revealed in this study are effector-specific, I used the promoter and signal peptide sequences of *PWL2* to drive a secreted protein that is not an effector. For this I used invertase, encoded by *INV1*, which is normally secreted from the fungus to break down sucrose into fructose and glucose (Lindsay et al., 2016). Inv1-mCh is localised to the apoplast where this enzyme activity resides (Lindsay et al., 2016). When *INV1* was expressed under control of the promoter and signal peptide sequences of *PWL2*, Inv1 was visualised at the BIC. This result strongly suggests that any protein can be delivered to the BIC when it is expressed under control of the promoter/signal peptide region of a cytoplasmic effector. Furthermore, plasmolysis experiments confirmed that this results in take-up of invertase into host cells. The sorting mechanism therefore is not effector-specific.

How then might the effector secretion process by controlled and why are the sequences at the 5'end of cytoplasmic effectors so important. Our current hypothesis is that 5'UTR of the gene may be important at the mRNA level. It is worth speculating that transcripts are sorted and transported based on signals in the 5'UTR region and that this spatial regulation of translation is necessary for delivery into both distinct secretory pathways. Recent evidence has revealed that local translation of mRNA may occur at hyphal tips (Riquelme, 2013). It has been shown for example that microtubule-dependent transport of septin mRNA occurs

in endosomes and that septin mRNA is translated on endosomes at the correct spatial location for their function (Baumann et al., 2014). It is possible that *M. oryzae* carries out a similar process, in which long-range transport of mRNAs for effectors occurs leading to their translation locally at either the hyphal tip– in the case of apoplastic effectors –or the BIC-associated cell– in the case of cytoplasmic effectors. This would explain why I observe the specific behaviour of the chimeras studied here.

How then could such a process be studied in future? One possibility would be to use similar methods to those employed by Baumann and co-workers to study mRNA trafficking using live cell imaging. They introduced a modified λN peptide fused to double Gfp ($\lambda N^*G^2$) that is able to bid to specific sites in mRNA that contain *boxB* binding sites. They introduced 16 copies of the *boxB* binding sites into the 3′ UTR of septin-encoding genes and thereby visualised the associated mRNA directly. I have undertaken a similar approach and introduced *boxB* binding sites into the *PWL2* gene at the 3'UTR in order to visualise how the transcript is moving and if undergoes long-range transport into the BIC-associated cell during plant infection. These experiments are in progress, but require considerable optimisation first to visualise mRNAs. In parallel, an examination of the predicted 5'UTR regions of effector-encoding genes is being carried out to see if specific RNA stem and loop motifs, might be associated with the 5'UTRs of each class of effector. This large-scale information study may be revealing in identifying if this sorting mechanism does occur at the mRNA level.

In summary, it is likely that a specific sorting mechanism exists that requires the 5'end of effector-encoding genes. This may occur at either the mRNA level or perhaps the protein level involving the most 5' end of the predicted signal peptide sequence. Future studies will need to dissect these two possibilities in detail using a combination of mutagenesis, and the functional assays developed in this study to determine precisely how cytoplasm and apoplastic effectors of *M. oryzae* are secreted and delivered to their specific destinations.

## Bibliography


Adachi, H., Kamoun, S., and Maqbool, A. 2019a. A resistosome-activated 'death switch'. Nat Plants 5:457-458.

Adachi, H., Contreras, M., Harant, A., Wu, C.-h., Derevnina, L., Sakai, T., Duggan, C., Moratto, E., Bozkurt, T.O., Maqbool, A., Win, J., and Kamoun, S. 2019b. An N-terminal motif in NLR immune receptors is functionally conserved across distantly related plant species. bioRxiv:693291.

Alfano, J.R., and Collmer, A. 2004. Type III secretion system effector proteins: double agents in bacterial disease and plant defense. Annu Rev Phytopathol 42:385-414.

Azizi, P., Rafii, M.Y., Mahmood, M., Abdullah, S.N., Hanafi, M.M., Nejat, N., Latif, M.A., and Sahebi, M. 2015. Differential Gene Expression Reflects Morphological Characteristics and Physiological Processes in Rice Immunity against Blast Pathogen Magnaporthe oryzae. PLoS One 10:e0126188.

Balhadere, P.V., and Talbot, N.J. 2001. PDE1 encodes a P-type ATPase involved in appressorium-mediated plant infection by the rice blast fungus Magnaporthe grisea. Plant Cell 13:1987-2004.

Baumann, S., König, J., Koepke, J., and Feldbrügge, M. 2014. Endosomal transport of septin mRNA and protein indicates local translation on endosomes and is required for correct septin filamentation. EMBO Rep 15:94-102.

Bayry, J., Aimanianda, V., Guijarro, J.I., Sunde, M., and Latge, J.P. 2012. Hydrophobins--unique fungal proteins. PLoS Pathog 8:e1002700.

Bebber, D.P., Ramotowski, M.A.T., and Gurr, S.J. 2013. Crop pests and pathogens move polewards in a warming world. Nature Climate Change 3:985.

Boddey, J.A., O'Neill, M.T., Lopaticki, S., Carvalho, T.G., Hodder, A.N., Nebl, T., Wawra, S., van West, P., Ebrahimzadeh, Z., Richard, D., Flemming, S., Spielmann, T., Przyborski, J., Babon, J.J., and Cowman, A.F. 2016. Export of malaria proteins requires co-translational processing of the PEXEL motif independent of phosphatidylinositol-3-phosphate binding. Nat Commun 7:10470.

Boevink, P.C., Wang, X., McLellan, H., He, Q., Naqvi, S., Armstrong, M.R., Zhang, W., Hein, I., Gilroy, E.M., Tian, Z., and Birch, P.R.J. 2016. A Phytophthora infestans RXLR effector targets plant PP1c isoforms that promote late blight disease. Nat Commun 7:10311.

Bohnert, H.U., Fudal, I., Dioh, W., Tharreau, D., Notteghem, J.L., and Lebrun, M.H. 2004. A putative polyketide synthase/peptide synthetase from Magnaporthe grisea signals pathogen attack to resistant rice. Plant Cell 16:2499-2513.

Bos, J.I.B., Armstrong, M.R., Gilroy, E.M., Boevink, P.C., Hein, I., Taylor, R.M., Zhendong, T., Engelhardt, S., Vetukuri, R.R., Harrower, B., Dixelius, C., Bryan, G., Sadanandom, A., Whisson, S.C., Kamoun, S., and Birch, P.R.J. 2010. Phytophthora infestans effector AVR3a is essential for virulence and manipulates plant immunity by stabilizing host E3 ligase CMPG1. Proceedings of the National Academy of Sciences of the United States of America 107:9909-9914.

Bourett, T.M., and Howard, R.J. 1990. In vitro development of penetration structures in the rice blast fungus Magnaporthe grisea. Canadian Journal of Botany 68:329-342.

Boutrot, F., and Zipfel, C. 2017. Function, Discovery, and Exploitation of Plant Pattern Recognition Receptors for Broad-Spectrum Disease Resistance. Annu Rev Phytopathol 55:257-286.

Bozkurt, T.O., Schornack, S., Banfield, M.J., and Kamoun, S. 2012. Oomycetes, effectors, and all that jazz. Curr Opin Plant Biol 15:483-492.

Bozkurt, T.O., Schornack, S., Win, J., Shindo, T., Ilyas, M., Oliva, R., Cano, L.M., Jones, A.M., Huitema, E., van der Hoorn, R.A., and Kamoun, S. 2011. Phytophthora infestans effector AVRblb2 prevents secretion of a plant immune protease at the haustorial interface. Proc Natl Acad Sci U S A 108:20832-20837.

Cai, Q., Qiao, L., Wang, M., He, B., Lin, F.M., Palmquist, J., Huang, S.D., and Jin, H. 2018. Plants send small RNAs in extracellular vesicles to fungal pathogen to silence virulence genes. Science 360:1126-1129.

Caillaud, M.C., Piquerez, S.J., Fabro, G., Steinbrenner, J., Ishaque, N., Beynon, J., and Jones, J.D. 2012. Subcellular localization of the Hpa RxLR effector repertoire identifies a tonoplast-associated protein HaRxL17 that confers enhanced plant susceptibility. Plant J 69:252-265.

Carbó, N., and Pérez-Martín, J. 2008. Spa2 is required for morphogenesis but it is dispensable for pathogenicity in the phytopathogenic fungus Ustilago maydis. Fungal Genetics and Biology 45:1315-1327.

Carvajal-Yepes, M., Cardwell, K., Nelson, A., Garrett, K.A., Giovani, B., Saunders, D.G.O., Kamoun, S., Legg, J.P., Verdier, V., Lessel, J., Neher, R.A., Day, R., Pardey, P., Gullino, M.L., Records, A.R., Bextine, B., Leach, J.E., Staiger, S., and Tohme, J. 2019. A global surveillance system for crop diseases. Science 364:1237-1239.

Cesari, S., Bernoux, M., Moncuquet, P., Kroj, T., and Dodds, P.N. 2014a. A novel conserved mechanism for plant NLR protein pairs: the "integrated decoy" hypothesis. Front Plant Sci 5:606.

Cesari, S., Kanzaki, H., Fujiwara, T., Bernoux, M., Chalvon, V., Kawano, Y., Shimamoto, K., Dodds, P., Terauchi, R., and Kroj, T. 2014b. The NB-LRR proteins RGA4 and RGA5 interact functionally and physically to confer disease resistance. EMBO J 33:1941-1959.

Cesari, S., Thilliez, G., Ribot, C., Chalvon, V., Michel, C., Jauneau, A., Rivas, S., Alaux, L., Kanzaki, H., Okuyama, Y., Morel, J.B., Fournier, E., Tharreau, D., Terauchi, R., and Kroj, T. 2013. The rice resistance protein pair RGA4/RGA5 recognizes the Magnaporthe oryzae effectors AVR-Pia and AVR1-CO39 by direct binding. Plant Cell 25:1463-1481.

Chen, C., Lian, B., Hu, J., Zhai, H., Wang, X., Venu, R.C., Liu, E., Wang, Z., Chen, M., Wang, B., Wang, G.L., Wang, Z., and Mitchell, T.K. 2013. Genome comparison of two Magnaporthe oryzae field isolates reveals genome variations and potential virulence effectors. BMC Genomics 14:887.

Chen, X.-L., Shi, T., Yang, J., Shi, W., Gao, X., Chen, D., Xu, X., Xu, J.-R., Talbot, N.J., and Peng, Y.-L. 2014. N-Glycosylation of Effector Proteins by an α-1,3-Mannosyltransferase Is Required for the Rice Blast Fungus to Evade Host Innate Immunity. The Plant Cell 26:1360.

Cheng, X., Lang, I., Adeniji, O.S., and Griffing, L. 2017. Plasmolysis-deplasmolysis causes changes in endoplasmic reticulum form, movement, flow, and cytoskeletal association. J Exp Bot 68:4075-4087.

Chinchilla, D., Bauer, Z., Regenass, M., Boller, T., and Felix, G. 2006. The Arabidopsis receptor kinase FLS2 binds flg22 and determines the specificity of flagellin perception. Plant Cell 18:465-476.

Choi, W., and Dean, R.A. 1997. The adenylate cyclase gene MAC1 of Magnaporthe grisea controls appressorium formation and other aspects of growth and development. Plant Cell 9:1973-1983.
Christie, P.J. 2019. The Rich Tapestry of Bacterial Protein Translocation Systems. Protein J 38:389-408.
Chumley, F.G.V., B. 1990. Genetic Analysis of Melanin-Deficient, Nonpathogenic Mutants of Magnaporthe grisea. Molecular Plant-Microbe Interactions 3:135-143.
Clancy, S.B., W. 2008. Translation: DNA to mRNA to Protein. Nature Education 1(1):101.
Couch, B.C., Fudal, I., Lebrun, M.H., Tharreau, D., Valent, B., van Kim, P., Notteghem, J.L., and Kohn, L.M. 2005. Origins of host-specific populations of the blast pathogen Magnaporthe oryzae in crop domestication with subsequent expansion of pandemic clones on rice and weeds of rice. Genetics 170:613-630.
Dagdas, Y.F., Yoshino, K., Dagdas, G., Ryder, L.S., Bielska, E., Steinberg, G., and Talbot, N.J. 2012. Septin-mediated plant cell invasion by the rice blast fungus, Magnaporthe oryzae. Science 336:1590-1595.
Damasceno, C.M., Bishop, J.G., Ripoll, D.R., Win, J., Kamoun, S., and Rose, J.K. 2008. Structure of the glucanase inhibitor protein (GIP) family from phytophthora species suggests coevolution with plant endo-beta-1,3-glucanases. Mol Plant Microbe Interact 21:820-830.
Dangl, J.L., and Jones, J.D. 2001. Plant pathogens and integrated defence responses to infection. Nature 411:826-833.
de Guillen, K., Ortiz-Vallejo, D., Gracy, J., Fournier, E., Kroj, T., and Padilla, A. 2015. Structure Analysis Uncovers a Highly Diverse but Structurally Conserved Effector Family in Phytopathogenic Fungi. PLoS Pathog 11:e1005228.
de Jong, J.C., McCormack, B.J., Smirnoff, N., and Talbot, N.J. 1997. Glycerol generates turgor in rice blast. Nature 389:244-244.
de Jonge, R., van Esse, H.P., Kombrink, A., Shinya, T., Desaki, Y., Bours, R., van der Krol, S., Shibuya, N., Joosten, M.H., and Thomma, B.P. 2010. Conserved fungal LysM effector Ecp6 prevents chitin-triggered immunity in plants. Science 329:953-955.
De la Concepcion, J.C., Franceschetti, M., Maqbool, A., Saitoh, H., Terauchi, R., Kamoun, S., and Banfield, M.J. 2018. Polymorphic residues in rice NLRs expand binding and response to effectors of the blast pathogen. Nat Plants 4:576-585.
Dean, R., Van Kan, J.A., Pretorius, Z.A., Hammond-Kosack, K.E., Di Pietro, A., Spanu, P.D., Rudd, J.J., Dickman, M., Kahmann, R., Ellis, J., and Foster, G.D. 2012. The Top 10 fungal pathogens in molecular plant pathology. Mol Plant Pathol 13:414-430.
Dean, R.A., Talbot, N.J., Ebbole, D.J., Farman, M.L., Mitchell, T.K., Orbach, M.J., Thon, M., Kulkarni, R., Xu, J.R., Pan, H., Read, N.D., Lee, Y.H., Carbone, I., Brown, D., Oh, Y.Y., Donofrio, N., Jeong, J.S., Soanes, D.M., Djonovic, S., Kolomiets, E., Rehmeyer, C., Li, W., Harding, M., Kim, S., Lebrun, M.H., Bohnert, H., Coughlan, S., Butler, J., Calvo, S., Ma, L.J., Nicol, R., Purcell, S., Nusbaum, C., Galagan, J.E., and Birren, B.W. 2005. The genome sequence of the rice blast fungus Magnaporthe grisea. Nature 434:980-986.

Delaunois, B., Jeandet, P., Clement, C., Baillieul, F., Dorey, S., and Cordelier, S. 2014. Uncovering plant-pathogen crosstalk through apoplastic proteomic studies. Front Plant Sci 5:249.

DeZwaan, T.M., Carroll, A.M., Valent, B., and Sweigard, J.A. 1999. Magnaporthe grisea; Pth11p Is a Novel Plasma Membrane Protein That Mediates Appressorium Differentiation in Response to Inductive Substrate Cues. The Plant Cell 11:2013.

Djamei, A., and Kahmann, R. 2012. Ustilago maydis: dissecting the molecular interface between pathogen and plant. PLoS Pathog 8:e1002955.

Djamei, A., Schipper, K., Rabe, F., Ghosh, A., Vincon, V., Kahnt, J., Osorio, S., Tohge, T., Fernie, A.R., Feussner, I., Feussner, K., Meinicke, P., Stierhof, Y.D., Schwarz, H., Macek, B., Mann, M., and Kahmann, R. 2011. Metabolic priming by a secreted fungal effector. Nature 478:395-398.

Doehlemann, G., van der Linde, K., Assmann, D., Schwammbach, D., Hof, A., Mohanty, A., Jackson, D., and Kahmann, R. 2009. Pep1, a secreted effector protein of Ustilago maydis, is required for successful invasion of plant cells. PLoS Pathog 5:e1000290.

Dutt, M., Dhekney, S.A., Soriano, L., Kandel, R., and Grosser, J.W. 2014. Temporal and spatial control of gene expression in horticultural crops. Hortic Res 1:14047.

Ebbole, D.J. 2007. Magnaporthe as a model for understanding host-pathogen interactions. Annu Rev Phytopathol 45:437-456.

Ebine, K., Fujimoto, M., Okatani, Y., Nishiyama, T., Goh, T., Ito, E., Dainobu, T., Nishitani, A., Uemura, T., Sato, M.H., Thordal-Christensen, H., Tsutsumi, N., Nakano, A., and Ueda, T. 2011. A membrane trafficking pathway regulated by the plant-specific RAB GTPase ARA6. Nat Cell Biol 13:853-859.

Ellis, J.G., and Dodds, P.N. 2011. Showdown at the RXLR motif: Serious differences of opinion in how effector proteins from filamentous eukaryotic pathogens enter plant cells. Proceedings of the National Academy of Sciences of the United States of America 108:14381-14382.

Fisher, M.C., Gow, N.A., and Gurr, S.J. 2016. Tackling emerging fungal threats to animal health, food security and ecosystem resilience. Philos Trans R Soc Lond B Biol Sci 371.

Fisher, M.C., Henk, D.A., Briggs, C.J., Brownstein, J.S., Madoff, L.C., McCraw, S.L., and Gurr, S.J. 2012. Emerging fungal threats to animal, plant and ecosystem health. Nature 484:186-194.

Flor. 1942. Inheritance of pathogenicity in Melampsora lini. Phytopath 32:653-669.

Fudal, I., Collemare, J., Böhnert, H.U., Melayah, D., and Lebrun, M.H. 2007. Expression of Magnaporthe grisea avirulence gene ACE1 is connected to the initiation of appressorium-mediated penetration. Eukaryot Cell 6:546-554.

Fujisaki, K., Abe, Y., Ito, A., Saitoh, H., Yoshida, K., Kanzaki, H., Kanzaki, E., Utsushi, H., Yamashita, T., Kamoun, S., and Terauchi, R. 2015. Rice Exo70 interacts with a fungal effector, AVR-Pii, and is required for AVR-Pii-triggered immunity. Plant J 83:875-887.

Gilbert, M.J., Thornton, C.R., Wakley, G.E., and Talbot, N.J. 2006. A P-type ATPase required for rice blast disease and induction of host resistance. Nature 440:535-539.

Gilbert, R.D., Johnson, A.M., and Dean, R.A. 1996. Chemical signals responsible for appressorium formation in the rice blast fungusMagnaporthe grisea. Physiological and Molecular Plant Pathology 48:335-346.

Giraldo, M.C., and Valent, B. 2013. Filamentous plant pathogen effectors in action. Nat Rev Microbiol 11:800-814.

Giraldo, M.C., Dagdas, Y.F., Gupta, Y.K., Mentlak, T.A., Yi, M., Martinez-Rocha, A.L., Saitoh, H., Terauchi, R., Talbot, N.J., and Valent, B. 2013. Two distinct secretion systems facilitate tissue invasion by the rice blast fungus Magnaporthe oryzae. Nat Commun 4:1996.

Godfray, H.C., Beddington, J.R., Crute, I.R., Haddad, L., Lawrence, D., Muir, J.F., Pretty, J., Robinson, S., Thomas, S.M., and Toulmin, C. 2010. Food security: the challenge of feeding 9 billion people. Science 327:812-818.

Goldberg, D.E., and Cowman, A.F. 2010. Moving in and renovating: exporting proteins from Plasmodium into host erythrocytes. Nat Rev Microbiol 8:617-621.

Gupta, Y.K., Dagdas, Y.F., Martinez-Rocha, A.-L., Kershaw, M.J., Littlejohn, G.R., Ryder, L.S., Sklenar, J., Menke, F., and Talbot, N.J. 2015. Septin-Dependent Assembly of the Exocyst Is Essential for Plant Infection by <em>Magnaporthe oryzae</em&gt. The Plant Cell 27:3277.

Hamel, L.P., Nicole, M.C., Duplessis, S., and Ellis, B.E. 2012. Mitogen-activated protein kinase signaling in plant-interacting fungi: distinct messages from conserved messengers. Plant Cell 24:1327-1351.

Hamer, J.E., Howard, R.J., Chumley, F.G., and Valent, B. 1988. A mechanism for surface attachment in spores of a plant pathogenic fungus. Science 239:288-290.

Hayakawa, Y., Ishikawa, E., Shoji, J.Y., Nakano, H., and Kitamoto, K. 2011. Septum-directed secretion in the filamentous fungus Aspergillus oryzae. Mol Microbiol 81:40-55.

Hemetsberger, C., Herrberger, C., Zechmann, B., Hillmer, M., and Doehlemann, G. 2012. The Ustilago maydis effector Pep1 suppresses plant immunity by inhibition of host peroxidase activity. PLoS Pathog 8:e1002684.

Howard, R.J., and Valent, B. 1996. Breaking and entering: host penetration by the fungal rice blast pathogen Magnaporthe grisea. Annu Rev Microbiol 50:491-512.

Howard, R.J., Ferrari, M.A., Roach, D.H., and Money, N.P. 1991. Penetration of hard substrates by a fungus employing enormous turgor pressures. Proc Natl Acad Sci U S A 88:11281-11284.

Islam, M.T., Kim, K.H., and Choi, J. 2019. Wheat Blast in Bangladesh: The Current Situation and Future Impacts. Plant Pathol J 35:1-10.

Islam, M.T., Croll, D., Gladieux, P., Soanes, D.M., Persoons, A., Bhattacharjee, P., Hossain, M.S., Gupta, D.R., Rahman, M.M., Mahboob, M.G., Cook, N., Salam, M.U., Surovy, M.Z., Sancho, V.B., Maciel, J.L., NhaniJunior, A., Castroagudin, V.L., Reges, J.T., Ceresini, P.C., Ravel, S., Kellner, R., Fournier, E., Tharreau, D., Lebrun, M.H., McDonald, B.A., Stitt, T., Swan, D., Talbot, N.J., Saunders, D.G., Win, J., and Kamoun, S. 2016. Emergence of wheat blast in Bangladesh was caused by a South American lineage of Magnaporthe oryzae. BMC Biol 14:84.

Janjusevic, R., Abramovitch, R.B., Martin, G.B., and Stebbins, C.E. 2006. A Bacterial Inhibitor of Host Programmed Cell Death Defenses Is an E3 Ubiquitin Ligase. Science 311:222.

Jia, Y., McAdams, S.A., Bryan, G.T., Hershey, H.P., and Valent, B. 2000. Direct interaction of resistance gene and avirulence gene products confers rice blast resistance. EMBO J 19:4004-4014.

Jones, J.D., and Dangl, J.L. 2006. The plant immune system. Nature 444:323-329.

Kale, S.D., Gu, B., Capelluto, D.G., Dou, D., Feldman, E., Rumore, A., Arredondo, F.D., Hanlon, R., Fudal, I., Rouxel, T., Lawrence, C.B., Shan, W., and Tyler, B.M. 2010. External lipid PI3P mediates entry of eukaryotic pathogen effectors into plant and animal host cells. Cell 142:284-295.

Kang, S., Sweigard, J.A., and Valent, B. 1995. The PWL host specificity gene family in the blast fungus Magnaporthe grisea. Mol Plant Microbe Interact 8:939-948.

Kankanala, P., Czymmek, K., and Valent, B. 2007. Roles for rice membrane dynamics and plasmodesmata during biotrophic invasion by the blast fungus. Plant Cell 19:706-724.

Kemen, E., Kemen, A., Ehlers, A., Voegele, R., and Mendgen, K. 2013. A novel structural effector from rust fungi is capable of fibril formation. Plant J 75:767-780.

Kemen, E., Kemen, A.C., Rafiqi, M., Hempel, U., Mendgen, K., Hahn, M., and Voegele, R.T. 2005. Identification of a protein from rust fungi transferred from haustoria into infected plant cells. Mol Plant Microbe Interact 18:1130-1139.

Kershaw, M.J., and Talbot, N.J. 2009. Genome-wide functional analysis reveals that infection-associated fungal autophagy is necessary for rice blast disease. Proc Natl Acad Sci U S A 106:15967-15972.

Khang, C.H., Berruyer, R., Giraldo, M.C., Kankanala, P., Park, S.Y., Czymmek, K., Kang, S., and Valent, B. 2010. Translocation of Magnaporthe oryzae effectors into rice cells and their subsequent cell-to-cell movement. Plant Cell 22:1388-1403.

Kihoro, J., Bosco, N.J., Murage, H., Ateka, E., and Makihara, D. 2013. Investigating the impact of rice blast disease on the livelihood of the local farmers in greater Mwea region of Kenya. Springerplus 2:308.

Kim, S., Hu, J., Oh, Y., Park, J., Choi, J., Lee, Y.H., Dean, R.A., and Mitchell, T.K. 2010. Combining ChIP-chip and expression profiling to model the MoCRZ1 mediated circuit for Ca/calcineurin signaling in the rice blast fungus. PLoS Pathog 6:e1000909.

Klausner, R.D., Donaldson, J.G., and Lippincott-Schwartz, J. 1992. Brefeldin A: insights into the control of membrane traffic and organelle structure. The Journal of cell biology 116:1071-1080.

Kleemann, J., Rincon-Rivera, L.J., Takahara, H., Neumann, U., Ver Loren van Themaat, E., van der Does, H.C., Hacquard, S., Stuber, K., Will, I., Schmalenbach, W., Schmelzer, E., and O'Connell, R.J. 2012. Sequential delivery of host-induced virulence effectors by appressoria and intracellular hyphae of the phytopathogen Colletotrichum higginsianum. PLoS Pathog 8:e1002643.

Knuepfer, E., Rug, M., Klonis, N., Tilley, L., and Cowman, A.F. 2005. Trafficking of the major virulence factor to the surface of transfected P. falciparum-infected erythrocytes. Blood 105:4078-4087.

Koga, H., Dohi, K., Nakayachi, O., and Mori, M. 2004. A novel inoculation method of Magnaporthe grisea for cytological observation of the infection process using intact leaf sheaths of rice plants. Physiological and Molecular Plant Pathology 64:67-72.

Kohn, C.a. 2002. <Couch, Kohn - 2002 - A multilocus gene genealogy concordant with host preference indicates segregation of a new species, Magnaporthe ory.pdf>.
Kombrink, A., and Thomma, B.P.H.J. 2013. LysM Effectors: Secreted Proteins Supporting Fungal Life. PLOS Pathogens 9:e1003769.
Konig, J., Baumann, S., Koepke, J., Pohlmann, T., Zarnack, K., and Feldbrugge, M. 2009. The fungal RNA-binding protein Rrm4 mediates long-distance transport of ubi1 and rho3 mRNAs. EMBO J 28:1855-1866.
Kroj, T., Chanclud, E., Michel-Romiti, C., Grand, X., and Morel, J.B. 2016. Integration of decoy domains derived from protein targets of pathogen effectors into plant immune receptors is widespread. New Phytol 210:618-626.
Kulkarni, R.D., Thon, M.R., Pan, H., and Dean, R.A. 2005. Novel G-protein-coupled receptor-like proteins in the plant pathogenic fungus Magnaporthe grisea. Genome Biol 6:R24.
Kurup, S., Runions, J., Kohler, U., Laplaze, L., Hodge, S., and Haseloff, J. 2005. Marking cell lineages in living tissues. Plant J 42:444-453.
Le Roux, C., Huet, G., Jauneau, A., Camborde, L., Tremousaygue, D., Kraut, A., Zhou, B., Levaillant, M., Adachi, H., Yoshioka, H., Raffaele, S., Berthome, R., Coute, Y., Parker, J.E., and Deslandes, L. 2015. A receptor pair with an integrated decoy converts pathogen disabling of transcription factors to immunity. Cell 161:1074-1088.
Li, C., Yang, J., Zhou, W., Chen, X.-L., Huang, J.-G., Cheng, Z.-H., Zhao, W.-S., Zhang, Y., and Peng, Y.-L. 2014. A spindle pole antigen gene MoSPA2 is important for polar cell growth of vegetative hyphae and conidia, but is dispensable for pathogenicity in Magnaporthe oryzae. Current Genetics 60:255-263.
Li, N., Han, X., Feng, D., Yuan, D., and Huang, L.-J. 2019. Signaling Crosstalk between Salicylic Acid and Ethylene/Jasmonate in Plant Defense: Do We Understand What They Are Whispering? Int J Mol Sci 20:671.
Li, W., Wang, B., Wu, J., Lu, G., Hu, Y., Zhang, X., Zhang, Z., Zhao, Q., Feng, Q., Zhang, H., Wang, Z., Wang, G., Han, B., Wang, Z., and Zhou, B. 2009. The Magnaporthe oryzae avirulence gene AvrPiz-t encodes a predicted secreted protein that triggers the immunity in rice mediated by the blast resistance gene Piz-t. Mol Plant Microbe Interact 22:411-420.
Lindsay, R.J., Kershaw, M.J., Pawlowska, B.J., Talbot, N.J., and Gudelj, I. 2016. Harbouring public good mutants within a pathogen population can increase both fitness and virulence. Elife 5.
Liu, X.H., Lu, J.P., Zhang, L., Dong, B., Min, H., and Lin, F.C. 2007. Involvement of a Magnaporthe grisea serine/threonine kinase gene, MgATG1, in appressorium turgor and pathogenesis. Eukaryot Cell 6:997-1005.
Manning, V.A., Hamilton, S.M., Karplus, P.A., and Ciuffetti, L.M. 2008. The Arg-Gly-Asp-containing, solvent-exposed loop of Ptr ToxA is required for internalization. Mol Plant Microbe Interact 21:315-325.
Maqbool, A., Saitoh, H., Franceschetti, M., Stevenson, C.E., Uemura, A., Kanzaki, H., Kamoun, S., Terauchi, R., and Banfield, M.J. 2015. Structural basis of pathogen recognition by an integrated HMA domain in a plant NLR immune receptor. Elife 4.
Marti, M., and Spielmann, T. 2013. Protein export in malaria parasites: many membranes to cross. Curr Opin Microbiol 16:445-451.
Mentlak, T.a., Kombrink, a., Shinya, T., Ryder, L.S., Otomo, I., Saitoh, H., Terauchi, R., Nishizawa, Y., Shibuya, N., Thomma, B.P.H.J., and Talbot,

N.J. 2012. Effector-Mediated Suppression of Chitin-Triggered Immunity by Magnaporthe oryzae Is Necessary for Rice Blast Disease. The Plant Cell 24:322-335.

Mosquera, G., Giraldo, M.C., Khang, C.H., Coughlan, S., and Valent, B. 2009. Interaction transcriptome analysis identifies Magnaporthe oryzae BAS1-4 as Biotrophy-associated secreted proteins in rice blast disease. Plant Cell 21:1273-1290.

Mueller, A.N., Ziemann, S., Treitschke, S., Assmann, D., and Doehlemann, G. 2013. Compatibility in the Ustilago maydis-maize interaction requires inhibition of host cysteine proteases by the fungal effector Pit2. PLoS Pathog 9:e1003177.

Nalley, L., Tsiboe, F., Durand-Morat, A., Shew, A., and Thoma, G. 2016. Economic and Environmental Impact of Rice Blast Pathogen (Magnaporthe oryzae) Alleviation in the United States. PLoS One 11:e0167295.

O'Connell, R.J., Thon, M.R., Hacquard, S., Amyotte, S.G., Kleemann, J., Torres, M.F., Damm, U., Buiate, E.A., Epstein, L., Alkan, N., Altmüller, J., Alvarado-Balderrama, L., Bauser, C.A., Becker, C., Birren, B.W., Chen, Z., Choi, J., Crouch, J.A., Duvick, J.P., Farman, M.A., Gan, P., Heiman, D., Henrissat, B., Howard, R.J., Kabbage, M., Koch, C., Kracher, B., Kubo, Y., Law, A.D., Lebrun, M.-H., Lee, Y.-H., Miyara, I., Moore, N., Neumann, U., Nordström, K., Panaccione, D.G., Panstruga, R., Place, M., Proctor, R.H., Prusky, D., Rech, G., Reinhardt, R., Rollins, J.A., Rounsley, S., Schardl, C.L., Schwartz, D.C., Shenoy, N., Shirasu, K., Sikhakolli, U.R., Stüber, K., Sukno, S.A., Sweigard, J.A., Takano, Y., Takahara, H., Trail, F., van der Does, H.C., Voll, L.M., Will, I., Young, S., Zeng, Q., Zhang, J., Zhou, S., Dickman, M.B., Schulze-Lefert, P., Ver Loren van Themaat, E., Ma, L.-J., and Vaillancourt, L.J. 2012. Lifestyle transitions in plant pathogenic Colletotrichum fungi deciphered by genome and transcriptome analyses. Nature Genetics 44:1060.

Orbach, M.J., Farrall, L., Sweigard, J.A., Chumley, F.G., and Valent, B. 2000. A telomeric avirulence gene determines efficacy for the rice blast resistance gene Pi-ta. Plant Cell 12:2019-2032.

Ortiz, D., de Guillen, K., Cesari, S., Chalvon, V., Gracy, J., Padilla, A., and Kroj, T. 2017. Recognition of the Magnaporthe oryzae Effector AVR-Pia by the Decoy Domain of the Rice NLR Immune Receptor RGA5. Plant Cell 29:156-168.

Oses-Ruiz, M., Sakulkoo, W., Littlejohn, G.R., Martin-Urdiroz, M., and Talbot, N.J. 2017. Two independent S-phase checkpoints regulate appressorium-mediated plant infection by the rice blast fungus Magnaporthe oryzae. Proc Natl Acad Sci U S A 114:E237-E244.

Pantazopoulou, A. 2016. The Golgi apparatus: insights from filamentous fungi. Mycologia 108:603-622.

Park, C.H., Chen, S., Shirsekar, G., Zhou, B., Khang, C.H., Songkumarn, P., Afzal, A.J., Ning, Y., Wang, R., Bellizzi, M., Valent, B., and Wang, G.L. 2012. The Magnaporthe oryzae effector AvrPiz-t targets the RING E3 ubiquitin ligase APIP6 to suppress pathogen-associated molecular pattern-triggered immunity in rice. Plant Cell 24:4748-4762.

Park, C.H., Shirsekar, G., Bellizzi, M., Chen, S., Songkumarn, P., Xie, X., Shi, X., Ning, Y., Zhou, B., Suttiviriya, P., Wang, M., Umemura, K., and Wang, G.L. 2016. The E3 Ligase APIP10 Connects the Effector AvrPiz-t to the NLR Receptor Piz-t in Rice. PLoS Pathog 12:e1005529.

Patkar, R.N., Benke, P.I., Qu, Z., Chen, Y.Y., Yang, F., Swarup, S., and Naqvi, N.I. 2015. A fungal monooxygenase-derived jasmonate attenuates host innate immunity. Nat Chem Biol 11:733-740.

Pelham, H.R. 1991. Multiple targets for brefeldin A. Cell 67:449-451.

Perez-Nadales, E., Nogueira, M.F., Baldin, C., Castanheira, S., El Ghalid, M., Grund, E., Lengeler, K., Marchegiani, E., Mehrotra, P.V., Moretti, M., Naik, V., Oses-Ruiz, M., Oskarsson, T., Schafer, K., Wasserstrom, L., Brakhage, A.A., Gow, N.A., Kahmann, R., Lebrun, M.H., Perez-Martin, J., Di Pietro, A., Talbot, N.J., Toquin, V., Walther, A., and Wendland, J. 2014. Fungal model systems and the elucidation of pathogenicity determinants. Fungal Genet Biol 70:42-67.

Petre, B., and Kamoun, S. 2014. How do filamentous pathogens deliver effector proteins into plant cells? PLoS biology 12:e1001801-e1001801.

Petre, B., Kopischke, M., Evrard, A., Robatzek, S., and Kamoun, S. 2016. Cell re-entry assays do not support models of pathogen-independent translocation of AvrM and AVR3a effectors into plant cells. bioRxiv:038232.

Peyyala, R., and Farman, M.L. 2006. Magnaporthe oryzae isolates causing gray leaf spot of perennial ryegrass possess a functional copy of the AVR1-CO39 avirulence gene. Mol Plant Pathol 7:157-165.

Pfeilmeier, S., Caly, D.L., and Malone, J.G. 2016. Bacterial pathogenesis of plants: future challenges from a microbial perspective: Challenges in Bacterial Molecular Plant Pathology. Molecular plant pathology 17:1298-1313.

Plett, J.M., Kemppainen, M., Kale, S.D., Kohler, A., Legue, V., Brun, A., Tyler, B.M., Pardo, A.G., and Martin, F. 2011. A secreted effector protein of Laccaria bicolor is required for symbiosis development. Curr Biol 21:1197-1203.

Pumplin, N., and Harrison, M.J. 2009. Live-cell imaging reveals periarbuscular membrane domains and organelle location in Medicago truncatula roots during arbuscular mycorrhizal symbiosis. Plant Physiol 151:809-819.

Pumplin, N., Zhang, X., Noar, R.D., and Harrison, M.J. 2012. Polar localization of a symbiosis-specific phosphate transporter is mediated by a transient reorientation of secretion. Proc Natl Acad Sci U S A 109:E665-672.

Qi, Y., Liang, Z., Wang, Z., Lu, G., and Li, G. 2015. Determination of Rab5 activity in the cell by effector pull-down assay. Methods Mol Biol 1298:259-270.

Rafiqi, M., Gan, P.H.P., Ravensdale, M., Lawrence, G.J., Ellis, J.G., Jones, D.A., Hardham, A.R., and Dodds, P.N. 2010. Internalization of Flax Rust Avirulence Proteins into Flax and Tobacco Cells Can Occur in the Absence of the Pathogen. The Plant Cell 22:2017.

Ribot, C., Cesari, S., Abidi, I., Chalvon, V., Bournaud, C., Vallet, J., Lebrun, M.H., Morel, J.B., and Kroj, T. 2013. The Magnaporthe oryzae effector AVR1-CO39 is translocated into rice cells independently of a fungal-derived machinery. Plant J 74:1-12.

Rico-Ramirez, A.M., Roberson, R.W., and Riquelme, M. 2018. Imaging the secretory compartments involved in the intracellular traffic of CHS-4, a class IV chitin synthase, in Neurospora crassa. Fungal Genet Biol 117:30-42.

Riquelme, M. 2013. Tip growth in filamentous fungi: a road trip to the apex. Annu Rev Microbiol 67:587-609.

Riquelme, M., Bartnicki-Garcia, S., Gonzalez-Prieto, J.M., Sanchez-Leon, E., Verdin-Ramos, J.A., Beltran-Aguilar, A., and Freitag, M. 2007.

Spitzenkorper localization and intracellular traffic of green fluorescent protein-labeled CHS-3 and CHS-6 chitin synthases in living hyphae of Neurospora crassa. Eukaryot Cell 6:1853-1864.

Riquelme, M., Aguirre, J., Bartnicki-Garcia, S., Braus, G.H., Feldbrugge, M., Fleig, U., Hansberg, W., Herrera-Estrella, A., Kamper, J., Kuck, U., Mourino-Perez, R.R., Takeshita, N., and Fischer, R. 2018. Fungal Morphogenesis, from the Polarized Growth of Hyphae to Complex Reproduction and Infection Structures. Microbiol Mol Biol Rev 82.

Rispail, N., Soanes, D.M., Ant, C., Czajkowski, R., Grunler, A., Huguet, R., Perez-Nadales, E., Poli, A., Sartorel, E., Valiante, V., Yang, M., Beffa, R., Brakhage, A.A., Gow, N.A., Kahmann, R., Lebrun, M.H., Lenasi, H., Perez-Martin, J., Talbot, N.J., Wendland, J., and Di Pietro, A. 2009. Comparative genomics of MAP kinase and calcium-calcineurin signalling components in plant and human pathogenic fungi. Fungal Genet Biol 46:287-298.

Rooney, H.C., Van't Klooster, J.W., van der Hoorn, R.A., Joosten, M.H., Jones, J.D., and de Wit, P.J. 2005. Cladosporium Avr2 inhibits tomato Rcr3 protease required for Cf-2-dependent disease resistance. Science 308:1783-1786.

Rose, J.K., Ham, K.S., Darvill, A.G., and Albersheim, P. 2002. Molecular cloning and characterization of glucanase inhibitor proteins: coevolution of a counterdefense mechanism by plant pathogens. Plant Cell 14:1329-1345.

Ryder, L.S., Dagdas, Y.F., Mentlak, T.A., Kershaw, M.J., Thornton, C.R., Schuster, M., Chen, J., Wang, Z., and Talbot, N.J. 2013. NADPH oxidases regulate septin-mediated cytoskeletal remodeling during plant infection by the rice blast fungus. Proc Natl Acad Sci U S A 110:3179-3184.

Saitoh, H., Fujisawa, S., Mitsuoka, C., Ito, A., Hirabuchi, A., Ikeda, K., Irieda, H., Yoshino, K., Yoshida, K., Matsumura, H., Tosa, Y., Win, J., Kamoun, S., Takano, Y., and Terauchi, R. 2012. Large-scale gene disruption in Magnaporthe oryzae identifies MC69, a secreted protein required for infection by monocot and dicot fungal pathogens. PLoS Pathog 8:e1002711.

Sakulkoo, W., Oses-Ruiz, M., Oliveira Garcia, E., Soanes, D.M., Littlejohn, G.R., Hacker, C., Correia, A., Valent, B., and Talbot, N.J. 2018. A single fungal MAP kinase controls plant cell-to-cell invasion by the rice blast fungus. Science 359:1399-1403.

Sambrook, J., and Russell, D.W. 2006. Southern blotting: capillary transfer of DNA to membranes. CSH Protoc 2006.

Sanchez-Leon, E., Bowman, B., Seidel, C., Fischer, R., Novick, P., and Riquelme, M. 2015. The Rab GTPase YPT-1 associates with Golgi cisternae and Spitzenkorper microvesicles in Neurospora crassa. Mol Microbiol 95:472-490.

Sarris, Panagiotis F., Duxbury, Z., Huh, Sung U., Ma, Y., Segonzac, C., Sklenar, J., Derbyshire, P., Cevik, V., Rallapalli, G., Saucet, Simon B., Wirthmueller, L., Menke, Frank L.H., Sohn, Kee H., and Jones, Jonathan D.G. 2015. A Plant Immune Receptor Detects Pathogen Effectors that Target WRKY Transcription Factors. Cell 161:1089-1100.

Saunders, D.G., Aves, S.J., and Talbot, N.J. 2010. Cell cycle-mediated regulation of plant infection by the rice blast fungus. Plant Cell 22:497-507.

Schornack, S., van Damme, M., Bozkurt, T.O., Cano, L.M., Smoker, M., Thines, M., Gaulin, E., Kamoun, S., and Huitema, E. 2010. Ancient class of translocated oomycete effectors targets the host nucleus. Proceedings of the National Academy of Sciences 107:17421.

Sheu, Y.J., Santos, B., Fortin, N., Costigan, C., and Snyder, M. 1998. Spa2p interacts with cell polarity proteins and signaling components involved in yeast cell morphogenesis. Mol Cell Biol 18:4053-4069.
Song, J., Win, J., Tian, M., Schornack, S., Kaschani, F., Ilyas, M., van der Hoorn, R.A., and Kamoun, S. 2009. Apoplastic effectors secreted by two unrelated eukaryotic plant pathogens target the tomato defense protease Rcr3. Proc Natl Acad Sci U S A 106:1654-1659.
Sornkom, W., Miki, S., Takeuchi, S., Abe, A., Asano, K., and Sone, T. 2017. Fluorescent reporter analysis revealed the timing and localization of AVR-Pia expression, an avirulence effector of Magnaporthe oryzae. Mol Plant Pathol 18:1138-1149.
Stam, R., Jupe, J., Howden, A.J., Morris, J.A., Boevink, P.C., Hedley, P.E., and Huitema, E. 2013. Identification and Characterisation CRN Effectors in Phytophthora capsici Shows Modularity and Functional Diversity. PLoS One 8:e59517.
Steinberg, G. 2016. The mechanism of peroxisome motility in filamentous fungi. Fungal Genet Biol 97:33-35.
Steinberg, G., Penalva, M.A., Riquelme, M., Wosten, H.A., and Harris, S.D. 2017. Cell Biology of Hyphal Growth. Microbiol Spectr 5.
Stergiopoulos, I., and de Wit, P.J. 2009. Fungal effector proteins. Annu Rev Phytopathol 47:233-263.
Strange, R.N., and Scott, P.R. 2005. Plant disease: a threat to global food security. Annu Rev Phytopathol 43:83-116.
Sun, C.B., Suresh, A., Deng, Y.Z., and Naqvi, N.I. 2006. A multidrug resistance transporter in Magnaporthe is required for host penetration and for survival during oxidative stress. Plant Cell 18:3686-3705.
Sweigard, J.A., Carroll, A.M., Kang, S., Farrall, L., Chumley, F.G., and Valent, B. 1995. Identification, cloning, and characterization of PWL2, a gene for host species specificity in the rice blast fungus. Plant Cell 7:1221-1233.
Takken, F.L.W., and Goverse, A. 2012. How to build a pathogen detector: structural basis of NB-LRR function. Current Opinion in Plant Biology 15:375-384.
Talbot, N.J. 1995. Having a blast: exploring the pathogenicity of Magnaporthe grisea. Trends Microbiol 3:9-16.
Talbot, N.J. 2003. On the trail of a cereal killer: Exploring the biology of Magnaporthe grisea. Annu Rev Microbiol 57:177-202.
Talbot, N.J. 2010. Living the sweet life: how does a plant pathogenic fungus acquire sugar from plants? PLoS Biol 8:e1000308.
Talbot, N.J. 2019. Appressoria. Curr Biol 29:R144-R146.
Talbot, N.J., Ebbole, D.J., and Hamer, J.E. 1993a. Identification and characterization of MPG1, a gene involved in pathogenicity from the rice blast fungus Magnaporthe grisea. Plant Cell 5:1575-1590.
Talbot, N.J., Salch, Y.P., Ma, M., and Hamer, J.E. 1993b. Karyotypic Variation within Clonal Lineages of the Rice Blast Fungus, Magnaporthe grisea. Appl Environ Microbiol 59:585-593.
Tanaka, S., Schweizer, G., Rossel, N., Fukada, F., Thines, M., and Kahmann, R. 2019. Neofunctionalization of the secreted Tin2 effector in the fungal pathogen Ustilago maydis. Nat Microbiol 4:251-257.
Tang, M., Ning, Y., Shu, X., Dong, B., Zhang, H., Wu, D., Wang, H., Wang, G.-L., and Zhou, B. 2017. The Nup98 Homolog APIP12 Targeted by the Effector AvrPiz-t is Involved in Rice Basal Resistance Against Magnaporthe oryzae. Rice (N Y) 10:5-5.

Trusch, F., Loebach, L., Wawra, S., Durward, E., Wuensch, A., Iberahim, N.A., de Bruijn, I., MacKenzie, K., Willems, A., Toloczko, A., Dieguez-Uribeondo, J., Rasmussen, T., Schrader, T., Bayer, P., Secombes, C.J., and van West, P. 2018. Cell entry of a host-targeting protein of oomycetes requires gp96. Nat Commun 9:2347.

Tyler, B.M., Kale, S.D., Wang, Q., Tao, K., Clark, H.R., Drews, K., Antignani, V., Rumore, A., Hayes, T., Plett, J.M., Fudal, I., Gu, B., Chen, Q., Affeldt, K.J., Berthier, E., Fischer, G.J., Dou, D., Shan, W., Keller, N.P., Martin, F., Rouxel, T., and Lawrence, C.B. 2013. Microbe-independent entry of oomycete RxLR effectors and fungal RxLR-like effectors into plant and animal cells is specific and reproducible. Mol Plant Microbe Interact 26:611-616.

Urban, M., Bhargava, T., and Hamer, J.E. 1999. An ATP-driven efflux pump is a novel pathogenicity factor in rice blast disease. EMBO J 18:512-521.

Valent, B., and Chumley, F.G. 1991. Molecular genetic analysis of the rice blast fungus, magnaporthe grisea. Annu Rev Phytopathol 29:443-467.

Valkonen, M., Kalkman, E.R., Saloheimo, M., Penttila, M., Read, N.D., and Duncan, R.R. 2007. Spatially segregated SNARE protein interactions in living fungal cells. J Biol Chem 282:22775-22785.

Van der Hoorn, R.A., and Kamoun, S. 2008. From Guard to Decoy: a new model for perception of plant pathogen effectors. Plant Cell 20:2009-2017.

Veneault-Fourrey, C., Barooah, M., Egan, M., Wakley, G., and Talbot, N.J. 2006. Autophagic fungal cell death is necessary for infection by the rice blast fungus. Science 312:580-583.

Wang, B.-h., Ebbole, D.J., and Wang, Z.-h. 2017a. The arms race between Magnaporthe oryzae and rice: Diversity and interaction of Avr and R genes. Journal of Integrative Agriculture 16:2746-2760.

Wang, J., Hu, M., Wang, J., Qi, J., Han, Z., Wang, G., Qi, Y., Wang, H.W., Zhou, J.M., and Chai, J. 2019a. Reconstitution and structure of a plant NLR resistosome conferring immunity. Science 364.

Wang, J., Wang, J., Hu, M., Wu, S., Qi, J., Wang, G., Han, Z., Qi, Y., Gao, N., Wang, H.W., Zhou, J.M., and Chai, J. 2019b. Ligand-triggered allosteric ADP release primes a plant NLR complex. Science 364.

Wang, R., Ning, Y., Shi, X., He, F., Zhang, C., Fan, J., Jiang, N., Zhang, Y., Zhang, T., Hu, Y., Bellizzi, M., and Wang, G.L. 2016. Immunity to Rice Blast Disease by Suppression of Effector-Triggered Necrosis. Curr Biol 26:2399-2411.

Wang, S., Boevink, P.C., Welsh, L., Zhang, R., Whisson, S.C., and Birch, P.R.J. 2017b. Delivery of cytoplasmic and apoplastic effectors from Phytophthora infestans haustoria by distinct secretion pathways. New Phytol 216:205-215.

Wang, S., Welsh, L., Thorpe, P., Whisson, S.C., Boevink, P.C., and Birch, P.R.J. 2018. The Phytophthora infestans Haustorium Is a Site for Secretion of Diverse Classes of Infection-Associated Proteins. MBio 9.

Wang, W., Wen, Y., Berkey, R., and Xiao, S. 2009. Specific targeting of the Arabidopsis resistance protein RPW8.2 to the interfacial membrane encasing the fungal Haustorium renders broad-spectrum resistance to powdery mildew. Plant Cell 21:2898-2913.

Wawra, S., Djamei, A., Albert, I., Nurnberger, T., Kahmann, R., and van West, P. 2013. In vitro translocation experiments with RxLR-reporter fusion proteins of Avr1b from Phytophthora sojae and AVR3a from Phytophthora

infestans fail to demonstrate specific autonomous uptake in plant and animal cells. Mol Plant Microbe Interact 26:528-536.
Wawra, S., Trusch, F., Matena, A., Apostolakis, K., Linne, U., Zhukov, I., Stanek, J., Kozminski, W., Davidson, I., Secombes, C.J., Bayer, P., and van West, P. 2017. The RxLR Motif of the Host Targeting Effector AVR3a of Phytophthora infestans Is Cleaved before Secretion. Plant Cell 29:1184-1195.
Whisson, S.C., Boevink, P.C., Moleleki, L., Avrova, A.O., Morales, J.G., Gilroy, E.M., Armstrong, M.R., Grouffaud, S., van West, P., Chapman, S., Hein, I., Toth, I.K., Pritchard, L., and Birch, P.R.J. 2007. A translocation signal for delivery of oomycete effector proteins into host plant cells. Nature 450:115.
Wilson, R.A., and Talbot, N.J. 2009. Under pressure: investigating the biology of plant infection by Magnaporthe oryzae. Nat Rev Microbiol 7:185-195.
Wu, C.H., Abd-El-Haliem, A., Bozkurt, T.O., Belhaj, K., Terauchi, R., Vossen, J.H., and Kamoun, S. 2017. NLR network mediates immunity to diverse plant pathogens. Proc Natl Acad Sci U S A 114:8113-8118.
Wu, J., Kou, Y., Bao, J., Li, Y., Tang, M., Zhu, X., Ponaya, A., Xiao, G., Li, J., Li, C., Song, M.Y., Cumagun, C.J., Deng, Q., Lu, G., Jeon, J.S., Naqvi, N.I., and Zhou, B. 2015. Comparative genomics identifies the Magnaporthe oryzae avirulence effector AvrPi9 that triggers Pi9-mediated blast resistance in rice. New Phytol 206:1463-1475.
Xu, G., Greene, G.H., Yoo, H., Liu, L., Marqués, J., Motley, J., and Dong, X. 2017. Global translational reprogramming is a fundamental layer of immune regulation in plants. Nature 545:487-490.
Xu, J.R., and Hamer, J.E. 1996. MAP kinase and cAMP signaling regulate infection structure formation and pathogenic growth in the rice blast fungus Magnaporthe grisea. Genes Dev 10:2696-2706.
Yaeno, T., Li, H., Chaparro-Garcia, A., Schornack, S., Koshiba, S., Watanabe, S., Kigawa, T., Kamoun, S., and Shirasu, K. 2011. Phosphatidylinositol monophosphate-binding interface in the oomycete RXLR effector AVR3a is required for its stability in host cells to modulate plant immunity. Proc Natl Acad Sci U S A 108:14682-14687.
Yang, C.D., Dang, X., Zheng, H.W., Chen, X.F., Lin, X.L., Zhang, D.M., Abubakar, Y.S., Chen, X., Lu, G., Wang, Z., Li, G., and Zhou, J. 2017. Two Rab5 Homologs Are Essential for the Development and Pathogenicity of the Rice Blast Fungus Magnaporthe oryzae. Front Plant Sci 8:620.
Yi, M., and Valent, B. 2013. Communication between filamentous pathogens and plants at the biotrophic interface. Annu Rev Phytopathol 51:587-611.
Yi, M., Chi, M.H., Khang, C.H., Park, S.Y., Kang, S., Valent, B., and Lee, Y.H. 2009. The ER chaperone LHS1 is involved in asexual development and rice infection by the blast fungus Magnaporthe oryzae. Plant Cell 21:681-695.
Yoshida, K., Saitoh, H., Fujisawa, S., Kanzaki, H., Matsumura, H., Yoshida, K., Tosa, Y., Chuma, I., Takano, Y., Win, J., Kamoun, S., and Terauchi, R. 2009. Association genetics reveals three novel avirulence genes from the rice blast fungal pathogen Magnaporthe oryzae. Plant Cell 21:1573-1591.
Zhang, S., and Xu, J.R. 2014. Effectors and effector delivery in Magnaporthe oryzae. PLoS Pathog 10:e1003826.
Zhang, S., Wang, L., Wu, W., He, L., Yang, X., and Pan, Q. 2015. Function and evolution of Magnaporthe oryzae avirulence gene AvrPib responding to the rice blast resistance gene Pib. Sci Rep 5:11642.

Zhang, Z.M., Zhang, X., Zhou, Z.R., Hu, H.Y., Liu, M., Zhou, B., and Zhou, J. 2013. Solution structure of the Magnaporthe oryzae avirulence protein AvrPiz-t. J Biomol NMR 55:219-223.

Zheng, H., Chen, S., Chen, X., Liu, S., Dang, X., Yang, C., Giraldo, M.C., Oliveira-Garcia, E., Zhou, J., Wang, Z., and Valent, B. 2016. The Small GTPase MoSec4 Is Involved in Vegetative Development and Pathogenicity by Regulating the Extracellular Protein Secretion in Magnaporthe oryzae. Front Plant Sci 7:1458.

Zipfel, C. 2009. Early molecular events in PAMP-triggered immunity. Curr Opin Plant Biol 12:414-420.

Zipfel, C., Kunze, G., Chinchilla, D., Caniard, A., Jones, J.D., Boller, T., and Felix, G. 2006. Perception of the bacterial PAMP EF-Tu by the receptor EFR restricts Agrobacterium-mediated transformation. Cell 125:749-760.